Report No. 77-2

COMPLETE STRESS-STRAIN CURVE OF CONCRETE AND ITS EFFECT ON DUCTILITY OF REINFORCED CONCRETE MEMBERS

by

Pao-Tsan Wang
Research Assistant

Surendra P. Shah
Professor of Civil Engineering

Antoine E. Naaman
Associate Professor of Structural Design

October 1977

ia/

COMPLETE STRESS-STRAIN CURVE OF CONCRETE AND ITS EFFECT ON DUCTILITY OF REINFORCED CONCRETE MEMBERS

by

P. T. Wang, S. P. Shah and A. E. Naaman
Department of Materials Engineering
University of Illinois at Chicago Circle
Chicago, Illinois 60680

ABSTRACT

A relatively simple experimental technique is developed to obtain the entire stress-strain curve of concrete including the descending portion. The experimental stress-strain curves of normal weight concretes of strengths up to 11,000 psi and lightweight concretes of strengths up to 8,000 psi are reported.

A general analytical expression for the stress-strain curve of concrete is proposed to reflect accurately experimental results. The expression has four constants which depend on the properties of both the ascending and the descending portions of the stress-strain curve and can be evaluated from the knowledge of four key points of the curve, namely; on the ascending portion, the peak point and the point corresponding to a stress of 45% of the peak, and, on the descending portion, the inflection point, and another point symmetric to the peak with respect to the inflection point. Furthermore, the coordinates of the four key points were expressed in function of the compressive strength of concrete so as to allow prediction of the entire curve solely from the knowledge of the compressive strength.

Similarly, an expression was developed to represent the entire stress-strain curve of Grade 60 reinforcing bars with yield strengths varying from about 60 to 75 ksi. This expression was based on the analysis of results from 50 random reinforcing bar specimens tested according to ASTM standards.

Based on the above results, a computerized nonlinear analysis program was developed to predict the structural response of reinforced concrete beams, and columns under combined axial load and uniaxial and biaxial bendings. The method takes into consideration actual material properties for both concrete and steel, and uses the general assumptions of equilibrium and compatibility. Using the above program, the comparison of theoretically generated information with some experimental data reported in technical literature is found acceptable.

The effects of high strength concrete, tensile and compressive reinforcement ratios, axial load and eccentricity on the structural behavior of reinforced concrete sections, such as ultimate load capacity, curvature and ductility are thoroughly explored. Load-moment-curvature-strain interaction diagrams are automatically generated and plotted.

An extensive parametric study of the concrete compression zone is undertaken and leads to recommendations on the appropriate values of the rectangular stress block parameters (ε_{cu}, β_1) for high strength normal weight and lightweight concretes.

ACKNOWLEDGEMENTS

This research was at first initiated by the need to characterize the stress-strain properties of portland cement mortar as used in ferrocement. The study on ferrocement was supported by a National Science Foundation Grant No. ENG 74-20829 to the University of Illinois at Chicago Circle. However, the completion of the first phase of this continuing investigation would not have been possible without the support of the Department of Materials Engineering and an internal grant from the University of Illinois Research Board. The help of the above three sponsors is greatly appreciated.

TABLE OF CONTENTS

TABLE OF CONTENTS (Cont'd)

TABLE OF CONTENTS (Cont'd)

LIST OF FIGURES

LIST OF TABLES

NOTATION

A,B,C,D	parameters used in $Y = (AX+BX^2)/(1+CX+DX^2)$
a	depth of equivalent rectangular stress block, ($= \beta_1 c$ in ACI code)
A_c	area of concrete at the cross-section considered (depending on the particular case it may be the net area, the gross area or the transformed area)
A_g	gross area of concrete at the cross section considered
A_s	area of non-prestressed tension reinforcement
A_s'	area of compression reinforcement
b	width of compression face of member
b_w or b'	web width of a flanged member
c	distance from extreme compression fiber to neutral axis
C	resulting compressive force on the concrete section due to the prestressing force and applied external forces
d	distance from extreme compression fiber to centroid of tension reinforcement
d''	distance from extreme compression fiber to centroid of compressive reinforcement
d'	thickness of concrete cover measured from the extreme tension fiber to the centroid of tension reinforcement
e	eccentricity of applied external load or of the C force on the concrete section parallel to axis measured from the centroid of the section
E_c	modulus of elasticity of concrete
E_o	f_o/ε_o, secant modulus of elasticity at the peak stress
E_s	modulus of elasticity of non-prestressed steel
f_c' or f_o	compressive strength of concrete
f_i	stress at the inflection point of stress-strain curve of concrete
f_{2i}	stress at ε_{2i}

f_f	stress at arbitrary point after the inflection point
f_s	stress in the non-prestressed tensile reinforcement
f'_s	stress in the compressive reinforcement
f_y	yield strength of non-prestressed tensile reinforcement
f'_y	yield strength of compressive reinforcement
h	overall thickness or depth of member
h_f	flange thickness of a flanged member (t is also used)
k	ratio of depth of neutral axis to d
M	moment in general
M_b	bending moment capacity at balanced conditions, i.e., at simultaneous assumed ultimate strain of concrete and yielding of tension steel
M_u	applied ultimate moment at section considered
P	concentrated external load in general
P_b	axial load capacity at balanced conditions, i.e., at simultaneous assumed ultimate strain of concrete and yielding of tension steel
P'_u or P_o	axial load capacity of compression member subject to pure compression (no moment)
t	thickness of the upper flange of flanged section (see also h_f)
T	tensile load
u	used as subscript for "ultimate"
X	$\varepsilon/\varepsilon_o$, strain in unit system
Y	f/f_o, stress in unit system
α	parameter used related to the resultant force of stress block of compression zone of concrete
β	stress block of compression zone of concrete

β_1	factor used to define the depth of the equivalent rectangular stress block at ultimate as a function of the neutral axis. According to ACI: $\beta_1 = 0.85$ for $f'_c \leq 4000$ psi $\beta_1 = 0.85 - 5\times10^{-5}\ (f'_c - 4000)$ for $4000 \leq f'_c \leq 8000$ psi $\beta_1 = 0.65$ for $f'_c \geq 8000$ psi
Δ	deflection in general
ε	strain in general
ε_c	concrete strain in general
ε_{cu}	concrete strain at ultimate on extreme compression fiber
ε_f	strain at arbitrary point after the inflection point
ε_i	strain at the inflection point of the stress-strain curve of concrete
ε_{2i}	$2\varepsilon_i - \varepsilon_o$, strain at twice the distance of the inflection point with respect to the peak point
ε_o	strain at peak stress of the stress-strain curve of concrete
θ	eccentricity angle for biaxial loading on column
μ	ϕ_u/ϕ_y, ductility factor
ρ	A_s/bd, ratio of non-prestressed tension reinforcement
ρ'	A'_s/bd, ratio of compression reinforcement
ρ_b	reinforcement ratio producing balanced condition
ρ_{min}	minimum specified reinforcement ratio
ρ_{max}	maximum specified reinforcement ratio
σ_s	ratio of volume of spiral reinforcement to total volume of core
σ or f	stress in general
ϕ	curvature of section

CHAPTER I

INTRODUCTION

1.1 GENERAL

In analyzing the behavior of any structural member, it is essential to have the accurate knowledge of the constitutive equations of the materials concerned. In reinforced-concrete structures, the material properties of the two major components, concrete and steel, can be best described by their stress-strain relationships, in compression for concrete and in tension for steel.

The stress-strain curve of concrete shows generally an ascending portion up to a maximum stress called peak stress, and a S-shaped descending portion after the peak stress. The ascending portion can be considered linear for all practical purposes up to about 45% of the peak stress, after which it becomes nonlinear with a decreasing slope. The test data regarding this portion can be obtained in any compression test machine. However, little data on the complete stress-strain curve of concrete including the descending portion, especially for high strengths, are available in existing technical literature. This is because it is difficult to actually record the descending portion of the curve. Many testing machines used for standard compression test apply increasing loads rather than increasing deformations. This results in an uncontrolled, sudden failure of the specimen immediately after the peak load because of the release of energy from the testing systems when the specimen is unloading. Even with the deformation controlled loading, the release of the energy stored in the testing machine, when the specimen is unloading, will influence the shape of the descending portion. In this research, a simple technique was developed to obtain the stress-strain

curve of concrete up to a strain of 0.006. Higher strains can also be achieved by slightly modifying the testing procedure.

The stress-strain curve of reinforcing steel of Grade 60 exhibits a strain-hardening portion up to the peak load. For a reinforced-concrete section with high percentage of compressive steel, the strain in the tensile steel always reaches the strain-hardening portion at ultimate; therefore, the accurate knowledge of the stress-strain relationship of reinforcing steels including the strain-hardening portion is needed. Furthermore, once the experimental stress-strain curves have been determined, an analytical expression must be developed in order to be used in computerized models of structural analysis.

In designing reinforced-concrete structures, there is a tendency to design the structural members with sufficient ductility, especially in an earthquake zone. Ductility implies the ability to sustain significant inelastic deformations after the peak load without a significant variation in the resisting capacity prior to collapse. The ductility of reinforced-concrete members can be improved by adding compressive steel in the concrete section, or by confining the concrete compressive zone which leads to an improvement in the ductility of the material. Note that improving the ductility of the materials generally leads to an improvement in the ductility of the reinforced-concrete section and/or member.

It is generally believed that higher strength concrete as a material has less ductility than lower strength; however, in analyzing the load-moment-curvature-strain interaction diagrams for typical reinforced-concrete sections, there is evidence that the same ductility factors, for the section and/or the member, can be obtained for all strengths of concrete.

Although high strength concrete does not significantly improve the moment capacity of beam sections under pure bending, it significantly improves the load capacity of column sections under combined flexural and compressive loadings. A thorough and careful investigation of the effects of using high strength concrete on the structural response of reinforced-concrete members should be undertaken. There is also a definite need to carry out a detailed study of the current design approaches, such as the ACI recommended stress block parameters at ultimate behavior, as to their applicability to structures made with high strength reinforced concrete.

1.2 OBJECTIVE AND SCOPE

The main objectives of this investigation are:

(1) To develop, if necessary, and assess methods for obtaining the complete stress-strain curve of concrete including the descending portion,

(2) To generate experimental information on the complete actual stress-strain curves of high strength normal weight and lightweight concretes,

(3) To evaluate existing analytical expressions for the stress-strain curves of concrete, to check if they represent actual experimental observations, to propose a new expression if others are found inadequate,

(4) To propose an analytical expression for the complete stress-strain curves of Grade 60 reinforcing bars which may show yield strengths between 60 to 75 ksi,

(5) To formulate a computerized nonlinear analysis model for the analysis of reinforced-concrete beams and columns under uniaxial and biaxial bending,

(6) To evaluate the effects of using high strength concrete on the structural response of reinforced-concrete members such as ultimate moment, curvature, ductility and deflections, and

(7) To conduct a parametric evaluation of high strength reinforced-concrete members in order to define appropriate values for the stress block parameters of the concrete compression zone to be recommended for design purposes.

The information from this investigation will provide a better understanding of the characteristics and behavior of high strength concrete, and its effects on the structural response of reinforced-concrete members. It will allow the designer to use high strength concrete with more confidence and take advantage of its properties when they are desired.

1.3 STRUCTURE OF THIS THESIS

Chapter II is devoted to study the existing analytic expressions for the stress-strain curve of concrete, to analyze the characteristic points of these curves, and to formulate an analytic relationship that is most representative of the observed behavior of various concretes. Chapter III is a similar study on reinforcing steels. Chapter IV describes a test procedure for obtaining the complete stress-strain curve of concrete in compression. The experimental program undertaken in this investigation is also described in Chapter IV and test results are presented. Furthermore,

the observed characteristic points of the curve are linearly related to the peak stress using regression analysis. Chapter V explains the nonlinear computerized analysis technique developed for reinforced-concrete sections under pure bending and bending combined with uniaxial and biaxial compressive loadings. Chapter VI explores the structural behavior of reinforced-concrete sections, namely, the ultimate moment, curvature, ductility and deflection for various concrete strengths and amounts of reinforcement. Chapter VII is a quantitative study of the ultimate strength parameters of the concrete compression zone to be used for the design of reinforced high strength concrete strengths. Chapter VIII presents the summary of conclusions.

CHAPTER II

COMPLETE STRESS-STRAIN CURVE OF CONCRETE

2.1 REVIEW OF EXISTING STRESS-STRAIN CURVES OF CONCRETE

2.1.1 Introduction

A complete stress-strain curve consists of two portions: an ascending portion before the peak, and a descending portion after the peak. Several expressions have been proposed to describe the σ-ε curve of concrete; unfortunately they have one or more shortcomings, which will be pointed out in each reviewed expression. In order to review the existing stress-strain expressions systematically, these expressions are grouped into several categories. They include: polynomial functions, exponential functions, fractional functions, and statistical distribution functions. For each of these analytic expressions, the following items were investigated:

(a) the boundary conditions, namely the peak stress, f_o, the strain at peak point, ε_o, the secant modulus of elasticity, E_c, at 0.45 f_o, the stresses and strains at the inflection point and another far point on the descending portion.

(b) the shape of the curve over its entire range.

(c) the comparation of the analytic curve with experimental data and its shortcomings if any.

2.1.2 Description of Mathematical Procedure

In order to review the various equations and their representative curve, a system for describing each curve is set up as follows:

A. Unit stress-strain system.

Unit stress and unit strain are used to express the stress-strain relationship. By this manner, the expression ensures itself a correct dimension, and all the parameters involved are dimensionless. A typical σ-ε curve is shown in Fig. 2.1 and the following notations will be used throughout this report:

$$X = \frac{\varepsilon}{\varepsilon_o}, \qquad Y = \frac{f_o}{\varepsilon_o}$$

$$E_o = \frac{f_o}{\varepsilon_o}, \qquad A = \frac{E_c}{E_o} \tag{2.1}$$

where

f and ε = stress and strain in general

f_o and ε_o = peak stress and corresponding strain

f_t and ε_t = stress and strain at 0.45 f_o

f_i and ε_i = stress and strain at inflection point

f_f and ε_f = stress and strain at far point on descending portion which was arbitrarily selected such that $\varepsilon_f - \varepsilon_i = \varepsilon_i - \varepsilon_o$ for this study

E_c = secant modulus of elasticity at 0.45 f_o

B. Boundary conditions for ascending portion.

BC1 - Curve passes through the peak point:

$$(\varepsilon = \varepsilon_o,\ f = f_o) \quad \text{or} \quad (X = X_o = 1,\ Y = Y_o = 1)$$

BC2 - At the peak point, the slope equal zero:

$$\left.\frac{df}{d\varepsilon}\right|_{(\varepsilon_o, f_o)} = 0, \qquad \text{or} \qquad \left.\frac{dY}{dX}\right|_{(1,1)} = 0$$

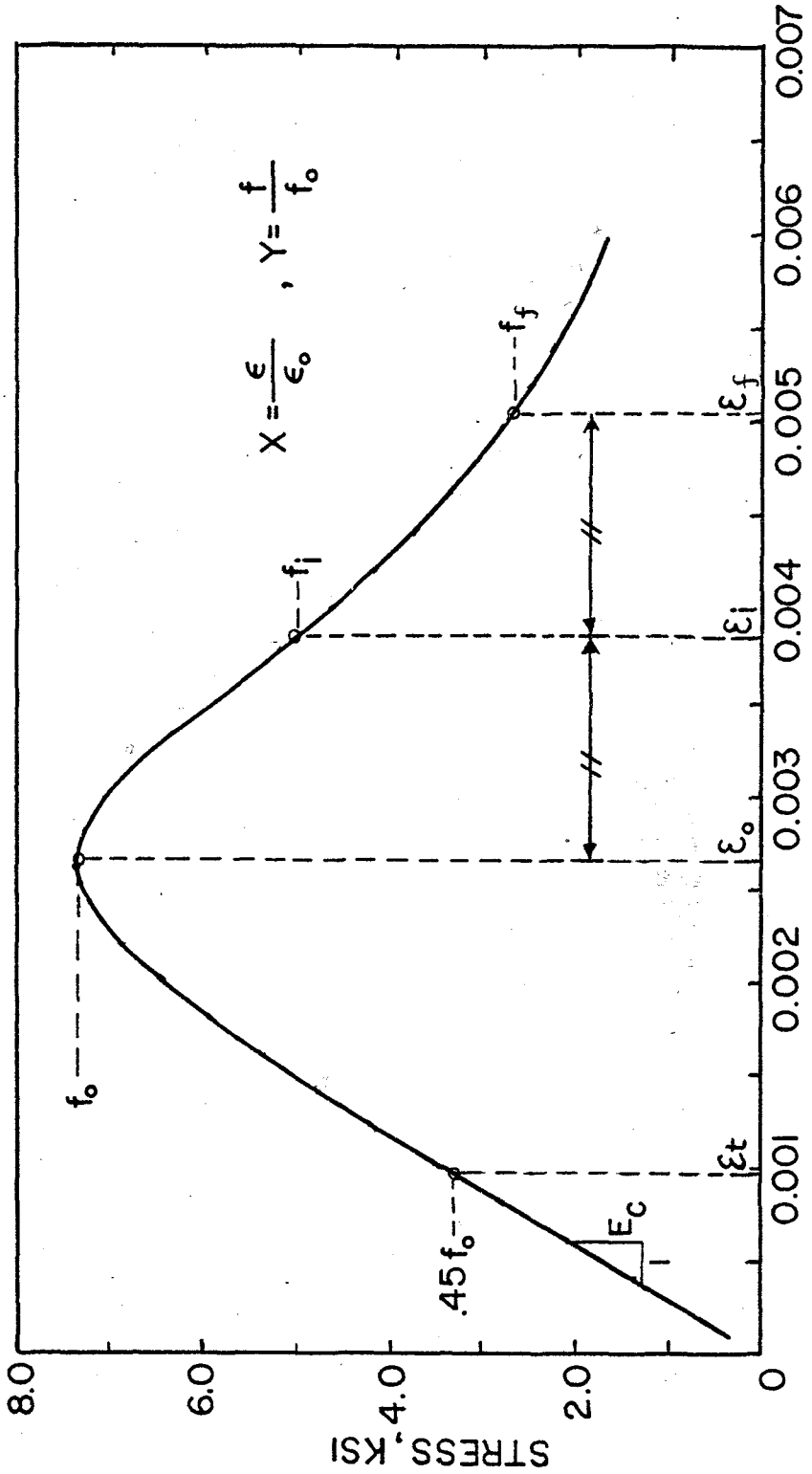

Fig. 2.1 Typical stress-strain curve.

BC3 - At the origin, the slope is equal to the initial modulus of elasticity:

$$\left.\frac{df}{d\varepsilon}\right|_{(0,0)} = E \qquad \text{or} \qquad \left.\frac{dY}{dX}\right|_{(0,0)} = A$$

BC4 - Curve passes through the point at $0.45f_o$:

$$\left(\varepsilon = \varepsilon_t = \frac{0.45f_o}{E} \quad , \quad f = f_t = 0.45f_o\right) \qquad \text{or}$$

$$\left(X = X_t = \frac{0.45}{A} \quad , \quad Y = Y_t = 0.45\right)$$

Note: E could be taken to be equal to E_c as per ACI.

C. Boundary conditions for descending portion.

BC1, BC2 } Same as for the ascending portion to ensure continuity at the peak point.

BC5 - Curve passes through the inflection point:

$$(\varepsilon = \varepsilon_i,\ f = f_i) \qquad \text{or} \qquad (X = X_i,\ Y = Y_i)$$

BC6 - Curve passes through a far point on the tail portion:

$$(\varepsilon = \varepsilon_f,\ f = f_f) \qquad \text{or} \qquad (X = X_f,\ Y = Y_f)$$

BC7 - Zero curvature at the inflection point:

$$\left.\frac{d^2f}{d\varepsilon^2}\right|_{(\varepsilon_i,f_i)} = 0 \qquad \text{or} \qquad \left.\frac{d^2Y}{dX^2}\right|_{(X_i,Y_i)} = 0$$

2.1.3 Categories of Stress-Strain Curves

As mentioned earlier, the expressions to be reviewed have been divided into four categories: exponential functions, polynomial functions,

fractional functions, and statistical distribution functions. For each expression, the original equation was transferred to the unit stress-strain system and the representative curve was plotted by using that system; then the boundary conditions were checked to see if they are satisfied.

A. Exponential functions.

1. Smith and Young [35] has proposed the following expression with two parameters: f_o and ε_o:

$$f = f_o(\varepsilon/\varepsilon_o)e^{(1 - \varepsilon/\varepsilon_o)} \tag{2.2}$$

which leads to the following dimensionless form (plotted in Fig. 2.2):

$$Y = Xe^{(1-X)} \tag{2.3}$$

and for which

$$\frac{dY}{dX} = (1-X)e^{(1-X)} \tag{2.4}$$

$$\frac{d^2Y}{dX^2} = (X-2)e^{(1-X)} \tag{2.5}$$

Checking boundary conditions:

BC1 $X = 1, Y = 1 \rightarrow 1 \equiv 1$ identity O.K.

BC2 $X = 1, \frac{dY}{dX} = 0 \rightarrow 0 \equiv 0$ identity O.K.

BC3 $X = 0, \frac{dY}{dX} = A \rightarrow A = e = 2.71828$ Constrained

Location of inflection point:

$$\frac{d^2Y}{dX^2} = 0 \rightarrow X_i = 2, \quad Y_i = \frac{2}{e} = 0.73576$$

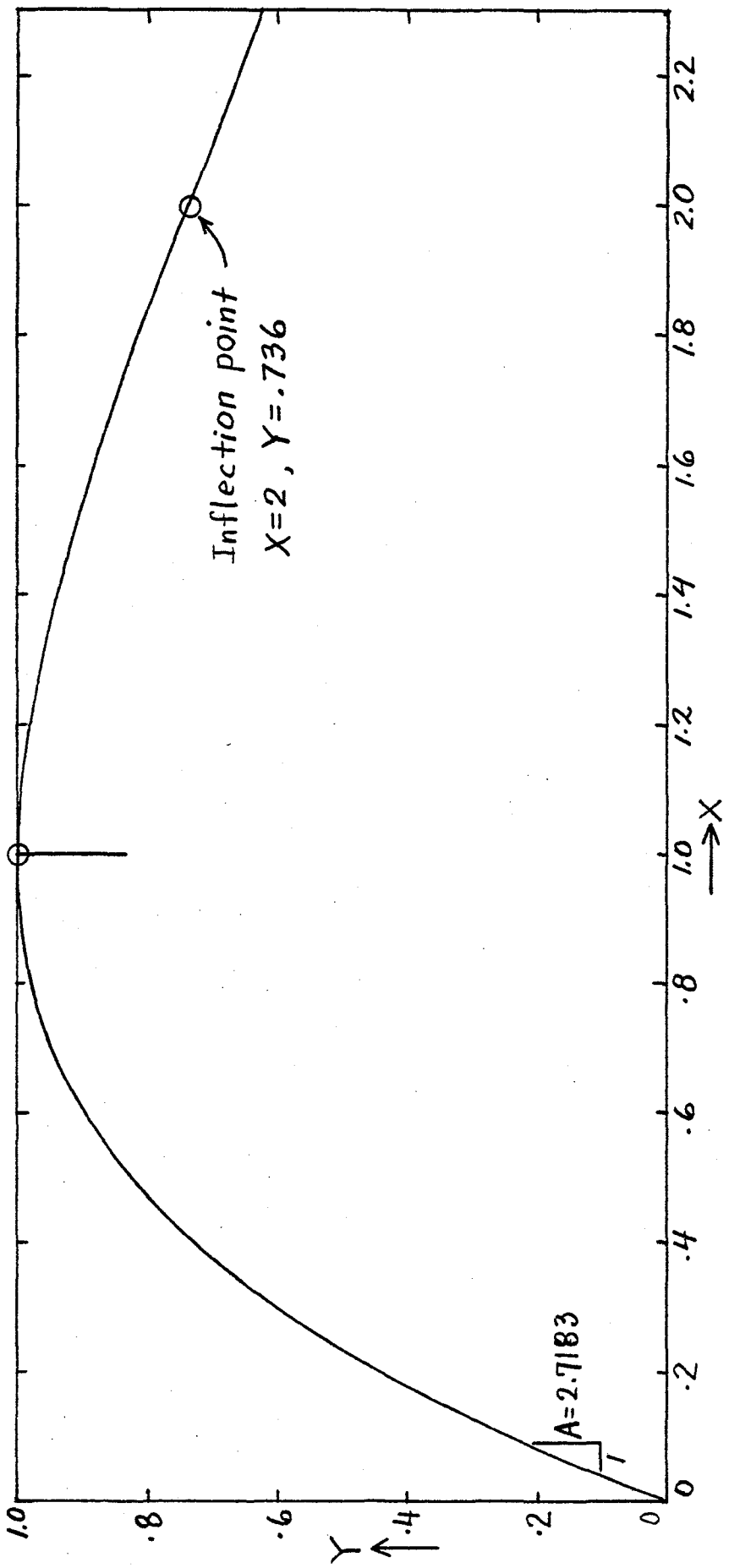

Fig. 2.2 Smith and Young's exponential function.

It can be seen that this expression has the following characteristics:

- It satisfies BC1 and BC2.
- It leads to an initial modulus fixed by A = 2.71828 for all values of f_o.
- It leads to an inflection point fixed by X = 2, Y = 0.73576 for all values of f_o.

B. Polynomial functions.

1. The European Concrete Committee has proposed the following expression (second-degree polynomial) with two parameters: E and ε_o

$$f = E\varepsilon\left(1 - \frac{\varepsilon}{2\varepsilon_o}\right) \tag{2.6}$$

which leads to the following dimensionless form (plotted in Fig. 2.3):

$$Y = A\left(X - \frac{1}{2}X^2\right) \tag{2.7}$$

and for which

$$\frac{dY}{dX} = A(1-X) \tag{2.8}$$

Checking boundary conditions:

BC1 $X = 1, Y = 1 \rightarrow A = 2$ Constrained

BC2 $X = 1, \frac{dY}{dX} = 0 \rightarrow 0 \equiv 0$ identity O.K.

BC3 $X = 0, \frac{dY}{dX} = A \rightarrow A \equiv A$ identity O.K.

It can be seen that this expression has the following characteristics:

- It satisfies BC1 and BC2
- It shows no inflection point
- It leads to an initial modulus fixed by A = 2 for all values of f_o

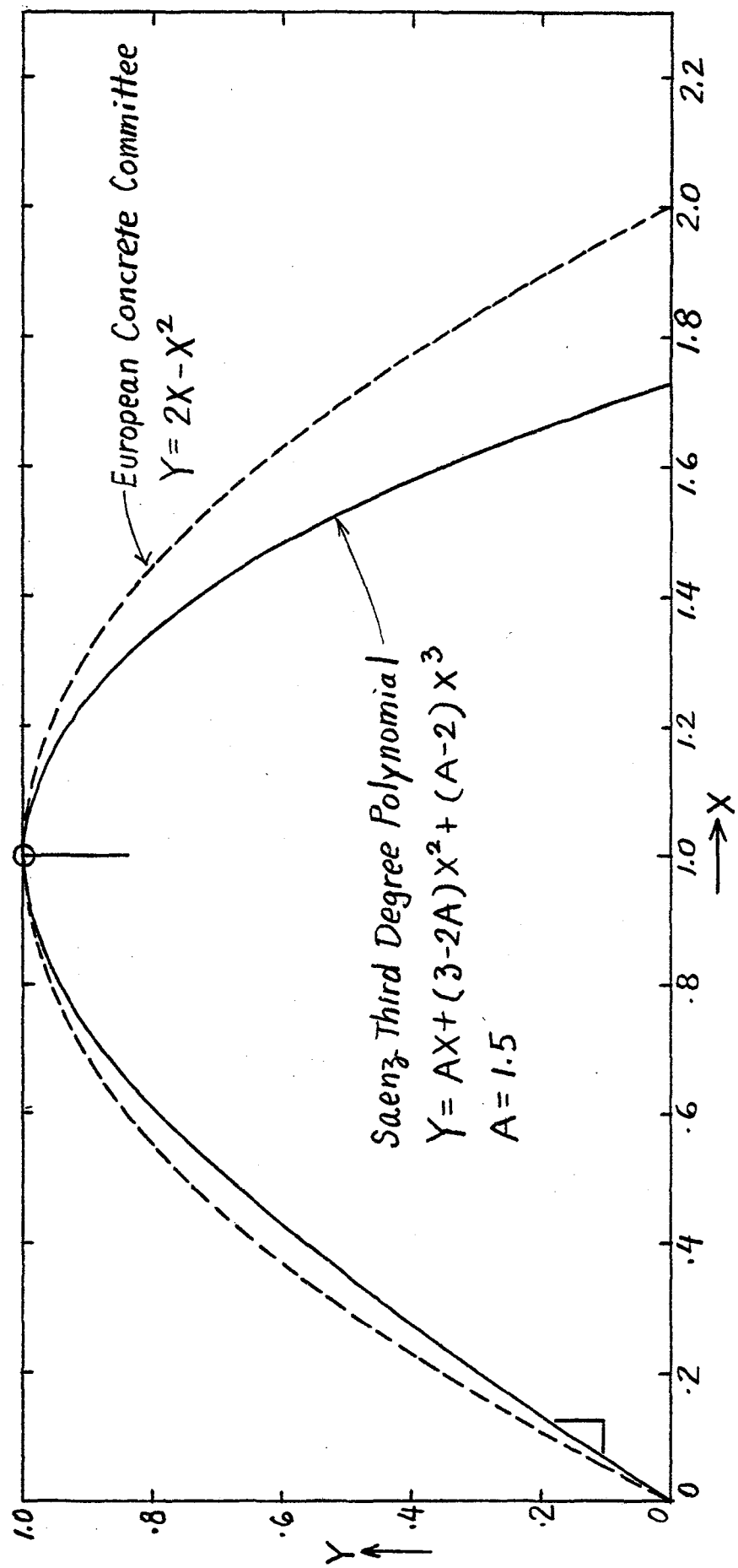

Fig. 2.3 Polynomial functions.

- It is symmetric with respect to the peak point (it may eventually lead to a negative stress for large strains).

2. Saenz [29] has proposed the following expression (third-degree polynomial) with three parameters: E, E_o, and ε_o

$$f = E\varepsilon \left\{ 1 + \left(\frac{3E_o}{E} - 2 \right) \left(\frac{\varepsilon}{\varepsilon_o} \right) + \left(1 - \frac{2E_o}{E} \right) \left(\frac{\varepsilon}{\varepsilon_o} \right)^2 \right\} \tag{2.9}$$

which lead to the following dimensionless form (plotted in Fig. 2.3):

$$Y = AX + (3-2A)X^2 + (A-2)X^3 \tag{2.10}$$

and for which

$$\frac{dY}{dX} = A + (6-4A)X + (3A-6)X^2 \tag{2.11}$$

$$\frac{d^2Y}{dX^2} = (6-4A) + (6A-12)X \tag{2.12}$$

Checking boundary conditions:

BC1 $X = 1,\ Y = 1 \rightarrow 1 \equiv 1$ identity O.K.

BC2 $X = 1,\ \frac{dY}{dX} = 0 \rightarrow 0 \equiv 0$ identity O.K.

BC3 $X = 0,\ \frac{dY}{dX} = A \rightarrow A \equiv A$ identity O.K.

Location of inflection point

$$\frac{d^2Y}{dX^2} = 0 \rightarrow X_i = \frac{3-2A}{6-3A}, \quad Y_i = \frac{(2A-3)(A^2+6A-18)}{27(A-2)^2} \tag{2.13}$$

It can be seen that this expression has the following characteristics:

- It satisfies BC1, BC2, and BC3

- It shows an inflection point fixed by $X_i = X_i(A)$, $Y_i = Y_i(A)$ which may not exist depending upon the value of A.
- It is asymmetric with respect to the inflection point, therefore it may lead to either negative stresses or very large stresses for large strains.

3. Sturman, Shah, and Winter [37] have proposed the following expressions with three parameters: A_1, A_2, and n

$$f = A_1\varepsilon + A_2\varepsilon^n \tag{2.14}$$

$$\frac{df}{d\varepsilon} = A_1 + A_2 n\varepsilon^{n-1} \tag{2.15}$$

$$\frac{d^2f}{d\varepsilon^2} = A_2 n(n-1)\varepsilon^{n-2} \tag{2.16}$$

which cannot be written in a dimensionless form before some conditions are satisfied.

Checking boundary conditions:

$$\left.\begin{array}{lll} \underline{\text{BC1}} & \varepsilon = \varepsilon_o\ ,\ f = f_o & \\ & \rightarrow & A_1 = \left(\frac{n}{n-1}\right)\frac{f_o}{\varepsilon_o} \\ \underline{\text{BC2}} & \varepsilon = \varepsilon_o\ ,\ \frac{df}{d\varepsilon} = 0 & A_2 = \frac{f_o}{(1-n)\varepsilon_o^n} \\ \underline{\text{BC3}} & \varepsilon = 0\ ,\ \frac{df}{d\varepsilon} = E \rightarrow & A_1 = E \end{array}\right\} \tag{2.17}$$

From Eqs. (2.17), it yields

$$A_1 = E\ ,\quad n = \frac{E}{E-E_o}\ ,\quad A_2 = \frac{f_o}{(1-n)\varepsilon_o^n} \tag{2.18}$$

After substituting Eqs. (2.17) into Eq. (2.14), it can be rewritten in the following dimensionless form (plotted in Fig. 2.4).

$$Y = \left(\frac{n}{n-1}\right)X - \left(\frac{1}{n-1}\right)X^n \tag{2.19}$$

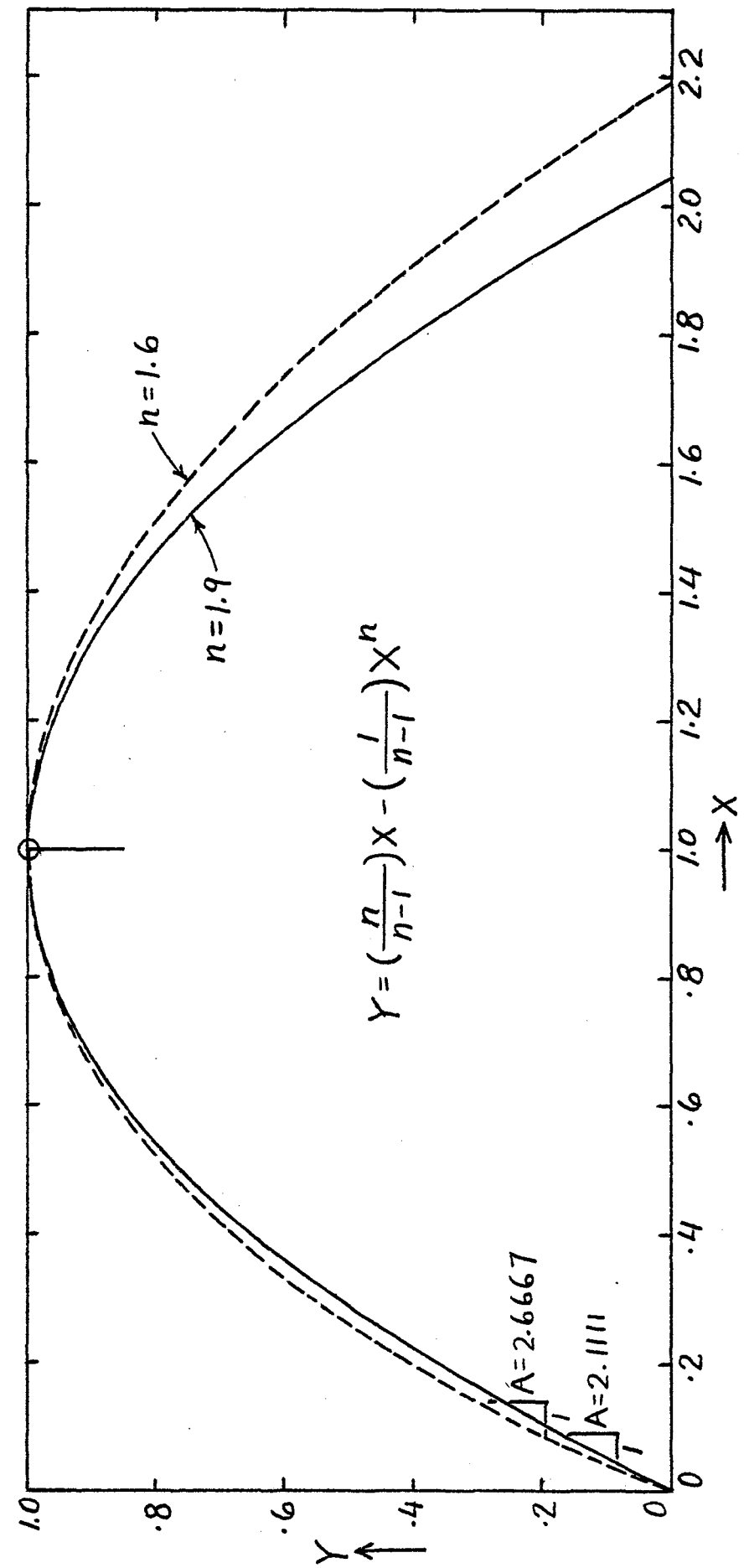

Fig. 2.4 Sturman, Shah and Winter's curve.

It can be seen that this expression has the following characteristics:

- It satisfies BC1, BC2, and BC3
- It shows an inflection point at the origin; there is no inflection point on the descending portion, its representative curve is concave downwards for all positive strains, therefore it leads to negative stresses for large strains.
- The value of n can be determined by a least square analysis which leads to: n = 1.9 for axial loading and n = 1.6 for eccentric loading.

C. Fractional functions.

1. Desay and Krishnan [12] have proposed the following expression with two parameters: E and ε_o

$$f = \frac{E\varepsilon}{1 + (\varepsilon/\varepsilon_o)^2} \tag{2.20}$$

which leads to the following dimensionless forms (plotted in Fig. 2.5):

$$Y = \frac{AX}{1+X^2} \tag{2.21}$$

and for which

$$\frac{dY}{dX} = \frac{A(1-X^2)}{(1+X^2)^2} \tag{2.22}$$

$$\frac{d^2Y}{dX^2} = \frac{A(-2X)(3-X^2)}{(1+X^2)^3} \tag{2.23}$$

Checking boundary conditions:

BC1 $X = 1,\ Y = 1 \rightarrow A = 2$ Constrained

BC2 $X = 1,\ \frac{dY}{dX} = 0 \rightarrow 0 \equiv 0$ identity O.K.

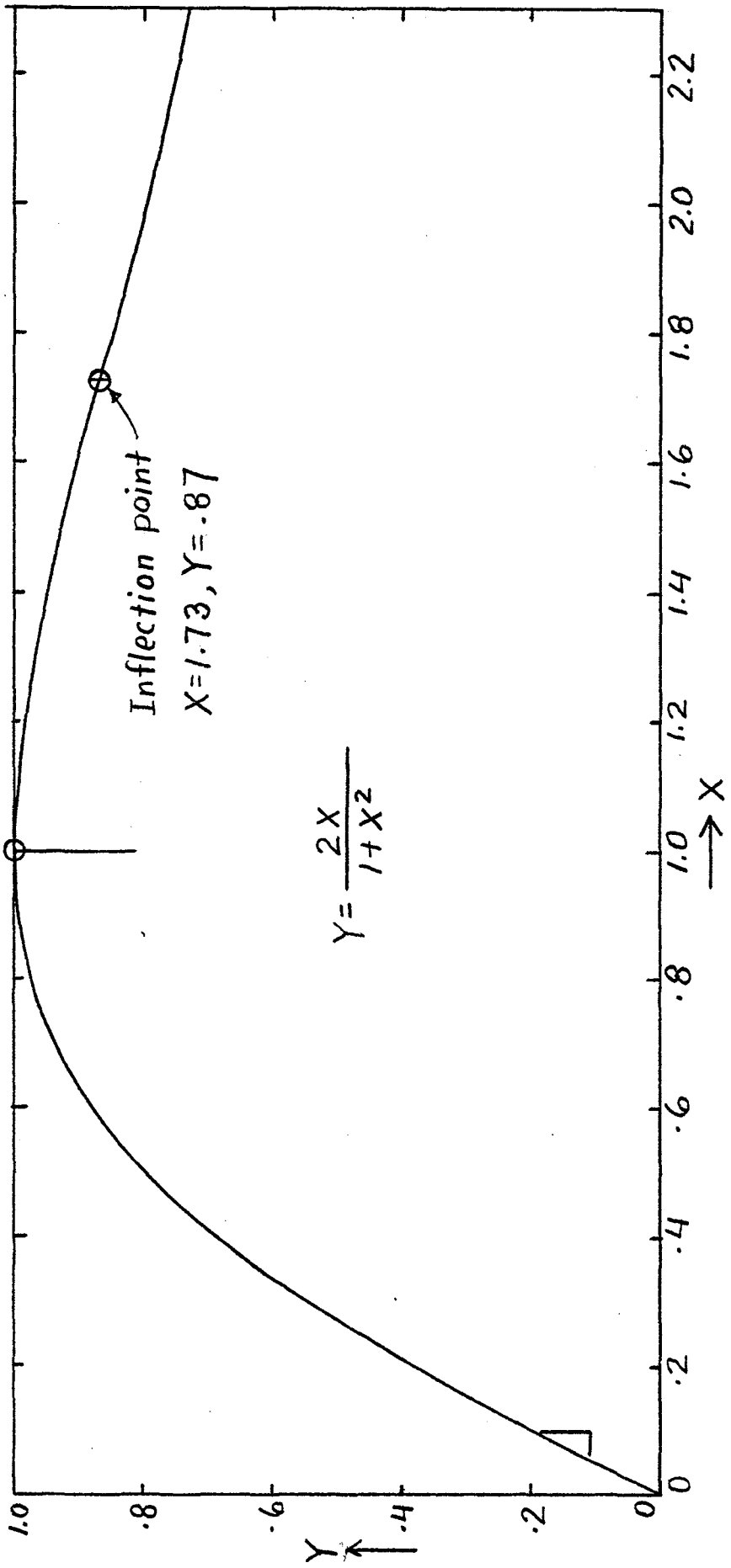

Fig. 2.5 Desay and Krishnan's curve.

BC3 $X = 0, \frac{dY}{dX} = A \rightarrow A = A$ identity O.K.

Location of inflection point

$$\frac{d^2Y}{dX^2} = 0 \rightarrow X_i = 1.73205 , \quad Y_i = 0.86603$$

It can be shown that this expression has the following characteristics:

- Its initial modulus is fixed by A = 2 for all values of f_o.
- Its inflection point is fixed by $X_i = 1.73205$, $Y_i = 0.86603$ for all value of f_o.
- Furthermore, it satisfies BC1 and BC2

2. Saenz [29] has proposed the following expression with three parameters: E, E_o, and ε_o

$$f = \frac{E\varepsilon}{1 + \left(\frac{E}{E_o} - 2\right)\left(\frac{\varepsilon}{\varepsilon_o}\right) + \left(\frac{\varepsilon}{\varepsilon_o}\right)^2} \tag{2.24}$$

which leads to the following dimensionless form (plotted in Fig. 2.6):

$$Y = \frac{AX}{1 + (A-2)X + X^2} \tag{2.25}$$

and for which

$$\frac{dY}{dX} = \frac{A(1-X^2)}{\{1 + (A-2)X + X^2\}^2} \tag{2.26}$$

$$\frac{d^2Y}{dX^2} = \frac{2A[X^3 - 3X - (A-2)]}{\{1 + (A-2)X + X^2\}^3} \tag{2.27}$$

Checking boundary conditions:

BC1 $X = 1, Y = 1 \rightarrow 1 \equiv 1$ identity O.K

BC2 $X = 1, \frac{dY}{dX} = 0 \rightarrow 0 \equiv 0$ identity O.K

BC3 $X = 0, \frac{dY}{dX} = A \rightarrow A \equiv A$ identity O.K

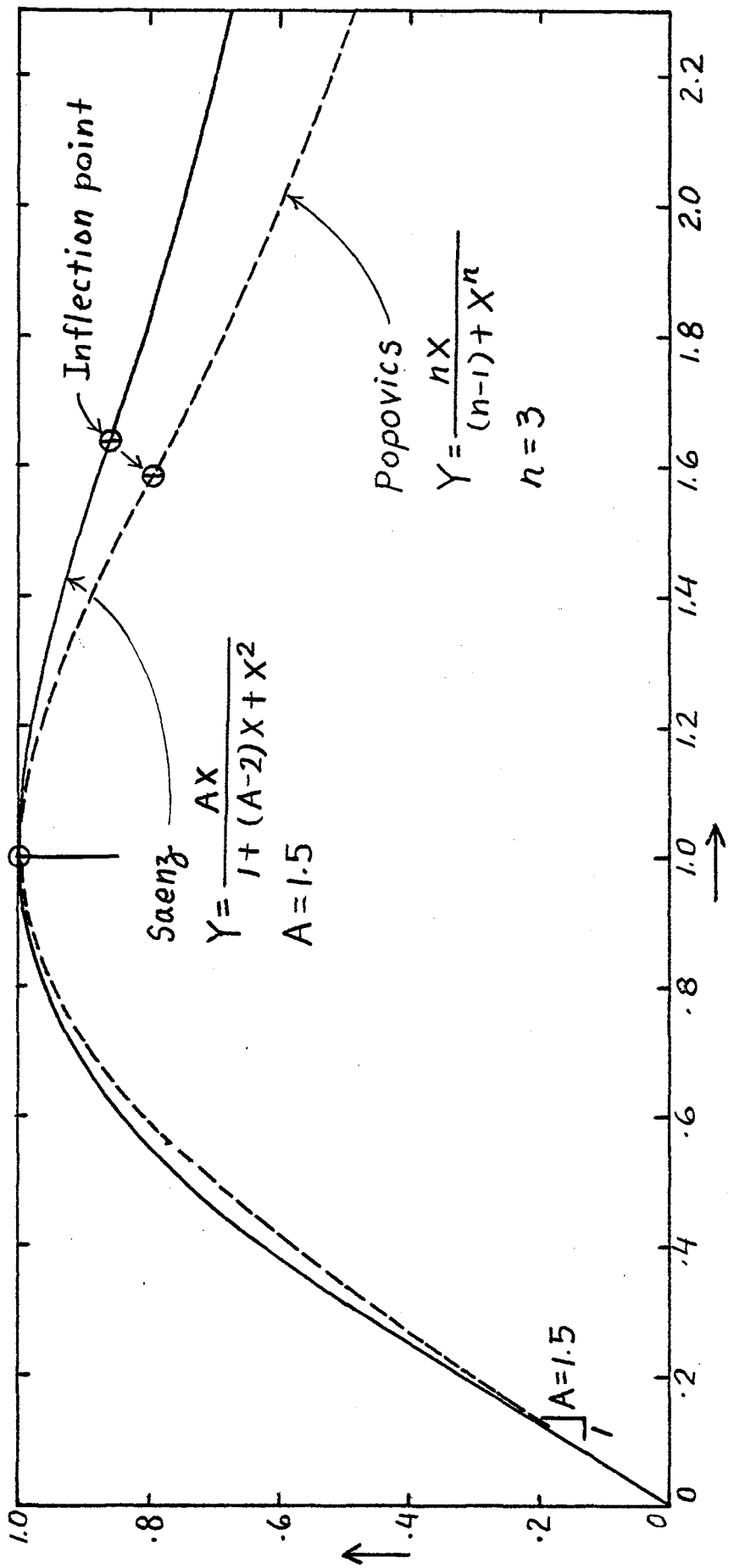

Fig. 2.6 Fractional functions by Popovics and Saenz.

Location of inflection point:

$$\frac{d^2Y}{dX^2} = 0 \quad \rightarrow \quad X^3 - 3X - (A-2) = 0 \tag{2.28}$$

for $A = 1.5$, $X_i = 1.64$, $Y_i = 0.86$

for $A = 2.0$, $X_i = 1.73$, $Y_i = 0.866$

It can be shown that this expression has the following characteristics:

- It satisfies BC1, BC2, and BC3.
- Its inflection point is fixed by a value of A determined from Eq. (2.28). This value of A simultaneously determines the initial modulus.

3. Popovics [26] has proposed the following expression with three parameters: f_o, ε_o, and n

$$\frac{f}{f_o} = \frac{\varepsilon}{\varepsilon_o} \frac{n}{(n-1) + (\varepsilon/\varepsilon_o)^n} \tag{2.29}$$

which leads to the following dimensionless form (plotted in Fig. 2.6):

$$Y = \frac{nX}{(n-1) + X^n} \tag{2.30}$$

and for which

$$\frac{dY}{dX} = \frac{n(n-1)(1-X^n)}{(n-1+X^n)^2} \tag{2.31}$$

$$\frac{d^2Y}{dX^2} = \frac{(nX^{n-1})(-n-1+X^n)}{(n-1+X^n)^3} \tag{2.32}$$

Checking boundary conditions:

BC1 $X = 1$, $Y = 1 \rightarrow 1 \equiv 1$ identity O.K.

BC2 $X = 1, \frac{dY}{dX} = 0 \rightarrow 0 \equiv 0$ identity O.K.

BC3 $X = 0, \frac{dY}{dX} = A \rightarrow A = \frac{n}{n-1} \rightarrow n = \frac{A}{A-1}$ (2.33)

Location of inflection point:

$$\frac{d^2Y}{dX^2} = 0 \rightarrow X_i = e^{\frac{\log(n+1)}{n}} \tag{2.34}$$

For example: $A = 1.5$, $n = 3$, $X_i = 1.587$, $Y_i = 0.794$

It can be shown that this expression has the following characteristics:

- It satisfies BC1, BC2, and BC3.
- Its inflection point is fixed by the value of n from Eq. (2.34) and the value of n is directly related to the initial modulus.

4. Saenz [29] has proposed the following expression with six parameters: f_o, ε_o, n, A, B, and C

$$\frac{f}{f_o} = \frac{A(\varepsilon/\varepsilon_o)}{1 + B(\varepsilon/\varepsilon_o) + C(\varepsilon/\varepsilon_o)^n} \tag{2.35}$$

which leads to the following dimensionless form (plotted in Fig. 2.7):

$$Y = \frac{AX}{1 + BX + CX^n} \tag{2.36}$$

and for which

$$\frac{dY}{dX} = \frac{A + (1-n)ACX^n}{(1+BX+CX^n)^2} \tag{2.37}$$

$$\frac{d^2Y}{dX^2} = \frac{-2AB - 2ACX^{n-1}\{n(n+1) + (n+1)(n-2)BX + n(1-n)CX^n\}}{(1+BX+CX^n)^3} \tag{2.38}$$

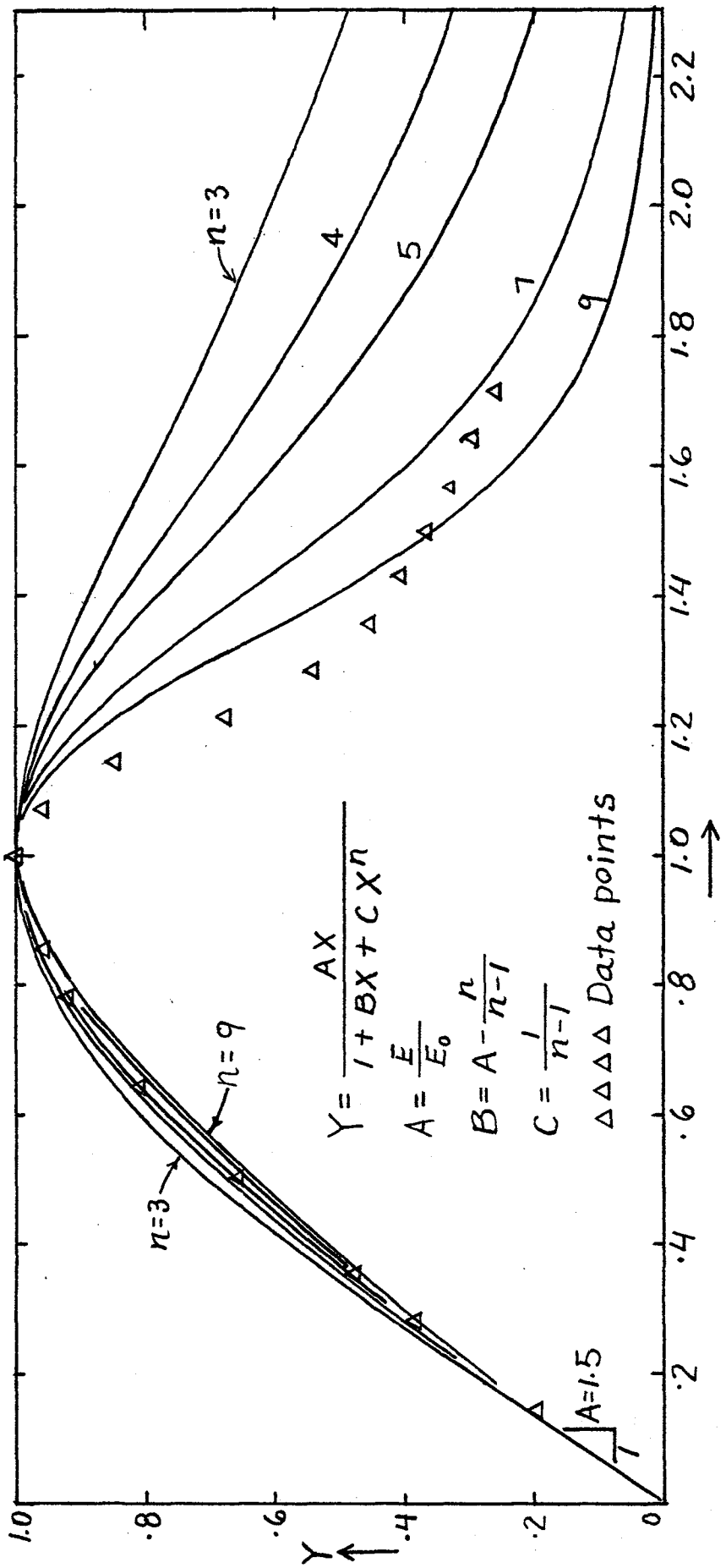

Fig. 2.7 Fractional function with six parameters by Saenz.

Checking boundary conditions:

$$\left.\begin{array}{ll} \underline{\text{BC1}} & X = 1,\ Y = 1 \\ \underline{\text{BC2}} & X = 1,\ \dfrac{dY}{dX} = 0 \end{array}\right\} \rightarrow \quad B = A - (n/n-1)\ , \quad C = 1/n-1 \qquad (2.39)$$

$\underline{\text{BC3}}$ $\quad X = 0,\ \dfrac{dY}{dX} = A \quad \rightarrow \quad A \equiv A$ identity O.K.

$\underline{\text{BC5}}$ $\quad X = Xd,\ Y = Yd$ (curve through arbitrary point on decending portion)

$$\rightarrow \quad Y_d = \frac{AX_d}{\left(1 + \left(A - \dfrac{n}{n-1}\right) X_d + \left(\dfrac{1}{n-1}\right)\left(X_d\right)^n\right.} \qquad (2.40)$$

The solution of Eq. (2.40) can be obtained by trial and error. For example $A = 1.5$, $X_d = 1.4$, $Y_d = 0.65$, $n = 7.021$.

It can be shown that this expression has the following characteristics:

- It satisfies BC1, BC2, BC3, and BC5.
- The value of n can only be obtained by solving Eq. (2.40) by trial and error.
- Its inflection point is fixed by Eq. (2.38) for all values of f_o.
- Salse [30] proposed an expression which can be derived from Saenz's equation after satisfying boundary condition.

2.1.4 Summary

(1) Most of the reviewed expressions have one or more of the following shortcomings: a) they are based only on the properties of the ascending portion [12,26,29,34,35]; b) they contain constants which can be changed to fit a given curve, but these constants are not based on any particular physical characteristic of the stress-strain curve [30,37]; and c) the descending portion does not

always have an inflection point or it does not show a long tail which is characteristic of concrete behavior [29].

(2) Generally, polynomial equations of order three or above exhibit an upward tail which cannot characterize actual concrete behavior.

(3) Saenz's expression has one parameter, n, which must be determined to fit the descending portion; however this parameter also affects the ascending portion. Since the descending portion is very important, one prescribed boundary condition does not seem sufficient. This expression by Saenz seems to be the best so far, however n has to be determined arbitrarily. More important, it was not possible to fit his expression to our experimental data (Fig. 2.7 shows one of our curves). This is because changing n changes both ascending and descending portions in such a way that the stiffer the ascending portion, the flatter the descending portion, which appears contrary to the observation.

(4) It seems desirable that an equation be developed which will accommodate independently the ascending and the descending portions of the curve, i.e., independent parameters will be used to describe each portion. Furthermore, for the descending portion, there should be at least two boundary conditions prescribed.

2.2 PROPOSED ANALYTIC STRESS-STRAIN CURVE OF CONCRETE

In a preliminary investigation, several forms of equations were tried to describe the stress-strain curve of concrete. For example, a gamma distribution function was used; this distribution function leads

to a family of exponential equations, one of which is the same as the equation proposed by Smith and Young [34]. It has the advantage however to allow for a variety of choices in the shape of the representative curve as can be seen in Fig 2.8; a six-degree polynomial function satisfying six boundary conditions was also used, but the intrinsic property of oscillation of polynomials between prescribed points leads to an unrealistic description of the σ-ε curve of concrete in the descending portion as shown in Fig. 2.9. Fractional functions were also tried, but generally the poles of these functions, if any, reduce the denominator to zero which creates a discontinuity at that pole (Fig. 2.10); therefore, such functions cannot be used to describe the entire stress-strain curve of concrete without special precautions; for example, they can be made to represent one portion of the curve only as shown in the following section.

After an extensive search for a suitable expression, the following fractional stress-strain relations were found to be most acceptable:

$$Y = \frac{AX + BX^2}{1 + CX + DX^2} \tag{2.41}$$

and

$$Y = \frac{AX + BX^2}{1 + CX + DX^2 + HX^3} \tag{2.42}$$

where A, B, C, D, and H = constants to be determined.

The accuracy of these expressions in representing the stress-strain curve was much improved when two separate sets of values of constants were used for the ascending and the descending portions. For the ascending portion, Eq. (2.41) was used and the values of the four constants were evaluated from the four boundary conditions described in Section 1.1.2. For the descending portion, Eqs. (2.41) and (2.42) were used and the

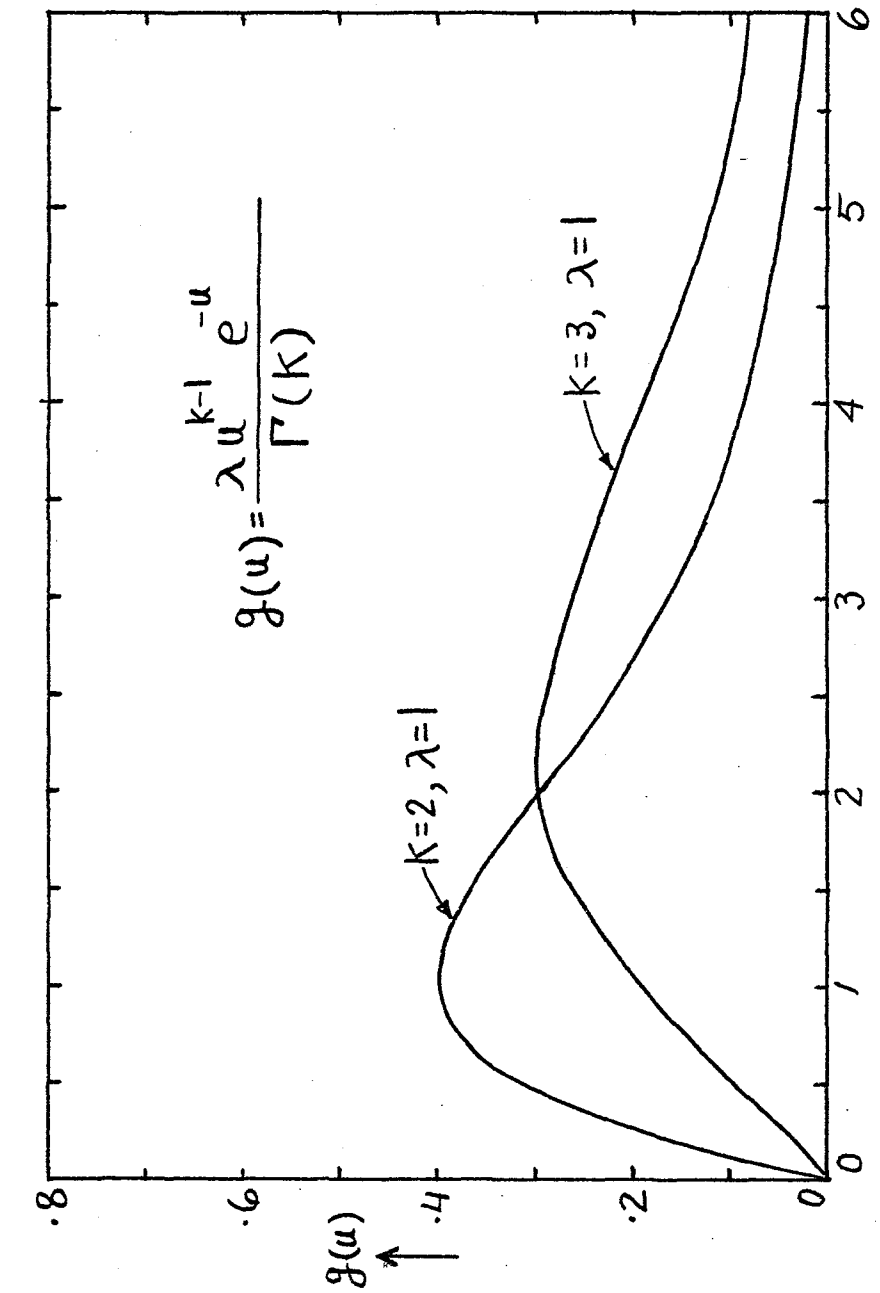

Fig. 2.8 Gamma distribution function.

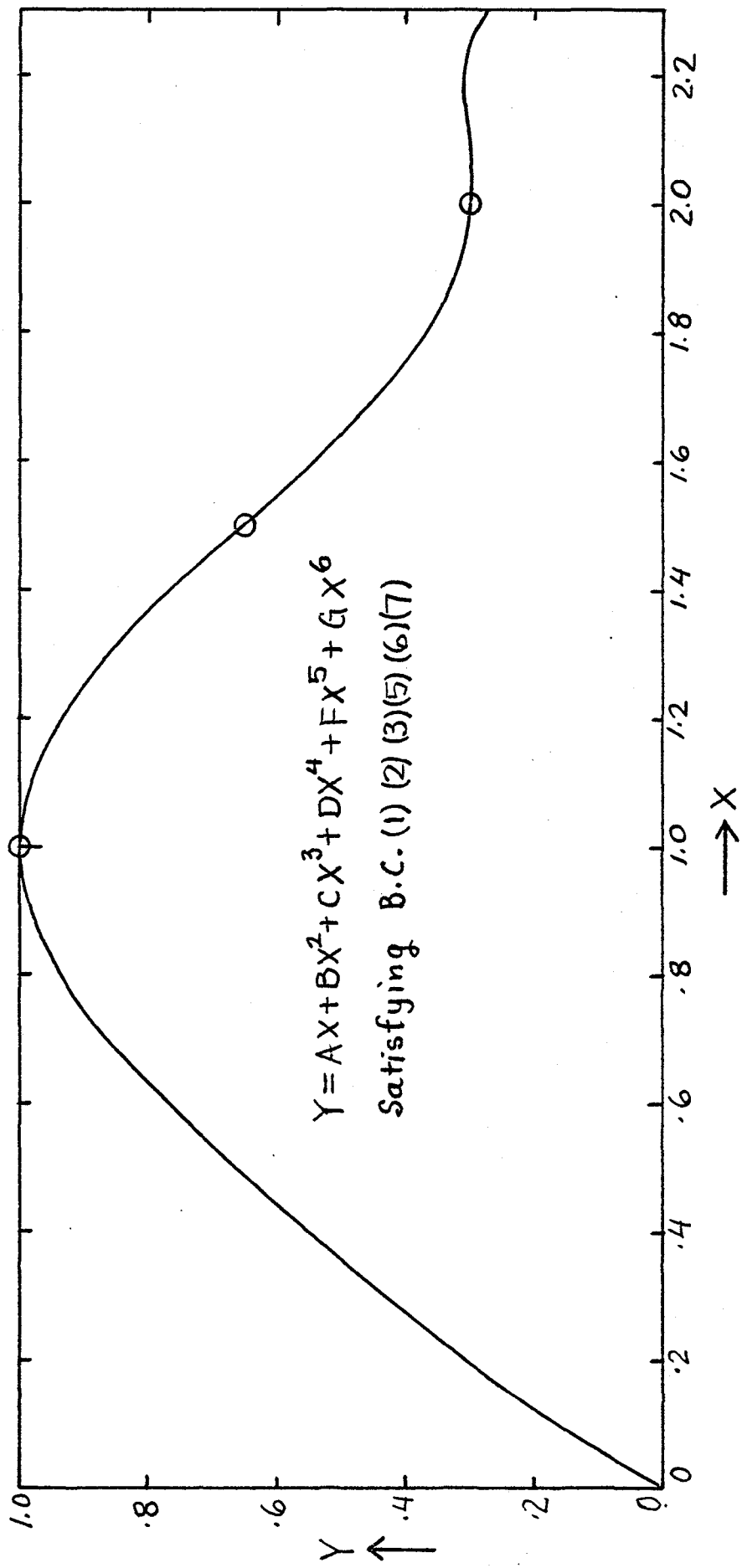

Fig. 2.9 Sixth degree polynomial,

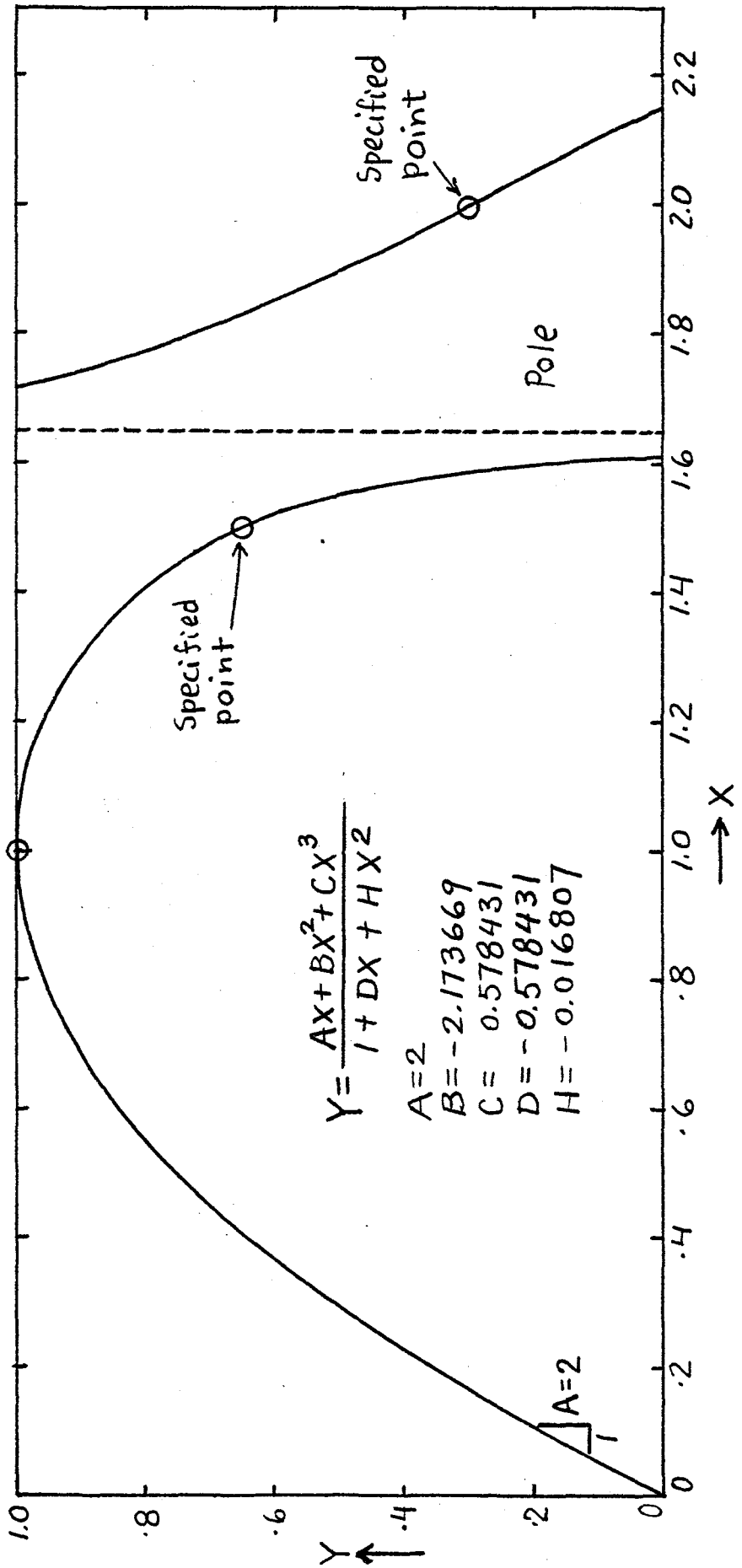

Fig. 2.10 Fractional function with a pole.

values of the constants were evaluated from the boundary conditions described in Section 2.1.2. After comparing the two expression Eqs. (2.41) was finally selected because it was simpler and led to about the same accuracy as explained in Section

2.2.1 Determination of the Four Constants for the Ascending Portion

The equation and its derivative are expressed as follows:

$$Y = \frac{AX+BX^2}{1+CX+DX^2} \tag{2.41}$$

$$\frac{dY}{dX} = \frac{(A+2BX)(1+CX+DX^2) - (AX+BX^2)(C+2DX)}{(1+CX+DX^2)^2} \tag{2.43}$$

Checking boundary condition:

$$\text{BC1} \quad X = 1,\ Y = 1 \rightarrow A+B = 1+C+D \tag{2.44}$$

$$\text{BC2} \quad X = 1,\ \frac{dY}{dX} = 0 \rightarrow (A+2B)(1+C+D) = (A+B)(C+2D) \tag{2.45}$$

$$\text{BC3} \quad X = 0,\ \frac{dY}{dX} = A \rightarrow A \equiv A \quad \text{identity}$$

$$\text{BC4} \quad X = X_t,\ Y = Y_t \rightarrow Y_t = \frac{AX_t + BX_t^2}{1+CX_t + DX_t^2} \tag{2.46}$$

From Eqs. (2.44) and (2.45)

$$\left.\begin{aligned} B &= D - 1 \\ C &= A - 2 \end{aligned}\right\} \tag{2.47}$$

From Eqs. (2.47) and (2.46)

$$D = \left(\frac{-A}{X_t}\right) + \left[\frac{Y_t - 2X_tY_t + X_t^2}{X_t^2(1-Y_t)}\right] \tag{2.48}$$

where $X_t = \frac{0.45}{A}$, $Y_t = 0.45$

Some typical ascending portions, represented by this expression, are shown in Fig. 2.11.

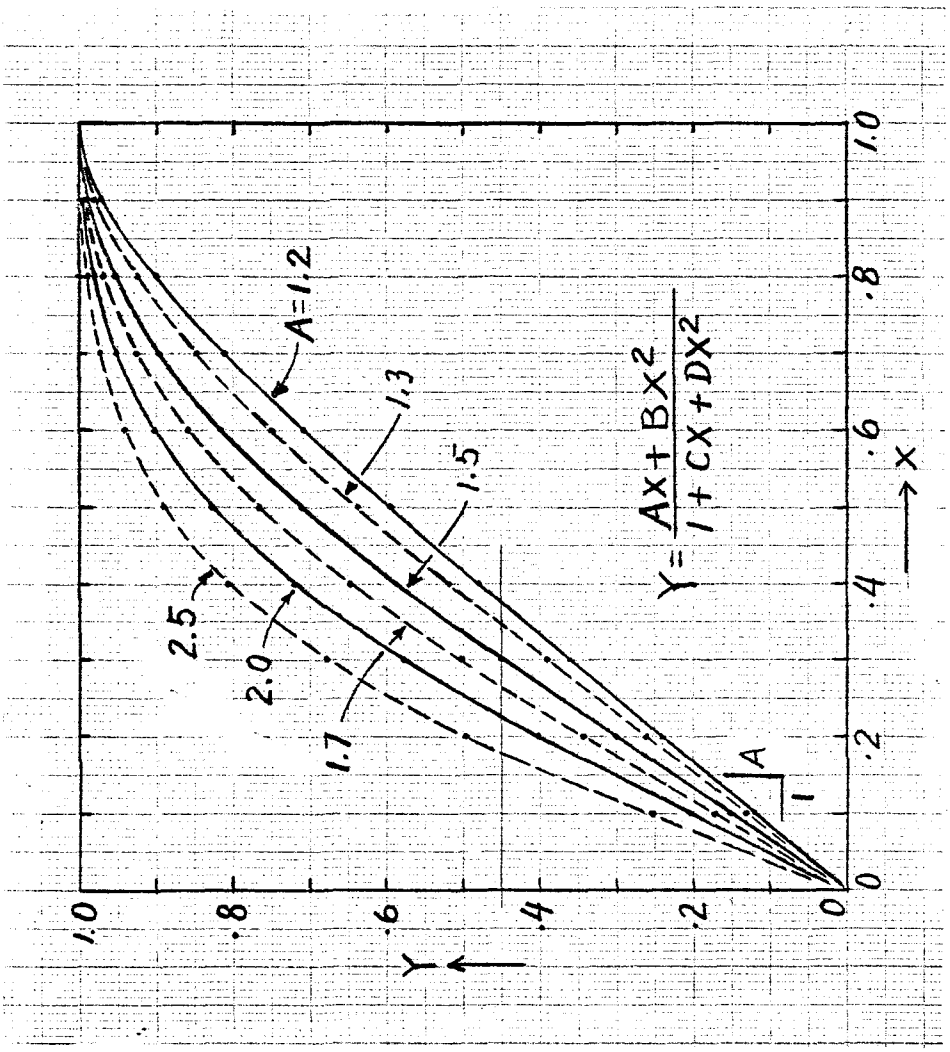

Fig. 2.11 Typical ascending portion.

2.2.2 Determination of the Constants for the Descending Portion

Three alternates for representing the descending portion are discussed in the following sections:

1. Alternate 1 - The curve is constrained to pass through two points, namely the inflection point and a far point on the tail portion of the curve, but the zero curvature condition is not prescribed at the inflection point. This approach is the one finally selected in this investigation for the analysis of experimental results. The equation and its derivatives are expressed as follows:

$$Y = \frac{AX+BX^2}{1+CX+DX^2} \tag{2.41}$$

$$\frac{dY}{dX} = \frac{(A+2BX)(1+CX+DX^2) - (AX+BX^2)(C+2DX)}{(1+CX+DX^2)^2}$$

or

$$\frac{dY}{dX} = \frac{A+2BX + (BC-AD)X^2}{(1+CX+DX^2)^2} \tag{2.43}$$

$$\frac{d^2Y}{dX^2} = \frac{-2\{(CA-B) + (BC+3AD)X + 4BCX^2 + D(BC-AD)X^3\}}{(1+CX+DX^2)^3} \tag{2.49}$$

Checking boundary conditions:

$$\left.\begin{array}{ll} \text{BC1} & X = 1,\ Y = 1 \\ \text{BC2} & X = 1,\ \dfrac{dY}{dX} = 0 \end{array}\right\} \rightarrow \left.\begin{array}{l} B = D - 1 \\ C = A - 2 \end{array}\right\} \tag{2.47}$$

$$\left.\begin{array}{ll} \text{BC5} & X = X_i,\ Y = Y_i \\ \text{BC6} & X = X_f,\ Y = Y_f \end{array}\right\} \rightarrow \left.\begin{array}{l} A = \dfrac{c_1b_2 - c_2b_1}{a_1b_2 - a_2b_1} \\ D = \dfrac{a_1c_2 - a_2c_1}{a_1b_2 - a_2b_1} \end{array}\right\} \tag{2.50}$$

where

$$\left.\begin{aligned} a_1 &= X_i - X_i Y_i, \quad b_1 = X_i^2 - X_i^2 Y_i, \quad c_1 = Y_i - 2X_i Y_i + X_i^2 \\ a_2 &= X_f - X_f Y_f, \quad b_1 = X_f^2 - X_f^2 Y_f, \quad c_2 = Y_f - 2X_f Y_f + X_f^2 \end{aligned}\right\} \tag{2.51}$$

(X_i, Y_i) = inflection point

(X_f, Y_f) = arbitrary far point on tail portion (chosen in this study such that $X_f - X_i = X_i - X_o \equiv X_i - 1$)

Two typical descending portions represented by this expression are shown in Fig. 2.12 for an arbitrary far point for which $X_f = 2$.

2. Alternate 2 - The curve is constrained to pass through the inflection point with zero curvature prescribed at that point. The equation and its derivatives are the same as that for Alternate 1.

Checking boundary conditions:

$$\left.\begin{aligned} &\text{BC1} \quad X = 1, \; Y = 1 \\ &\text{BC2} \quad X = 1, \; \frac{dY}{dX} = 0 \end{aligned}\right\} \rightarrow \left.\begin{aligned} B &= D - 1 \\ C &= A - 2 \end{aligned}\right\} \tag{2.47}$$

$$\left.\begin{aligned} &\text{BC5} \quad X = X_i, \; Y = Y_i \rightarrow A = qD + P \\ &\text{where} \quad q = X_i, \quad P = \frac{Y_i - 2X_i Y_i + X_i^2}{X_i - X_i Y_i} \end{aligned}\right\} \tag{2.52}$$

$$\text{BC7} \quad X = X_i \; \frac{d^2Y}{dX^2} = 0 \rightarrow \tag{2.53}$$

$$-A^2 + AD(X_i^3 - 3X_i) + D^2(2X_i^3 - 3X_i^2) + A(2) + D(-2X_i^3 + 3X_i^2 + 1) - 1 = 0$$

Substituting Eq. (2.47) into Eq. (2.53) leads to a quadratic equation for D as follows:

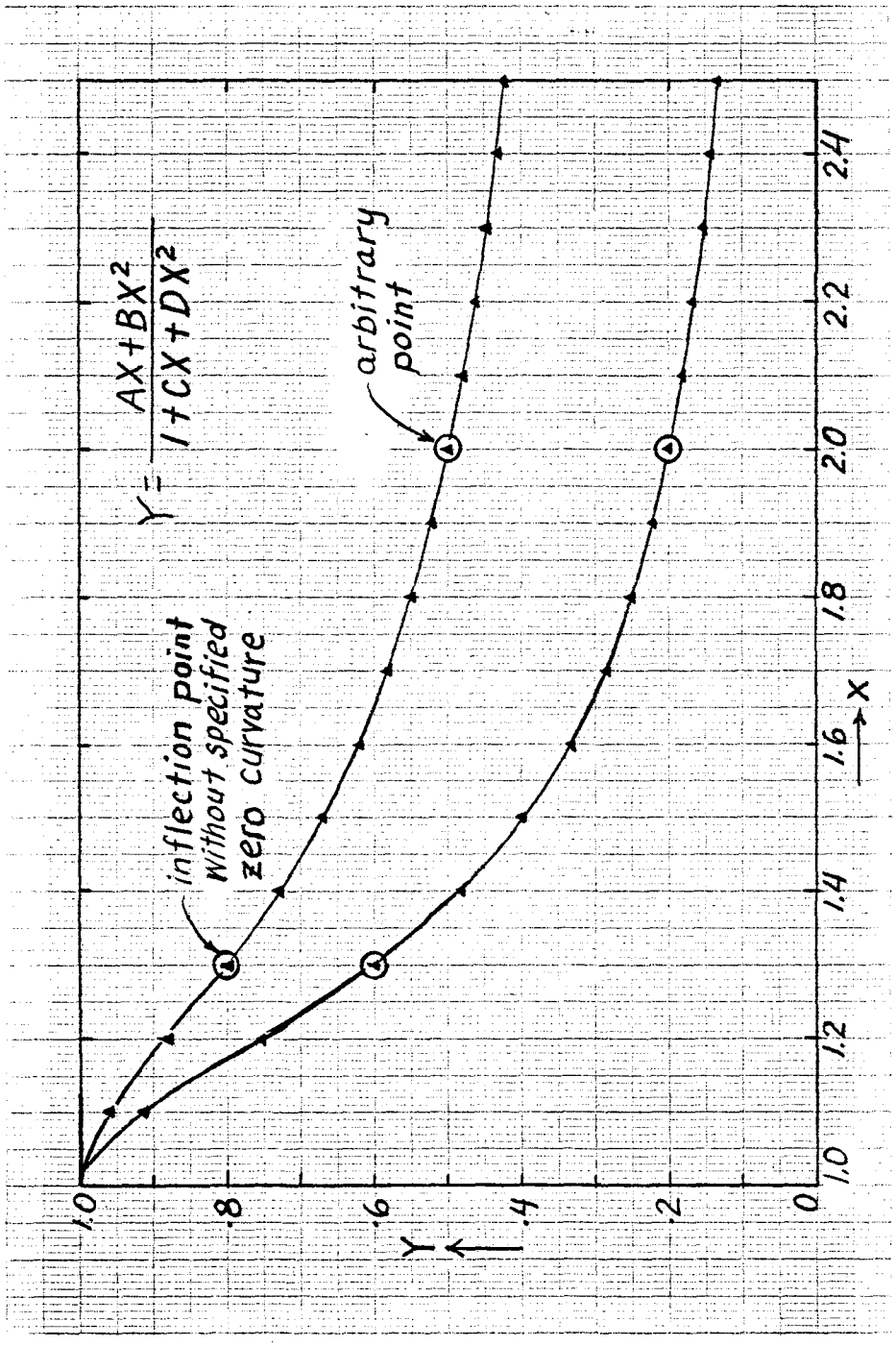

Fig. 2.12 Descending portion through two points.

$$mD^2 + nD + \ell = 0 \tag{2.54}$$

and the two solutions are

$$D = \frac{-n + \sqrt{n^2 - 4m\ell}}{2m} \quad \text{first solution}$$

or (2.55)

$$D = \frac{-n - \sqrt{n^2 - 4m\ell}}{2m} \quad \text{second solution}$$

where

$$m = 2X_i^3 - 3X_i^3 - q^2 + q(X_i^3 - 3X_i)$$

$$n = -2X_i^3 + 3X_i^2 + 1 + 2q + p(X_i^3 - 3X_i) - 2pq$$

$$\ell = -1 + 2p - p^2 \tag{2.56}$$

$$q = -X_i$$

$$p = \frac{Y_i - 2X_iY_i + X_i^2}{X_i - X_iY_i}$$

The first solution of the quadratic equation for D yields a lower bound solution, and is selected in this expression. The curves for both solutions are shown in Fig. 2.13. It can be seen that these two solutions are very close.

3. Alternate 3 - The curve is constrained to pass through two points, namely the inflection point and a far point on the tail portion the curve, and the zero curvature condition is prescribed at the inflection point. Its equation has one more constant as compared to Alternate 1 or 2. The equation and its derivatives are expressed as follows:

$$Y = \frac{AX+BX^2}{1+CX+DX^2+HX^3} \tag{2.42}$$

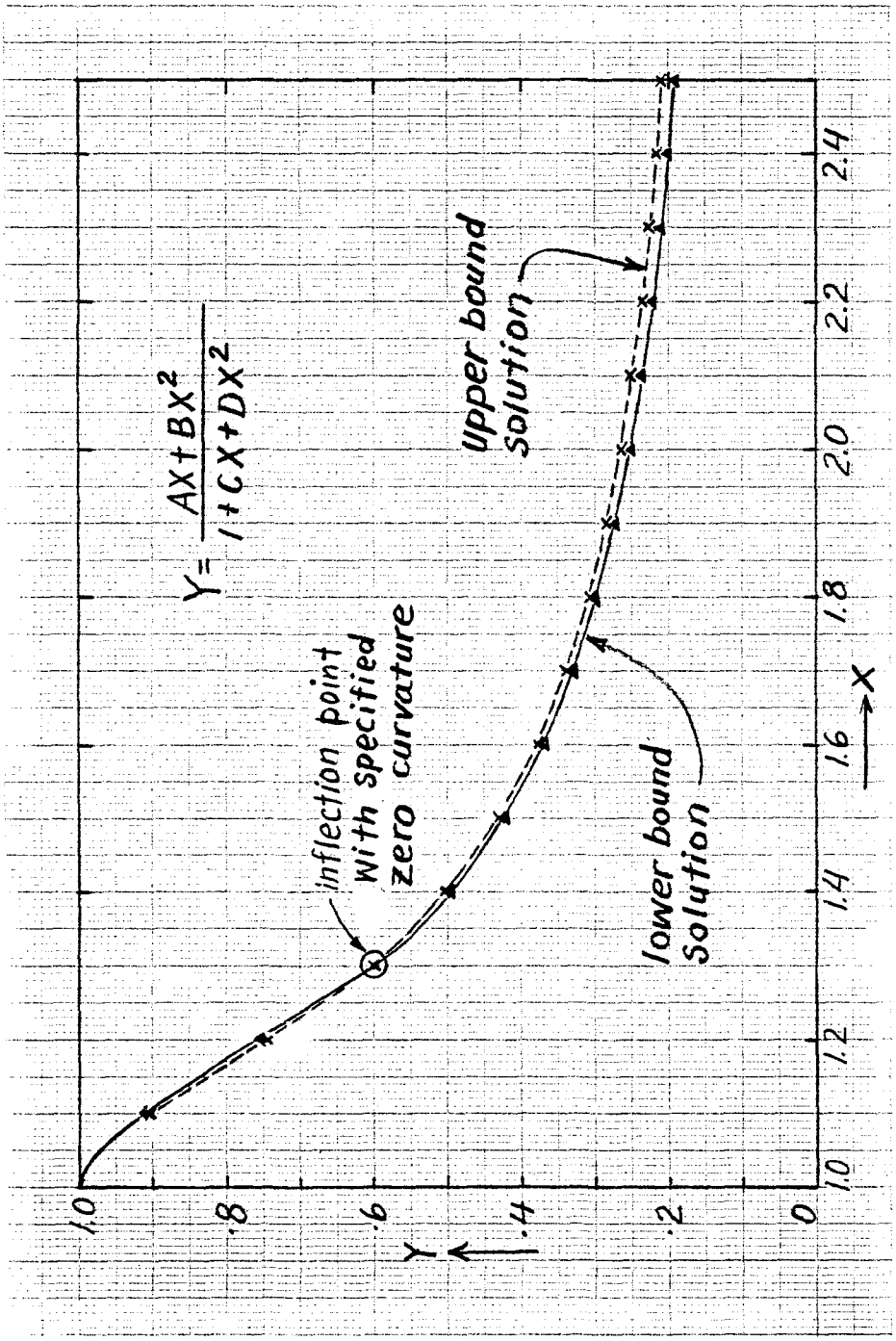

Fig. 2.13 Descending portion through inflection point.

$$\frac{dY}{dX} = \frac{(A+2BX)(1+CX+DX^2+HX^3) - (AX+BX^2)(C+2DX+3HX^2)}{(1+CX+DX^2+HX^3)}$$

or

$$\frac{dY}{dX} = \frac{A+2BX+(BC-AD)X^2 - 2AHX^3 - BHX^4}{(1+CX+DX^2+HX^3)^2} \tag{2.57}$$

the equation for satisfying zero curvature, i.e. $\frac{d^2Y}{dX^2} = 0$, is

$$\{B+(BC-AD)X - 3AHX^2 - 2BHX^3\}(1+CX+DX^2+HX^3) - (C+2DX+3HX^2)\{A+2BX+(BC-AD)X^2-2AHX^3-BHX^4\} = 0 \tag{2.58}$$

Checking boundary conditions:

BC1 $X = 1,\ Y = 1$

BC2 $X = 1,\ \frac{dY}{dX} = 0$

BC5 $X = X_i,\ Y = Y_i$

BC6 $X = X_f,\ Y = Y_f$

BC7 $X = X_i,\ \frac{d^2Y}{dX^2} = 0$

By using boundary conditions, the results obtained are summarized as follows:

$$\begin{aligned} A &= t + \nu H \\ B &= m + nH \\ C &= f + gH \\ D &= p + qH \end{aligned} \tag{2.59}$$

and

$$aH^3 + bH^2 + cH + d = 0 \tag{2.60}$$

where

$$t = - X_i p + r_i , \qquad \nu = s_i - X_i q$$

$$m = p - 1 , \qquad n = q + 2$$

$$f = t - 2 , \qquad g = \nu + 1$$

$$p = \frac{r_i - r_f}{X_i - X_f} , \qquad q = \frac{s_i - s_f}{X_i - X_f}$$

$$r_i = \frac{X_i^2 - 2X_iY_i + Y_i}{X_i - X_iY_i} , \qquad r_f = \frac{X_f^2 - 2X_fY_f + Y_f}{X_f - X_fY_f}$$

$$s_i = \frac{Y_i + X_i^2Y_i - 2X_i}{1 - Y_i} , \qquad s_f = \frac{Y_f + X_f^2Y_f - 2X_f}{1 - Y_f}$$

$$a = X_i^3(-ngq+\nu q^2+2\nu g)+X_i^4(2ng)+X_i^5(-3\nu-3ng+3\nu q)+X_i^6(-2n+6\nu)+X_i^7(3n)$$

$$b = X_i^3(-mgq-fnq-png+2pq\nu+tq^2+2tg+2\nu f)+2X^4(mg+nf)$$
$$+3X_i^5(-t-mg-nf+tq+\nu p)+X_i^6(-2m+6t)+3X_i^7m-(\nu g)$$
$$-3X\nu q-3X_i^2(\nu+nq)-X_i^3(n+3\nu)-6nX_i^4$$

$$c = X_i^3(-mfg-fpn-mpg+2pqt+\nu p^2+2tf)+2mfX_i^4+3X_i^5(-mf+tp)$$
$$-(tg+\nu f)-3X_i(tq+\nu p)-3X_i^2(t+mq+np)-X_i^3(m+3t)-6mX_i^4+n$$

$$d = X_i^3(-mfp+tp^2)-tf-3tpX_i-3mpX_i^2+m$$

The solutions of the cubic Eq. (2.60) yields three roots for H; in most cases, one real root and two imaginary roots are obtained; if however three real roots are encountered one of them should be selected to better fit the data. Typical curves are shown in Fig. 2.14. It can be seen that when three real roots are obtained, the representative curves are very close to each other.

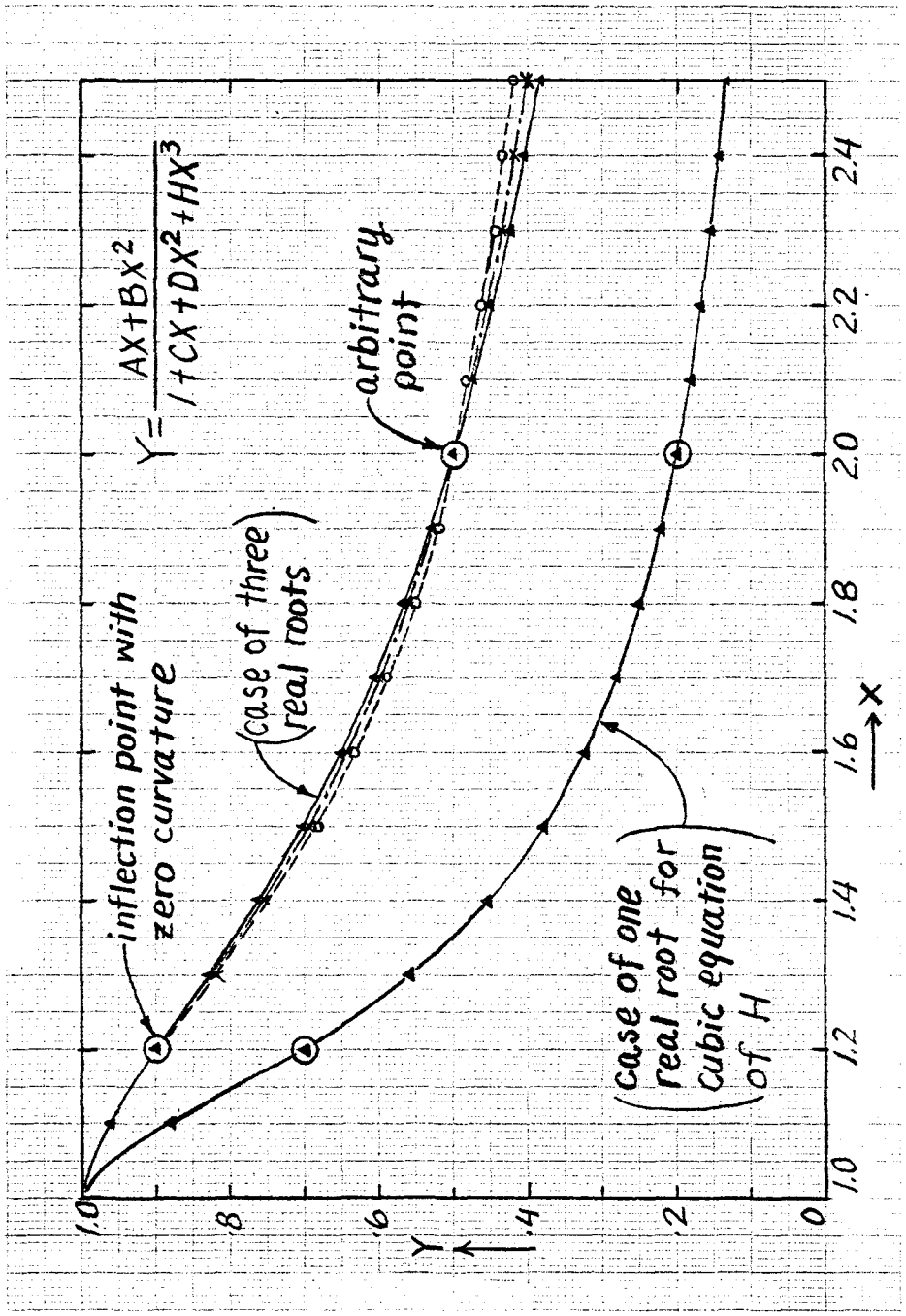

Fig. 2.14 Descending portion through inflection and arbitrary points.

2.2.3 Comparison of the Three Alternatives Used to Describe the Descending Portion of the Curve

Three different approaches were described in the preceding section to determine the parameters of the descending portion. The first two required four parameters while the third one required five parameters. In order to select the most appropriate alternative, the three generated curves were compared to actual stress-strain relationships. In Figs. 2.15a and 2.15b, Alternates 1 and 2 were compared, and it can be seen that Alternate 1 leads to a better fit. Also Alternates 1 and 3 are very comparable and lead to about the same fit. Therefore, Alternate 1 was finally selected for the following reasons:

(1) It is superior to Alternate 2.

(2) The result in fitting the data is as good as Alternate 3.

(3) The number of parameters is less than that of Alternate 3.

(4) It has the same form as the equation representing the ascending portion.

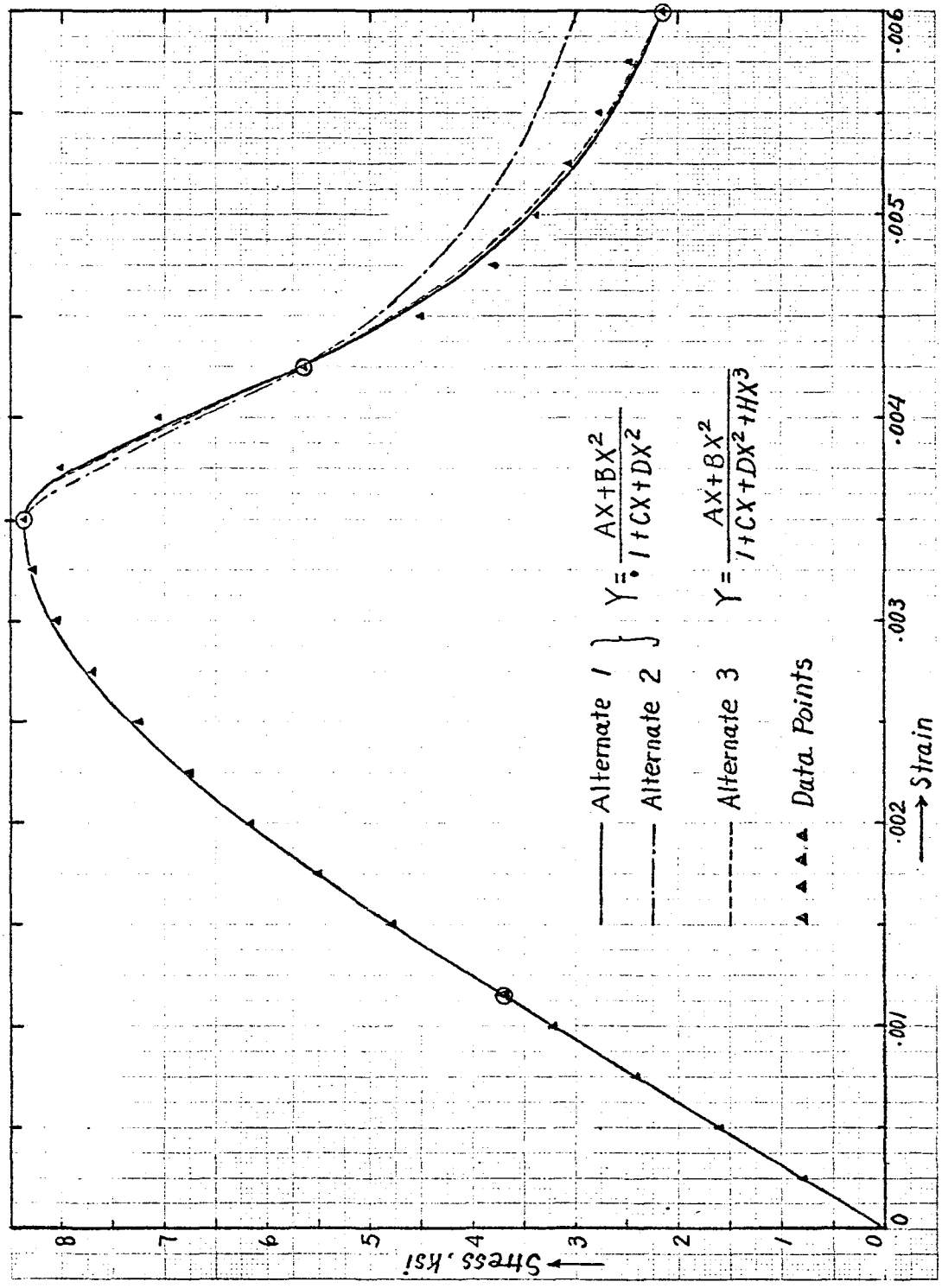

Fig. 2.15a Comparison between alternates 1, 2 and 3 for descending portion.

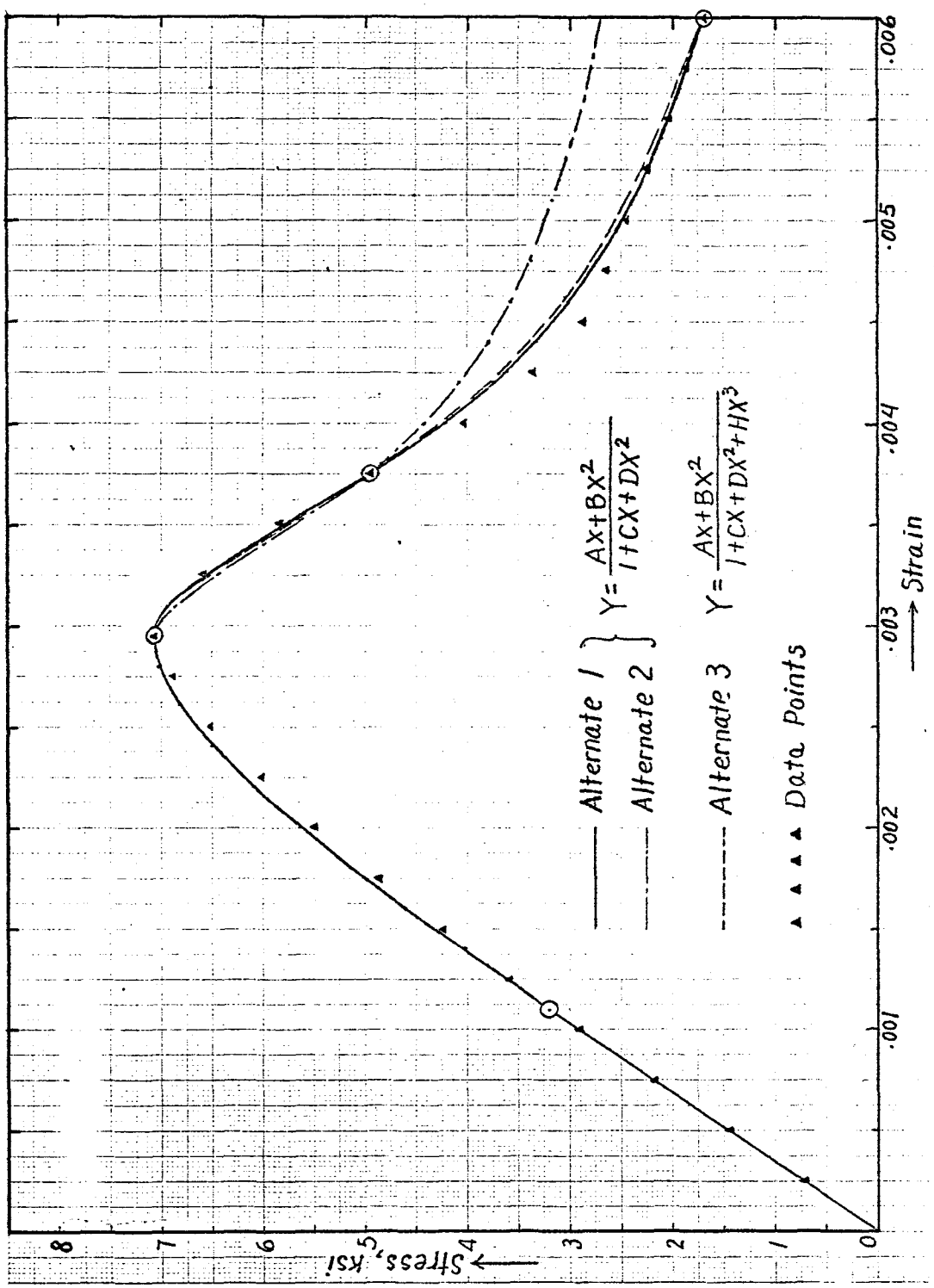

Fig. 2.15b Comparison between alternates 1, 2 and 3 for descending portion.

CHAPTER III

STRESS-STRAIN CURVES OF REINFORCING STEEL

3.1 INTRODUCTION

Reinforcing steels, used in reinforced concrete structures, will be classified here into two categories as regard to their σ-ε curves: the first with a definite yield plateau, and the other with no definite yield point. For the first category, the appearance of the σ-ε curve over its entire range up to failure will be described as follows:

(a) an initial elastic portion up to the yield point,

(b) a yield plateau up to the strain-hardening portion,

(c) a strain-hardening portion.

For the second category, the σ-ε curve consists essentially of two portions:

(a) an approximately linear portion up to the proportional limit which cannot generally be identified except as specified in codes of practice such as 0.2% offset,

(b) a strain-hardening portion.

A third category of steel, which will not be described here, consists of prestressing steels for which the σ-ε curve shows three portions:

(a) an initial elastic portion up to the proportional limit,

(b) a curvilinear portion up to about 95% of ultimate strength,

(c) an asymptotic straight-line portion up to ultimate.

The main purpose of this chapter is to find a suitable analytic expression for the σ-ε curves of the first two groups of reinforcing steels described above. A discussion of the available expression is also included.

3.2 STRESS-STRAIN CURVE OF MILD STEEL WITH DEFINITE YIELD PLATEAU

Various expressions to represent the σ-ε curve of this category of steel have been proposed. The ACI (318-71) proposed a design curve consisting of only two portions: an initial elastic portion and a yield plateau, assuming that in the design the steel does not reach the strain-hardening stage. Heimdahl and Bianchini [18] and Bresler [4] both proposed a curve consisting of three portions: an initial elastic portion, a yield plateau, and a strain-hardening portion represented by a straight-line up to ultimate. Their curves are shown in Fig. 3.1 for A615 Grade 60 steel.

Sargin [32] proposed a curve consisting of three portions: an initial elastic portion, a yield plateau, and a strain-hardening portion up to failure which was represented by a parabola. This expression is more representative of the real behavior of this category of steels, and will be discussed in detail next.

3.2.1 Sargin's σ-ε Curve for Mild Steel with Definite Yield Plateau

The proposed expression has five parameters: E_s, E_{sh}, f_y, f_{su}, and ε_{sh}, which are identified in Fig. 3.2 where a typical σ-ε curve is plotted. The three portions of the curve are given by the following equations:

$$f_s = E_s \varepsilon_s \quad \text{for} \quad 0 < \varepsilon_s \leq \varepsilon_y \tag{3.1}$$

$$f_s = f_y \quad \text{for} \quad \varepsilon_y < \varepsilon_s \leq \varepsilon_{sh} \tag{3.2}$$

$$f_s = f_y + E_{sh}(\varepsilon_s - \varepsilon_{sh}) \left[1 - \frac{E_{sh}(\varepsilon_s - \varepsilon_{sh})}{4(f_{su} - f_y)}\right] \quad \text{for } \varepsilon_s > \varepsilon_{sh} \tag{3.3}$$

The first derivative of Eq. (3.3) leads to:

$$\frac{df_s}{d\varepsilon_s} = E_{sh} - \frac{E_{sh}^2}{2(f_{su} - f_y)} (\varepsilon_s - \varepsilon_{sh}) \tag{3.4}$$

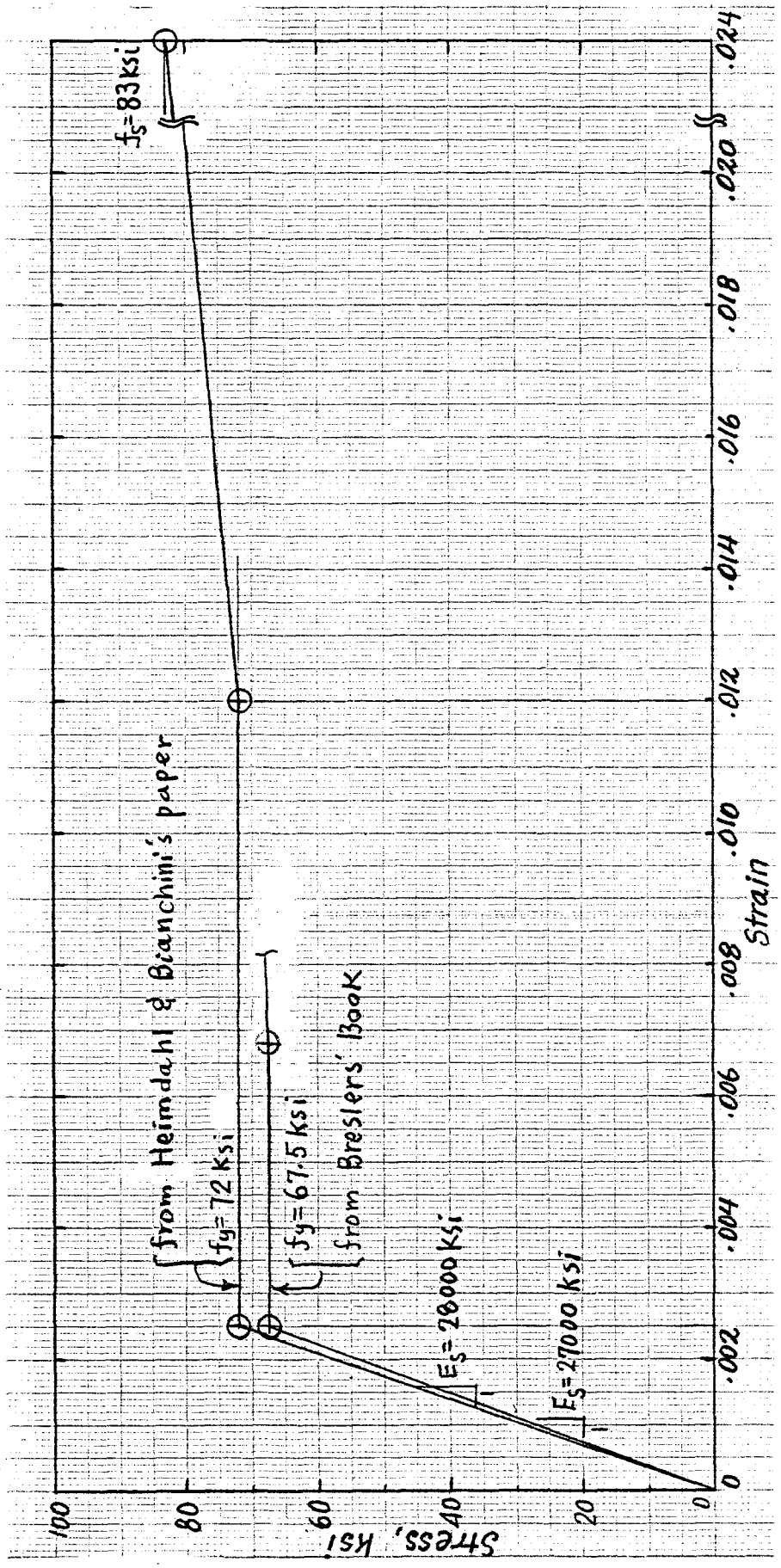

Fig. 3.1 Bresler and Heimdahl's stress-strain curve for grade 60 steel.

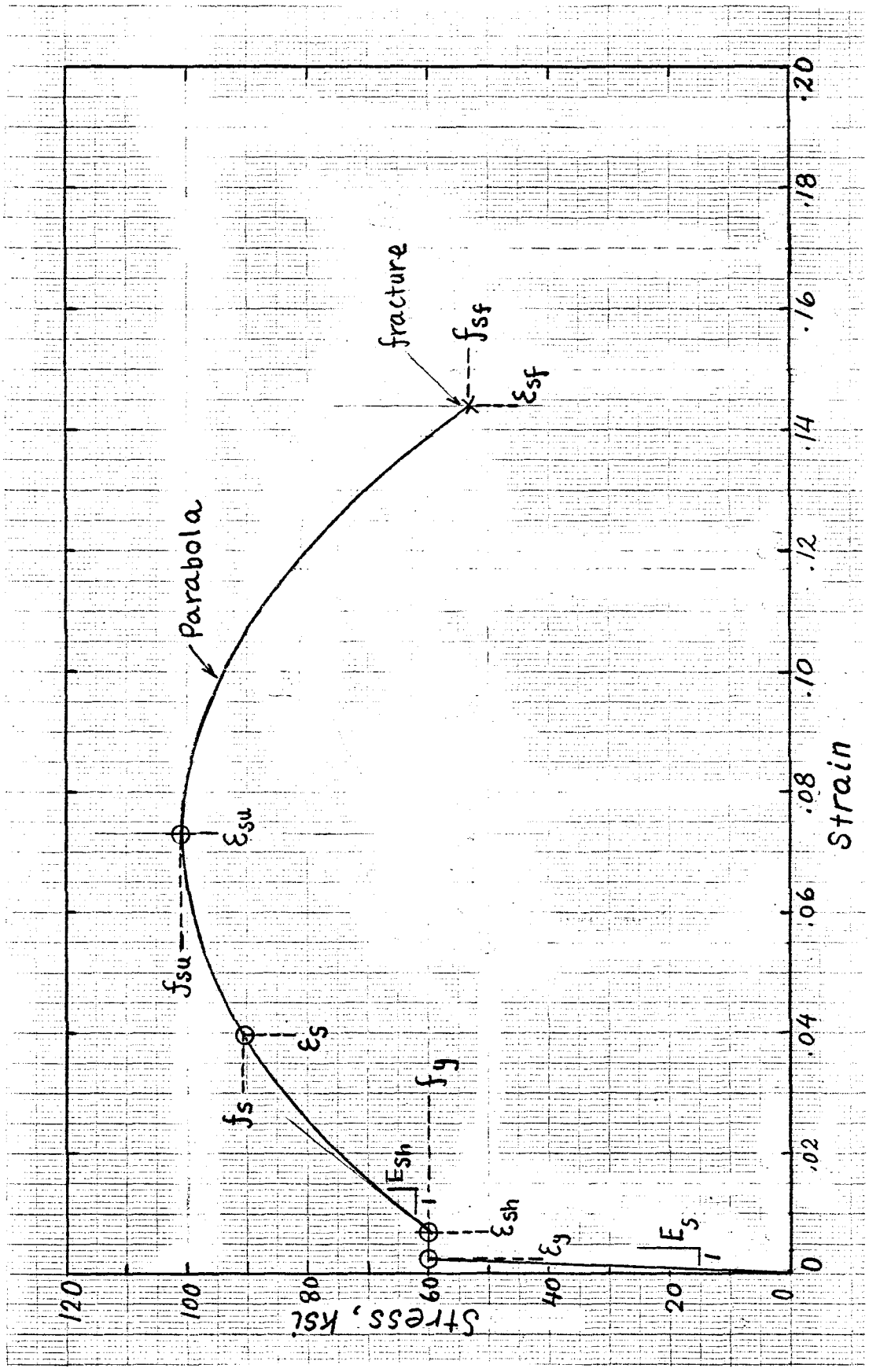

Fig. 3.2 Sargin's stress-strain curve for grade 60 steel.

and the strain at the peak point is given by equating Eq. (3.4) to zero, which leads to:

$$\varepsilon_{su} = \varepsilon_{sh} + \frac{2(f_{su} - f_y)}{E_{sh}} \tag{3.5}$$

It can be seen that this expression has the following characteristics:

(a) the strain-hardening portion is represented by a parabola which is symmetric to the peak point,

(b) the value of strain at the peak point is determined by Eq. (3.5).

3.2.2 Proposed Expression to Represent the Strain-Hardening Portion for Mild Steel with Definite Yield Plateau

The parabolic curve for representing the strain-hardening portion proposed by Sargin [32] does not seem, as will be shown latter, to properly fit the observed experimental data after the peak load. Although we are seldom interested in reinforcing bars in the strain beyond the peak, and although the ultimate strength of concrete sections always occur at a tensile strain of steel less than the strain at the peak, it may be important to know more exactly their behavior up to the exact failure point; the failure point is a characteristic point of the complete stress-strain curve of steel and can be obtained in a tensile test of reinforcing bars; therefore, the following expression is proposed when such need arises

$$Y = \frac{AX + BX^2}{1 + CX + DX^2} \tag{3.6}$$

Its derivative is given by:

$$\frac{dY}{dX} = \frac{(A + 2BX)(1 + CX + DX^2) - (AX + BX^2)(C + 2DX)}{(1 + CX + DX^2)^2} \tag{3.7}$$

where

$$\left.\begin{aligned} X &= \frac{\varepsilon_s - \varepsilon_{sh}}{\varepsilon_o} \\ Y &= \frac{f_s - f_y}{f_o} \end{aligned}\right\} \qquad (3.8)$$

f_s and ε_s = stress and strain in general (Fig. 3.3)

f_{su} and ε_{su} = peak stress and corresponding strain

f_{sf} and ε_{sf} = stress and strain at failure point

ε_{sh} and ε_{su} = strains at onset of strain-hardening and peak point

E_s = Young's modulus

E_{sh} = strain-hardening modulus

A,B,C,D = constants

$\varepsilon_o = \varepsilon_{su} - \varepsilon_{sh}$

$f_o = f_{su} - f_y$

$E_o = f_o/\varepsilon_o$

$A = E_{sh}/E_o$

The curve is constrained to satisfy the following four boundary conditions.

BC1 Curve passes through the peak point

$(\varepsilon_s = \varepsilon_{su},\ f_s = f_{su})$ or $(X = X_o \equiv 1,\ Y = Y_o \equiv 1)$

BC2 At the peak point, the slope equals zero

$\left(\varepsilon_s = \varepsilon_{su},\ \frac{df_s}{d\varepsilon_s} = 0\right)$ or $\left(X = X_o \equiv 1,\ \frac{dY}{dX} = 0\right)$

BC3 At the onset of strain-hardening, the slope is equal to the strain-hardening modulus

$\left(\varepsilon_s = \varepsilon_{sh},\ \frac{df_s}{d\varepsilon_s} = E_{sh}\right)$ or $\left(X = X_{sh},\ \frac{dY}{dX} = A\right)$

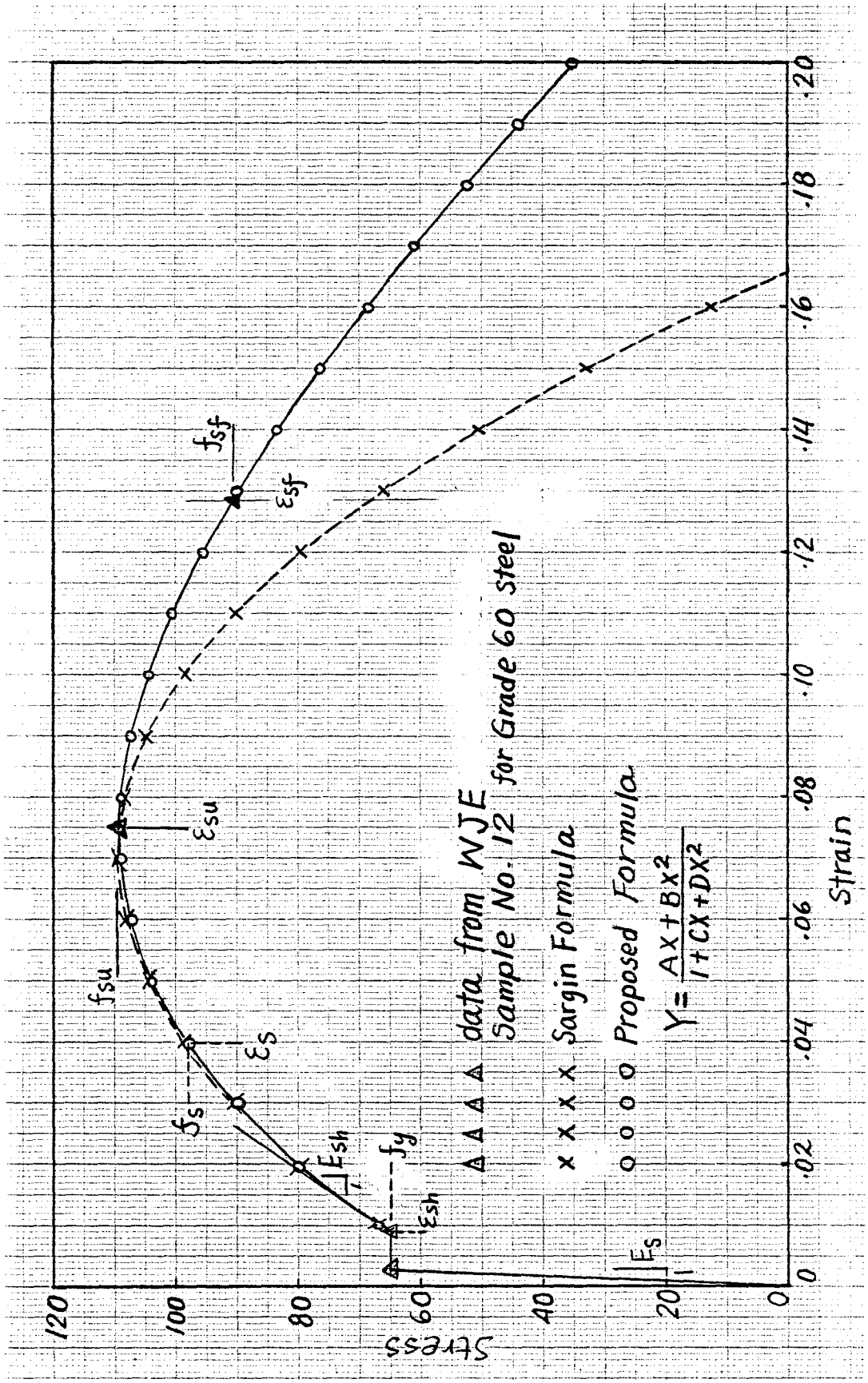

Fig. 3.3 Comparison between Sargin's and revised formulas for representing the stress and strain curve of grade 60 steel up to a strain of 0.200.

BC4 Curve passes through the failure point

$$(\varepsilon_s = \varepsilon_{sf},\ f_s = f_{sf}) \qquad \text{or} \qquad (X = X_{sf},\ Y = Y_{sf})$$

By using the boundary conditions, the four constants are determined as follows:

$$\left.\begin{aligned} A &= \frac{E_{sh}}{E_o} \\ B &= D - 1 \\ C &= A - 2 \\ D &= \frac{Y_{sf} + (A-2)X_{sf}Y_{sf} - AX_{sf} + X_{sf}^2}{X_{sf}^2 - X_{sf}^2 Y_{sf}} \end{aligned}\right\} \qquad (3.9)$$

where

$$X_{sf} = \frac{\varepsilon_{sf} - \varepsilon_y}{\varepsilon_o}$$

$$Y_{sf} = \frac{f_{sf} - f_y}{f_o}$$

The curve is plotted in Fig. 3.3 as well as that proposed by Sargin. It can be seen that this new expression can represent more accurately the observed data.

3.3 STRESS-STRAIN CURVE OF STEEL WITHOUT DEFINITE YIELD POINT SUCH AS HIGH STRENGTH REINFORCING BARS

A typical stress-strain curve (Ref. 39) for a reinforcing bar in this category is shown in Fig. 3.4. It can be seen that in the strain-hardening portion there are an ascending part and a descending part, and that a high value of strain (0.12) can be reached. Several stress-strain equations have been proposed to represent the experimental behavior of these steels. They are discussed next.

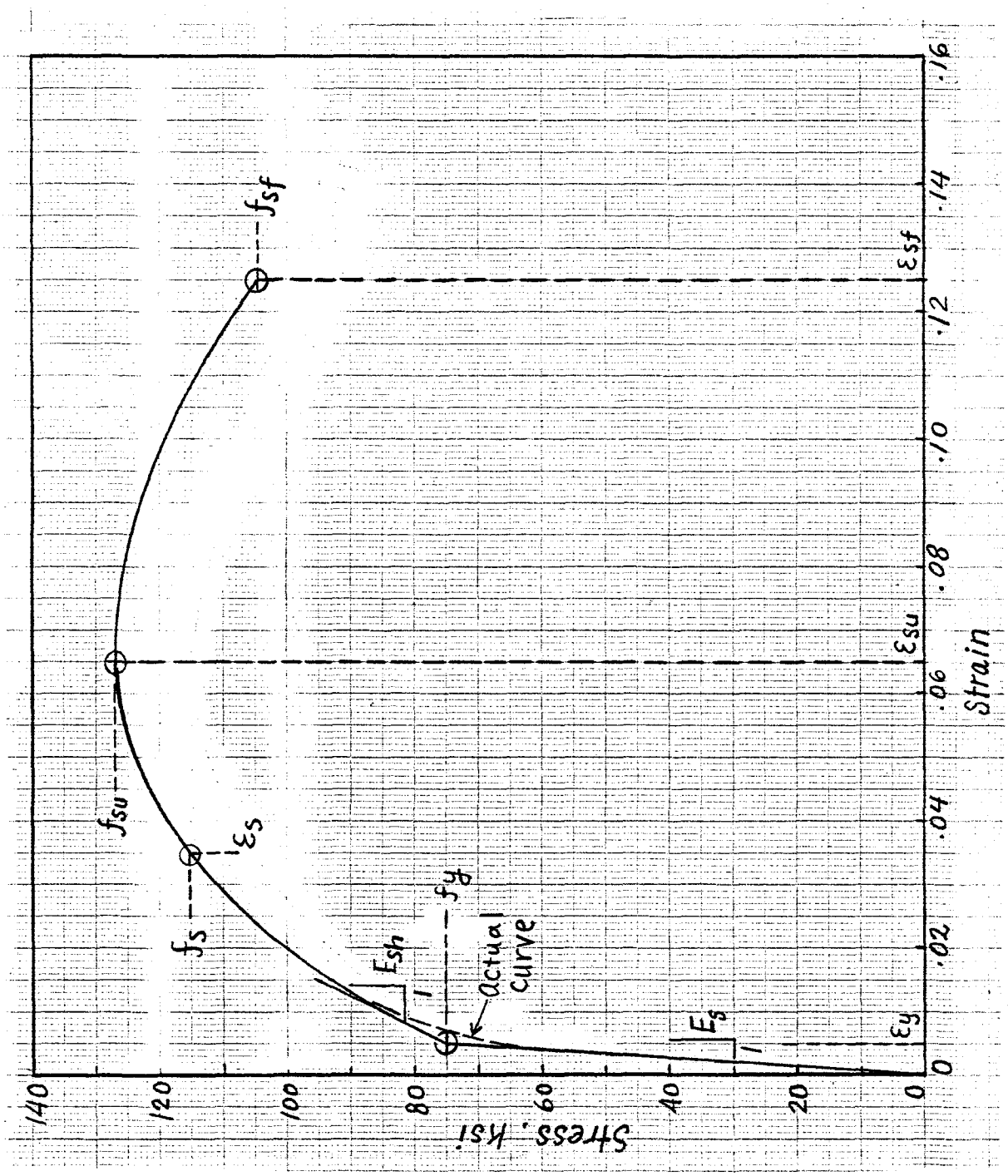

Fig. 3.4 Typical stress-strain curve of steel without definite yield point.

3.3.1 Sargin's Equation

Sargin [32] has proposed the following two-part stress-strain relationship in which the nonlinear part is the inverse of the Ramberg-Osgood polynomial [27]; the expression is as follows:

$$f_s = E_s \varepsilon_s \qquad \text{for} \quad 0 \leq \varepsilon_s \leq \varepsilon_e \tag{3.10}$$

$$f_s = f_e + (f_{su} - f_e) \frac{Z}{(1 + Z^v)^{1/v}} \qquad \text{for} \quad \varepsilon_e < \varepsilon_s \leq \varepsilon_{sf} \tag{3.11}$$

where

$$Z = \frac{(\varepsilon_s - \varepsilon_e)E_s}{f_{su} - f_e} \tag{3.12}$$

and

f_{su} = ultimate strength

f_e, ε_e = stress and strain at elastic limit

E_s = Young's modulus

v = constant

By translating the coordinate system as shown in Fig. 3.5, Eqs. (3.11) and (3.12) can be rewritten as follows:

$$Y = Y_o \frac{Z}{(1 + Z^v)^{1/v}} \tag{3.13}$$

$$Z = \frac{E_s X}{Y_o} \tag{3.14}$$

The first-order derivatives are as follows:

$$\frac{dY}{dX} = \frac{E_s}{(1 + Z^v)^{1/v}} \tag{3.15}$$

$$\frac{dZ}{dX} = \frac{E_s}{Y_o} \tag{3.16}$$

where

$X = \varepsilon_s - \varepsilon_e$

$Y = f_s - f_e$

$Y_o = f_{su} - f_e$

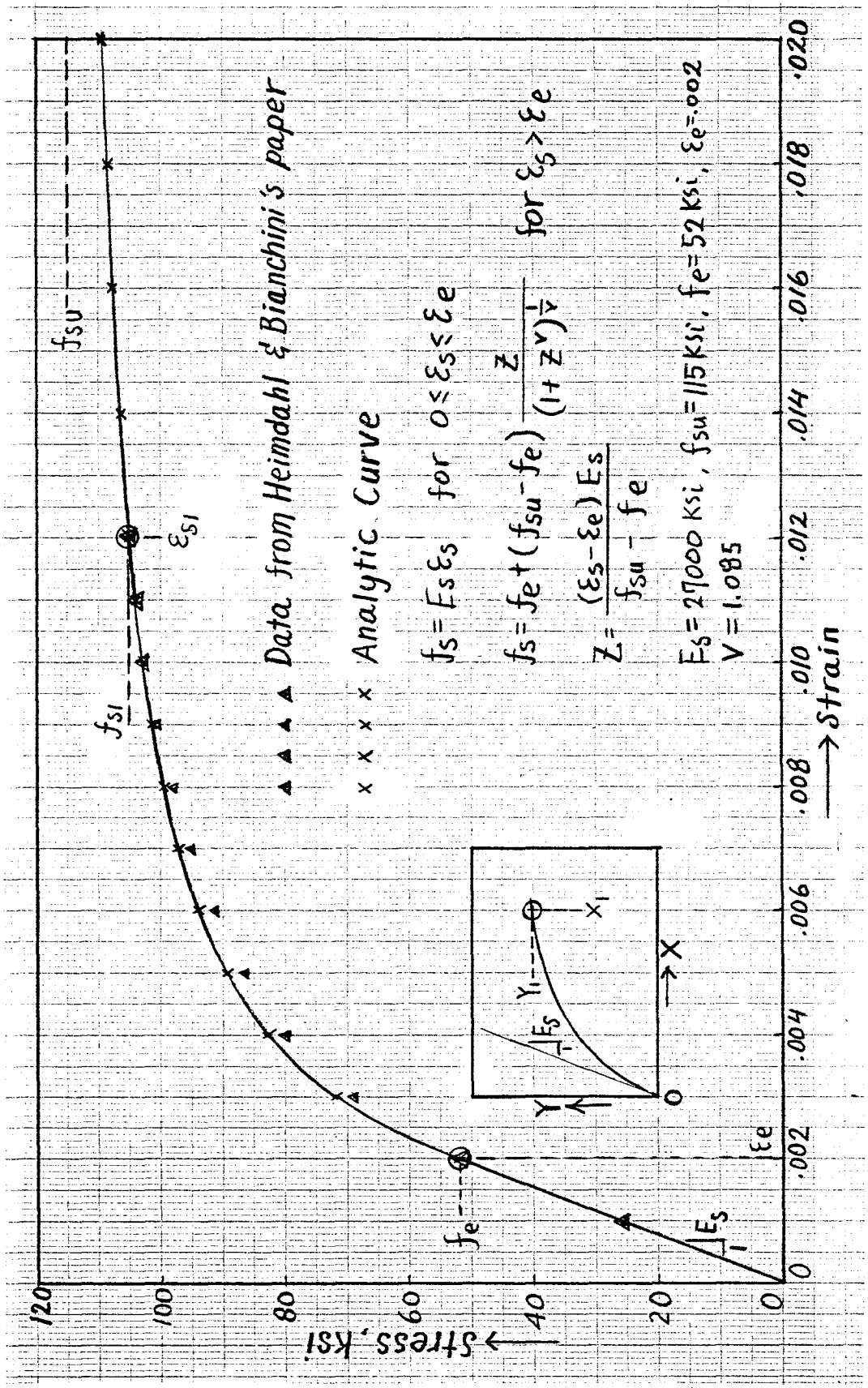

Fig. 3.5 Sargin curve for high strength reinforcing bar.

The curve is constrained to satisfy the following two boundary conditions:

BC1 At the point of the proportional limit (ε_e, f_e), the slope is equal to Young's modulus, E_s

$$\left(\left.\frac{df_s}{d\varepsilon_s}\right|_{(\varepsilon_e, f_e)} = E_s\right), \quad \text{or} \quad \left(\left.\frac{dY}{dX}\right|_{(0,0)} = E_s\right) \tag{3.17}$$

BC2 Curve passes through any specified point $(\varepsilon_{s1}, f_{s1})$

$(\varepsilon_s = \varepsilon_{s1},\ f_s = f_{s1})$ or $(X = X_1 \equiv \varepsilon_{s1} - \varepsilon_e,\ Y = Y_1 \equiv f_{s1} - f_e)$

Checking boundary conditions to determine v

BC1 $E_s = E_s$ identity

BC2
$$\frac{Y_1}{Y_o} = \frac{Z_1}{(1 + Z_1^v)^{1/v}} \tag{3.18}$$

and

$$Z_1 = \frac{E_s}{Y_o} X_1 \tag{3.19}$$

From Eq. (3.18)

$$\frac{1}{v} \log (1 + Z_1^v) = \log Z_1 + \log \left(\frac{Y_o}{Y_1}\right) \tag{3.20}$$

The constant v is determined by trial and error from Eq. (3.20); for example, given

$$E_s = 27000 \text{ ksi}, \quad f_{su} = 115 \text{ ksi}, \quad f_e = 52 \text{ ksi},$$

$$\varepsilon_e = 0.002, \quad f_{s1} = 105 \text{ ksi}, \quad \varepsilon_{s1} = 0.012$$

then

$$Y_o = 63 \text{ ksi}, \quad Y_1 = 53 \text{ ksi}, \quad X_1 = 0.010, \quad Z_1 = 4.28571$$

and

$$v = 1.085$$

The curve for the above example is plotted in Fig. 3.5. Its characteristic points are taken from the data of Heimdahl and Bianchini [18]. The following results are drawn:

- For the range of strain considered (up to 0.012), the fit is quite good.
- The curve is monotonously increasing, i.e., $\varepsilon_s = 0.2$, $f_s = 114.5$ ksi and $\varepsilon_s = \infty$, $f_s = f_{su} = 115$ ksi; so, there is no peak point.
- For the entire range of the strain (up to 0.200), as shown in Fig. 3.4, this expression cannot predict the real stress-strain behavior of steel, since there is no descending portion.

3.3.2 Goldberg and Richard's Equation

Goldberg and Richard [16] have proposed the following expression:

$$f_s = \frac{E_s \varepsilon_s}{\left[1 + \left(\frac{E_s \varepsilon_s}{f_{su}}\right)^N\right]^{1/N}} \tag{3.21}$$

where N can be determined from

$$N = \frac{\log 2}{\log\left(\frac{f_{su}}{f_y}\right)} \tag{3.22}$$

and

f_s, ε_s = stress and strain in the steel

f_{su} = ultimate strength

f_y = yield strength

E_s = Young's modulus

Equation (3.21) can be rewritten as follows:

$$f_s = f_{su} \frac{Z}{\left[1 + Z^N\right]^{1/N}} \tag{3.23}$$

where

$$Z = \frac{E_s \varepsilon_s}{f_{su}} \tag{3.24}$$

The first derivatives of Eqs. (3.23) and (3.24) are given by:

$$\frac{df_s}{d\varepsilon_s} = \frac{E_s}{(1 + Z^v)^{(1 + 1/v)}} \tag{3.25}$$

$$\frac{dZ}{d\varepsilon_s} = \frac{E_s}{f_{su}} \tag{3.26}$$

It can be seen that Eqs. (3.23), (3.24), (3.25), and (3.26) are similar to Eqs. (3.13), (3.14), (3.15), and (3.16) given by Sargin in the preceding section.

The value of N in Eq. (3.21) is determined from Eq. (3.22); N can also be determined independently by satisfying the following two boundary conditions:

BC1 At the origin, the slope is equal to E_s, the Young's modulus

$$\left(\left.\frac{df_s}{d\varepsilon_s}\right|_{(0,0)} = E_s\right)$$

BC2 Curve passes through a specified point such as $(\varepsilon_{s1}, f_{s1})$

$(\varepsilon_s = \varepsilon_{s1},\ f_s = f_{s1})$

Checking the boundary conditions to determine N:

BC1 $E_s = E_s$ identity

BC2
$$f_{s1} = f_{su} \frac{Z_1}{\left[1 + Z_1^N\right]^{1/N}} \tag{3.27}$$

where

$$Z_1 = \frac{E_s \varepsilon_{s1}}{f_{s1}} \tag{3.28}$$

Equation (3.27) can be rewritten as:

$$\frac{1}{N} \log (1 + Z_1^N) = \log Z_1 + \log \left(\frac{f_{su}}{f_{s1}} \right) \tag{3.29}$$

The constant N is then determined by trial and error from Eq. (3.29); for example, given

$$E_s = 27000 \text{ ksi}, \quad f_{su} = 115 \text{ ksi}, \quad f_{s1} = 105 \text{ ksi}, \quad \varepsilon_{s1} = 0.012$$

then

N = 1.7165 from Eq. (3.29)

N = 1.7169 from Eq. (3.22)

The curve for the above example is plotted in Fig. 3.6. Its characteristic points are taken from the data of Heimdahl and Bianchini [18]. The following results are drawn:

- For the range of strain considered (up to 0.012), the fit is good, since there is only one expression used in comparison to the two-portion curve proposed by Sargin in the preceding section.
- The curve is monotonously increasing, i.e., $\varepsilon_s = 0.2$, $f_s = 114.9$ ksi and $\varepsilon_s = \infty$, $f_s = f_{su} = 115$ ksi; so, there is no peak point.
- For the entire range of the strain (up to 0.200), as shown in Fig. 3.4, this expression cannot predict the real stress-strain behavior of the steel since there is no descending portion.

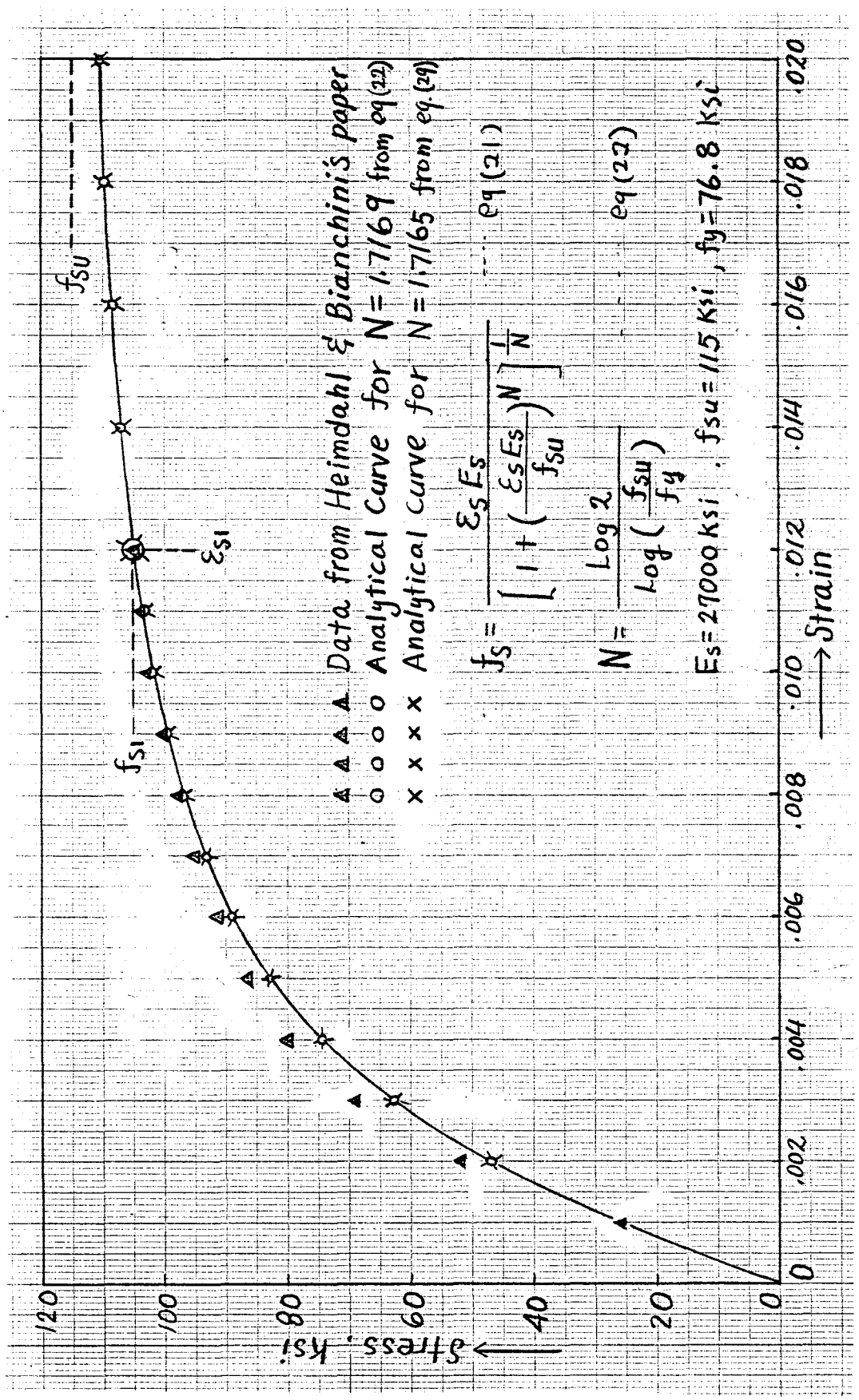

Fig. 3.6 Goldberg and Richard's curve for high strength reinforcing bars.

3.3.3 Proposed Expression to Represent the Entire Stress-Strain Relation Up to a Strain of 0.200 for Steel without a Definite Yield Point Such as High Strength Reinforcing Bars

The conclusion from the preceding two sections shows that both Sargin's expression and Goldberg's expression cannot predict well the typical curve over its entire range, as shown in Fig. 3.4, for this category of steel. The proposed expression consists of two parts as follows:

(a) Initial elastic portion

$$f_s = E_s \varepsilon_s \qquad \text{for} \quad 0 < \varepsilon_s < \varepsilon_y \tag{3.30}$$

(b) Strain-hardening portion

$$Y = \frac{AX + BX^2}{1 + CX + DX^2} \tag{3.31}$$

The expression for the strain-hardening portion has the same equation as that in Section 2.2.2 for mild steel with a definite yield point. The constants A, B, C, D and the boundary conditions are determined by the same manner described in that section, and will not be repeated here.

The curve represented by Eqs. (3.30) and (3.31) has the following characteristics:

- The representative curve is an idealized curve, so there is a gap existing between the analytical curve and the actual data points near the yield point, as shown in Fig. 3.4. Consequently, the discontinuity in the slope at the yield point is a result of that idealization.
- To improve the fit on the entire strain-hardening portion, the values of f_y and E_{sh} can be adjusted.

3.4 ANALYSIS OF AVAILABLE EXPERIMENTAL DATA

The data used here for analysis were obtained from Weiss, Janney, Elstner and Associates, Inc. and was submitted in a report to the Technical Committee of the Associated Reinforcing Bar Producers [41]. The testing variables are as follows:

(a) Type of steel: A615 Grade 60

(b) Bar size: #3, #4, #5, #8, #11 (from various manufacturers)

(c) Strain measurement: ASTM Standard

3.4.1 Synthesis of Results

About two hundred specimens of reinforcing bars from different manufacturers were tested and recorded for various bar sizes. In order to see the trend in the variability of the data, 46 specimens of bar sizes from #3 to #11 were studied. Two categories of stress-strain curves were observed from these data: one with a yield plateau, one without a definite yield point. For the first category, a typical stress-strain curve for Specimen No. 9 from Table 3.1 is shown in Fig. 3.7; for the second category, a typical stress-strain curve for Specimen No. 44 is shown in Fig. 3.8. The characteristic variables of the data are summarized in Tables 3.1 and 3.2 for these specimens, and are explained below:

f_y = yield strength

f_{su}, ε_{su} = stress and strain at the peak point

f_{sf}, ε_{sf} = stress and strain at the failure point

ε_{sh} = strain at the onset of strain-hardening

E_s = Young's modulus

E_{sh} = strain-hardening modulus

TABLE 3.1

Characteristic Parameters of Grade 60 Steel

Wiss, Janney, Elstner & Associates, Inc.

Specimen No.	Code No.	f_y ksi	f_{su} ksi	f_{sf} ksi	ε_{sh} 0.0001	ε_{su} 0.0001	ε_{sf} 0.0001	E_s 10^3 ksi	E_{sh} 10^3 ksi
1	110503	70	120.0	105	62	600	1400	29.4	1.07
2	10301	74	114.0	106	46	600	787	27.9	1.50
3	10303	65	91.0	76	125	687	1470	28.6	0.76
4	20501	64	110.0	100	75	700	1330	29.4	1.36
5	20502	67	114.0	106	87	870	1340	29.1	1.36
6	20503	67	117.0	106	40	725	1180	29.1	1.50
7	20504	69	116.0	104	57	500	1120	29.9	1.25
8	20505	68	114.0	105	120	912	1490	29.2	1.12
9	30501	65	109.0	96	85	750	1190	28.9	1.45
10	30502	73	122.0	96	28	687	1150	28.6	1.50
11	40401	68	97.0	78	100	625	1400	29.0	0.64
12	40503	72	100.0	81	100	662	1710	29.8	0.72
13	40504	71	98.0	85	120	725	1710	29.0	0.72
14	50503	72	97.0	88	125	750	1520	29.2	0.64
15	50504	74	105.0	90	90	750	1210	29.9	0.80
16	60401	69	114.0	92	60	780	1400	30.1	1.32
17	60504	64	106.0	84	80	687	1590	29.6	1.28
18	60505	72	117.0	99	65	725	1150	29.5	1.28
19	60506	68	117.0	102	80	687	1090	30.2	1.44
20	70302	74	120.0	108	65	820	1190	28.3	1.28
21	80501	62	108.0	89	85	635	1610	28.6	1.28
22	80503	62	108.0	90	75	650	1410	29.4	1.28
23	80505	62	109.0	92	60	660	1460	28.6	1.28
24	110501	64	114.0	101	75	625	1490	29.6	1.28
25	110502	64	115.0	105	65	620	1370	30.1	1.44
26	130401	68	107.0	98	103	580	1130	28.1	1.44
27	130402	68	108.0	98	75	662	1320	28.9	1.04
28	180401	68	118.0	109	70	650	1070	29.8	1.48
29	200501	68	102.0	86	75	625	1770	30.0	0.88
30	170803	64	113.1	105	62	780	1410	29.98	1.28
31	150812	64	122.3	116	50	720	1350	29.84	1.36
32	140810	66	100.2	92	80	660	1540	30.34	1.04
33	90808	60	104.1	93	75	750	1590	30.46	1.20
34	80808	64	100.0	88	100	820	1710	29.81	0.96
35	80806	63	94.3	88	130	780	1420	29.86	0.96
36	81111	64	107.8	93	100	840	1330	29.65	1.04
37	81112	63	101.2	90	110	850	1570	29.69	0.96
38	81115	64	96.9	80	130	810	1650	30.03	0.88
39	91101	66	110.0	102	100	700	1420	29.42	1.44
40	131115	60	103.2	98	80	710	1480	29.76	1.28
41	141111	68	98.4	90	100	750	1710	28.64	0.96
42	141112	66	100.1	92	80	750	1400	29.28	0.88

TABLE 3.1 (Cont'd)

Characteristic Parameters of Grade 60 Steel

Wiss, Janney, Elstner & Associates, Inc.

Specimen No.	Code No.	f_y ksi	f_{su} ksi	f_{sf} ksi	ε_{sh} 0.0001	ε_{su} 0.0001	ε_{sf} 0.0001	E_s 10^3 ksi	E_{sh} 10^3 ksi
43	210401	55	100.0	80	*	840	1500	28.8	*
44	210810	55	100.0	89	*	690	1770	31.2	*
45	210709	52	99.0	90	*	500	1580	28.0	*
46	210708	55	113.0	106	*	850	1510	28.7	*

*The stress-strain curve has no definite yield point

TABLE 3.2

PCA Steel Curve for Steel A615 Grade 60

Specimen No.	f_y ksi	f_{su} ksi	f_{sf} ksi	ε_{sh} 0.0001	ε_{su} 0.0001	ε_{sf} 0.0001	E_s 10^3 ksi	E_{sh} 10^3 ksi
1	74.2	110.0	-	103	-	1250	27.8	1.22
2	64.9	102.6	-	79	-	1290	28.2	1.25
3	60.0	100.8	-	65	-	1440	30.2	1.24

TABLE 3.3

Regression Equations for the Characteristic Variables of the Stress-Strain Curve of A615 Grade 60 Steel from WJE

y*	f_{su} ksi	f_{sf} ksi	E_s ksi	E_{sh} ksi	ε_{sh}	ε_{su}	ε_{sf}
a	+ 0.523	+ 0.274	- 54.39	- 9.44	- 0.00009	- 0.00023	- 0.00221
b	+ 73.2	+ 77.0	+ 33023	+ 1788	+ 0.0145	+ 0.0867	+ 0.2868

*$y = a[f_y(ksi)] + b$

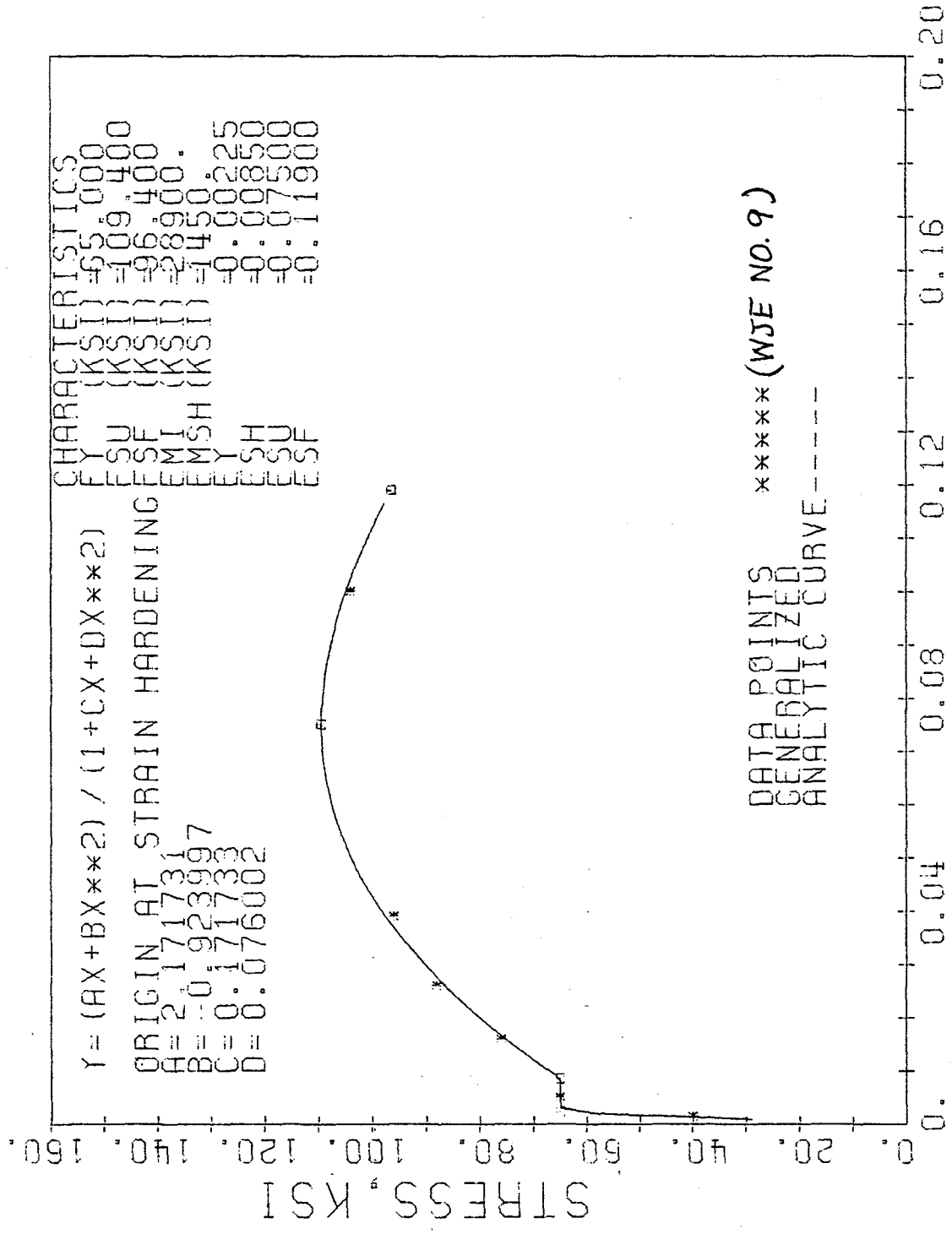

Fig. 3.7 Comparison between proposed formula and actual data of grade 60 steel.

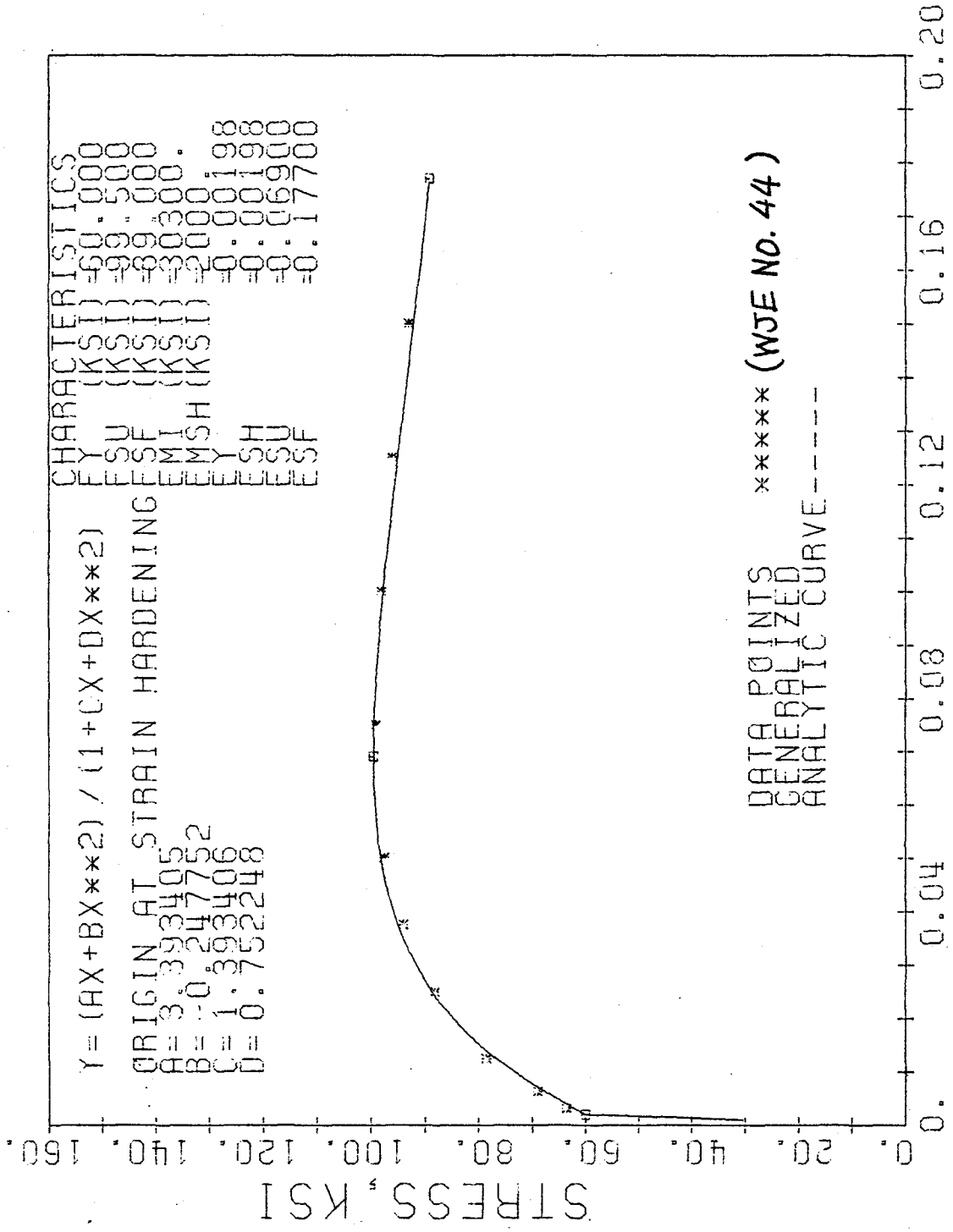

Fig. 3.8 Comparison between proposed formula and actual data of steel having no definite yield point.

The proposed analytic expressions for these two categories of the σ-ε curve described in Sections (3.2.2) and (3.3.3), are applied to fit the data of Specimens No. 9 and No. 44; the fittings are considered excellent as can be seen in Figs. 3.7 and 3.8.

For analyzing the first category of steel with a yield plateau, the next step is to relate the characteristic variables of the curve to the yield strength, so as to make it possible to generate a stress-strain curve solely from the knowledge of the yield strength. For this purpose, the characteristic variables were statistically related to the yield strength. In the statistical analysis, a linear relation is used to see the trend of the scattering of the data. The data points and the linear regression lines for these characteristic variables are plotted in Figs. 3.9, 3.10 and 3.11. The corresponding coefficients of the regression equation are summarized in Table 3.3. The large scatter of the data points is due to the various bar sizes and the different manufacturers as mentioned before (a more detailed analysis would be to separate the effect of bar sizes).

Based on the above results, a computer program was written to generate a stress-strain curve for any given yield strength. Such generated curves are shown in Fig. 3.12 and Table 3.4 for yield strengths equal to 60 ksi, 65 ksi, 70 ksi, and 75 ksi, respectively. In Fig. 3.13, seven experimental curves whose yield strengths were 68 ksi are compared with an analytical curve generated for a yield strength equal to 68 ksi. From this comparison, it appears that the analytic expression is quite satisfactory.

3.5 CONCLUSIONS

(1) Although available expressions (Sargin, Goldberg, et al.) for the stress-strain curve of reinforcing bars made of steels with no yield

TABLE 3.4

Characteristics and Constants of Equation for Generalized Stress-Strain Curves of Grade 60 Steel with Yield Strength of 60, 65, 70 and 75 ksi

Characteristics

f_y ksi	f_{su} ksi	f_{sf} ksi	ε_{sh}	ε_{su}	ε_{sf}	E_s 10^3 ksi	E_{sh} 10^3 ksi
60	104.6	93.4	0.0091	0.0729	0.1542	29.76	1.222
65	107.2	94.8	0.0086	0.0717	0.1431	29.49	1.174
70	109.8	96.2	0.0082	0.0706	0.1321	29.22	1.127
75	112.4	97.5	0.0077	0.0694	0.1210	28.94	1.080

Constants of Equation for Representing Strain-Hardening Portion*

f_y ksi	A	B	C	D
60	1.748272	0.173674	-0.251726	1.173672
65	1.756240	-0.145637	-0.243758	0.854363
70	1.766823	-0.416587	-0.233175	0.583412
75	1.780521	-0.655189	-0.219478	0.344811

$$*Y = \frac{AX+BX^2}{1+CX+DX^2}$$

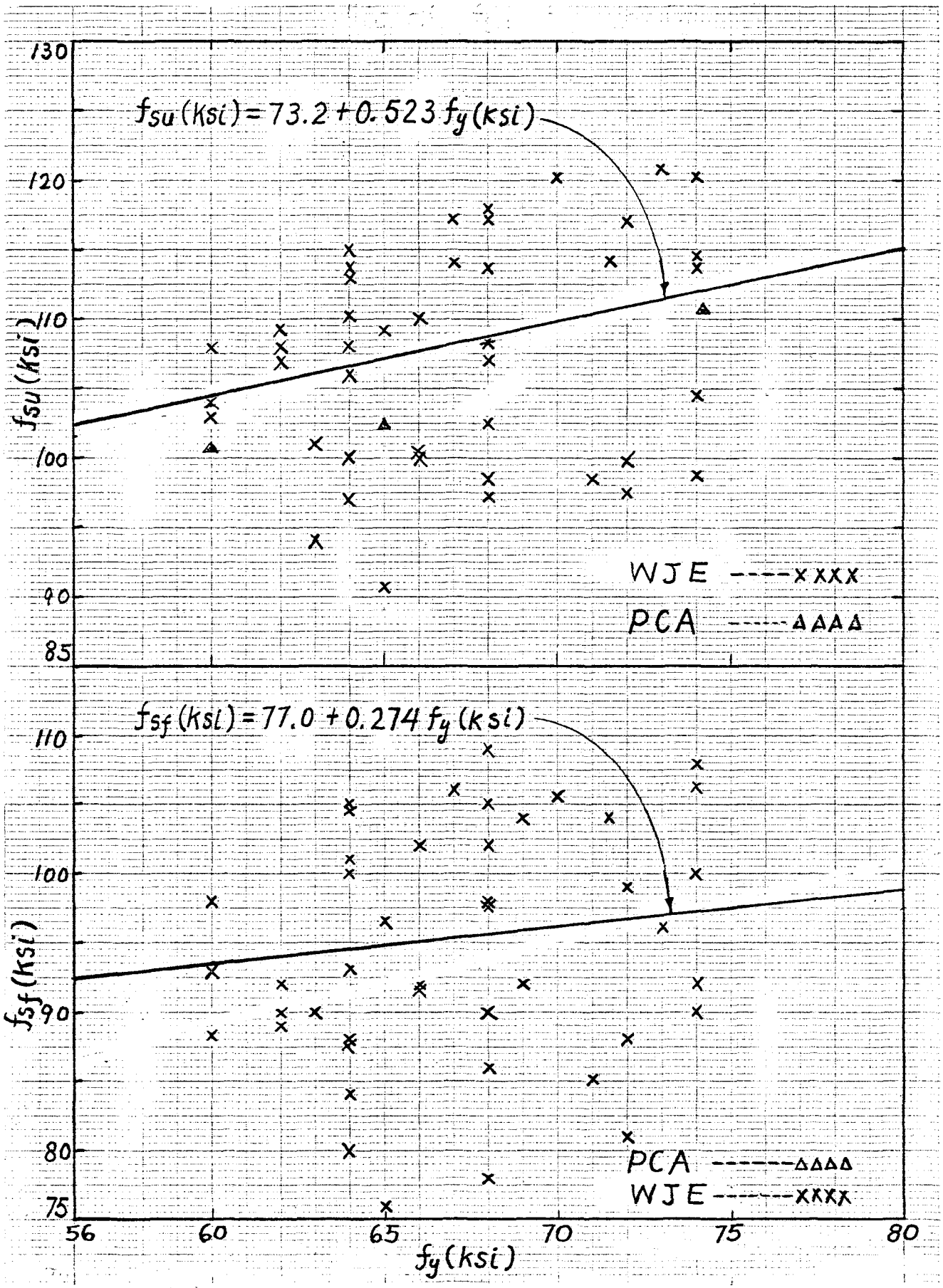

Fig. 3.9 f_{su}, f_{sf} vs. f_y .

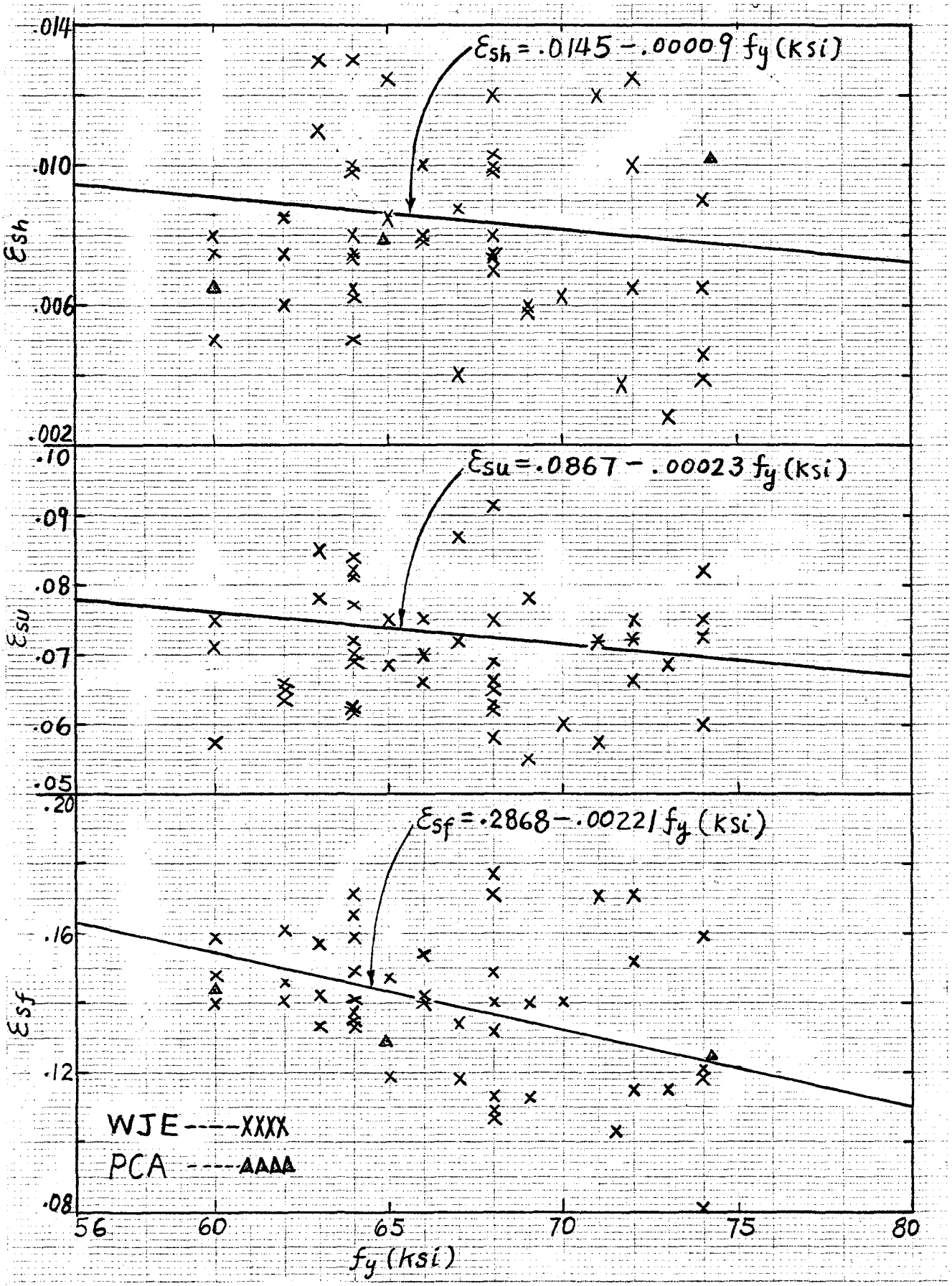

Fig. 3.10 ε_{sh}, ε_{su}, ε_{sf} vs. f_y .

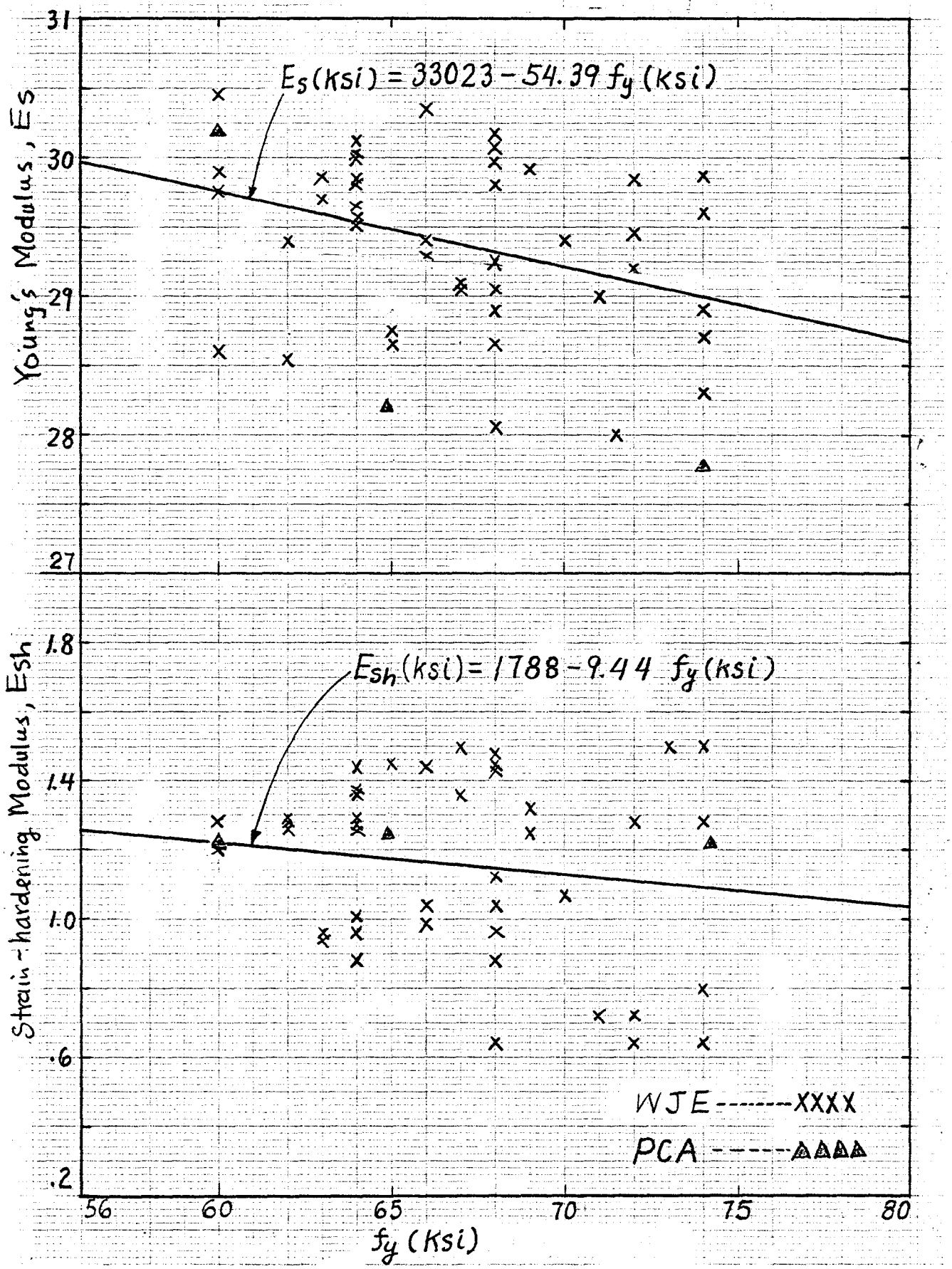

Fig. 3.11 E_s, E_{sh} vs. f_y .

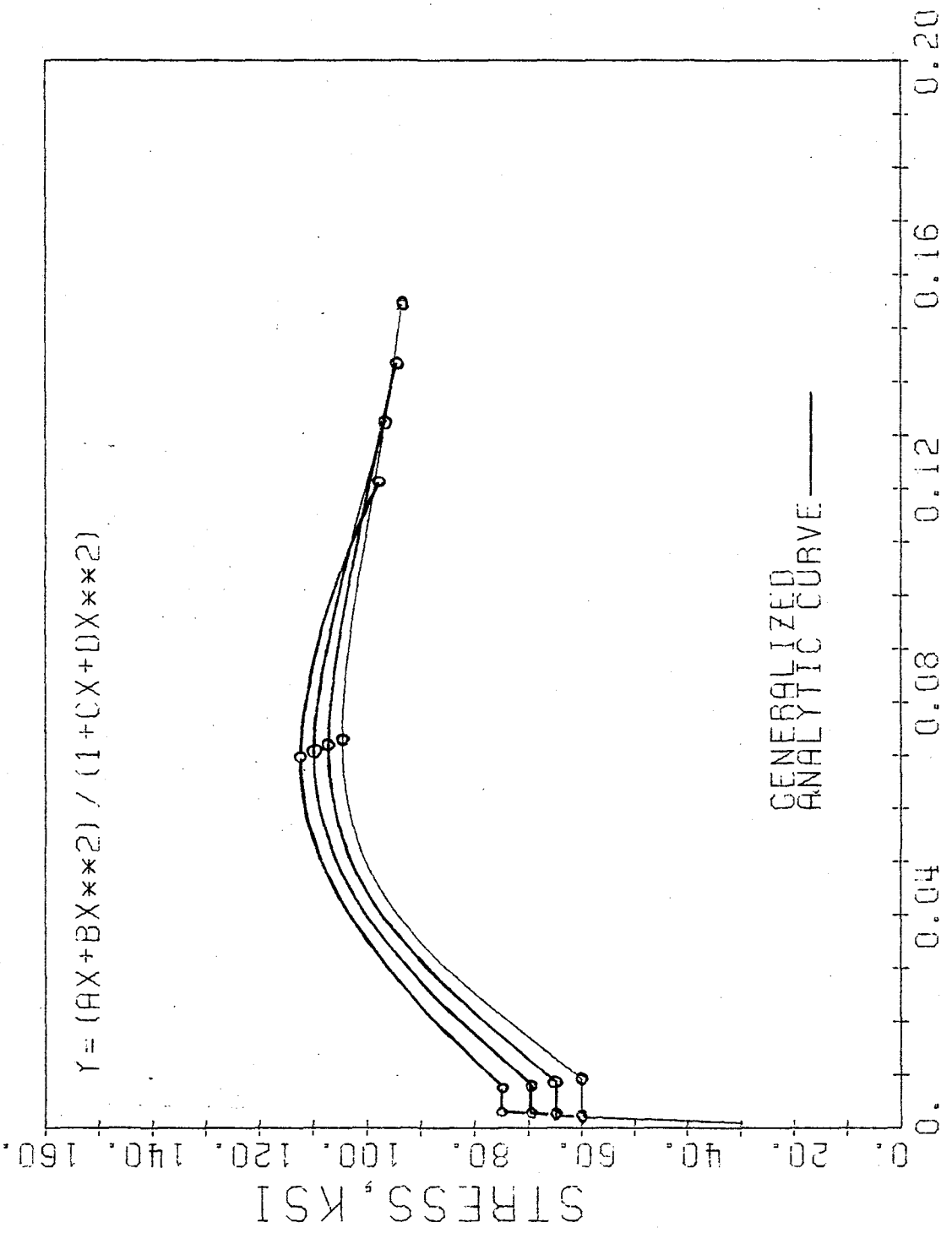

Fig. 3.12 Generalized stress-strain curves of grade 60 steel with yield strengths of 60, 65, 70 and 75 ksi.

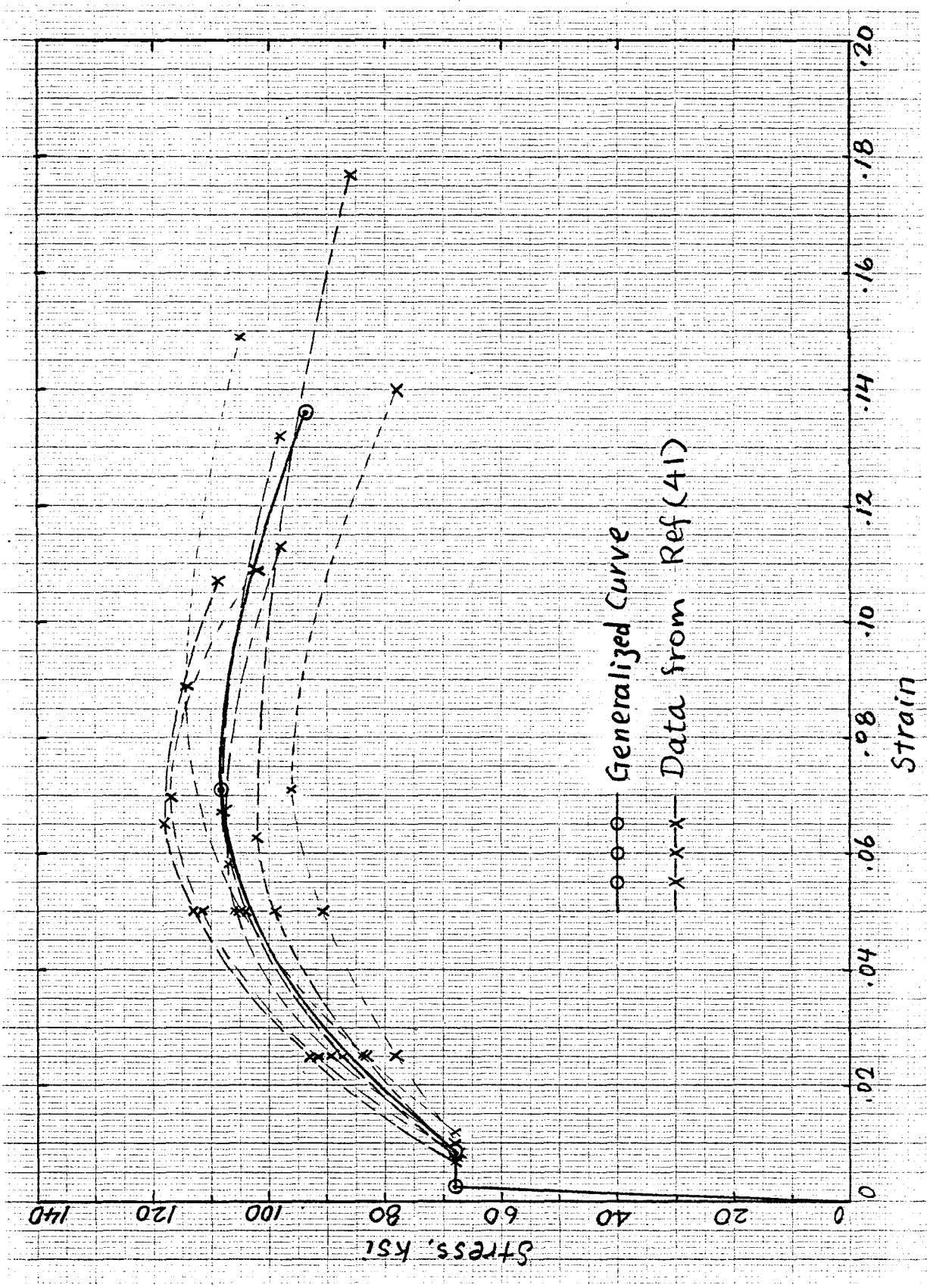

Fig. 3.13 Variation of data for f_y = 68 ksi.

plateau adequately describe their actual behavior well after the yield point (say up to a strain of 0.08), they do not seem to be representative at a higher value of strains (say up to a strain of 0.20).

(2) For steels whose stress-strain curves show a yield plateau, the expression proposed by Sargin [32] seems to be descriptive of the actual behavior, especially before the peak point. As the expression needs five parameters, none of which describe the fracture point, the curve is not necessarily representative after the peak.

(3) The expression proposed to represent the strain-hardening portion of the stress-strain curve of steels with yield plateau, and the nonlinear portion of steels without yield plateau, can be made to exactly describe the actual behavior up to the fracture point. It needs four constants which can be derived from the characteristic parameters of the curve; namely, the strain-hardening modulus, the stresses and strains at the peak point and the fracture point.

(4) The regression equation proposed in this chapter to predict the characteristic parameters of the stress-strain curve from the knowledge of the yield strength only, seems to lead to an adequate prediction of the entire stress-strain curve of steels with a yield plateau. (Note, however, that some of the regression equations show relatively poor correlation as the variation in bar size was not taken into consideration in this analysis.)

CHAPTER IV

TEXT PROGRAM AND VALIDATION OF RESULTS

This chapter is comprised of two major parts: the first describes the experimental program and results obtained on the stress-strain curve of concrete specimens in compression; the second compares actual curves with those obtained from the analytical expression described in Chapter II, and checks if the analytical expression is representative of the actual behavior of concrete from this investigation and other investigations.

4.1 EXPERIMENTAL PROGRAM

The primary purpose of the experimental program was to experimentally obtain the stress-strain curve in compression of normal weight and lightweight concrete specimens, and to define, from the observed data, the regression equations to predict the characteristic parameters needed in generating the analytical stress-strain curves for any concrete. The stress-strain curves were obtained from testing, up to a strain of 0.006, normal weight concrete cylinders with compressive strength varying from 3000 to 11000 psi (21 to 77 MN/m^2), and lightweight concrete cylinders with strength from 3000 to 8000 psi (21 to 56 MN/m^2).

4.2 TESTING METHOD

One of the reasons why there is insufficient experimental or analytic information on the shape of the stress-strain curve beyond the peak stress is the difficulty in experimentally measuring the descending portion of the curve. Many testing machines used for standard compression test apply increasing loads rather than increasing deformations. This results in an uncontrolled, sudden failure immediately after the peak load. Even with

the deformation controlled loading, the release of the energy stored in the testing machine, when the specimen is unloading, will influence the shape of the descending portion. Several investigators have developed techniques to obtain the complete stress-strain curves of concrete [2,6,31,38]. Some of these techniques are costly, require testing machines which may not be available in a normal quality control laboratory or require extensive modifications to a standard testing machine. In this research, a simple technique was developed to obtain the stress-strain curve of concrete up to the strain of 0.006 (Fig. 4.1).

Concrete cylinders were loaded parallel with a steel tube. The steel tube was made of 4142 alloy steel and was case-hardened to 43-45 RC (Rockwell Hardness No.) so that its stress-strain curve was linearly elastic up to the strain of 0.006. The specimens were capped in the testing machine to assure that the load will be shared simultaneously by both the tube and the cylinder immediately on loading. The thickness of the tube wall was such that the sum of the load carried by the steel tube and the concrete cylinder was always increasing up to the strain of 0.006. Thus, there was no release of energy from the testing machine. During loading, the strains in the steel tube were measured with two foil-type resistance strain gages. These strains gave not only the amount of load taken by the steel tube, but were also used to obtain nominal strains in concrete. Thus, knowing the total load and the corresponding steel strain, the stress-strain relationship for concrete can be obtained. In a preliminary study, the ascending portions of the stress-strain curves of two sets of 15 specimens each, one tested with the steel tube and one without, were compared and were found similar. With this procedure, reproducible

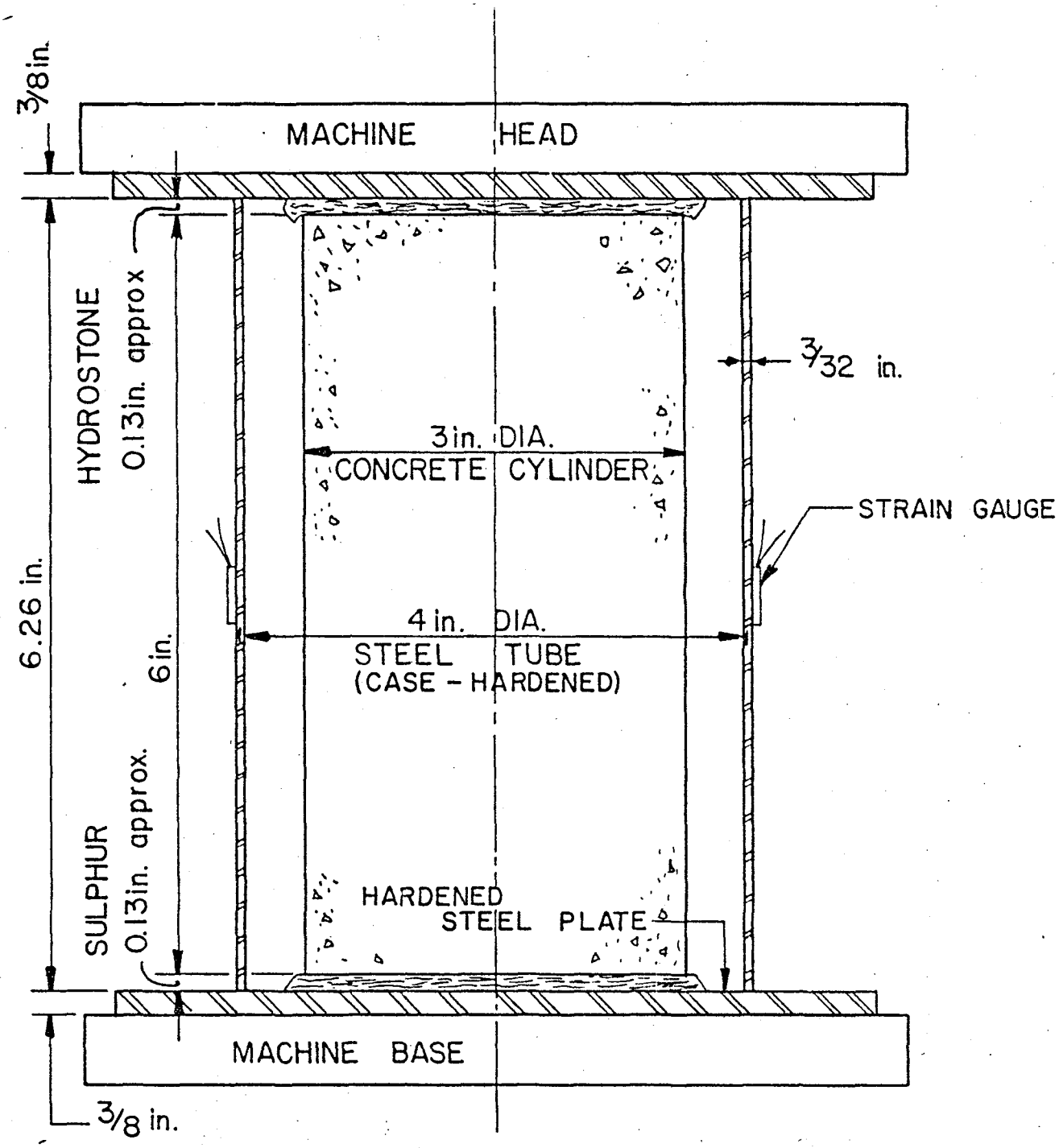

Fig. 4.1 Test set-up.

descending portions of the stress-strain curves were obtained for more than 150 concrete specimens. The rate of loading was 10 micro-strain per second.

Although the method developed is simple and gives satisfactory results, it has certain limitations: (1) the testing machine must apply a load to both the steel tube and concrete cylinder; thus the size of the cylinder is limited by the capacity of the machine; (2) the limit of 0.006 for final strain may be too small when the concrete is confined with lateral reinforcement; (3) the definition of strain is such that the deformations of the thin capping materials and those of the end zones of concrete specimens (where purely uniaxial state of stress does not exist) are included; (4) the presence of the steel tube precludes any observation of the failure modes of the specimen during testing.

4.3 FABRICATIONS AND MATERIALS

The specimens used were 3 x 6 in. (7.5 x 15 cm) cylinders. For normal weight concrete, three batches of thirty cylinders each were made. To obtain different values of compressive strength, the age of testing was varied from 2 days to 125 days. The specimens were cured in a fog room (70°F - 21°C, 100% R.H.) until a day before testing. At each testing age, six cylinders were tested. After each set of tests, the steel tube was also tested by itself up to the strain of 0.006, in order to check its linear elastic response. The specimens from the first batch were used for developing the testing method and for the preliminary testing mentioned earlier. For the statistical analysis of the results, the first batch was not included. All normal weight concrete specimens were made with Type I cement, silicious sand and 3/8 in. (9.5 mm) maximum size of dolomitic limestone coarse

aggregates. The water-cement, sand-cement and aggregate-cement ratios by weight were 0.45, 2.0 and 3.0.

Thirty lightweight concrete specimens were supplied by the Material Service Corporation of Chicago. These 30 cylinders were made with five different mix proportions (Table 4.1), all containing expanded shale with 3/8 in. (9.5 mm) maximum size aggregates and normal weight sand. They were cured for 28 days in a fog room and tested within three days after curing. Each set of six cylinders were designed to give a 28-day compressive strength varying from 3000 to 8000 psi (21 to 56 MN/m^2).

4.4 TEST RESULTS

Typical stress-strain curves for normal weight and lightweight concrete specimens are shown in Figs. 4.2 and 4.3, respectively. The following remarks can be made about these stress-strain curves: (1) every stress-strain curve showed an inflection point; at about the strain corresponding to this point, a slight drop in the load was observed and a cracking noise was often heard; (2) the failure of all the specimens was gradual, even the normal weight specimens with compressive strength of 11000 psi (77 MN/m^2) and the light-weight specimens with compressive strength of 8000 psi (56 MN/m^2) showed extensive vertical splitting cracks around the surface of the cylinders; the failure patterns for normal weight and lightweight concrete specimens are shown in Figs. 4.4 and 4.5; (3) for normal weight concrete, the strain at the peak stress as well as that at the inflection point did not seem to vary substantially with the compressive strength; (4) for lightweight concrete, both of these strains seem to increase with the compressive strength.

TABLE 4.1

Mix Proportions (lb/cu yd)

Normal Weight

Source of Specimen	Type I Cement	Fly Ash	Sand	Aggregate (3/8" max.)	Water	Admixture
UICC	628	-	1256	1884	282	-
Material Service Corp.	850	100	1070	1700	320	Water Reduc. + Air Entraining

Lightweight

Design Strength (psi)	Type I Cement	Fly Ash	Sand	Fine Materialite	Medium Materialite (3/8" max.)	Water	Admixture
3000	470	-	1180	900	300	300	Water Reduc. + Air Entraining
4000	560	-	1100	900	300	315	Water Reduc. + Air Entraining
5000	635	100	940	900	300	330	Water Reduc. + Air Entraining
6000	752	100	1000	900	300	340	Water Reduc.
7000	785	100	1040	860	300	335	Water Reduc.

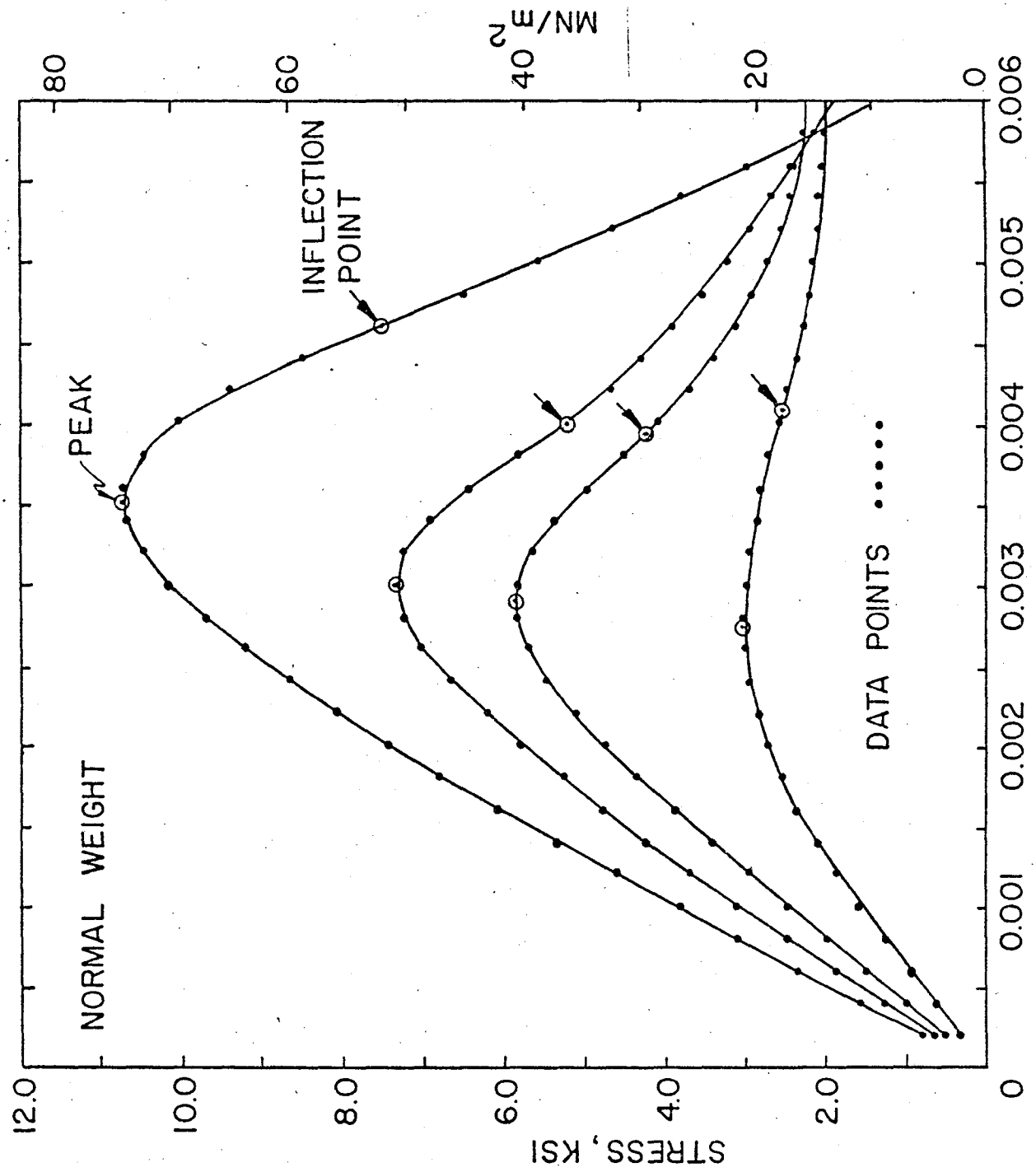

Fig. 4.2 Typical stress-strain curves for normal weight concrete.

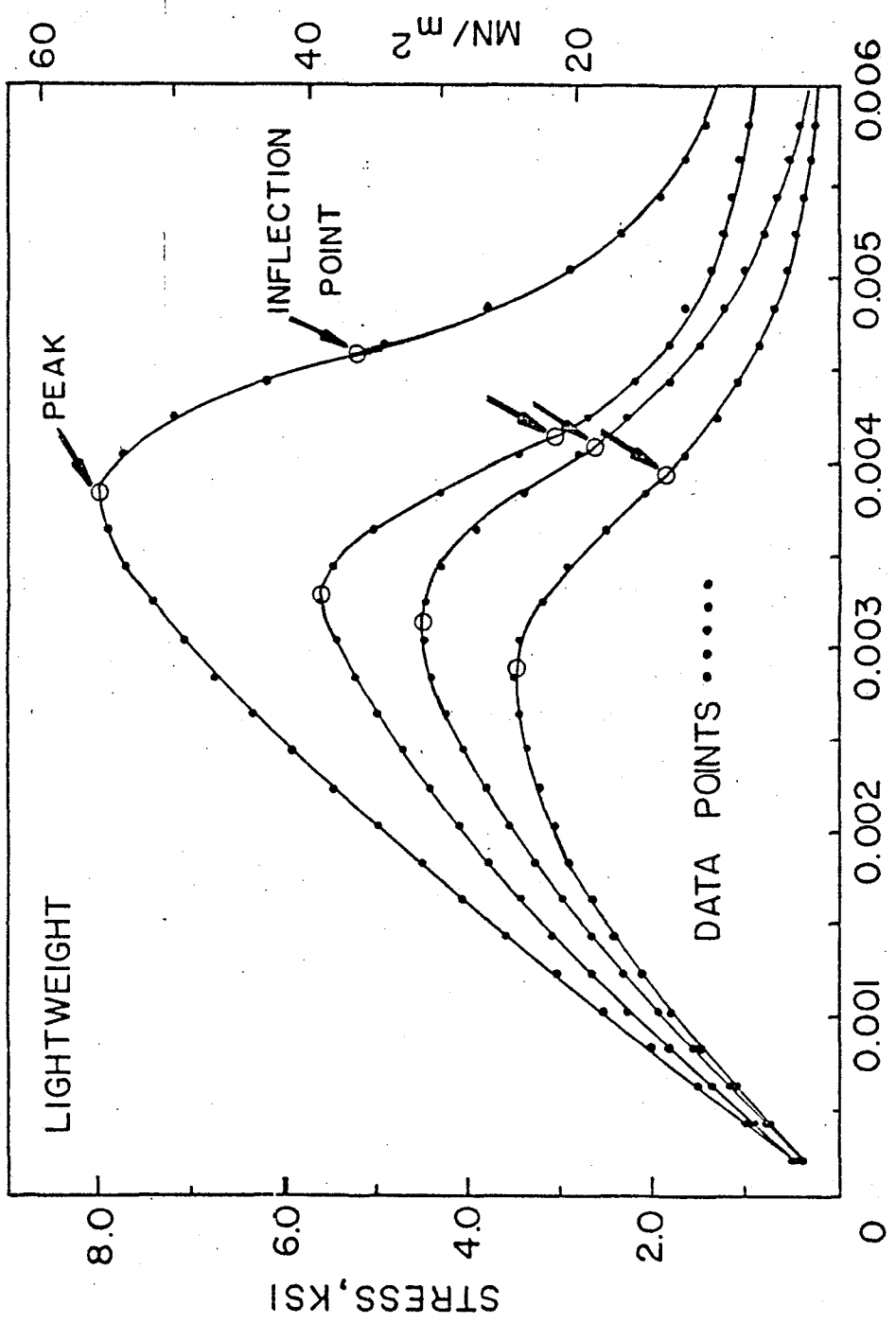

Fig. 4.3 Typical stress-strain curves for lightweight concrete.

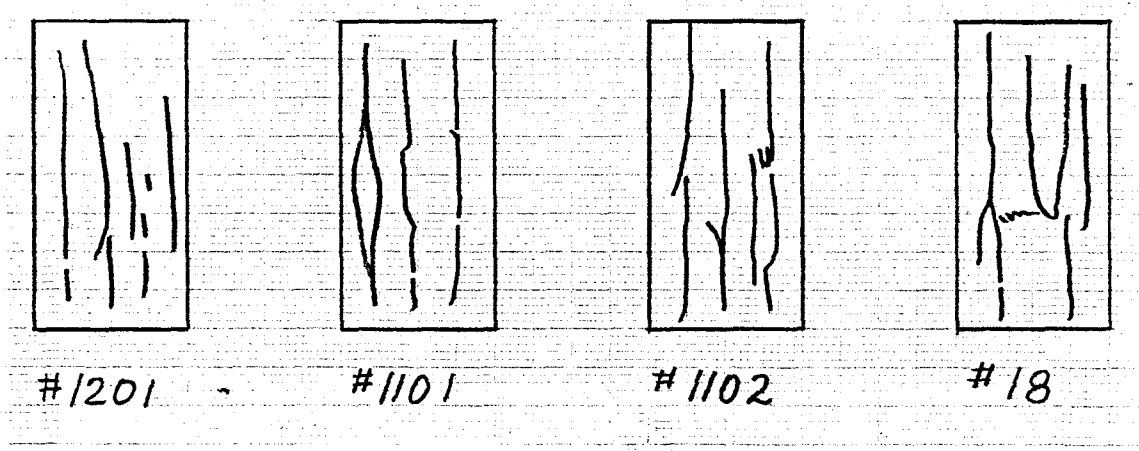

Fig. 4.4 Failure patterns for normal weight concrete.

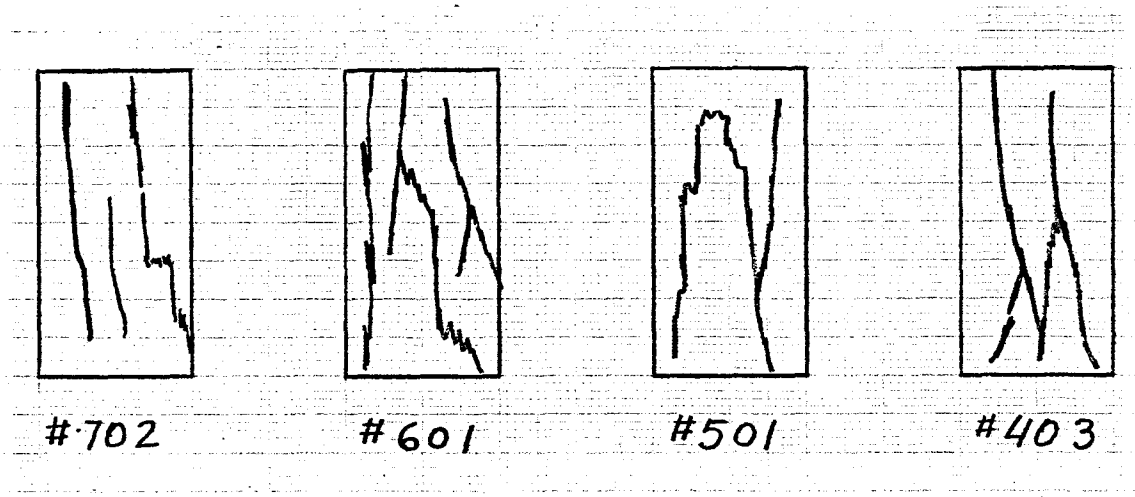

Fig. 4.5 Failure patterns for lightweight concrete.

In Fig. 4.6, a selected comparison is made between the stress-strain curves of normal weight and lightweight concrete having essentially the same compressive strengths of about 4300 and 7400 psi (30.1 and 51.8 MN/m^2). It can be seen that for a similar strength, lightweight concrete exhibits a more steeper drop of the descending part of the stress-strain curve than normal weight concrete. This means that if an analytic stress-strain curve is expressed as a function of the compressive strength alone, a separate expression would be required for each type of concrete. The two stress-strain curves for normal weight and lightweight concrete with the compressive strength of about 4300 psi (30.1 MN/m^2) have ascending portions which are quite similar but have widely varying descending portions. This means that the expression for the analytic stress-strain curves cannot be based just on the parameters of the ascending portions alone, as have often been done in the past.

4.5 GENERATING THE CONSTANTS OF THE ANALYTIC EXPRESSION FOR THE STRESS-STRAIN CURVE

The observed stress-strain relationship of concrete has to be expressed analytically in order to be useful in the analysis and design of structural members. The expression discussed in Chapter II, Section 2.2 is used here to check its validity in respresenting the actual behavior of concrete. As it is also desirable that the constants of this expression be evaluated solely from the key physical parameters of the stress-strain curve, these key parameters were expressed in terms of the readily available material properties such as compressive strength, type of aggregate (normal or lightweight) and amount of confinement. In this manner, the entire stress-strain curve can be generated only from the knowledge of these few material properties.

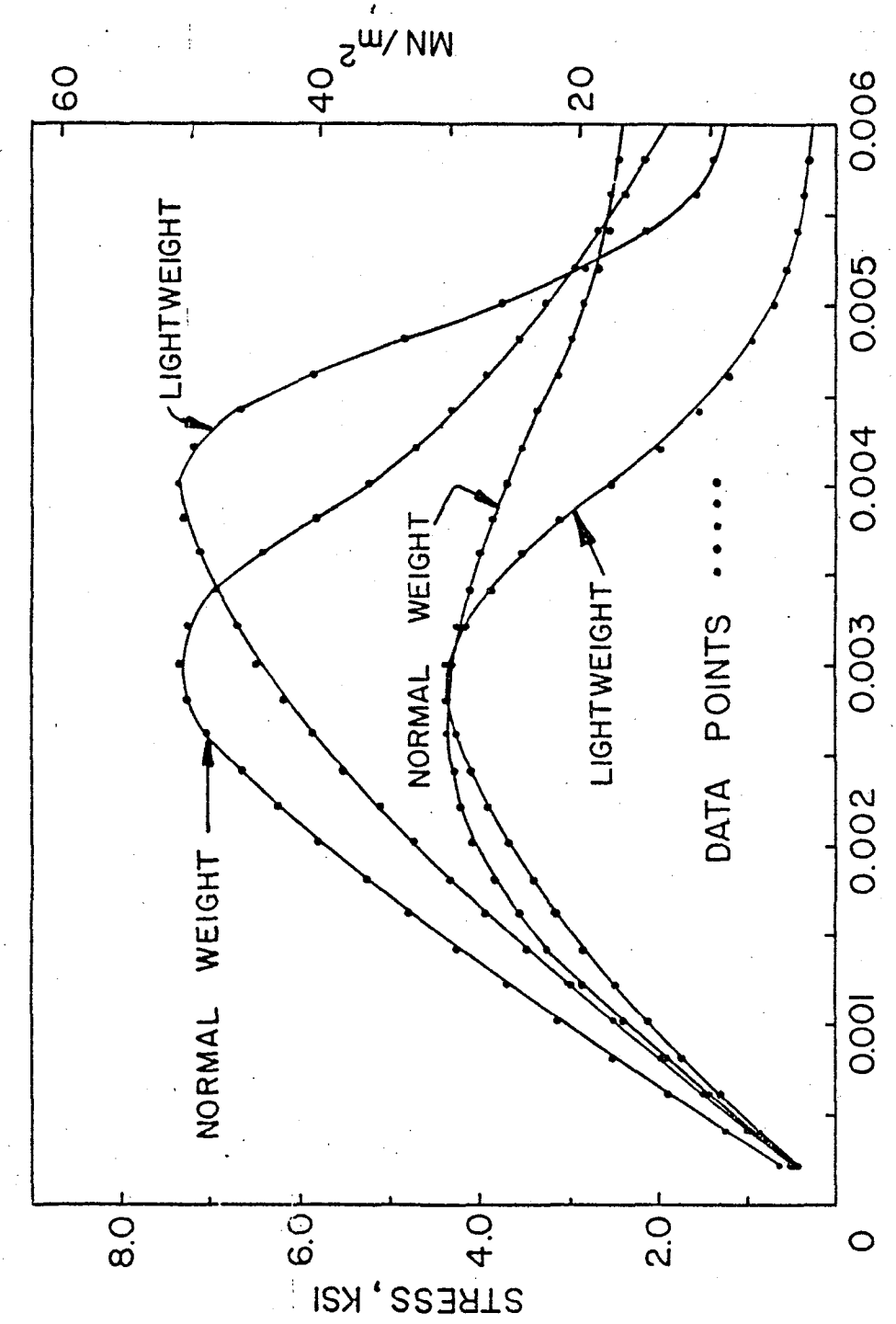

Fig. 4.6 Comparison between normal weight and lightweight concrete stress-strain curves.

The stress-strain relation used is given by:

$$Y = \frac{AX + BX^2}{1 + CX + DX^2} \tag{4.1}$$

where

$Y = f/f_o$

$X = \varepsilon/\varepsilon_o$

f and ε = stress and strain in general

f_o and ε_o = peak stress and corresponding strain

A, B, C, D = constants

$E_o = f_o/\varepsilon_o$ = secant modulus of elasticity at the peak stress

Two different sets of constants A, B, C and D were used for the ascending and descending portions of the curve. For the ascending portion, the values of the four constants were evaluated from the following four conditions, for which E_c represents the secant modulus of elasticity at $0.45\, f_o$:

$$\begin{cases} \dfrac{dY}{dX} = \dfrac{E_c}{E_o} & \text{at the origin } (Y = 0,\ X = 0) \\ Y = 0.45 & \text{for } X = \dfrac{0.45}{E_c/E_o} \\ Y = 1 & \text{for } X = 1 \\ \dfrac{dY}{dX} = 0 & \text{for the peak point } (Y = 1,\ X = 1) \end{cases} \tag{4.2}$$

For the descending portion, the conditions for determining the four constants were:

$$\begin{cases} Y = 1 & \text{for } X = 1 \\ \dfrac{dY}{dX} = 0 & \text{for the peak point } (Y = 1,\ X = 1) \\ Y = \dfrac{f_i}{f_o} & \text{for } X = \dfrac{\varepsilon_i}{\varepsilon_o} \\ Y = \dfrac{f_{2i}}{f_o} & \text{for } X = \dfrac{\varepsilon_{2i}}{\varepsilon_o} \end{cases} \tag{4.3}$$

where f_i and ε_i are the stress and the strain at the inflection point, and f_{2i} and ε_{2i} refer to a point which was arbitrarily selected (Fig. 4.7) such that: $\varepsilon_{2i} - \varepsilon_i = \varepsilon_i - \varepsilon_o$.

With this approach an analytic stress-strain curve can be generated from the knowledge of four key points of the experimental curve, namely: stress and strain at the peak; stress and strain at $0.45 f_o$ (or the secant modulus of elasticity at that point); stress and strain at the inflection point, and stress and strain at a point symmetric to the peak with respect to the inflection point. The characteristics of the four key points from the test data have been tabulated for normal weight and lightweight concrete in Tables 4.2 and 4.3. Due to the definition of strain used in this investigation, the characteristics obtained may have to be adjusted for comparison with data from other techniques.

It can be seen from Fig. 4.7 that Eq. (4.1) fits a given curve rather well when the four constants are determined according to the above procedure.

The next step was to relate the four key points of the curve to the compressive strength, so as to make it possible to generate a stress-strain curve solely from the knowledge of the compressive strength. For this purpose, the above four points (Fig. 4.7) were statistically related to the compressive strength (f_o) for the experimental data of both the normal weight and lightweight concrete specimens. The corresponding least square fitting lines relating the characteristics of the four key points to the peak stress are shown in Figs. 4.8 to 4.15 for both lightweight and normal weight concrete. In the statistical analysis, it was generally observed that a linear relation is quite acceptable and a relation either in terms

TABLE 4.2

Characteristic Points of Normal Weight Concrete

Batch 1 (Cast on February 5, 1976)

Days of Strength	Specimen Number	f_o psi	ε_o 0.001	f_i psi	ε_i 0.001	f_{2i} psi	ε_{2i} 0.001	E_c 10^3 psi	W lb/cu ft
7	6	5425	3.20	3380	4.90	1720	6.60	2222	147.3
	30	5990	2.85	4140	4.60	2405	6.35	2974	147.3
	4	5240	2.95	3100	4.70	850	6.45	2447	147.9
	23	5190	2.85	3820	4.40	2270	6.45	2583	147.3
	13	4960	3.00	2855	4.65	820	6.20	2343	147.5
	25	5515	2.80	4130	4.30	2945	5.80	3001	146.9
	2	8065	3.05	5545	3.95	3000	4.85	3812	151.3
	8	4980	3.20	2830	4.70	835	6.20	1887	148.3
	1	5350	3.20	3535	4.95	1980	6.70	2372	148.9
14	12	6505	2.95	4695	4.05	3185	5.15	2585	149.7
	14	5940	2.60	4175	3.60	2955	4.80	2808	148.0
	10	5870	2.90	4245	3.95	2745	5.00	2460	150.0
	15	6365	3.20	4525	4.10	2660	5.00	2320	150.6
	11	5615	2.50	4030	3.60	2545	4.70	2829	148.9
	9	5940	3.20	4525	4.10	3255	5.00	2146	150.5
28	17	8500	3.70	5660	4.70	2675	5.70	2829	148.2
	16	7370	3.55	4880	4.85	2455	6.15	2770	148.2
	27	7500	3.55	5095	4.90	2715	6.25	2705	148.2
	20	7370	3.60	5405	4.75	3580	5.90	2716	148.2
	28	6760	3.45	5375	4.90	3720	6.35	2476	148.0
56	26	7995	3.90	5090	4.85	2530	5.80	2587	150.7
	22	7355	2.95	5090	3.75	2815	4.55	3339	149.1
	24	7285	3.65	5305	4.80	3325	5.95	2711	150.4
	18	6805	3.70	5090	4.65	3550	5.60	2274	150.4
	31	6670	3.65	4810	4.60	3100	5.55	2360	148.7
	19	5770	2.95	4245	4.45	3100	5.95	2493	148.7

Batch 2 (Cast on February 21, 1976)

2	76	2945	3.05	2545	4.50	2065	5.95	1700	149.1
	61	3610	2.70	3110	3.95	2690	5.20	2000	150.9
	74	3140	2.90	2830	3.80	2460	4.70	1785	150.0
	58	3040	2.75	2545	4.10	2090	5.45	1555	149.6
	64	3085	2.90	2660	4.05	2263	5.20	1905	150.0
	65	2945	2.60	2545	3.95	2135	5.30	1650	150.0

TABLE 4.2 (Cont'd)

Batch 2 (Cast on February 21, 1976)

Days of Strength	Specimen Number	f_o psi	ε_o 0.001	f_i psi	ε_1 0.001	f_{2i} psi	ε_{2i} 0.001	E_c 10^3 psi	W lb/cu ft
3	56	4175	2.55	3255	4.10	2390	5.65	2315	150.9
	54	3790	3.25	2945	4.75	2220	6.25	1705	150.9
	53	4215	2.75	3000	4.40	1950	6.25	2475	150.0
	52	4145	2.75	3680	4.00	3135	5.25	1865	150.0
	51	4355	2.70	3395	4.35	2405	6.00	2330	150.4
	55	4100	2.60	3110	4.10	2265	5.65	2120	151.3
28	79	7510	2.70	5515	3.45	3820	4.20	3615	150.0
	70	7215	2.60	4810	3.70	2065	4.80	3660	150.0
	80	7640	2.70	4690	3.75	2290	4.80	3590	150.0
	69	7285	2.85	4950	3.85	2900	4.80	3395	150.2
	77	7355	2.65	5020	3.85	2690	5.05	3445	150.0
	83	7355	3.00	5660	3.85	3775	4.70	3110	150.0
90	60	8405	3.33	5235	4.20	1415	5.10	3605	150.9
125	72	9480	3.05	5660	4.25	1785	5.45	3885	150.9
	67	9870	2.90	6790	3.60	3395	4.30	4570	150.4
	62	10645	3.05	6860	4.00	2545	4.95	4580	151.3
	73	11035	3.20	7780	4.05	3465	4.90	4500	150.4

Specimens from Materials Service Co.

56*	1102	10185	3.30	6365	4.20	2265	5.10	3735	147.6
	1103	9905	3.65	6365	4.50	2690	5.35	3715	149.6
	1104	10470	3.80	6790	4.75	2120	5.70	3825	149.1
125*	1106	10750	3.50	7500	4.60	2545	5.70	3850	152.0
210+	1201	10270	3.85	6735	4.70	3165	5.55	3440	151.9
	1202	10100	4.10	6230	5.00	1765	6.00	3495	151.4

*Materials Service Co. Concrete Laboratory Specimen

+Riverside Plaza Column Core

TABLE 4.3

Characteristic Points of Lightweight Concrete

Specimens from Materials Service Co. (Tested on June 17, 1976)

Design Strength	Specimen Number	f_o psi	ε_o 0.001	f_i psi	ε_i 0.001	f_{2i} psi	ε_{2i} 0.001	E_c 10^3 psi	W lb/cu ft
3000	301	3535	2.85	1910	3.90	635	4.95	1885	118.4
	302	3610	2.85	2265	3.80	820	4.75	1915	119.1
	303	3090	3.00	1700	4.00	850	5.00	1570	118.7
	304	3655	3.15	2265	4.10	850	5.05	1625	117.9
	305	4105	2.95	2830	4.10	1910	5.25	1670	110.6
	306	4355	3.00	2845	4.10	1700	5.20	1835	110.6
4000	401	4385	2.90	2545	4.00	705	5.10	2160	119.2
	402	4540	3.10	2690	4.05	1060	5.00	1980	118.7
	403	4555	3.05	2545	3.85	705	4.65	2065	120.0
	404	4555	3.15	2405	4.10	850	5.05	2065	118.6
	405	5095	3.25	3270	4.00	1625	4.75	1850	110.2
	406	4400	2.90	2860	3.65	1685	4.40	1840	110.2
5000	501	5235	3.25	2545	4.05	425	4.85	2155	118.9
	502	5660	3.25	3110	4.10	1555	4.95	2315	118.2
	503	5870	3.45	3395	4.30	565	5.15	2425	118.2
	504	5955	3.20	3535	3.95	1130	4.95	2445	116.9
	505	5095	3.15	3185	3.80	1485	4.50	1885	109.5
	506	5305	3.25	3535	3.90	1625	4.55	1860	109.5
6000	605	7780	3.75	5165	4.55	1910	5.35	2560	116.8
	606	6510	3.55	4030	4.30	1840	5.05	2220	116.8
7000	702	7780	3.55	4950	4.40	2150	5.25	2565	125.2
	703	7355	4.00	4810	4.80	1585	5.60	2450	124.4
	704	7780	4.00	5095	4.80	1840	5.60	2375	125.4
	705	8065	3.80	5235	4.55	2195	5.30	2580	118.6
	706	7500	3.50	5095	4.35	2690	5.20	2425	118.6

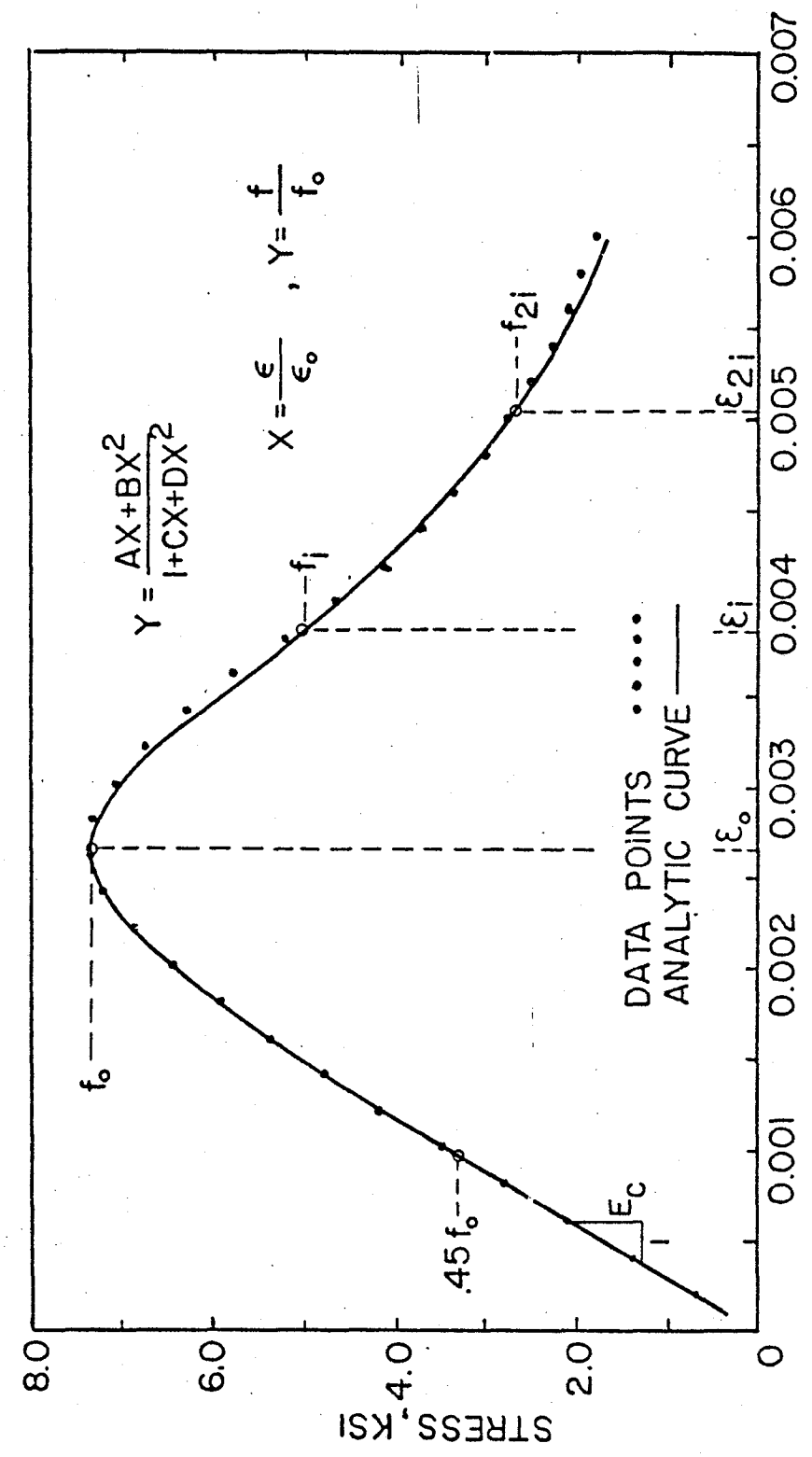

Fig. 4.7 The four key points for the proposed analytic stress-strain curve.

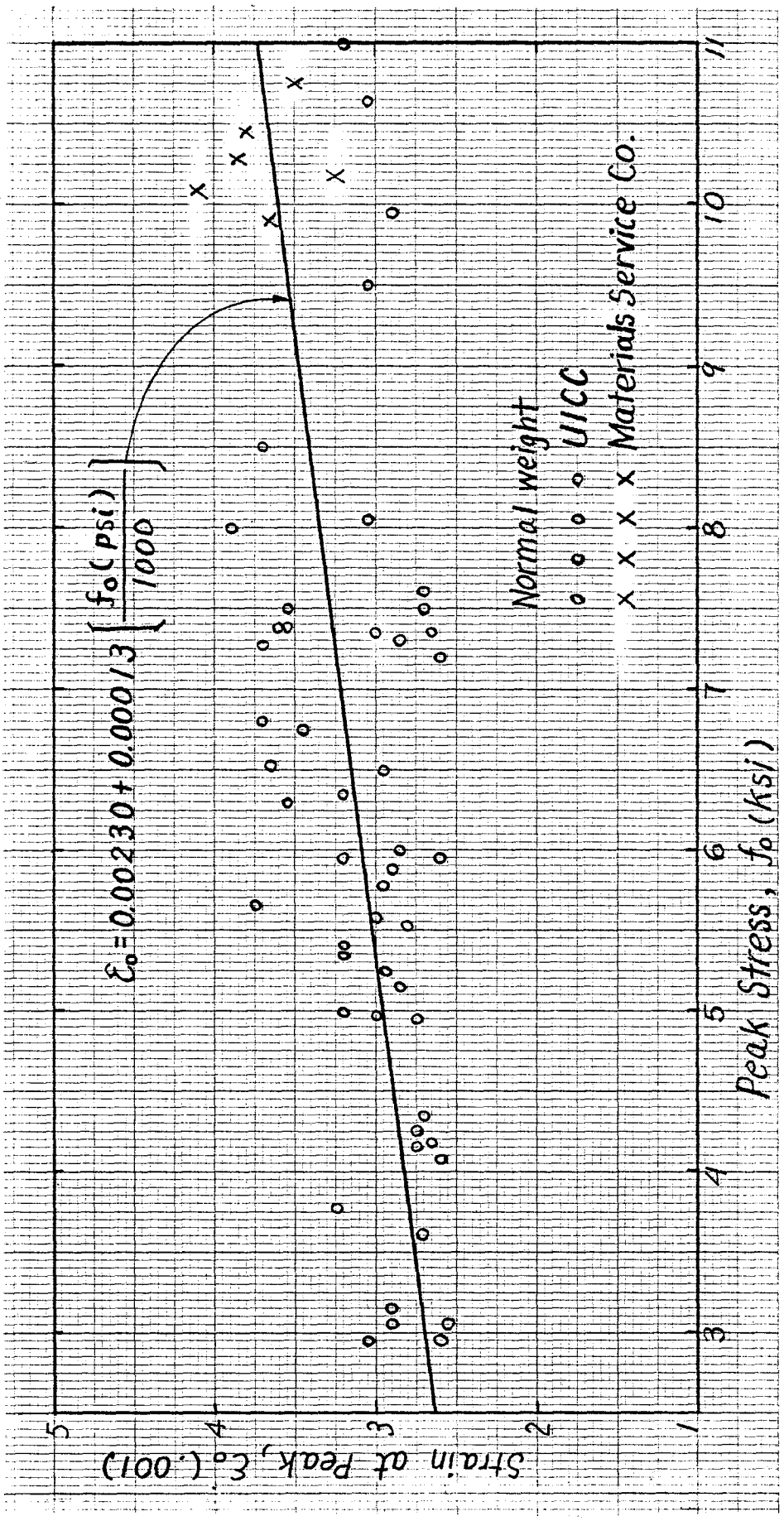

Fig. 4.8 Linear relation between ε_o and f_o for normal weight concrete.

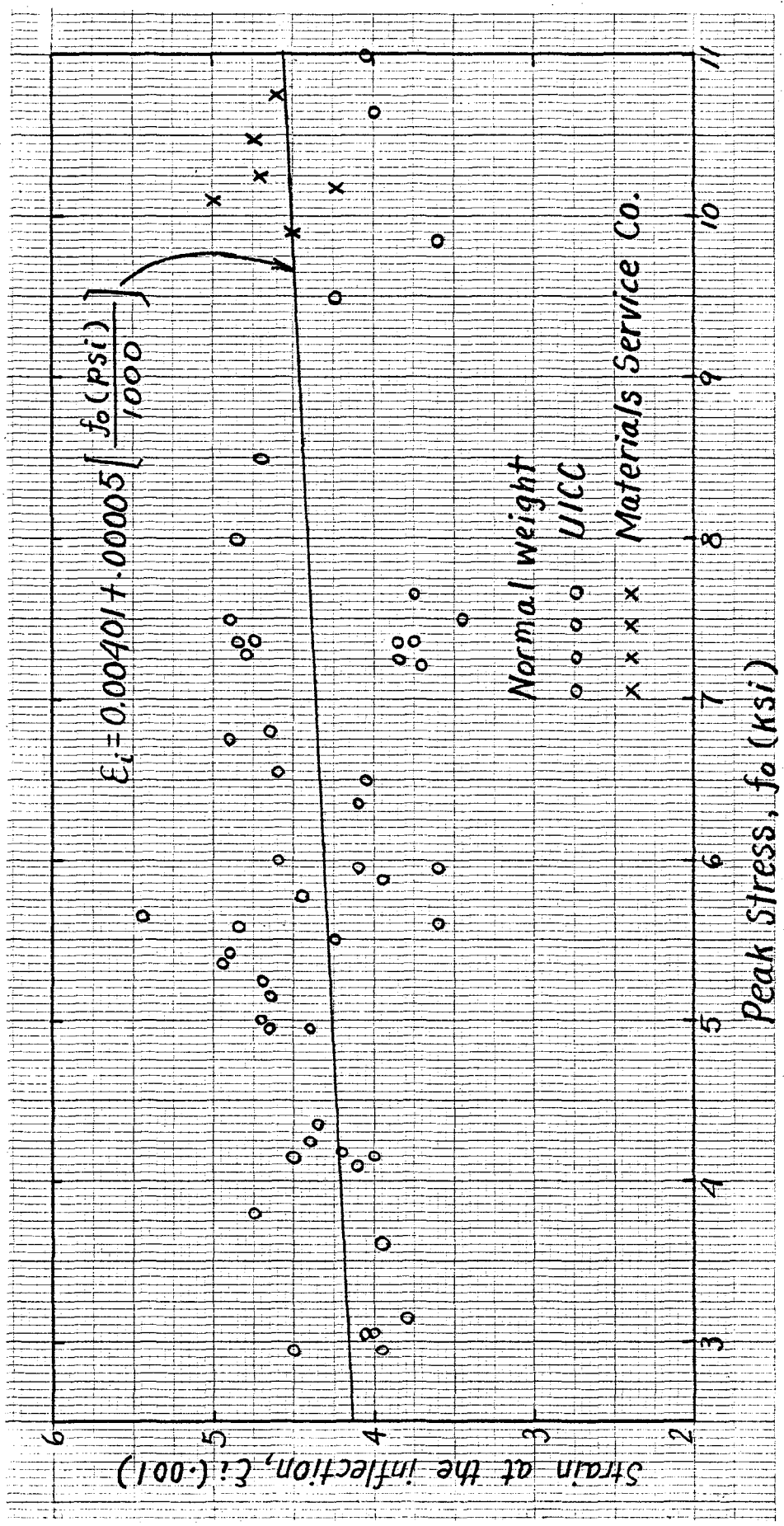

Fig. 4.9 Linear relation between ε_1 and f_o for normal weight concrete.

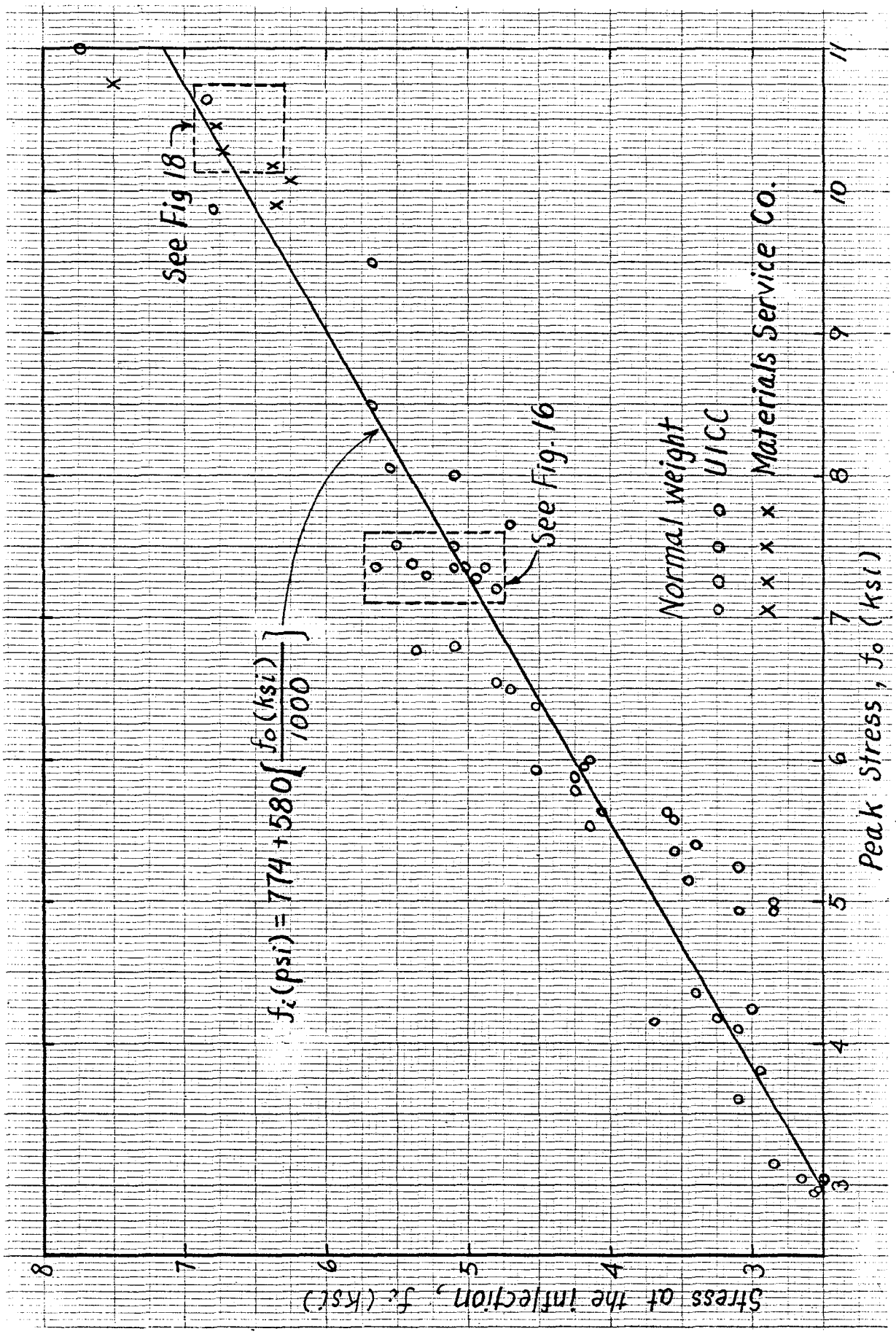

Fig. 4.10 Linear relation between f_i and f_o for normal weight concrete.

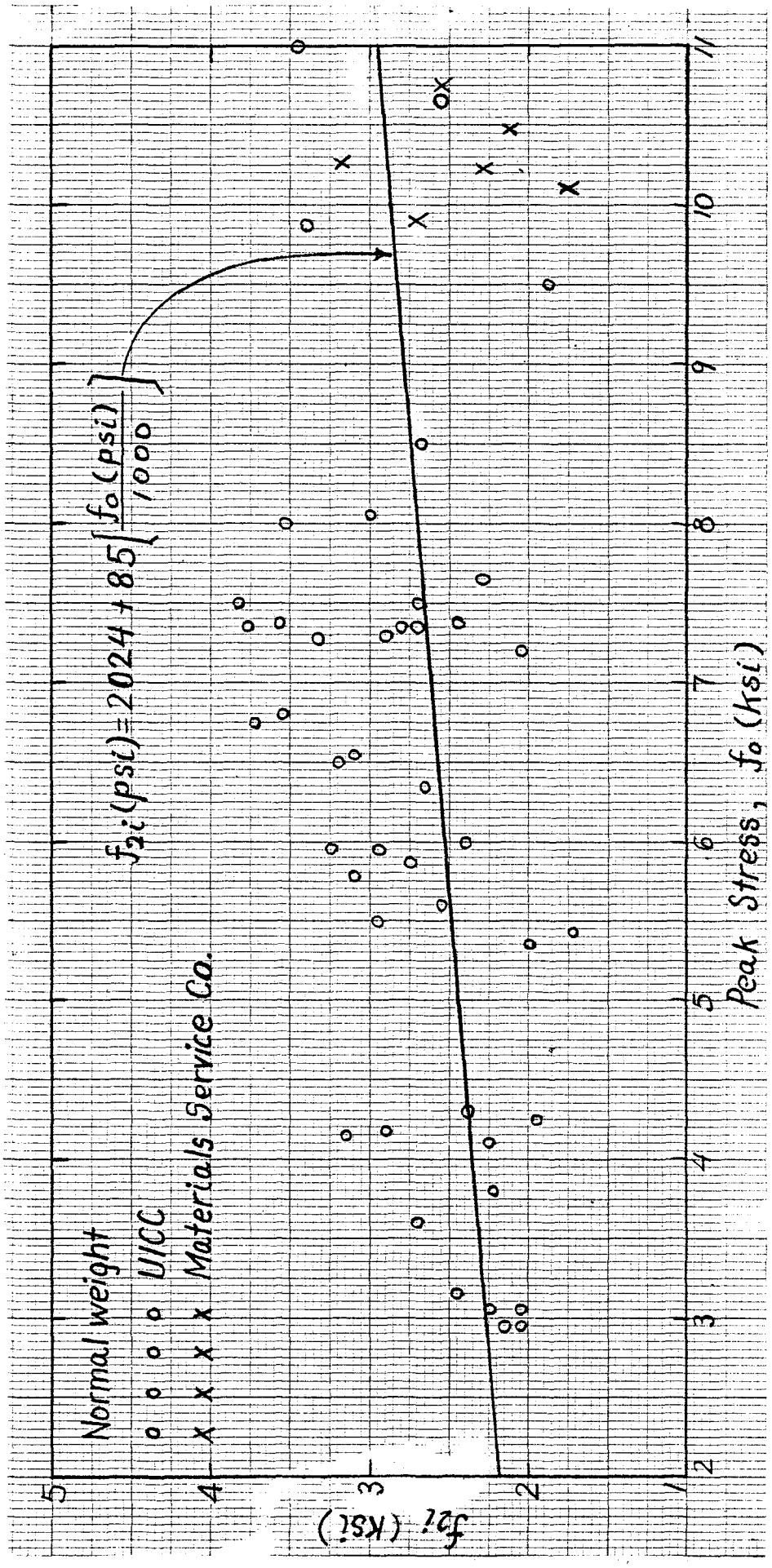

Fig. 4.11 Linear relation between f_{2i} and f_o for normal weight concrete.

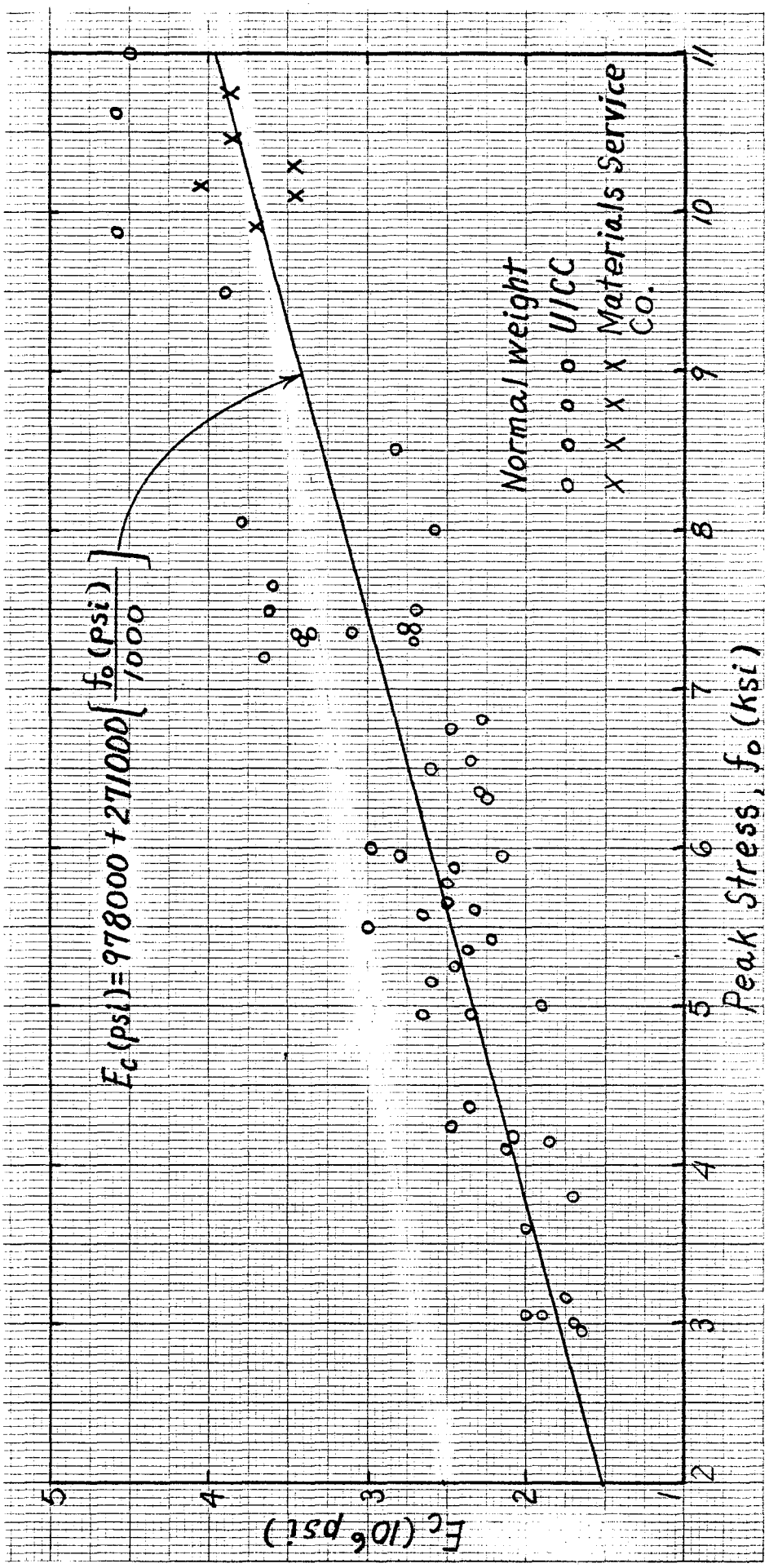

Fig. 4.12 Linear relation between E_c and f_o for normal weight concrete.

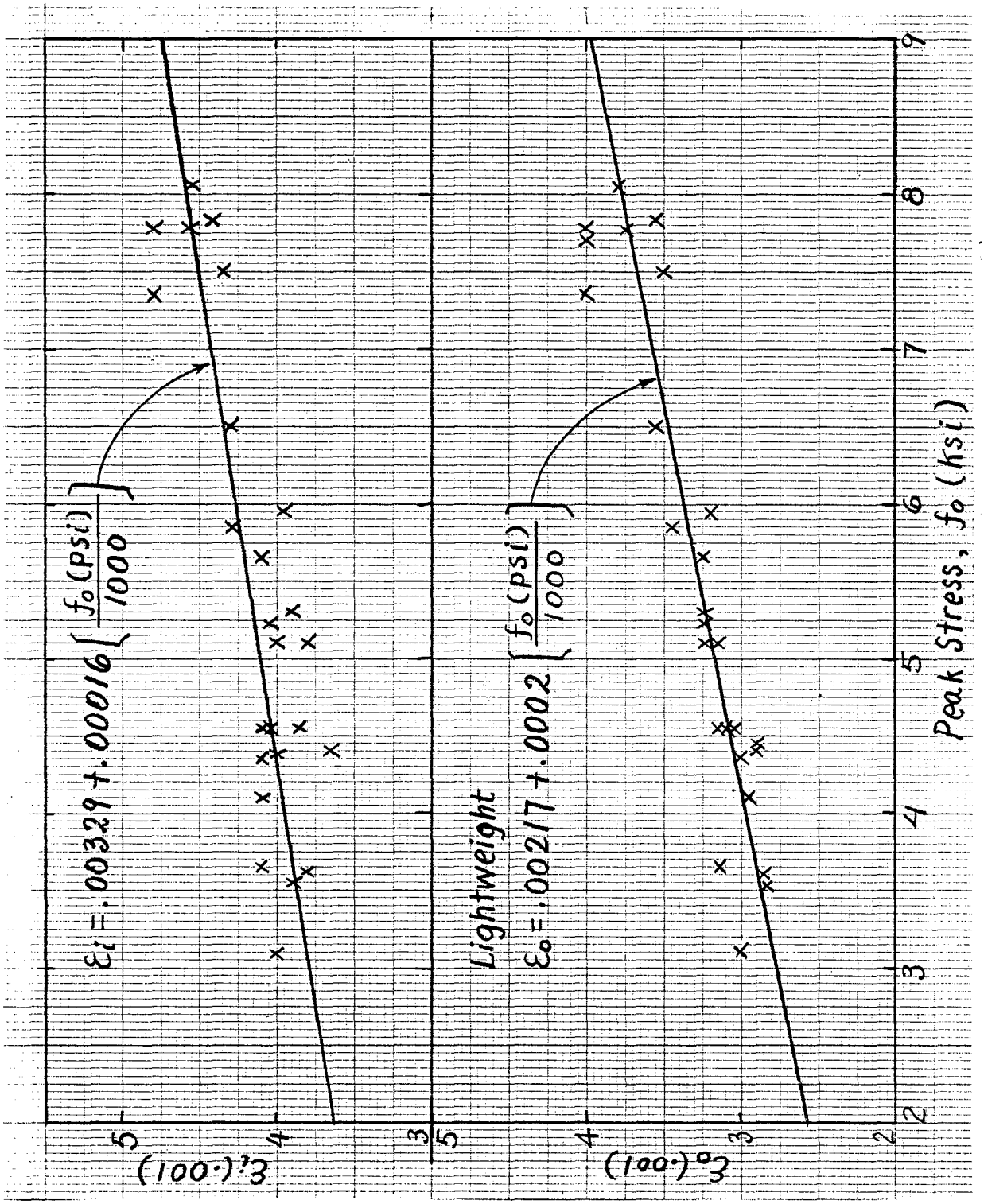

Fig. 4.13 Linear relation between ε_o, ε_i and f_o for lightweight concrete.

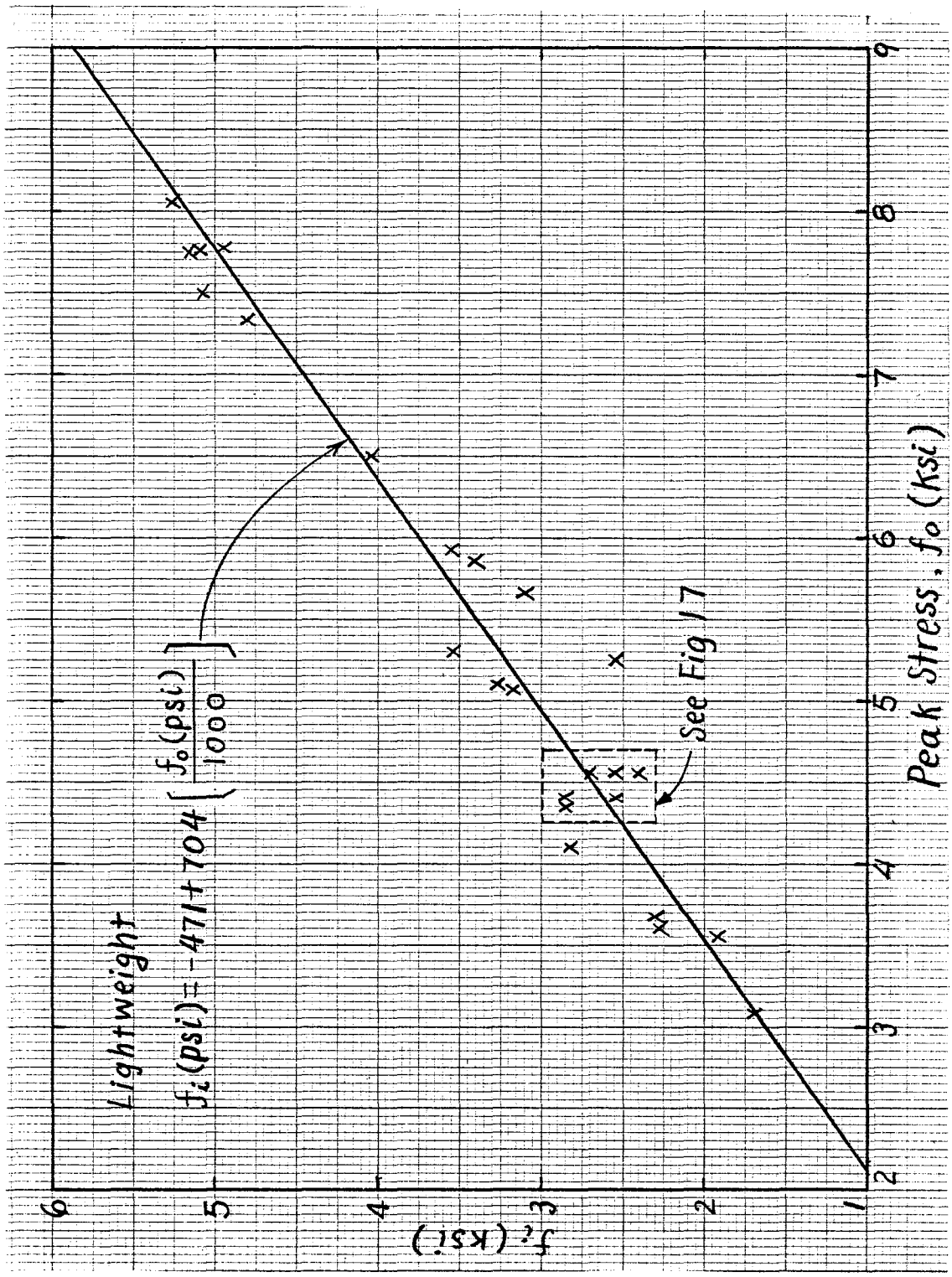

Fig. 4.14 Linear relation between f_i and f_o for lightweight concrete.

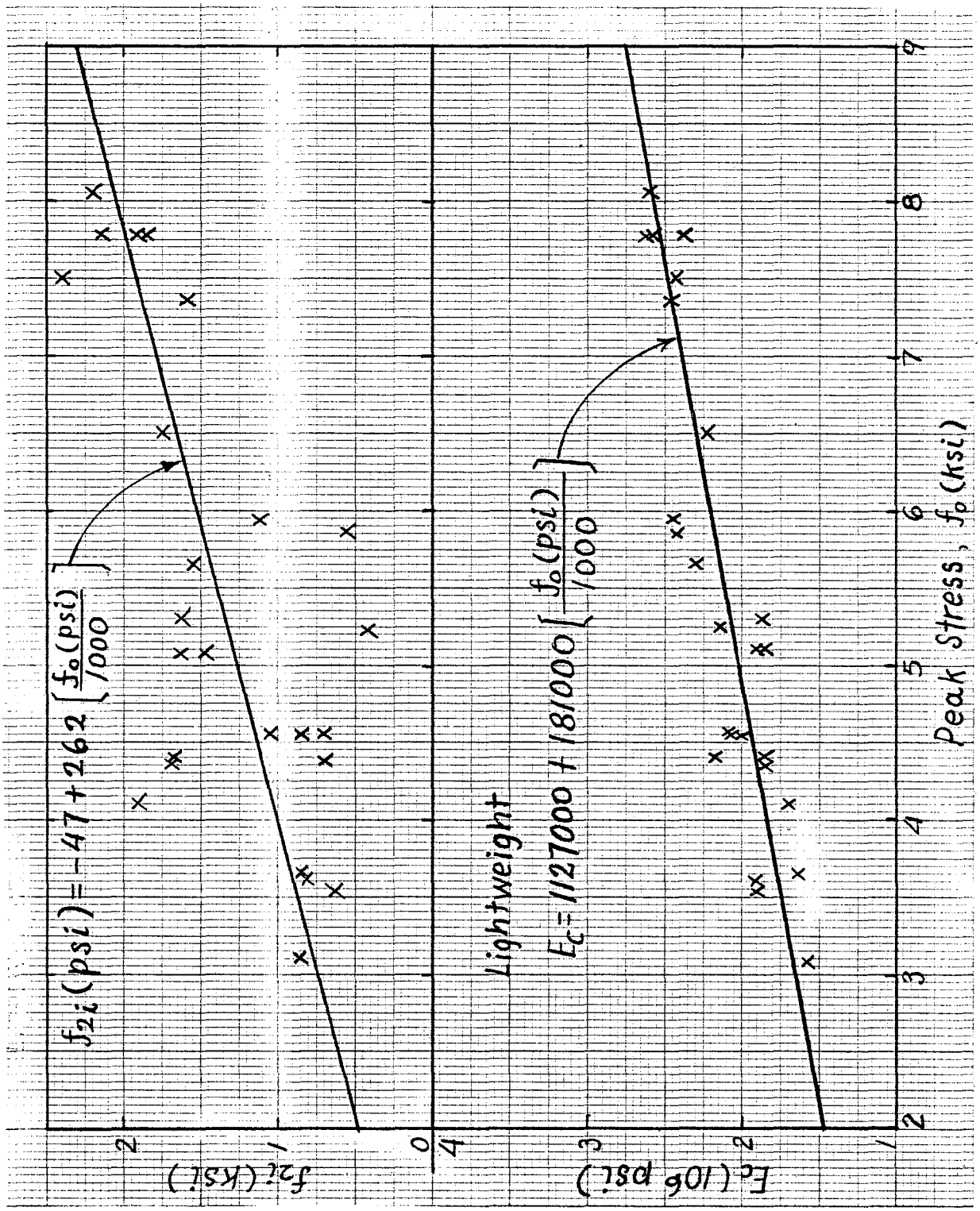

Fig. 4.15 Linear relation between E_c, f_{2i} and f_o for lightweight concrete.

of f_o^2 or $\sqrt{f_o}$ did not improve the fit. The linear regression equations relating the peak stress (independent variable) to the four key points of the curve are shown in Table 4.4. These lines are of the form $y = ax + b$ where y is the dependent variable, $x = f_o$ the peak stress, $\underline{a}$ the slope of the line and $\underline{b}$ the intercept. Also shown are some statistical characteristics of the data including the coefficients of correlation which indicate how well the data are approximated by a straight-line. It can be seen that for normal weight concrete the coefficients of correlation are poor for ε_o and ε_i. This seems to confirm the experimental observation that these parameters are almost constant for all values of f_o. Note also that the predicted values of the modulus of elasticity E_c given in Table 4.4 are generally smaller than those resulting from a standard ACI-ASTM test to determine the modulus using a compressometer attached to the middle portion of the cylinder; this is due to the different definitions of strain as used in this investigation.

Based on the above results, a computer program was written to generate a stress-strain curve for any given compressive strength and for a given type of aggregate (normal weight or lightweight). First the program calculates the coordinates of the four key points of the curve for the given compressive strength, from the relations shown in Table 4.4. Once these four points are determined, the four constants A, B, C and D of Eq. (4.1) are calculated separately as shown in Table 4.5 for the ascending and the descending portion of the curve by satisfying the conditions mentioned earlier. In Fig. 4.16, eight experimental curves whose compressive strength was about 7400 psi (51.8 MN/m^2) are compared with an analytic curve generated for a compressive strength equal to their average experimental compressive

TABLE 4.4

Regression Equations for the Key Parameters of the Stress-Strain Curve

	y*	a	b	Std. Dev.*	Coefficient of Variation*	Correlation Coefficient
Normal Weight	ε_o	0.000125	0.00230	0.000326	0.105	0.636
	f_i (psi)	580	774	326	0.073	0.966
	ε_i	0.00005	0.00401	0.000422	0.097	0.239
	f_{2i} (psi)	85	2024	656	0.256	0.263
	E_c (psi)	271,000	978,000	331,528	0.123	0.865
Lightweight	ε_o	0.00020	0.00217	0.000138	0.042	0.913
	f_i (psi)	704	-471	243	0.073	0.975
	ε_i	0.00016	0.00329	0.000176	0.043	0.801
	f_{2i} (psi)	262	-47	443	0.322	0.666
	E_c (psi)	180,900	1,127,000	143,778	0.068	0.885

*$y = a[f_o(\text{psi})/1000] + b$; Std. Dev. = $\sqrt{\Sigma(y_{data} - y)^2/n-1}$; coefficient of variation = (Std. Dev.) divided by the mean value of the dependent variable over the range considered.

TABLE 4.5

Constants of Equation for Generalized Stress-Strain Curves

	f_o psi	ε_o	Ascending				Descending			
			A	B	C	D	A	B	C	D
Normal Weight	3000	.00267	1.596973	-0.352041	-0.403025	0.647959	-1.275769	1.479520	-3.275768	2.479519
	4000	.0028	1.443399	-0.642542	-0.556601	0.357458	0.115286	0.306384	-1.884714	1.306384
	5000	.00292	1.364803	-0.758033	-0.635195	0.241966	0.326434	0.047969	-1.673565	1.047969
	6000	.00305	1.323699	-0.809490	-0.676301	0.190510	0.365932	-0.050730	-1.634068	0.949270
	7000	.00317	1.304016	-0.831952	-0.695982	0.168047	0.357600	-0.095550	-1.642398	0.904450
	8000	.00330	1.297725	-0.838836	-0.702275	0.161164	0.332631	-0.116274	-1.667369	0.883726
	9000	.00342	1.300356	-0.835973	-0.699641	0.164026	0.301863	-0.124428	-1.698136	0.875572
	10000	.00355	1.309239	-0.826130	-0.690761	0.173870	0.269654	-0.125315	-1.730346	0.874685
	11000	.00367	1.322664	-0.810704	-0.677334	0.189295	0.238022	-0.121764	-1.761977	0.878235
	12000	.00380	1.339499	-0.790439	-0.660501	0.209561	0.207840	-0.115354	-1.792160	0.884646
	13000	.00392	1.358955	-0.765731	-0.641044	0.234268	0.179552	-0.107095	-1.820446	0.892904
Lightweight	3000	.00277	1.541688	-0.466498	-0.458311	0.533502	0.178520	-0.046208	-1.821479	0.953791
	4000	.00297	1.374069	-0.745587	-0.625931	0.254413	0.223037	-0.084008	-1.776963	0.915992
	5000	.00317	1.287968	-0.849226	-0.712030	0.150773	0.235274	-0.103281	-1.764724	0.896719
	6000	.00337	1.242631	-0.892965	-0.757369	0.107035	0.231553	-0.112001	-1.768447	0.887999
	7000	.00357	1.220581	-0.911535	-0.779418	0.088464	0.219928	-0.114448	-1.780071	0.885551

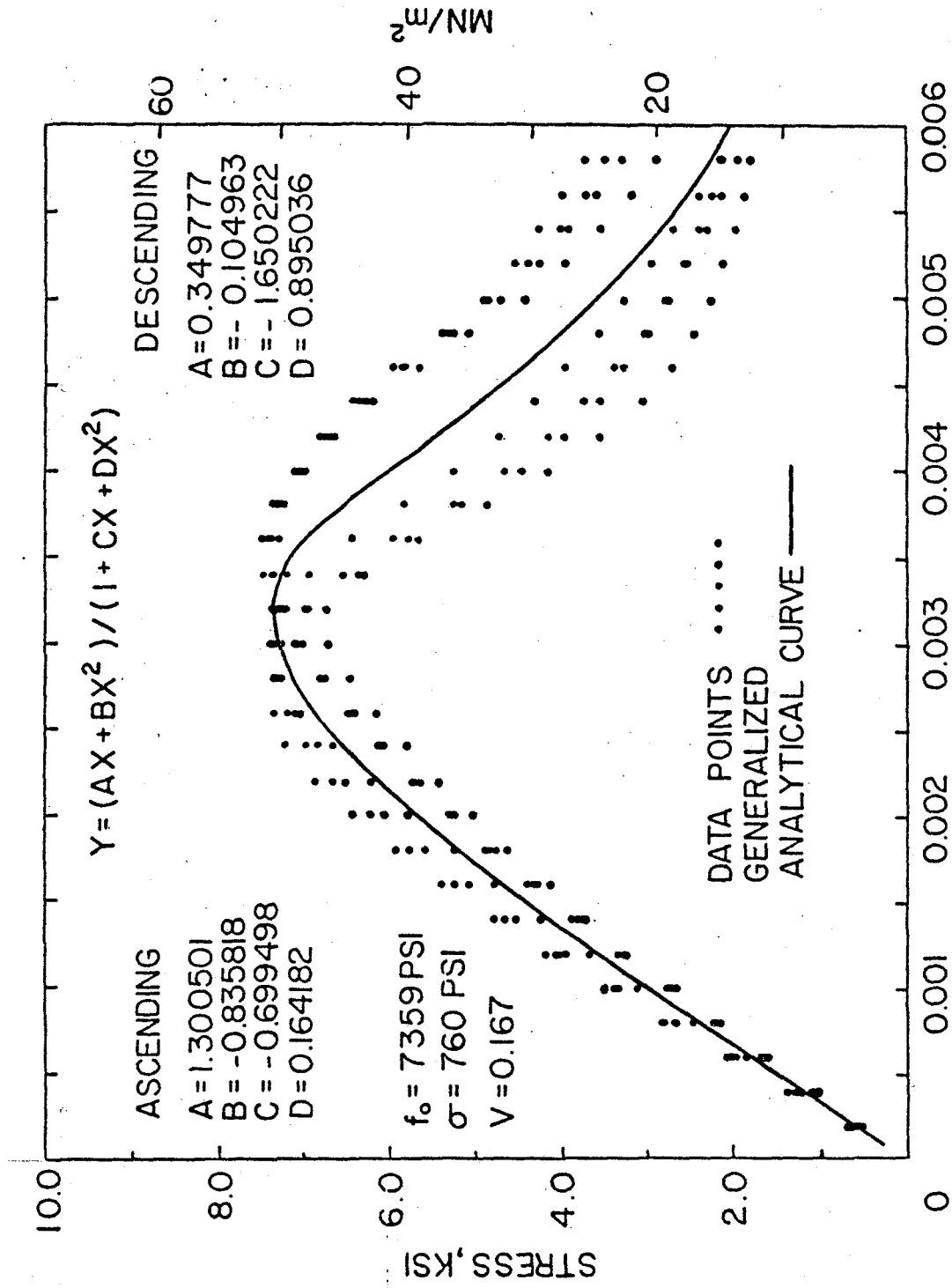

Fig. 4.16 Comparison of experimental data with the generalized analytic curve for normal weight concrete.

strength. From this comparison, it appears that the analytic expression is quite satisfactory. The experimental curves in Fig. 4.16 also illustrate the reproducibility of the descending portion of the stress-strain curve and the type of scatter that might be expected. A similar comparison is shown in Fig. 4.17 for lightweight concrete specimens whose compressive strength was about 4500 psi (31.5 MN/m^2).

4.6 VALIDATION OF THE ANALYTICAL EXPRESSION

Is the analytical procedure described here well suited to include the effect of lateral reinforcement which influences primarily the descending portion of the stress-strain curve? The answer is yes because the four constants for each the ascending and the descending portions of the curve are separately controlled as shown earlier.

Can the analytic curves generated from the experimental data of this investigation be valid for concrete made with different mix proportions? Or, how valid is the assumption that the stress-strain curve for a given type of concrete (normal weight or lightweight) can be expressed solely as a function of compressive strength, regardless of the mix proportions and age at testing? Although more experiments are needed to completely examine this assumption, some partial verification was obtained from the results of tests on six additional high strength, normal weight concrete cylinders. These cylinders were supplied by Material Service Corporation of Chicago and their mix proportions are shown in Table 4.1. Four of the cylinders were made in their laboratory, cured in the fog room for 55 days and tested at 56 days. The other two were cylindrical cores cut from an experimental column cast at the site of the Riverside Plaza structure in Chicago [8].

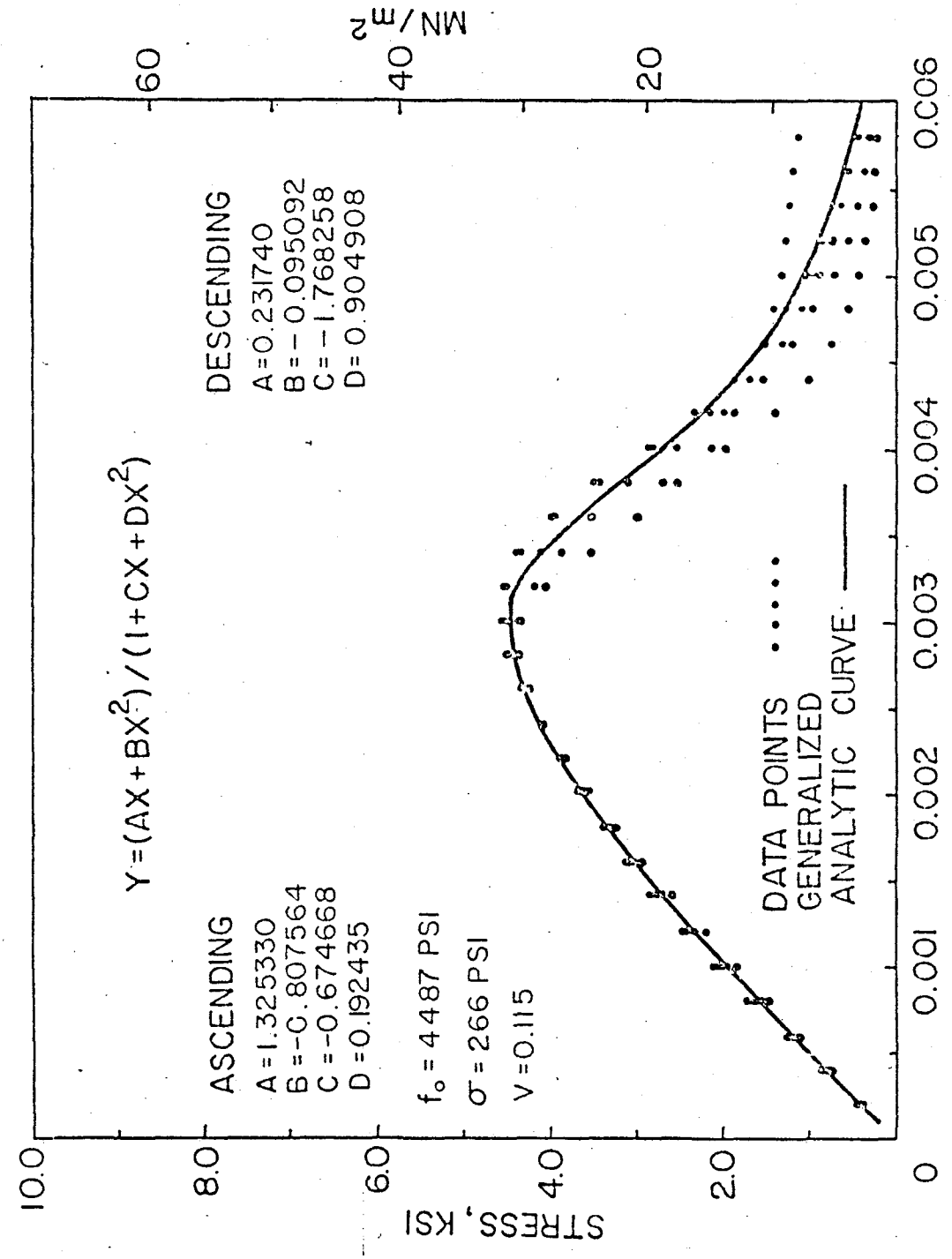

Fig. 4.17 Comparison of experimental data with the generalized analytic curve for lightweight concrete.

The cores were tested at 210 days after casting. The comparison of some of the data from these cylinders with a cylinder of comparable strength reported previously (UICC) can be seen in Fig. 4.18 along with the analytical curve generated for a compressive strength equal to the average of the data shown (10,366 psi or 72.5 MN/m^2).

How well the analytic expression would represent concrete behavior beyond a strain of 0.006 (which was the limiting strain of the experimental results)? Sangha and Dhir [31] have reported some experimental stress-strain curves of concrete cylinders up to a strain of 0.020. These curves were obtained by loading 2 in. (5 cm) diameter specimens at a rate of 2.5 micro-strain per second, in a very stiff machine of 5.85 MN (1200 kips) capacity. Equation (4.1) was fitted to the four key points of their curve and a comparison is shown in Fig. 4.19. It can be seen that the analytic expression is acceptable beyond the strain of 0.006.

The stress-strain curves reported here were obtained by testing concrete cylinders with length to diameter ratio of 2. Testing longer cylinders will reduce the effects of end restraints and may lead to different curves especially in the descending portion, as reported in [31, 36].

4.7 CONCLUSIONS

It has been shown in this investigation that:

1. High strength, normal weight and lightweight concretes do not fail in a brittle manner (provided special precautions are taken during testing) and exhibit a reproducible descending portion of the stress-strain curve.

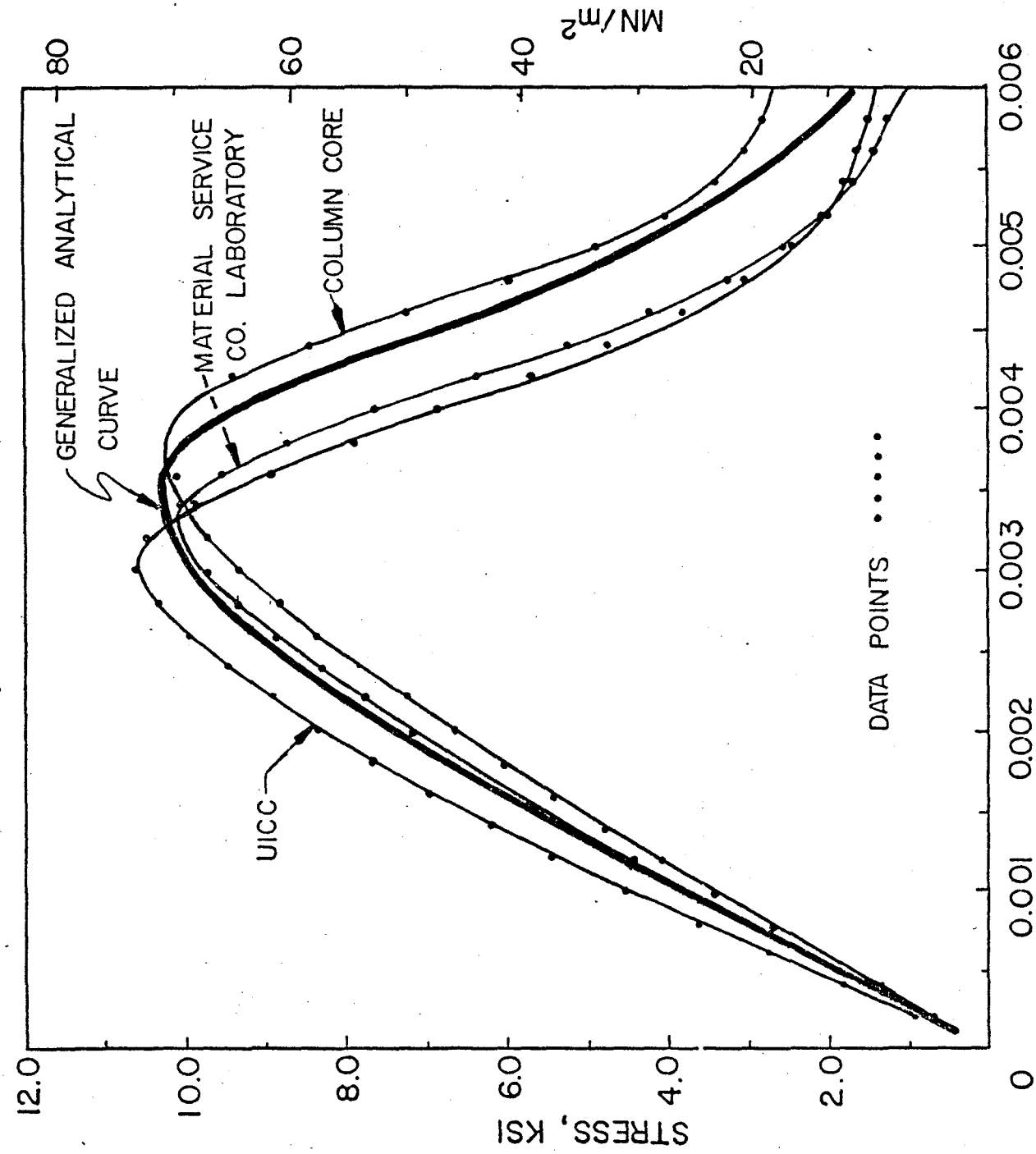

Fig. 4.18 Comparison of stress-strain curves for concrete from different sources.

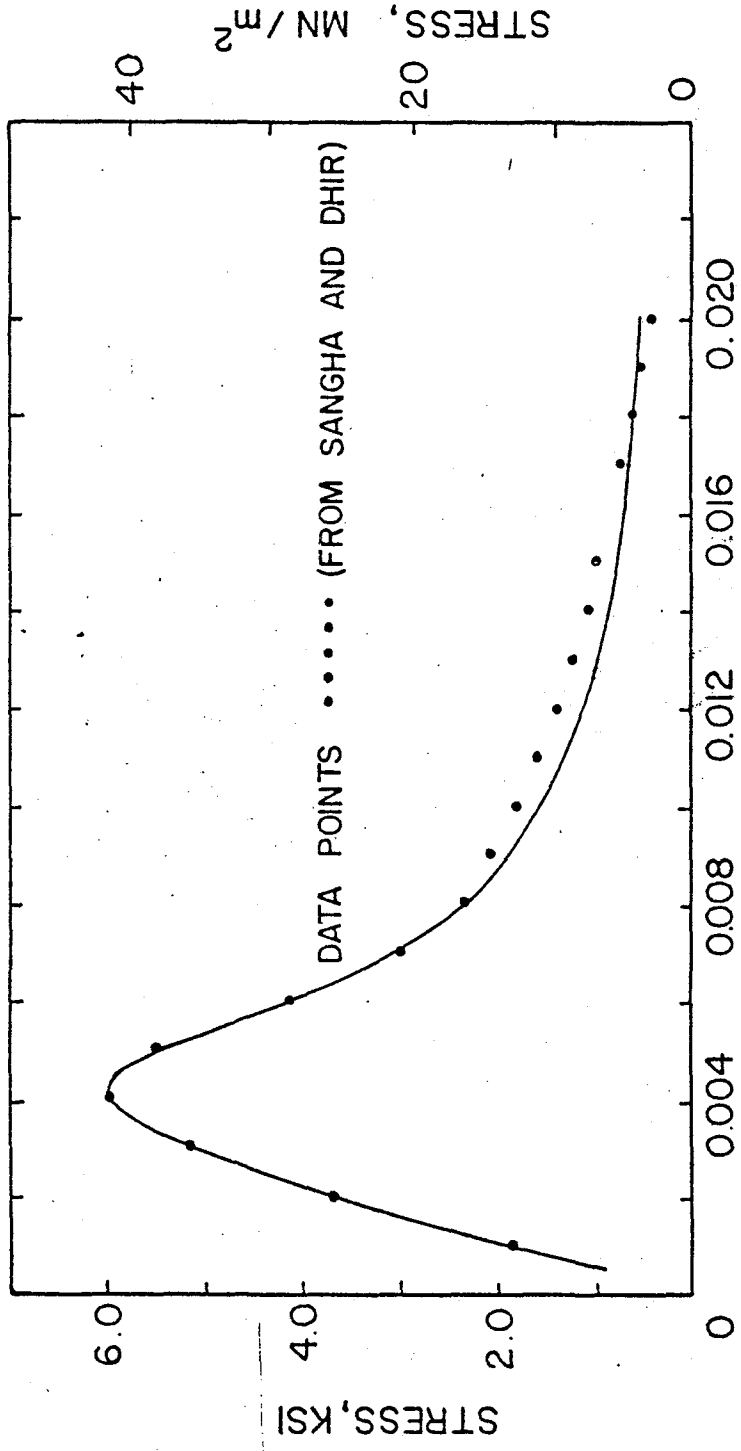

Fig. 4.19 Validation of the generalized curve up to a strain of 0.020.

2. The analytic expression for the stress-strain curve should contain constants which reflect not only the properties of the ascending portion but also those of the descending portion. The presence of lateral reinforcement can then be accounted for more rationally.

3. An inflection point was generally observed along the descending portion of the stress-strain curves. For normal weight concretes strains at the inflection point and at the peak did not change substantially with the compressive strength; whereas for lightweight concrete these strain values increased almost linearly with strength.

4. There is some indication that the coordinates of the inflection point may be a property of the material and thus are useful in the analytic characterization of the descending portion of the stress-strain curve.

5. The analytic expression developed here for the stress-strain curves of concretes in compression correlates well with experimental observations up to strains of 0.020.

CHAPTER V

A COMPUTER PROGRAM FOR THE NONLINEAR ANALYSIS OF REINFORCED CONCRETE SECTIONS

5.1 INTRODUCTION

A computer program was written to perform a nonlinear analysis of reinforced concrete sections, which include rectangular and T-beam, uniaxially-eccentrically-loaded and biaxially eccentrically-loaded columns. A general procedure for analyzing typical beam and column sections is explained, in which the actual stress-strain curves of concrete and steel were used, and no limiting concrete strain criterion was applied. The computer program accommodates the above variables. Theoretically predicted values of moments and curvatures are compared with some experimental results from the technical literature, and with the 1971 ACI code values to check the safety margin provided by the code.

5.2 GENERAL PROCEDURE FOR THE NONLINEAR ANALYSIS OF BEAM AND COLUMN SECTIONS

5.2.1 Assumptions

The following assumptions are used:

(a) Linear distribution of strains across the section (i.e., plane section remains plane after loading).

(b) Concrete has no strength in tension.

(c) Perfect bond exists between concrete and reinforcement (i.e., the same change in strain in the steel and concrete at the level of the steel).

(d) No limiting concrete strain criterion was assumed.

(e) The stress-strain relationships of concrete and steel are known.

(f) At all times, equilibrium of forces and moments must be satisfied.

5.2.2 General Equations in Determining Ultimate Capacity

Equilibrium of internal forces and external loads leads to:

$$C - T = P \tag{5.1}$$

where

C = compression on concrete and steel

T = tension on steel, tension on concrete being neglected

P = external load

Equilibrium of internal and external moments leads to:

$$M_{int} = M_{ext} \tag{5.2}$$

The compatibility of strains on concrete and steel, and the linear distribution of strain along the depth of the section even after cracking leads to:

$$\left.\begin{aligned} \varepsilon_s &= \frac{d-c}{c}\,\varepsilon_c \\ \varepsilon_s' &= \frac{c-d''}{c}\,\varepsilon_c \end{aligned}\right\} \tag{5.3}$$

where

c = depth of neutral axis

d = distance from extreme fiber to centroid of tension steel

d'' = distance from extreme fiber to centroid of compression steel

ε_c = strain on extreme compressive fiber

ε_s = strain at centroid of tension steel

ε'_s = strain at centroid of compression steel

The constitutive equations of concrete in compression and steel in tension are assumed to be of the general forms:

$$f_c = f(\varepsilon_c) \tag{5.4}$$

$$f_s = f(\varepsilon_s) \tag{5.5}$$

The above general equations will be applied to the cases of beams and columns in the following sections.

5.3 BEAM UNDER PURE BENDING

5.3.1 Behavior of Beam

The position of the neutral axis, the strain on the extreme compressive fiber, and the tensile strain in the steel are the key characteristics for describing the beam behavior during loading. The maximum compressive strain on the concrete, ε_c, increases with the applied moment and takes on values such as ε_{c1}, ε_{c2}, ... until failure as shown in Fig. 5.1; simultaneously the neutral axis shifts upwards or downwards as shown in Figs. 5.3 and 5.4; the tensile strain in the steel at ultimate observed capacity, determine the failure patterns of the beam, i.e. either a ductile or a brittle failure. Due to the different failure patterns, beam sections are classified as follows:

1. Under-reinforced Beams

   The tensile strain in the steel at ultimate moment capacity of the section is greater than the yield strain, i.e. $\varepsilon_s > \varepsilon_y$ as shown in Fig. 5.2, the failure pattern is ductile, and the neutral axis shifts

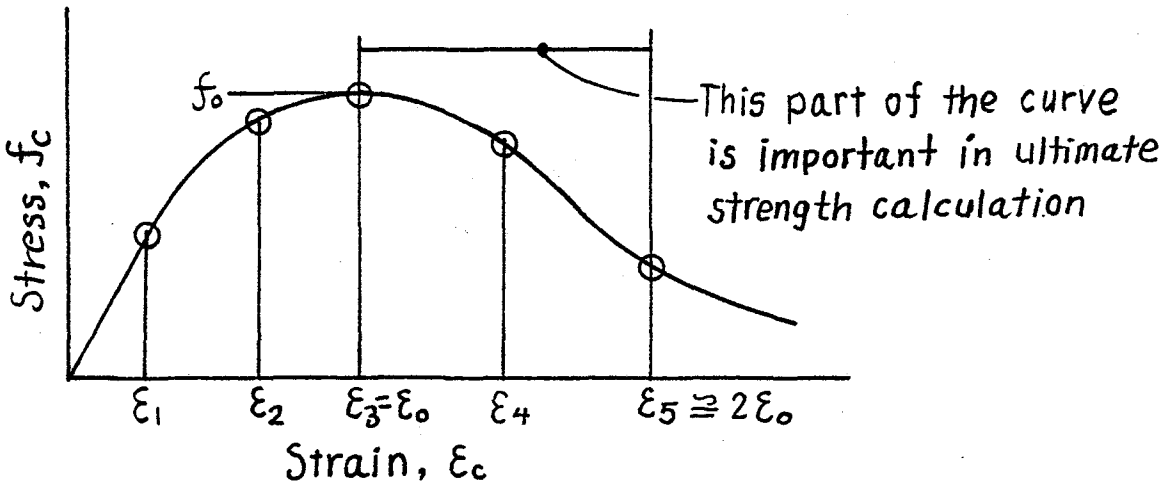

Fig. 5.1 Stress-strain curve of concrete.

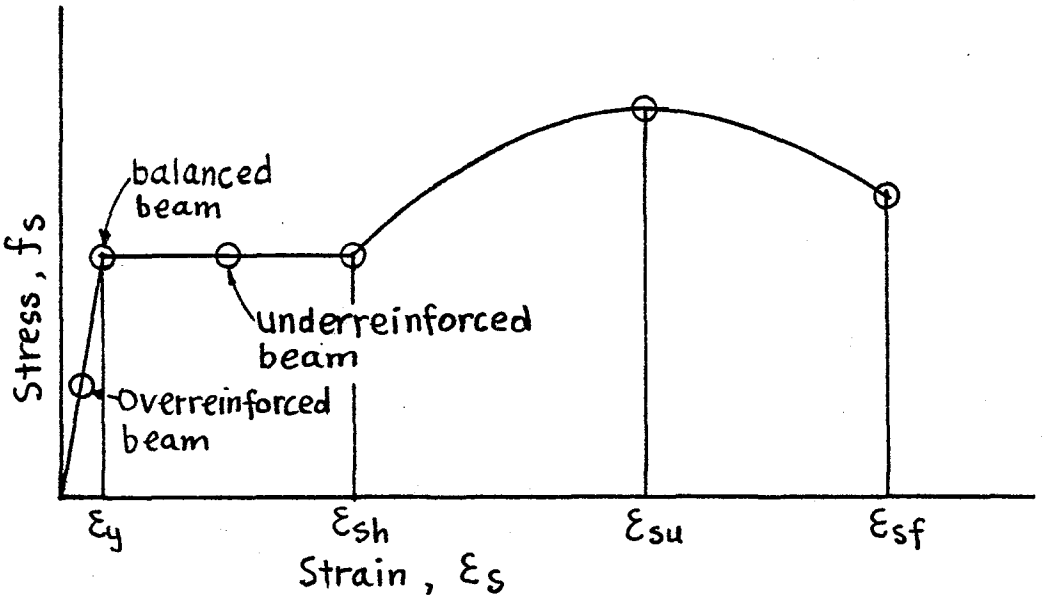

Fig. 5.2 Stress-strain curve of grade 60 steel.

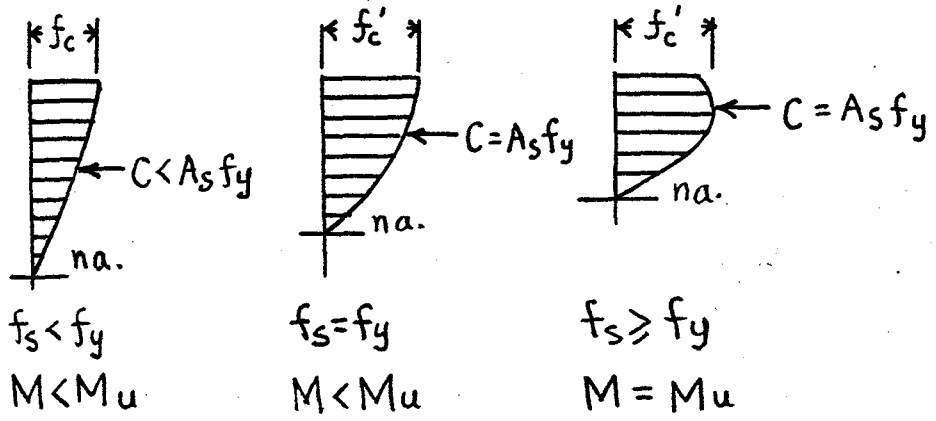

Fig. 5.3 Upwards shifting of neutral axial under loading for underreinforced beams.

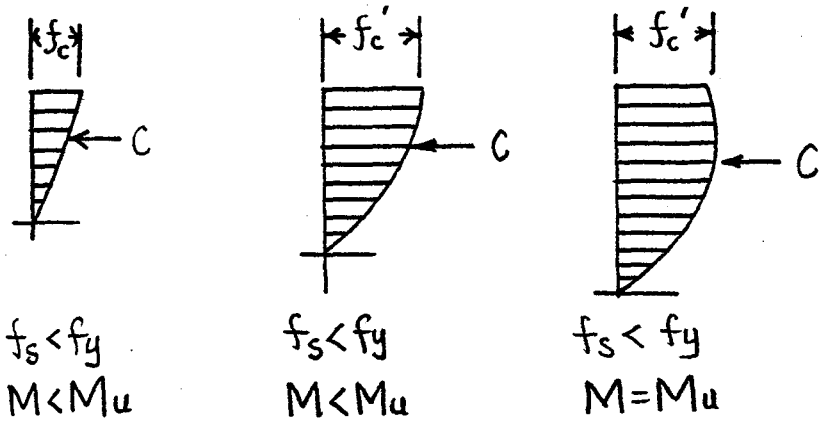

Fig. 5.4 Downwards shifting of neutral axial under loading for overreinforced beams.

upwards under loading toward the extreme compressive fiber as shown in Fig. 5.3.

2. Overreinforced Beams

The tensile strain in the steel at ultimate moment capacity of the section is smaller than the yield strain, i.e. $\varepsilon_s < \varepsilon_y$, as shown in Fig. 5.2 the failure pattern is brittle and the neutral axis shifts downwards toward the extreme tensile fiber as shown in Fig. 5.4.

3. Balanced Beams

The tensile strain in the steel at ultimate moment capacity of the section is exactly equal to the yield strain, i.e. $\varepsilon_s = \varepsilon_y$, as shown in Fig. 5.2; the balanced beam in ultimate strength design is not a practical beam, but the concept is fundamental to guide the design procedure to avoid a brittle failure pattern, i.e. overreinforced beam design.

Two types of beam cross sections, i.e. rectangular and T-beam, will be analyzed next according to the theoretical procedure described in Section 5.2. The ACI code formula will not be repeated here, although they will be used to compare the results.

5.3.2 Rectangular Beam

Rectangular beams can be either singly reinforced or doubly reinforced as shown in Fig. 5.6. The nonlinear analysis procedure as applied to rectangular beams is explained below; the corresponding general equations are given first as:

Equilibrium equations

$$\alpha f'_c bc + A'_s f'_s - A_s f_s = 0 \qquad (5.6)$$

$$\alpha f'_c bc(d-\beta c) + A'_s f'_s (d-d'') = M \tag{5.7}$$

Compatibility Equations

$$\left.\begin{aligned} \varepsilon_s &= \frac{d-c}{c}\,\varepsilon_c \\ \varepsilon'_s &= \frac{c-d''}{c}\,\varepsilon_c \end{aligned}\right\} \tag{5.8}$$

Constitutive Equations

$$\left.\begin{aligned} f_s &= f(\varepsilon_s) \\ f'_s &= f(\varepsilon'_s) \end{aligned}\right\} \tag{5.9}$$

$$\left.\begin{aligned} \alpha &= \alpha(\varepsilon_c) \\ \beta &= \beta(\varepsilon_c) \end{aligned}\right\} \tag{5.10}$$

where α and β are explained in Fig. 5.5

Curvature

$$\phi = \frac{\varepsilon_c}{c} \tag{5.11}$$

In the above equations, there are only two independent parameters, namely the depth of neutral axis, c, and strain at extreme compressive fiber, ε_c. Generally, ε_c is assumed first, then the depth of neutral axis c is determined by trial and error in order to satisfy equilibrium equations (5.6), through the use of compatibility and constitutive equations; then the corresponding moment M, and curavture ϕ are calculated from Eqs. (5.7) and (5.11). Typical variations between M and ε_c are shown in Fig. 5.7 from which the maximum moment capacity M_u can be determined. The logical flowchart for generating the moment-curvature relationship of a given beam

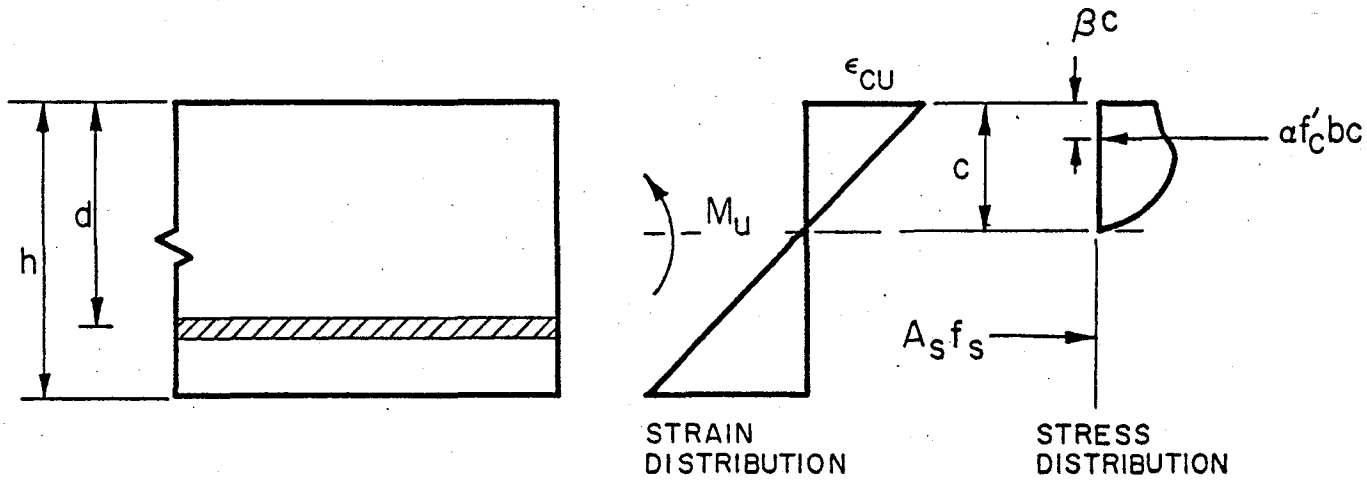

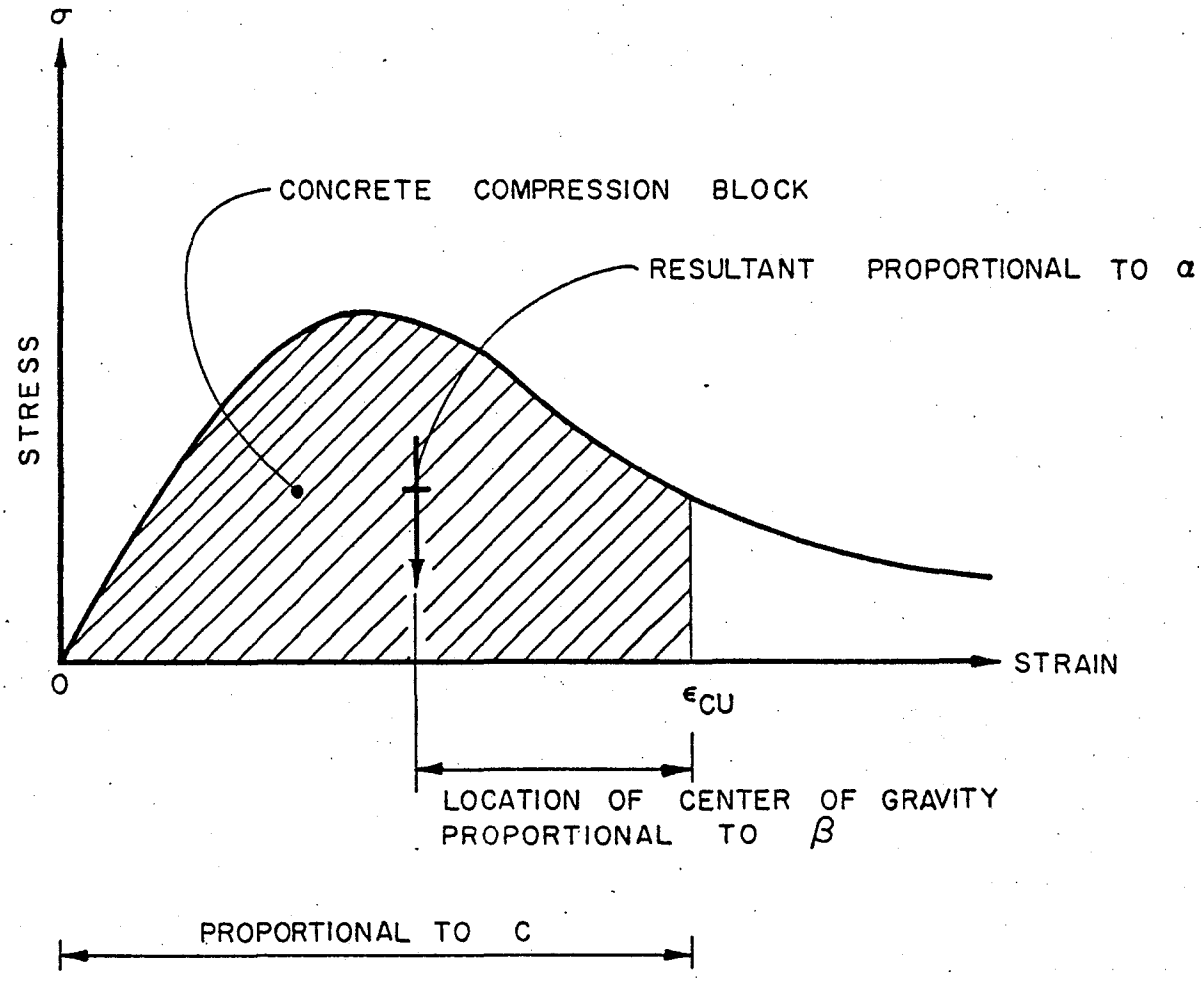

Fig. 5.5 Parameters α and β for stress block of concrete compression zone.

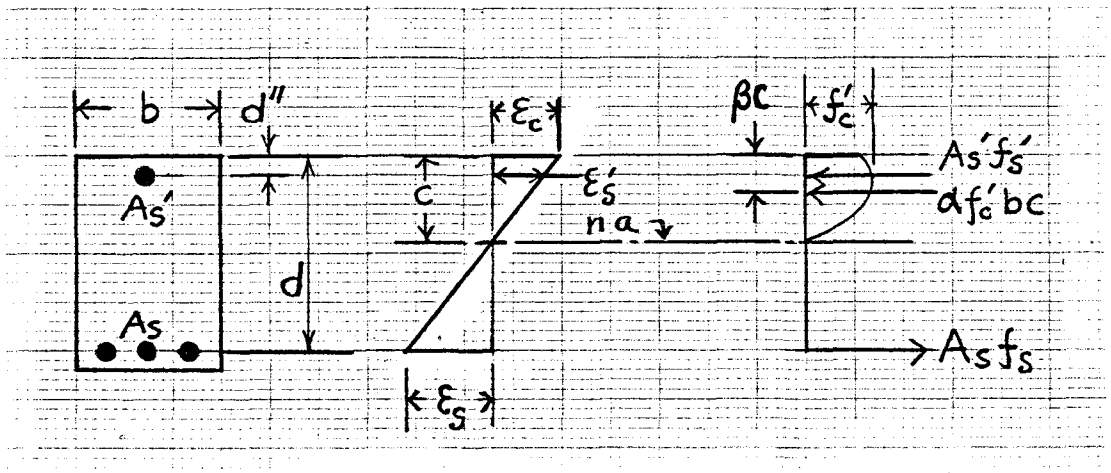

Fig. 5.6 Forces in rectangular beam.

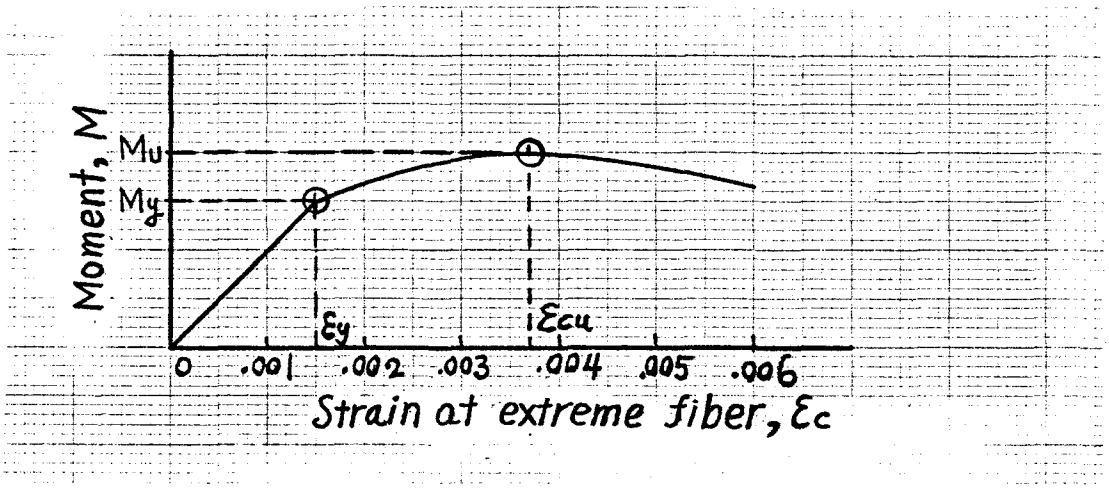

Fig. 5.7 Relationship of M-ε_c.

cross section is given in Table 5.1, the corresponding computer program (Appendix I), and for typical relationships of $M-\varepsilon_c$ and $M-\phi$ as generated by the program for a given beam cross section are shown in Figs. 5.8a and 5.8b.

5.3.3 T-Beam

When a T-beam does not act as a rectangular beam, its compression zone may be divided, for the purpose of this analysis, into two parts as shown in Fig. 5.9; part (1) with dimension (bxc), and part (2) with dimension (b-b') x (c-t). The corresponding general equations for the T-sections are given below:

Equilibrium Equations

$$\alpha_1 f'_c bc + A'_s f'_s - \alpha_2 f'_c (b-b')(c-t) - A_s f_s = 0 \tag{5.12}$$

$$\alpha_1 f'_c bc(d-\beta_1 c) + A'_s f'_s (d-d'') - \alpha_2 f'_c (b-b')(c-t)[d-t-\beta_2(c-t)] = M_{ext} \tag{5.13}$$

Compatibility Equations

$$\left.\begin{aligned} \varepsilon_s &= \frac{d-c}{c}\varepsilon_c \\ \varepsilon_s &= \frac{c-d''}{c}\varepsilon_c \\ \varepsilon_{fb} &= \frac{c-t}{c}\varepsilon_c \end{aligned}\right\} \tag{5.14}$$

Constitutive Equations

$$\left.\begin{aligned} f_s &= f_s(\varepsilon_s) \\ f'_s &= f_s(\varepsilon_s) \end{aligned}\right\} \tag{5.15}$$

TABLE 5.1

Flowchart - Rectangular and T-Beam Under Pure Bending (Generate Beam M-ϕ Curve)

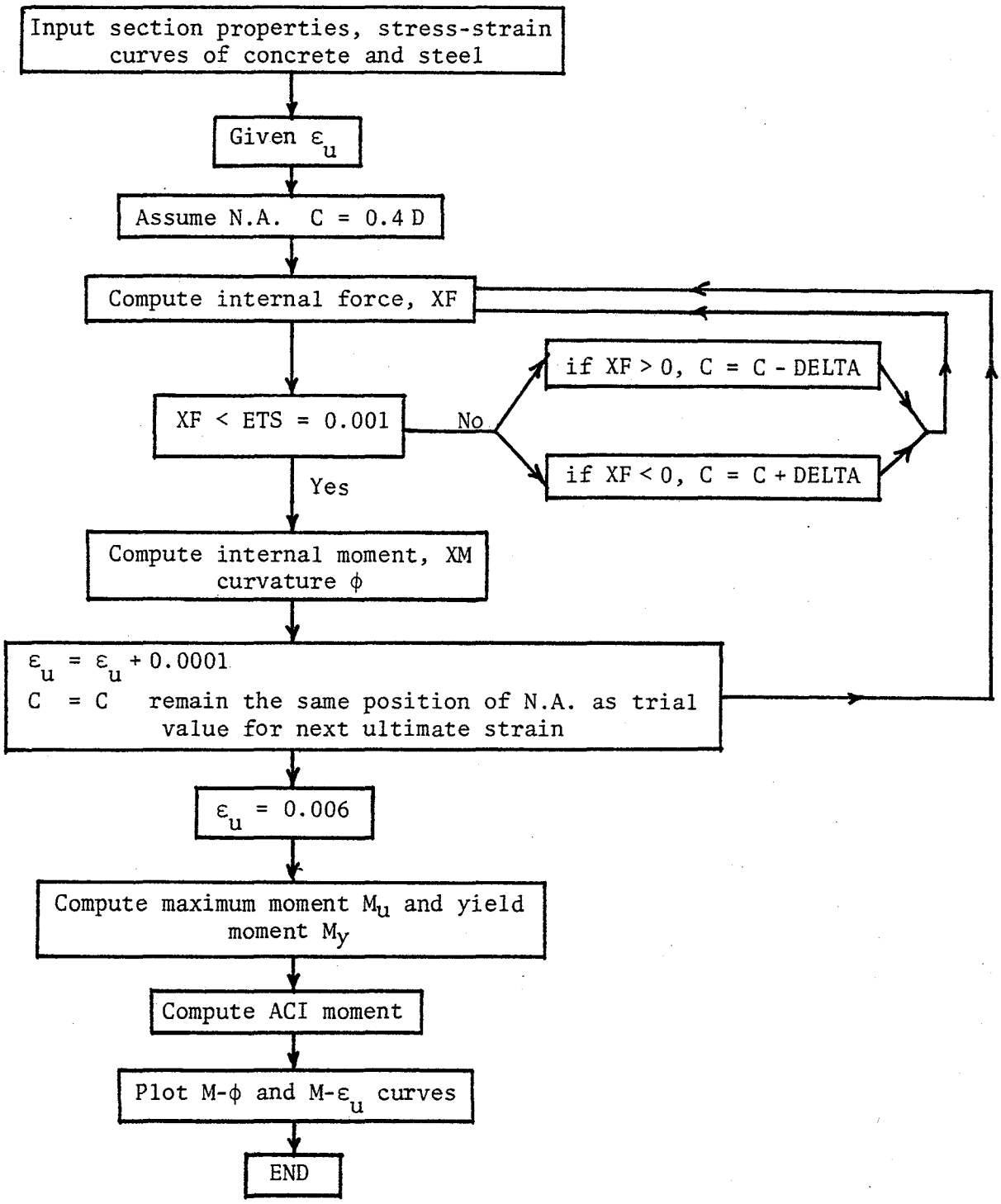

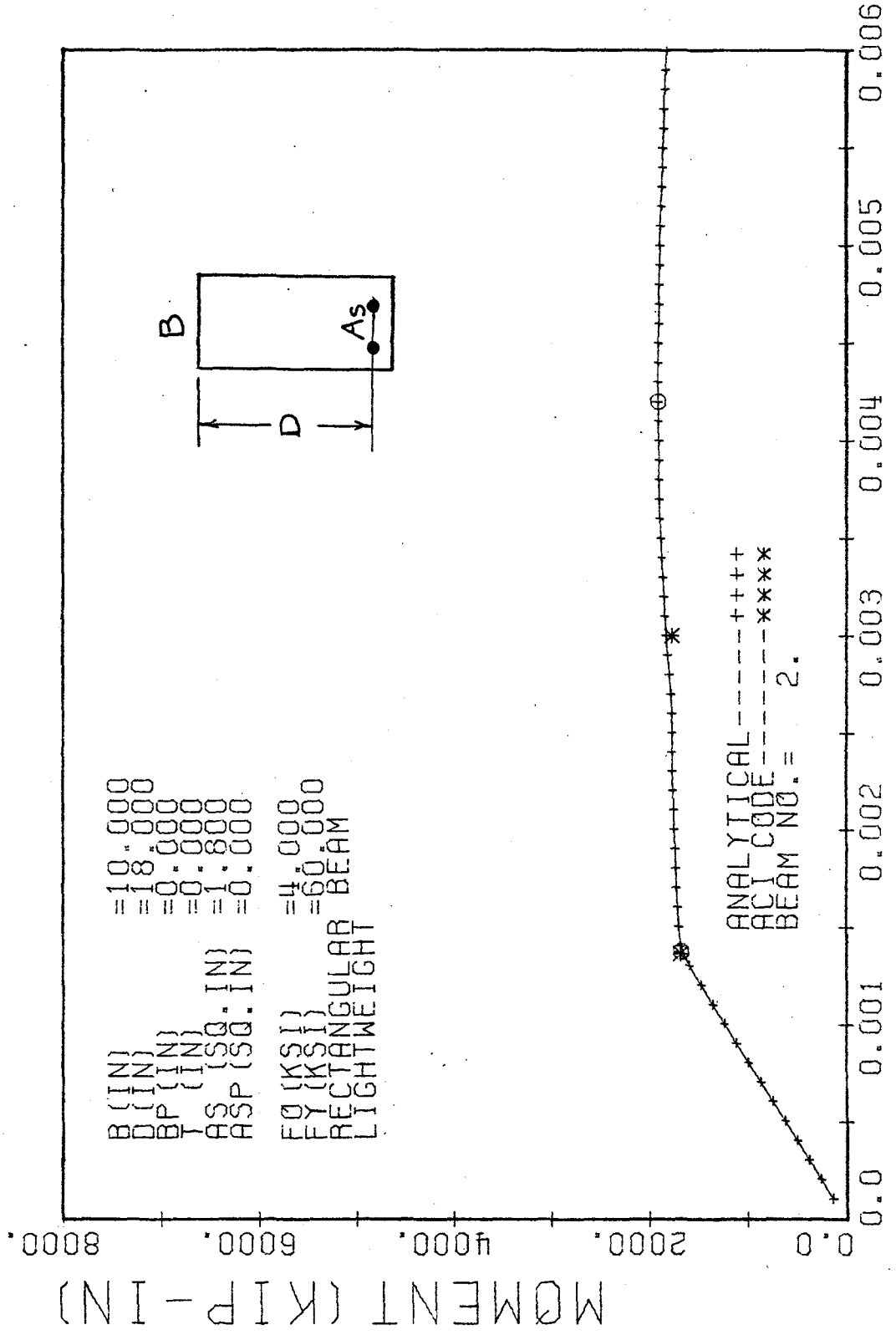

Fig. 5.8a M-ε_c relationship for rectangular beam.

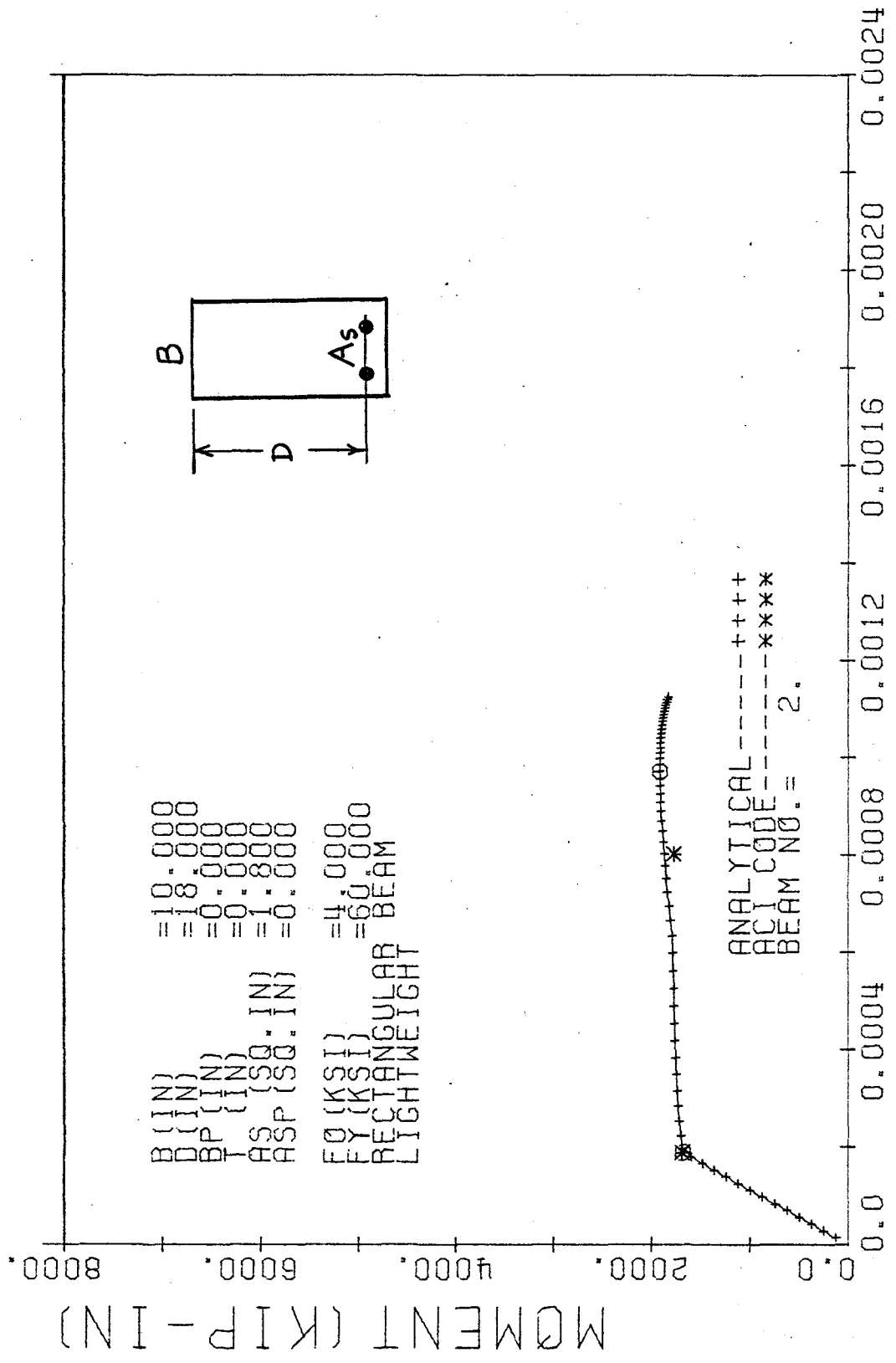

Fig. 5.8b M-ϕ relationship for rectangular beam.

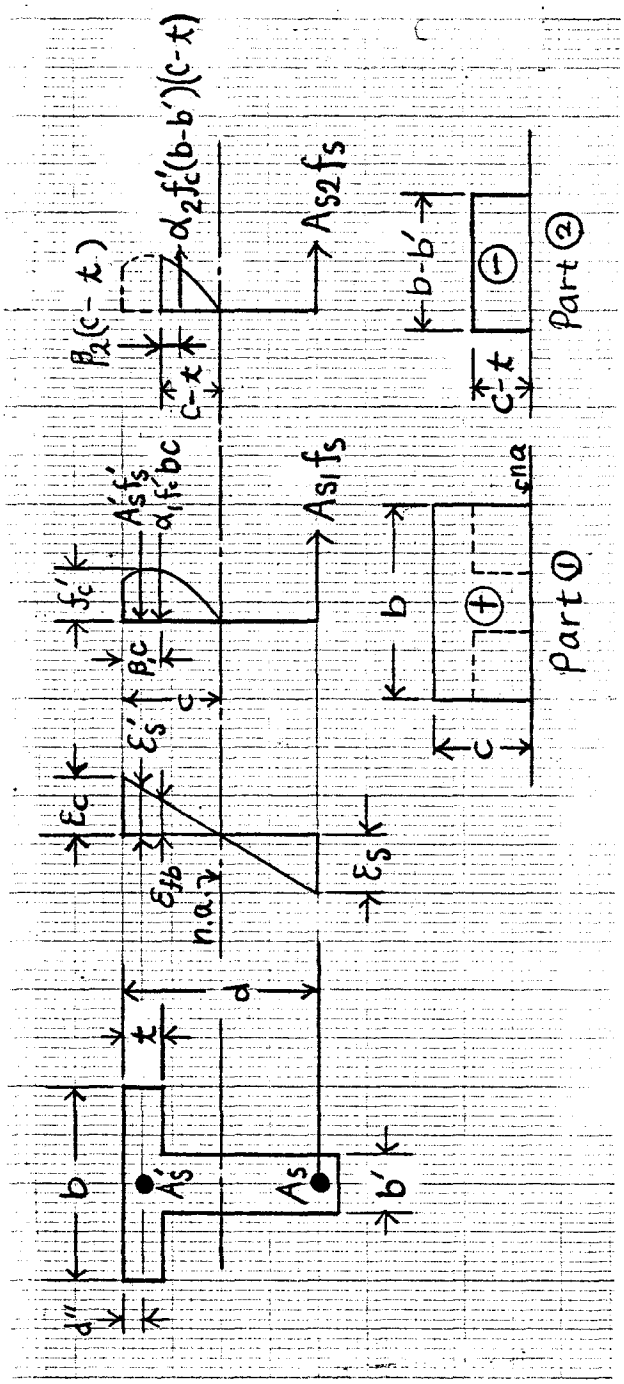

Fig. 5.9 Forces in T-beam.

$$\left.\begin{aligned} \alpha_1 &= \alpha(\varepsilon_c) \\ \beta_1 &= \beta(\varepsilon_c) \\ \alpha_2 &= \alpha(\varepsilon_{fb}) \\ \beta_2 &= \beta(\varepsilon_{fb}) \end{aligned}\right\} \qquad (5.16)$$

where ε_{fb} is the strain at the joint of flange and web

Curvature

$$\phi = \frac{\varepsilon_c}{c} \qquad (5.17)$$

The logical flowchart is the same as that for the rectangular section as shown in Table 5.1, and the corresponding computer program is given in Appendix 5.1. Typical computer outputs are shown in Figs. 5.10a and 5.10b.

5.4 COLUMN UNDER AXIAL LOAD AND BENDING

5.4.1 Behavior of Columns

A reinforced-concrete column may reach its strength under enumerable combinations of bending moments and axial loads. These may vary from a maximum axial load, P_o, which is associated with zero bending moment, to a maximum moment, M_o, associated with a zero axial load. It can be assumed that axial load and bending moment act independently of each other on a given cross section of a column. Figure 5.11 shows a schematic representation of a column under a bending moment, M, and an axial load, P, and Fig. 5.12, a statically equivalent system in which M = Pe. The locus of the combinations of axial load, P, and moment, M, at which a column attains its strength is usually represented by an interaction diagram or P-M diagram. A typical diagram is shown schematically in Fig. 5.13 for a rectangular cross section. Because the eccentricity e = M/P may be

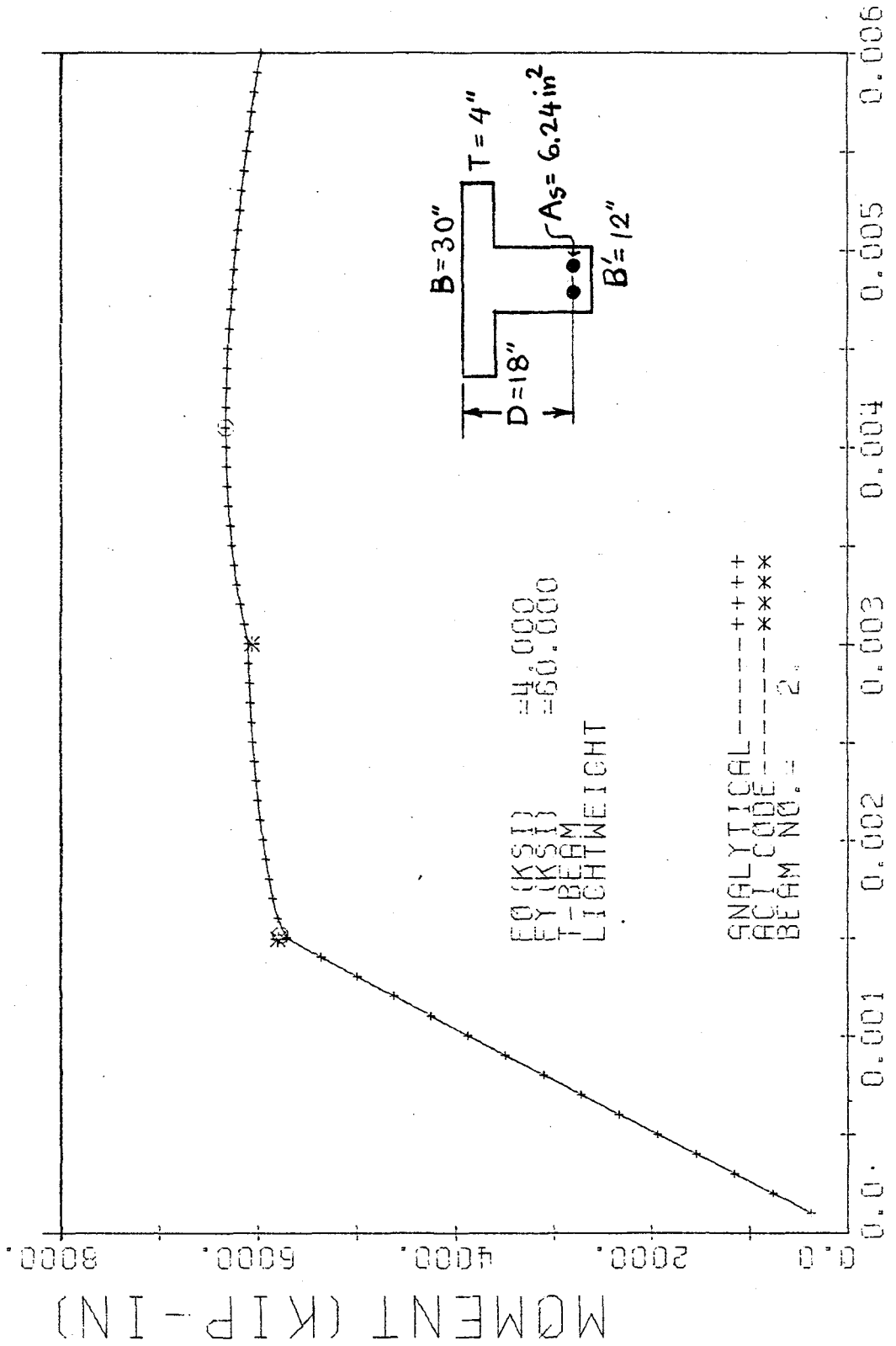

Figure 5.10a M-ε_c relationship for T-beam.

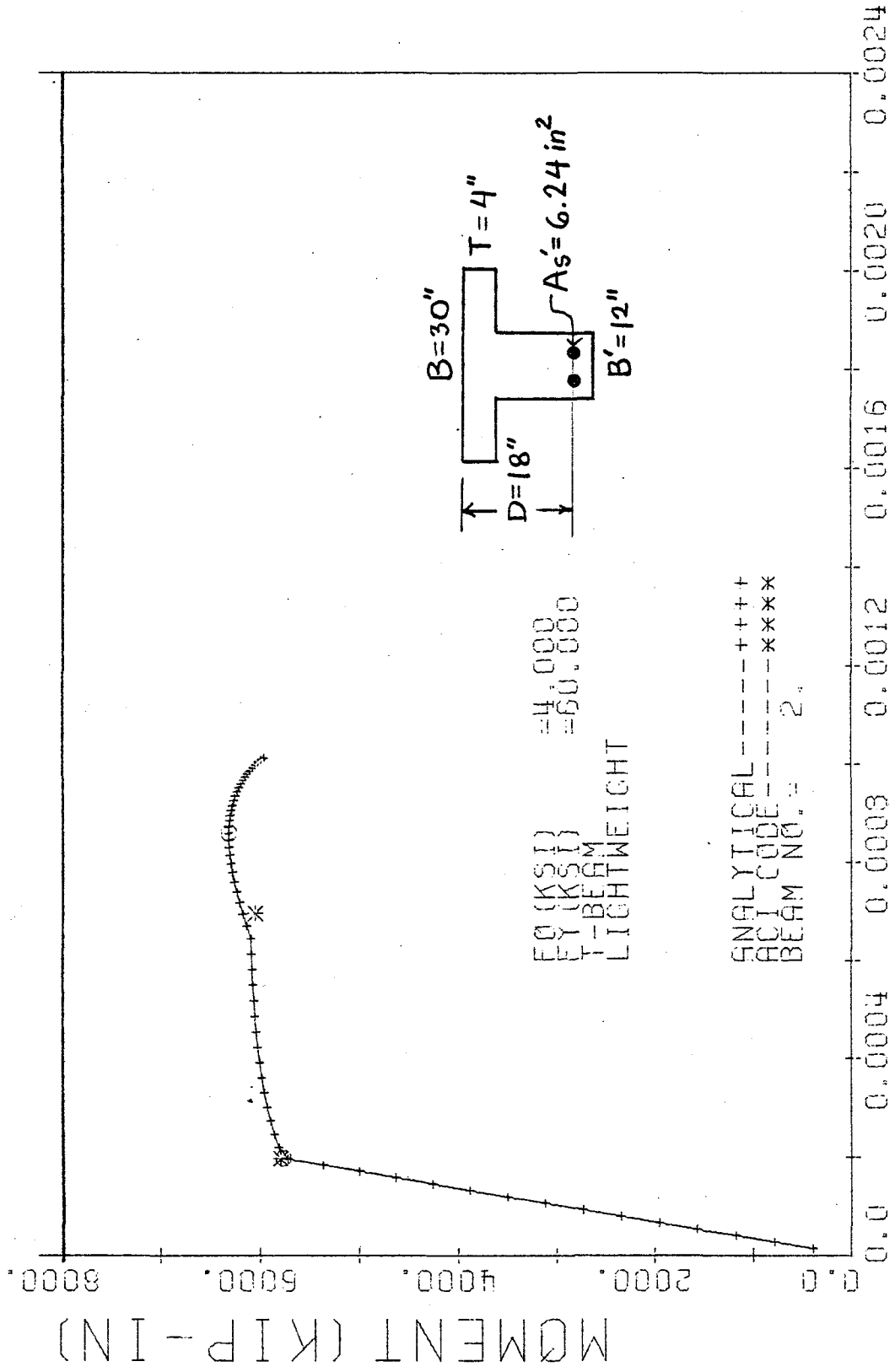

Fig. 5.10b M-φ relationship for T-beam.

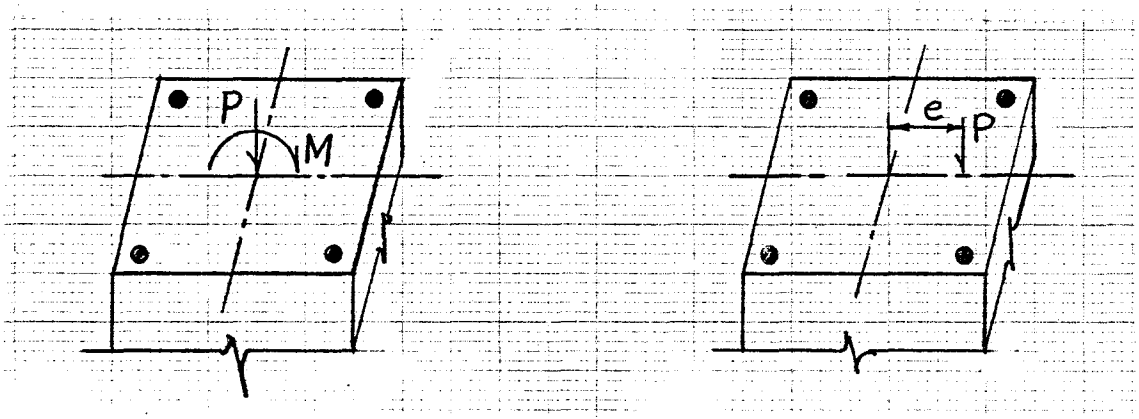

Fig. 5.11 Column under axial and flexural loads.

Fig. 5.12 Column under uniaxially eccentric load.

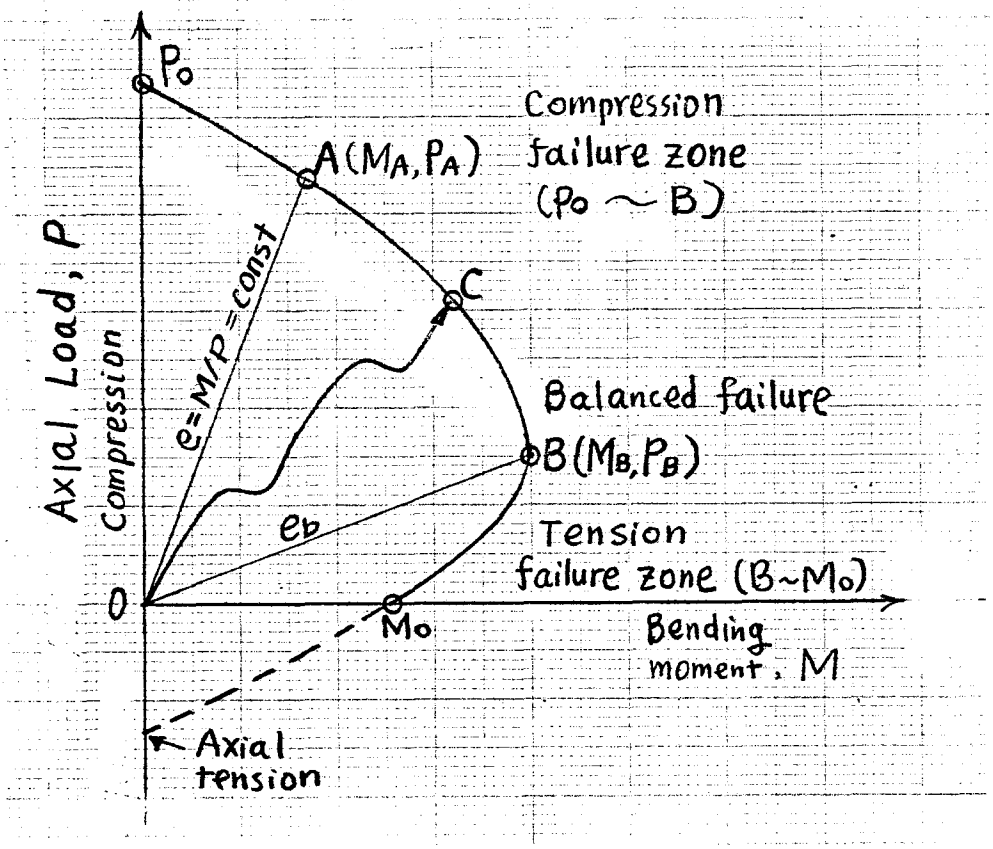

Fig. 5.13 Interaction P-M diagram.

obtained from any two values of M and P, an interaction diagram can also be defined as the locus of the maximum values of axial load which can be applied to a short column, when the eccentricity of the load varies from zero (concentric compression) to infinity (pure bending). Line OA in Fig. 5.13 represents a case in which the external load varies in such a way that the values of axial load and moment increase in the same proportion. The slope of this line is the eccentricity $e = M/P$. The strength of the column for this case would be M_A, P_A. Line OC represents an arbitrary loading history where axial load and bending moment do not increase in the same proportion. Point B represents the balanced condition; i.e., under simultaneous action of the axial load, P_b, and moment, M_b, the column will reach its ultimate strength, simultaneously with the tension steel reaching its yield stress.

The interaction diagram shown in Fig. 5.13 corresponds to a column with a given cross section under single bending. For the cross section shown in Fig. 5.12, the plane of bending coincides with a plane of symmetry.

The failure patterns of column under loading can be characterized as compression failure, balanced failure, and tension failure as shown in Fig. 5.13. Their failure patterns correspond to those for overreinforced beams, balanced beams, and underreinforced beams, respectively, as discussed in the previous section.

Two types of loadings on columns will be considered in the following sections: uniaxially eccentrical load, i.e. axial load plus single bending, and biaxially eccentrical load, i.e. axial load plus biaxial bending.

5.4.2 Column with Uniaxially Eccentrical Load

For a rectangular column reinforced by A_s and A_s' along the two faces parallel to the axis of bending as shown in Fig. 5.14, the analysis procedure can be divided into two parts: one corresponds to the case where the neutral axis falls inside the column section, and one where the neutral axis falls outside the section. The corresponding general equations are given below:

(a) The neutral axis falls inside the column section

Equilibrium Equations

$$\alpha f_c' bc + A_s' f_s' - A_s f_s = P \tag{5.18}$$

$$\alpha f_c' bc(h/2 - \beta c) + A_s' f_s'(h/2 - d'') + A_s f_s(h/2 - c) = Pe = M \tag{5.19}$$

where the plastic center and the centroid of the cross-section are assumed to coincide, and e is the eccentricity of the equivalent axial load with respect to the centroid.

Compatibility Equations

$$\left.\begin{aligned} \varepsilon_s &= \frac{d-c}{c}\varepsilon_c \\ \varepsilon_s &= \frac{c-d''}{c}\varepsilon_c \end{aligned}\right\} \tag{5.20}$$

Constitutive Equations

$$\left.\begin{aligned} f_s &= f_s(\varepsilon_s) \\ f_s' &= f_s(\varepsilon_s') \end{aligned}\right\} \tag{5.21}$$

$$\left.\begin{aligned} \alpha &= \alpha(\varepsilon_c) \\ \beta &= \beta(\varepsilon_c) \end{aligned}\right\} \tag{5.22}$$

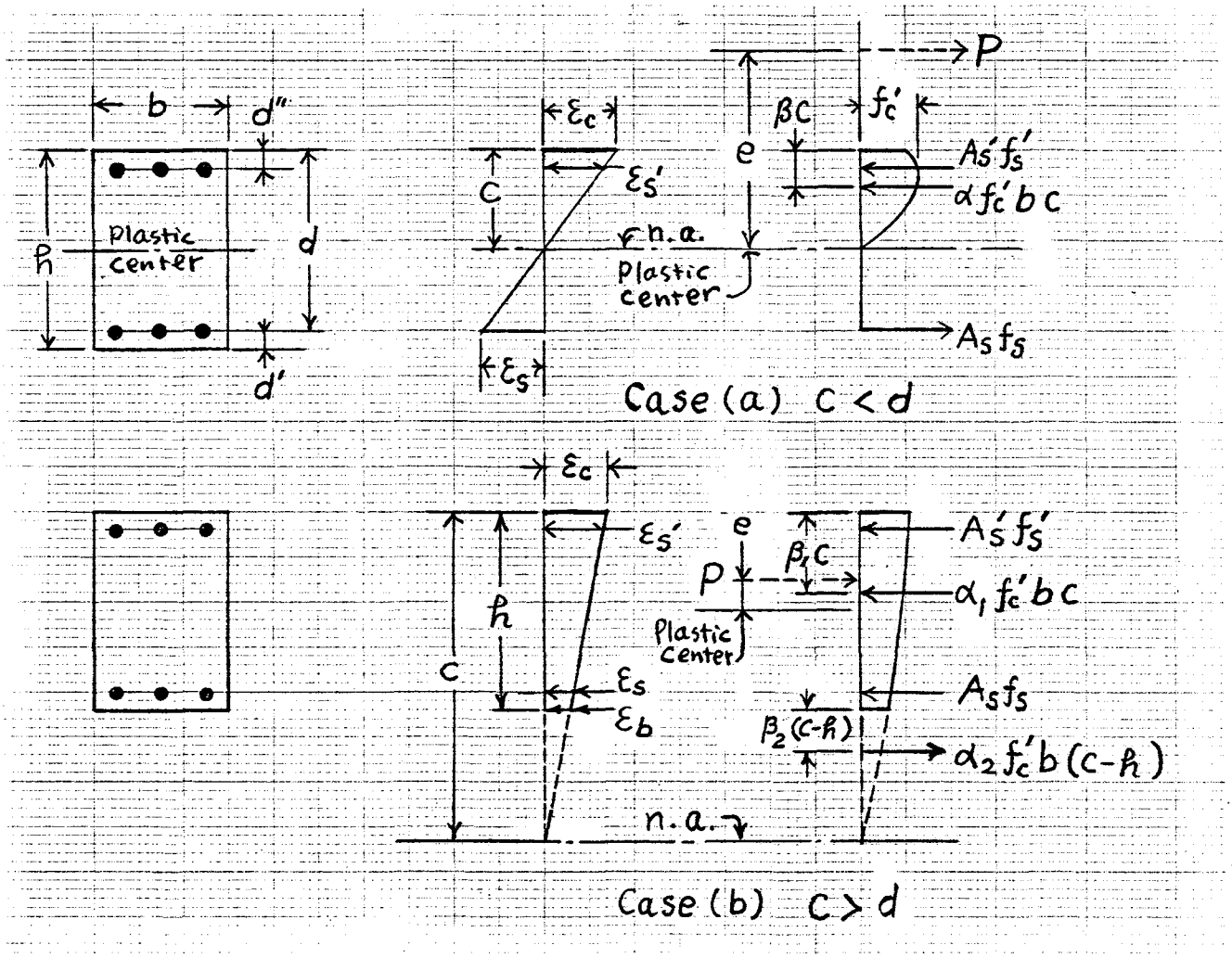

Fig. 5.14 Forces in uniaxially eccentrically loaded column.

Curvature

$$\phi = \frac{\varepsilon_c}{c} \tag{5.23}$$

(b) The neutral axis falls outside the column section

Equilibrium Equations

$$\alpha_1 f'_c bc - \alpha_2 f'_c b(c-h) + A'_s f'_s + A_s f_s = P \tag{5.24}$$

$$\alpha_1 f'_c bc(h/2 - \beta_1 c) - \alpha_2 f'_c b(c-h)[h/2 + \beta_2(c-h)] + A'_s f'_s(h/2 - d'') - A_s f_s(h/2 - d') = Pe = M \tag{5.25}$$

where e is the eccentricity with respect to the centroid of the cross section.

Compatibility Equations

$$\left.\begin{aligned} \varepsilon_s &= \frac{c-d}{c}\varepsilon_c \\ \varepsilon'_s &= \frac{c-d''}{c}\varepsilon_c \\ \varepsilon_b &= \frac{c-h}{c}\varepsilon_c \end{aligned}\right\} \tag{5.26}$$

where ε_b is the strain at bottom fiber of section.

Constitutive Equations

$$\left.\begin{aligned} f_s &= f_s(\varepsilon_s) \\ f'_s &= f_s(\varepsilon'_s) \end{aligned}\right\} \tag{5.27}$$

$$\left.\begin{aligned} \alpha_1 &= \alpha(\varepsilon_c) \\ \alpha_2 &= \alpha(\varepsilon_b) \\ \beta_1 &= \beta(\varepsilon_c) \\ \beta_2 &= \beta(\varepsilon_b) \end{aligned}\right\} \tag{5.28}$$

Curvature

$$\phi = \frac{\varepsilon_c}{c} \tag{5.29}$$

A typical computer graphical output for a typical column load-moment interaction diagram is shown in Fig. 5.15 where the values corresponding to the ACI-1971 code procedure are also plotted for comparison. The locigal flowchart for generating the interaction diagram is given in Table 5.2 and the corresponding computer program is listed in Appendix II. For the column with reinforcing bars placed along four faces will be treated as a special case of biaxially eccentrically-loaded columns with the angle of eccentricity equal to zero. The biaxially-loaded column will be discussed next.

5.4.3 Column with Biaxially Eccentrical Load

A. Introduction

For a given column of square cross-section, the most complicated calculations result when the load is applied at an angle of eccentricity between the symmetric case of 0° and 45° measured from an axis of symmetry of the cross section. The major difficulty involves the location of the neutral axis which is not necessarily perpendicular to the moment arm of the applied load in the general case; furthermore, its location translates across the cross section with variations in the magnitude of the applied eccentricity.

A typical biaxially eccentrically loaded column is shown in Fig. 5.16, and an arbitrary neutral axis is defined in Fig. 5.17. The analysis procedure is described in the following sections; the corresponding logical flowchart is shown in Table 5.3 and the computer program is listed in Appendix III. A typical computer output is shown in Fig. 5.26.

TABLE 5.2

Flowchart - Uniaxially Loaded Column (Generate Column Interaction Diagram)

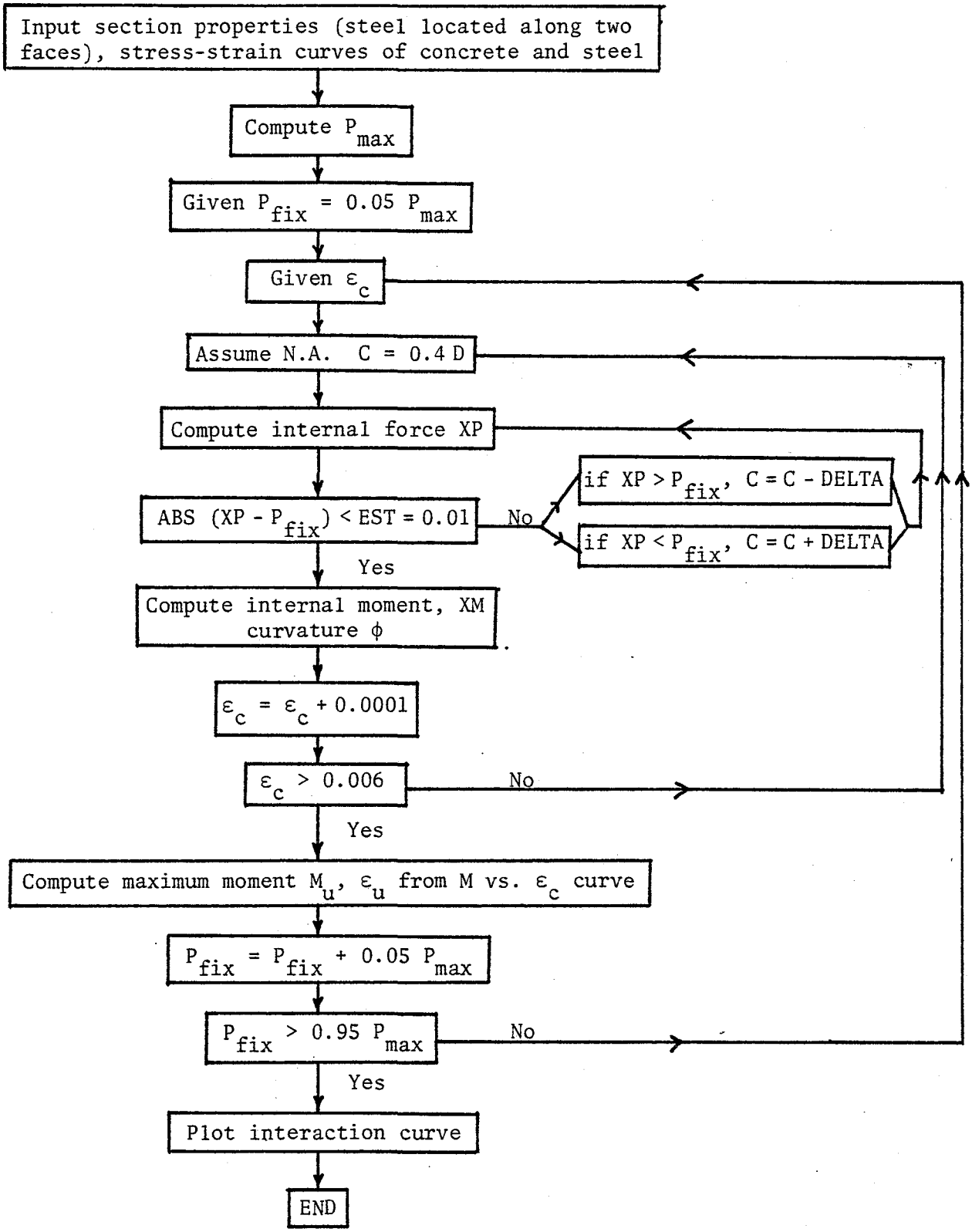

TABLE 5.3

Flowchart - Biaxially Loaded Column (Generate Column Interaction Diagram for Given Angle of Eccentricity)

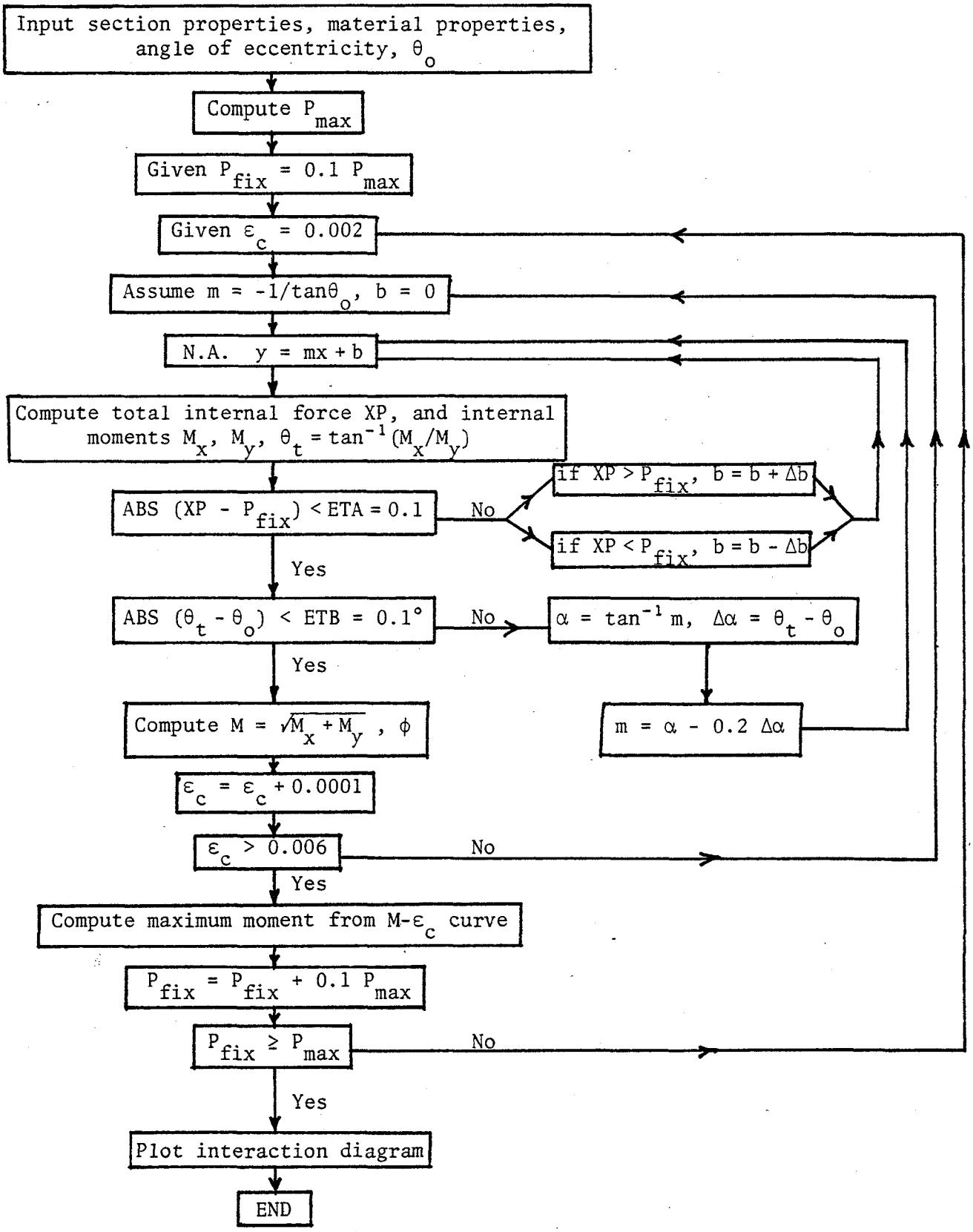

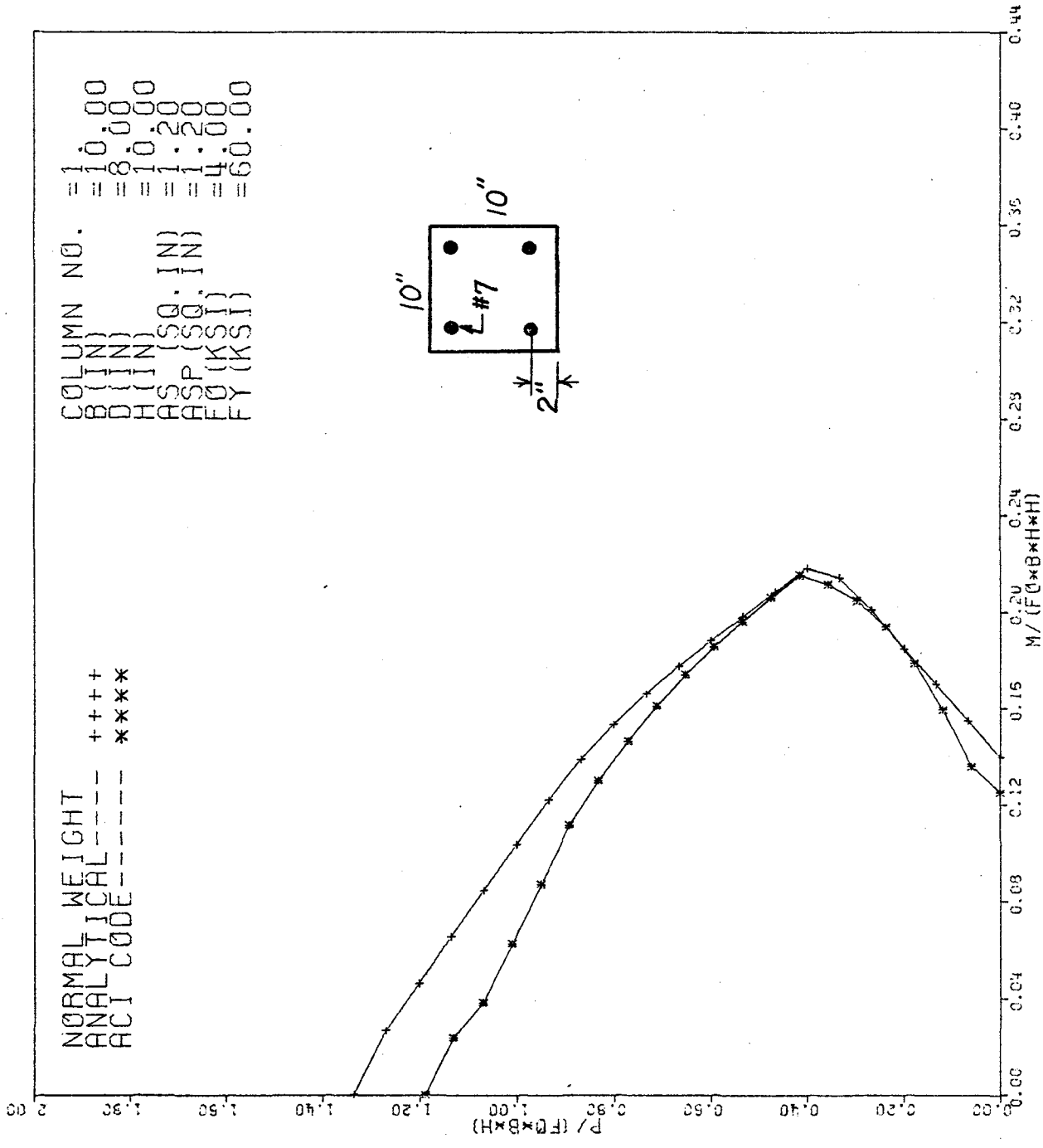

Fig. 5.15 Interaction P-M diagram of uniaxially loaded column.

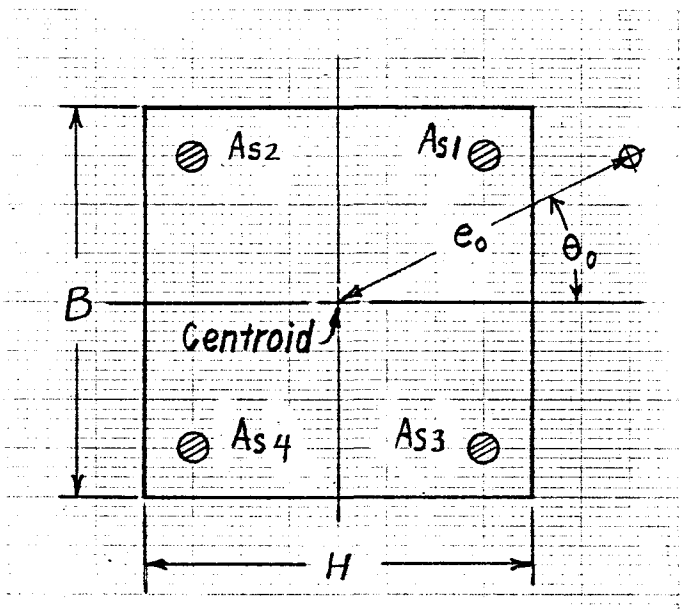

Fig. 5.16 Column cross section.

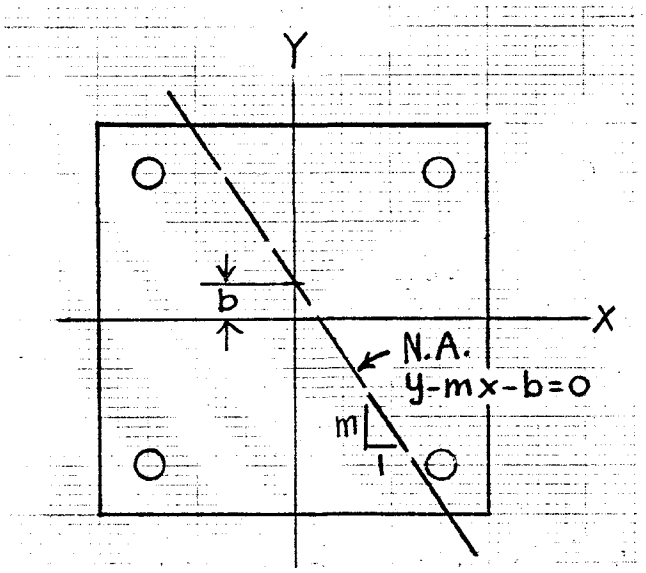

Fig. 5.17 Neutral axial position.

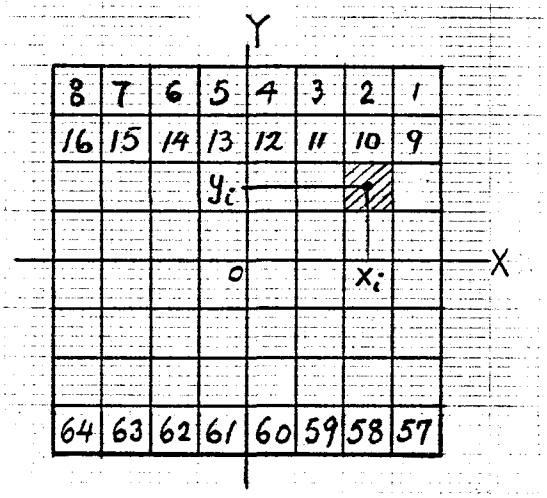

Fig. 5.18 Finite element mesh.

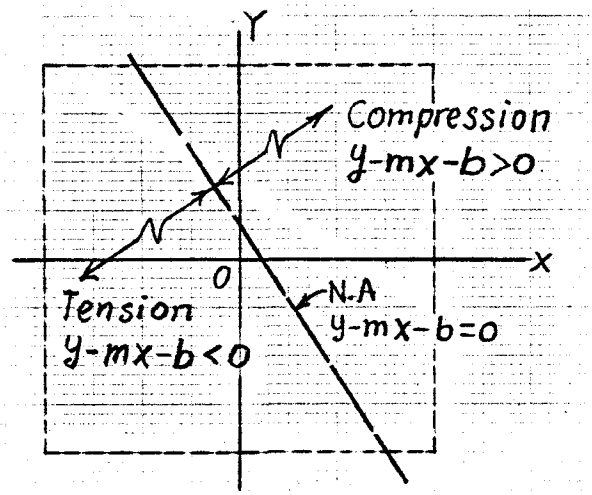

Fig. 5.19 Determining the compression zone.

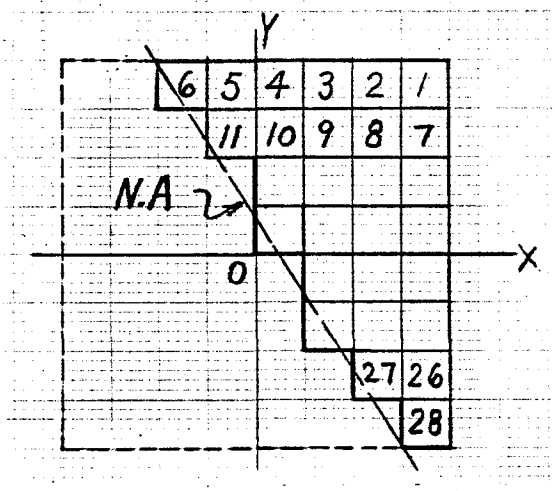

Fig. 5.20 Numbering sequence in compression zone.

B. Analysis procedure for generating the interaction diagram for a given angle of eccentricity θ (Fig. 5.16)

The following steps are used:

1. Divide the column cross section into finite elements as shown in Fig. 5.18 for each element an identity number is given; the coordinates of the element are computed with respect to the coordinate system fixed at the centroid of the cross section.

2. Compute the cross section area and the coordinates for each reinforcing bar.

3. Assume a starting value for the concrete strain, ε_c, acting at the extreme compression corner.

4. Assume a slope, m, for the neutral axis as shown in Fig. 5.17. A good initial approximation is obtained by positioning the neutral axis perpendicular to the moment arm of the applied load. For the square column in which the angle of eccentricity is 0° or 45°, the neutral axis will be always perpendicular to the moment arm.

5. Assume a value, b, for the intercept of the neutral axis with the y-axis as shown in Fig. 5.17.

6. Determine the concrete elements which are in compression, i.e. those elements located on one side of the neutral axis by the method explained in Fig. 5.19, and renumber the elements under compression in sequence as shown in Fig. 5.20. Note that the tensile strength of concrete is neglected.

7. Determine the strains at the center of each reinforcing bar and each concrete element from the assumed planar strain distribution as shown in Fig. 5.21. A corresponding concrete stress distribution is shown in Fig. 5.22.

8. Determine the forces on each concrete element and each reinforcing bar, and their corresponding moments with respect to the two coordinates axes, i.e.:

Force on each concrete element (see Fig. 5.23).

$$C_i = A_i f_i \tag{5.30}$$

where

C_i = force on concrete incremental area

A_i = concrete incremental area

f_i = stress on the centroid of element

Moment about coordinate axes due to concrete element.

$$\left.\begin{aligned} (M_{xc})_i &= C_i \bar{y}_i \\ (M_{yc})_i &= C_i \bar{x}_i \end{aligned}\right\} \tag{5.31}$$

Total force and moments from concrete elements.

$$\left.\begin{aligned} C_c &= \sum_{i=1,n} C_i \\ M_{xc} &= \sum_{i=1,n} (M_{xc})_i \\ M_{yc} &= \sum_{i=1,n} (M_{yc})_i \end{aligned}\right\} \tag{5.32}$$

Force and moment on each reinforcing bar.

$$(C_s)_i = (A_s)_i * (f_s)_i \tag{5.33}$$

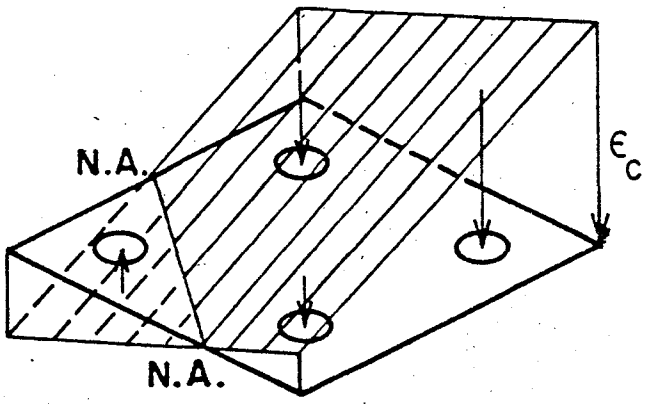

Fig. 5.21 Strain distribution.

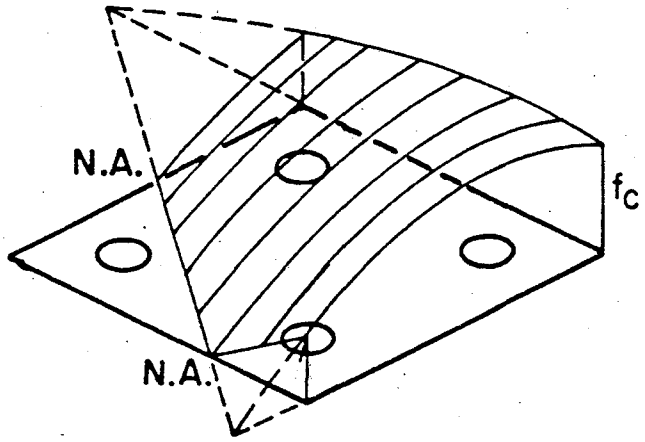

Fig. 5.22 Concrete stress distribution.

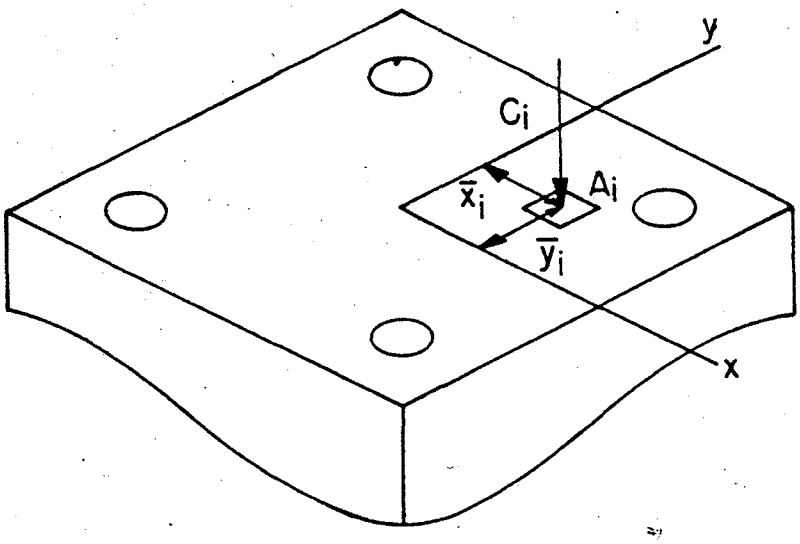

Fig. 5.23 Concrete force acting on each element.

$$\left.\begin{aligned}(M_{xs})_i &= (C_s)_i * (y_s)_i \\ (M_{ys})_i &= (C_s)_i * (x_s)_i\end{aligned}\right\} \quad (5.33)\ \text{Cont'd}$$

Total force and moments from reinforcing bars.

$$\left.\begin{aligned}C_s &= \sum_{i=1,k} (C_s)_i \\ M_{xs} &= \sum_{i=1,k} (M_{xs})_i \\ M_{ys} &= \sum_{i=1,k} (M_{ys})_i\end{aligned}\right\} \quad (5.34)$$

Total force and moments from concrete and steel.

$$\left.\begin{aligned}P &= C_c + C_s \\ M_x &= M_{xc} + M_{xs} \\ M_y &= M_{yc} + M_{ys}\end{aligned}\right\} \quad (5.35)$$

Check if P is sufficiently close to (P_o) given

Resultant of internal moments.

$$M = \sqrt{M_x^2 + M_y^2} \quad (5.36)$$

The position of eccentricity from centroid of cross section.

$$e_t = \frac{M}{P} \quad (5.37)$$

The inclination angle of eccentricity.

$$\theta_t = \tan^{-1}(M_x/M_y) \quad (5.38)$$

Check if θ_t is sufficiently close to (θ_o) given

9. Iteration procedures - the triple iteration procedure will be described as follows:

(a) Iteration on intercept, b, of the neutral axis with the y-axis as shown in Fig. 5.24:

i) $b = 0$ for first cycle analysis

ii) $b = \left\{ \begin{matrix} b + \Delta b & \text{if} \quad P > (P)_{given} \\ b - \Delta b & \text{if} \quad P < (P)_{given} \end{matrix} \right\}$ for second cycle analysis

(b) Iteration on slope, m, of the neutral axis as shown in Fig. 5.25:

i) Assume that the neutral axis perpendicular to the applied moment arm as shown in Fig. 5.25 for the first cycle analysis, i.e. $m = -1/\tan\theta_o$ and compute the inclination angle of the neutral axis, $\alpha = \tan^{-1}(m)$, as shown in Fig. 5.25.

ii) $m = \dfrac{-1}{\tan(\alpha - \Delta\alpha)}$ for second cycle analysis

where $\Delta\alpha = (0.2)(\theta_t - \theta_o)$ from Eq. (5.38) .

(c) Iteration on extreme compressive strain, ε_c, for determining the maximum-moment capacity at the given loading.

i) $\varepsilon_c = 0.002$ (arbitrary starting value but not greater than ε_o).

ii) $\varepsilon_c = \varepsilon_c + 0.001$ for the next assigned strain up to 0.006.

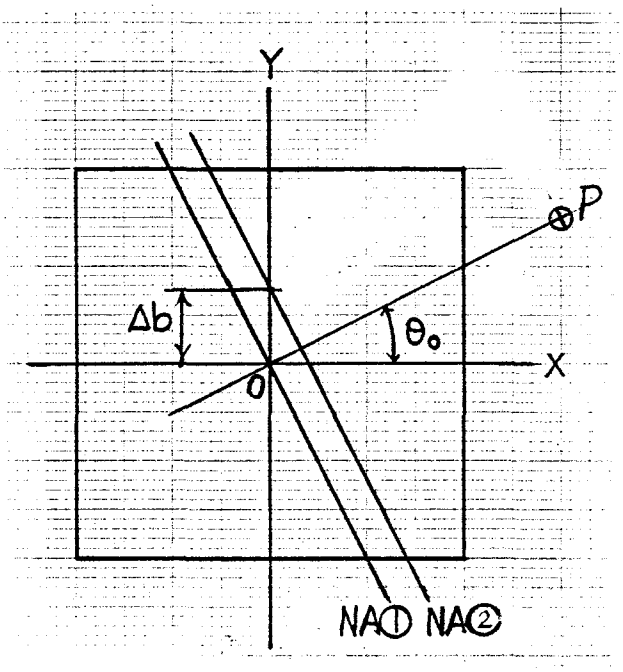

Fig. 5.24 Iteration on position of neutral axis.

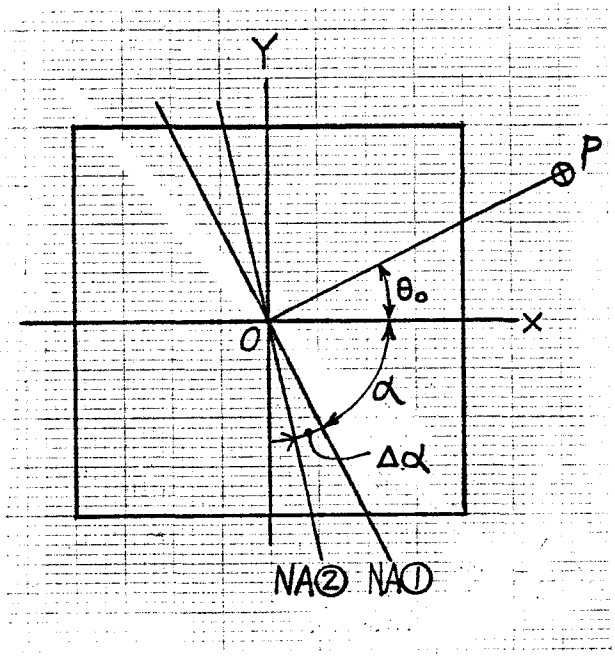

Fig. 5.25 Iteration on inclination angle of neutral axis.

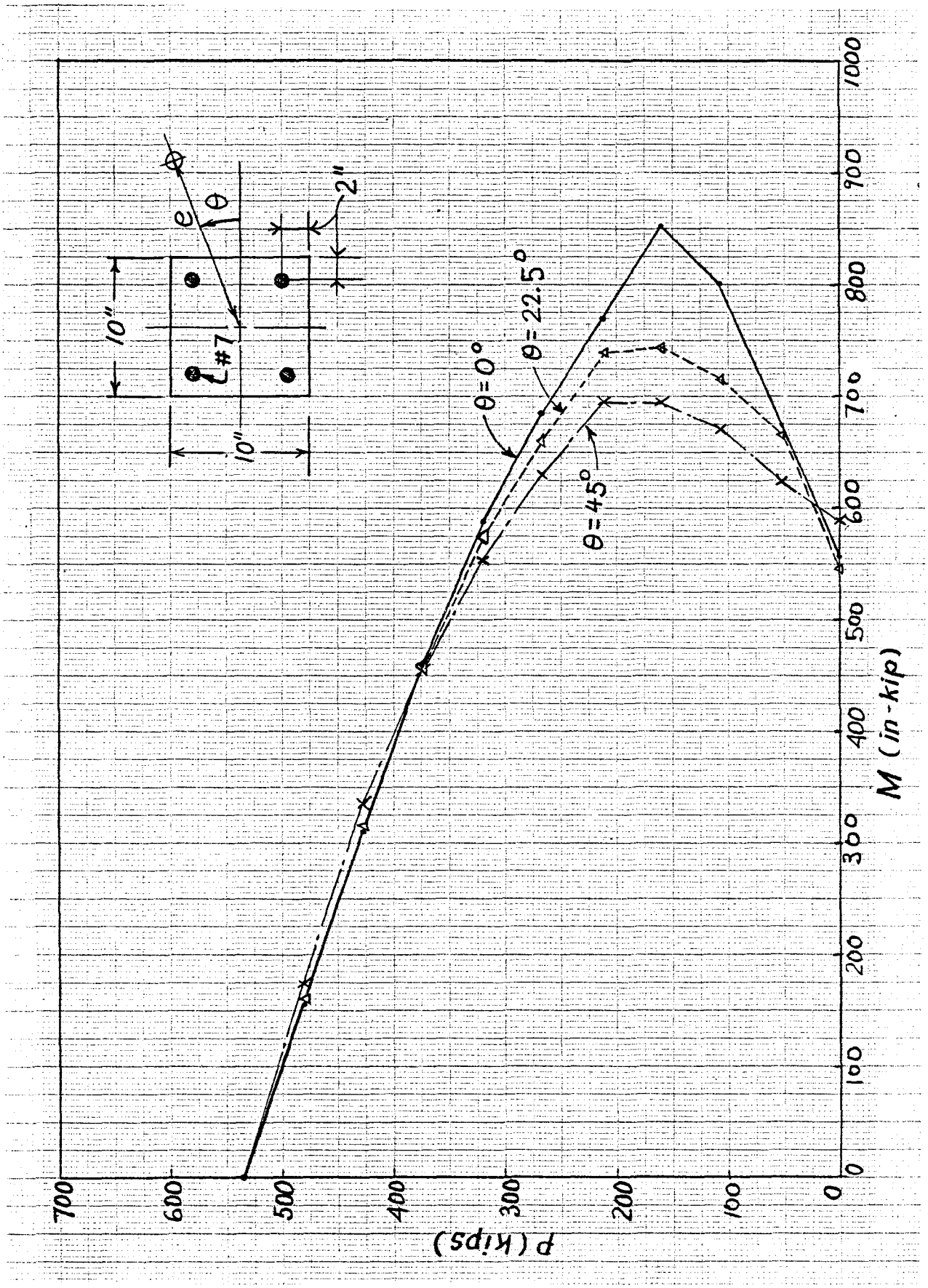

Fig. 5.26 Typical interaction diagram of biaxially loaded column.

CHAPTER VI

DUCTILITY OF REINFORCED-CONCRETE MEMBERS

6.1 INTRODUCTION

A ductile material is one that can undergo large strain while resisting loads. When applied to reinforced-concrete members and structures, the term ductility implies the ability to sustain significant inelastic deformations without a significant variation in the resisting capacity prior to collapse. This ability is, generally, quantitatively described by a parameter called "ductility factor" or "ductility ratio."

The objectives of this chapter are: to investigate the ductility behavior at the level of the materials, sections, and structural concrete members; to formulate a precise method for computing the corresponding ductility factors; and to compare these factors with the ACI code requirements.

6.2 DUCTILITY OF PLAIN CONCRETE

6.2.1 Unconfined (Uniaxial Loading)

The typical stress-strain curves of plain concrete under uniaxial loading for normal weight and lightweight concretes are shown in Fig. 6.3. It can be seen that for the same type of concrete the higher the strength the lower the ductility, and, for the same level of strength, normal weight concrete is more ductile than lightweight concrete. For a given material the ductility can be measured, for example, by the toughness, i.e., the area under the complete stress-strain curve, or by the strain ε_{50} at 50% of the peak load on the descending portion of the stress-strain curve [28]. Since the ductility of concrete depends on the steepness of the descending

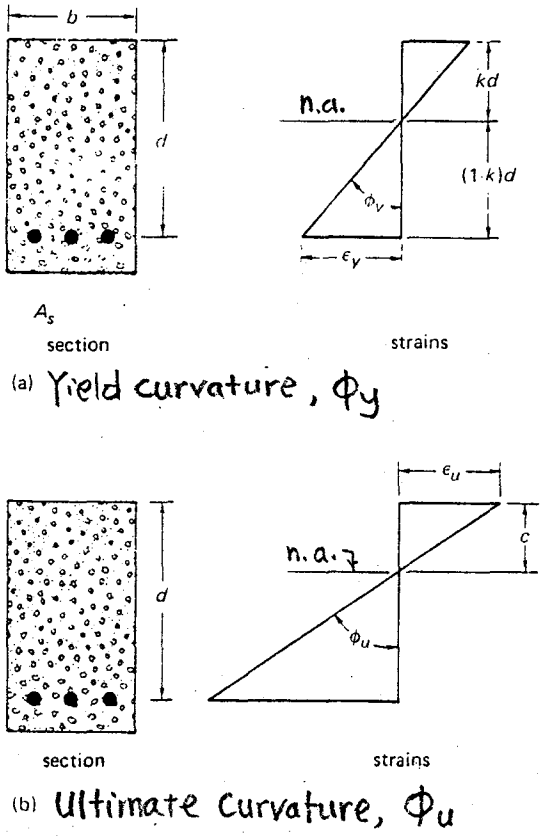

Fig. 6.1 Calculation of curvatures.

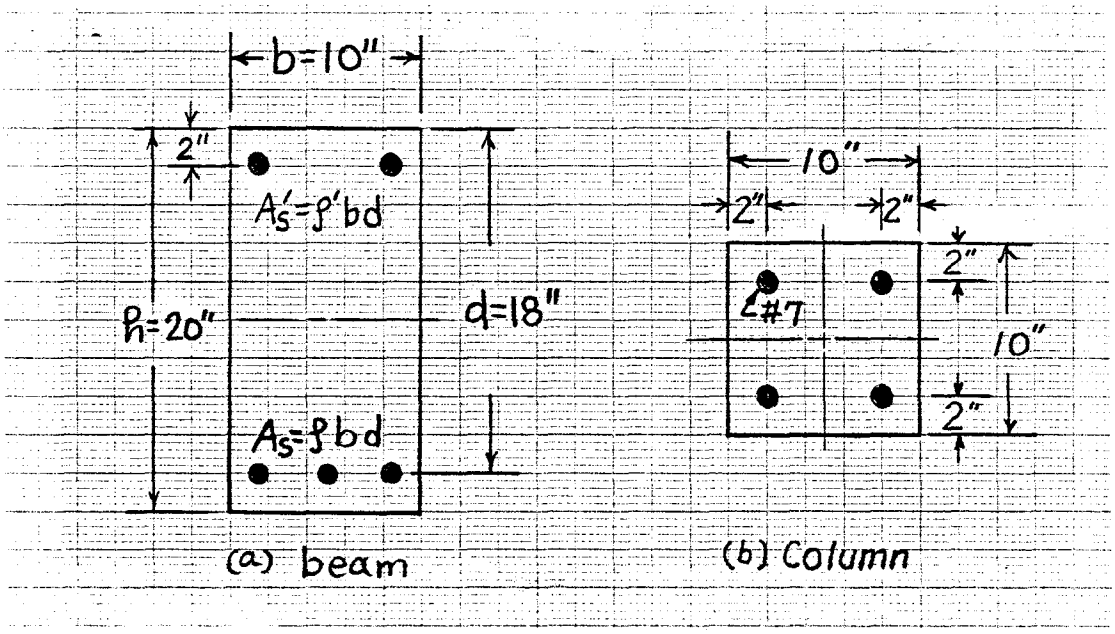

Fig. 6.2 Typical cross sections.

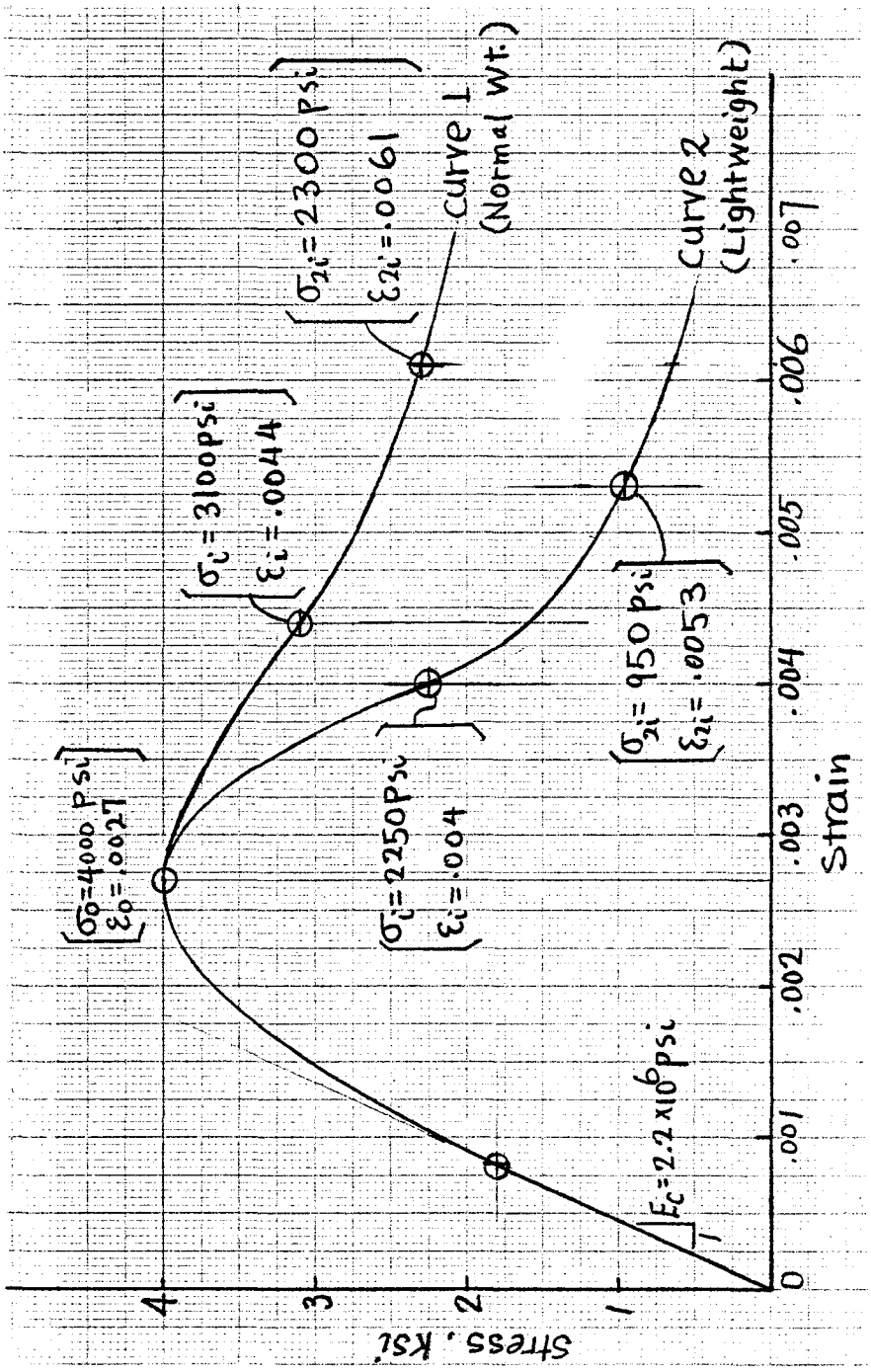

Fig. 6.3 Concrete stress-strain curve.

portion of the curve, it may also be defined as the slope at a certain characteristic point on the descending portion; such a point may be taken as the inflection point as described in Chapter II.

6.2.2 Effect of Confinement

Roy and Sozen [28] showed that although the load-carrying capacity of axially-loaded concrete specimens is not significantly improved by the use of rectangular ties, there is a considerable increase in ductility as expressed in the function of ε_{50} (the strain at 50% of peak stress on the descending portion) as follows:

$$\varepsilon_{50} = 0.015 \frac{h}{s}$$

or

$$\varepsilon_{50} = \frac{3}{4} \frac{p''h}{s}$$

where

h = dimension of square column

s = tie spacing

p'' = confinement reinforcement ratio

The above investigation was based on compressive specimens with the dimensions of 5" x 5" x 25" and the concrete strength on prisms of about 3500 psi.

In a related investigation Shah and Rangan [33] showed that stirrups are most effective in increasing the ductility of overreinforced beams as compared to fibers and compression reinforcement. The investigation was based on the flexural test of a beam specimen with the dimension of 2" x 3" x 34" and the concrete strength of 4000 psi.

6.3 DUCTILITY OF REINFORCED-CONCRETE BEAM SECTIONS

Using the moment-curvature diagram of reinforced concrete sections, Cohn and Ghosh [10] defined the ductility factor as the ratio of ultimate curvature to yield curvature, i.e., $\mu = \phi_u/\phi_y$. The yield curvature ϕ_y is defined as the curvature at which the tension steel reaches its yield stress, and the ultimate curvature ϕ_u is the one associated with the strain ε_u, load P_u or moment M_u at the ultimate stage. The ultimate stage, depending on each particular case, is defined as the point of maximum moment or load, or the point at which a specified strain is reached.

6.3.1 Calculation of Yield and Ultimate Curvatures According to ACI Code

A typical reinforced-concrete section with tension reinforcement only and its corresponding strain distribution at the yield and ultimate stages are shown in Figs. 6.1a and 6.1b. The curvature calculations are given by the following equations:

At Yield

$$\phi_y = \frac{\varepsilon_y}{d(1-k)} \tag{6.1}$$

where k can be determined by assuming the linear stress distribution on the concrete compression zone and satisfying the equilibrium condition of forces. This leads to:

$$\left.\begin{aligned} k &= -\rho n + \sqrt{2\rho n + \rho^2 n^2} \\ \rho &= \frac{A_s}{bd} \\ n &= \frac{E_s}{E_c} \end{aligned}\right\} \tag{6.2}$$

At Ultimate

$$\phi_u = \frac{\varepsilon_u}{c} \tag{6.3}$$

where

ε_u = concrete compression strain at crushing of concrete or at ultimate moment

c = depth of compression zone at ultimate, can be determined by satisfying equilibrium equation of forces

$$= \frac{\rho f_y}{f'_c} \frac{d}{0.85\beta_1} \tag{6.4}$$

where

$$\beta_1 = \begin{cases} 0.85 - 0.05\left(\frac{f'_c}{1000} - 4\right) & \text{for } f'_c \leq 8000 \text{ psi} \\ 0.65 & \text{for } f'_c > 8000 \text{ psi} \end{cases} \tag{6.5}$$

The addition of compression reinforcement to a beam will shift the neutral axis upwards, and increase the ultimate curvature substantially, although it has little effect on its yield strength or yield curvature. The term c in Eq. (6.4) then becomes

$$c = \left(\rho - \frac{\rho' f'_s}{f_y}\right) \frac{f_y d}{0.85\beta_1 f'_c} \tag{6.6}$$

where

$$\rho' = \frac{A'_s}{bd}$$

f'_s = stress in the compression reinforcement

From Eqs. (6.1) and (6.3), the ductility factor, μ, is defined as:

$$\mu = \frac{\phi_u}{\phi_y} \tag{6.7}$$

For research purposes, it is possible to determine ϕ_u and ϕ_y from the moment-curvature diagram which was derived in Chapter V using an iterative calculation procedure based on the actual stress-strain curves of concrete and steel, and for which a computer program was written.

6.3.2 Effects of Concrete Stress-Strain Curve on the Ductility of Reinforced Concrete Beam Sections

It has been shown in previous investigations that the confining reinforcement increases the ductility of concrete at the material level, and in turn, increases the flexural ductility of reinforced-concrete sections. Furthermore, most investigators agree that lateral confinement does not significantly affect the peak stress of the σ-ε curve and its ascending portion, but it influences the descending portion drastically. A case study is presented here to explore possible inferences between material and sectional ductilities for two different concrete stress-strain curves with identical ascending portions but different descending portions. The section properties for the above case study and the actual stress-strain curves of concretes and steel are shown in Figs. 6.2, 6.3 and 6.4. The computer program described in Chapter V was used to generate information on the curvature and ductility factors.

The effect of different stress-strain curves on the ductility of beam sections are shown in Figs. 6.5 for various tension and compression steel ratios. For underreinforced beams, the ultimate moment always occurs at a concrete compressive strain far beyond the peak strain; thus the descending portion of the stress-strain curve of concrete becomes important for ductility purposes. The effect can be seen in Fig. 6.5 for

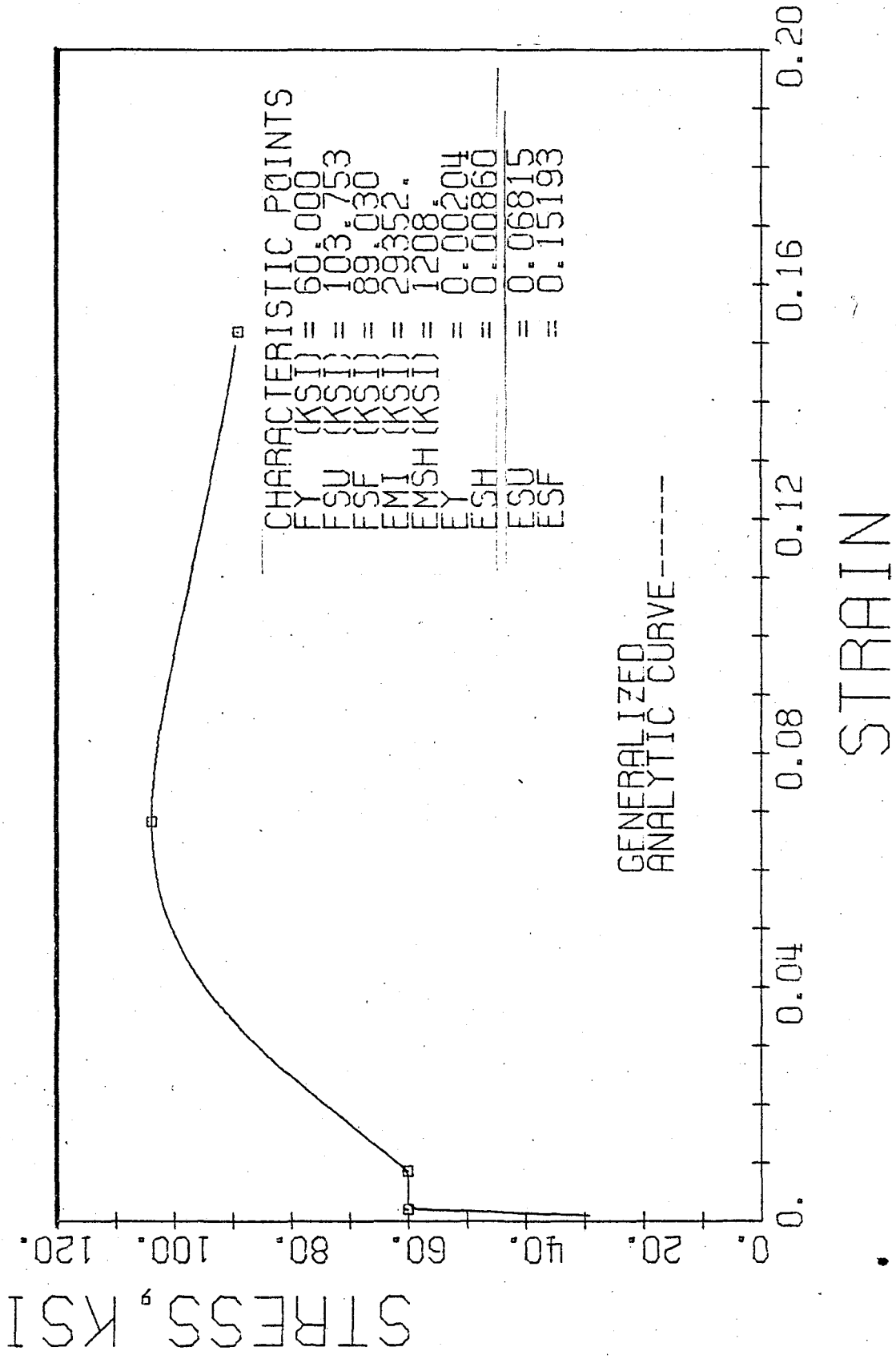

Fig. 6.4 Stress-strain curve of grade 60 steel with f_y = 60 ksi.

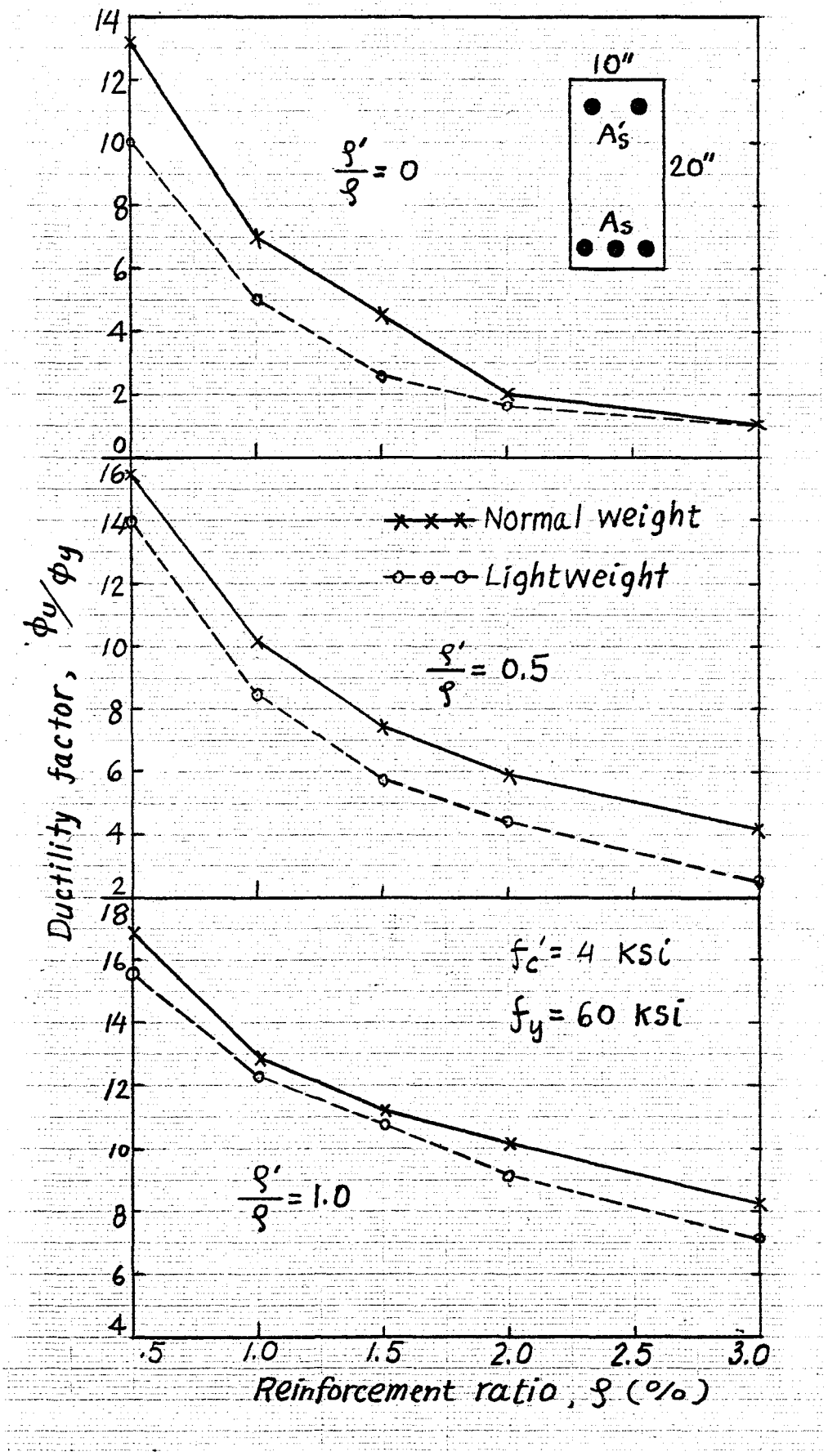

Fig. 6.5 Comparison of ductility between normal and lightweight concrete.

the beam with tension steel only (note that the two concretes have the same ascending portion). The effect of compression steel on the improvement of ductility can be observed from Fig. 6.5. The comparison of ductility between theoretical and ACI code values for normal and lightweight concretes are shown in Figs. 6.6 and 6.7. Note that the higher the reinforcement ratio, the higher the influence of compression steel on ductility. The safety margin on ductility as provided by the ACI code for lightweight concrete is very small as can be seen from Fig. 6.7a for $\rho' = 0$.

The effect of compression reinforcement on the ductility of the section as analytically derived is shown in Figs. 6.8 and 6.9 for normal and lightweight concretes where the moment-curvature diagrams are plotted. It can be seen that the addition of compression reinforcement to a beam has relatively little effect on its yield moment or yield curvature. It does, however, greatly increase the ultimate curvature and lead to a substantial increase in the ultimate moment.

The effect of axial loads on the ductility of the section is shown in Figs. 6.10 and 6.11 for normal and lightweight concretes, respectively. These figures show that the ductility decreases drastically when the axial load approaches about 30% of the axial load-capacity of the section. The corresponding load-moment interaction diagrams for the section with $\rho'/\rho = 1$ are shown in Figs. 6.12 and 6.13.

6.4 DUCTILITY OF REINFORCED-CONCRETE COLUMN SECTIONS

Reinforced-concrete column sections under uniaxial and biaxial bending are examined here. The effect of axial loads on the moment-curvature diagrams of the reinforced-concrete sections (uniaxial bending) are shown

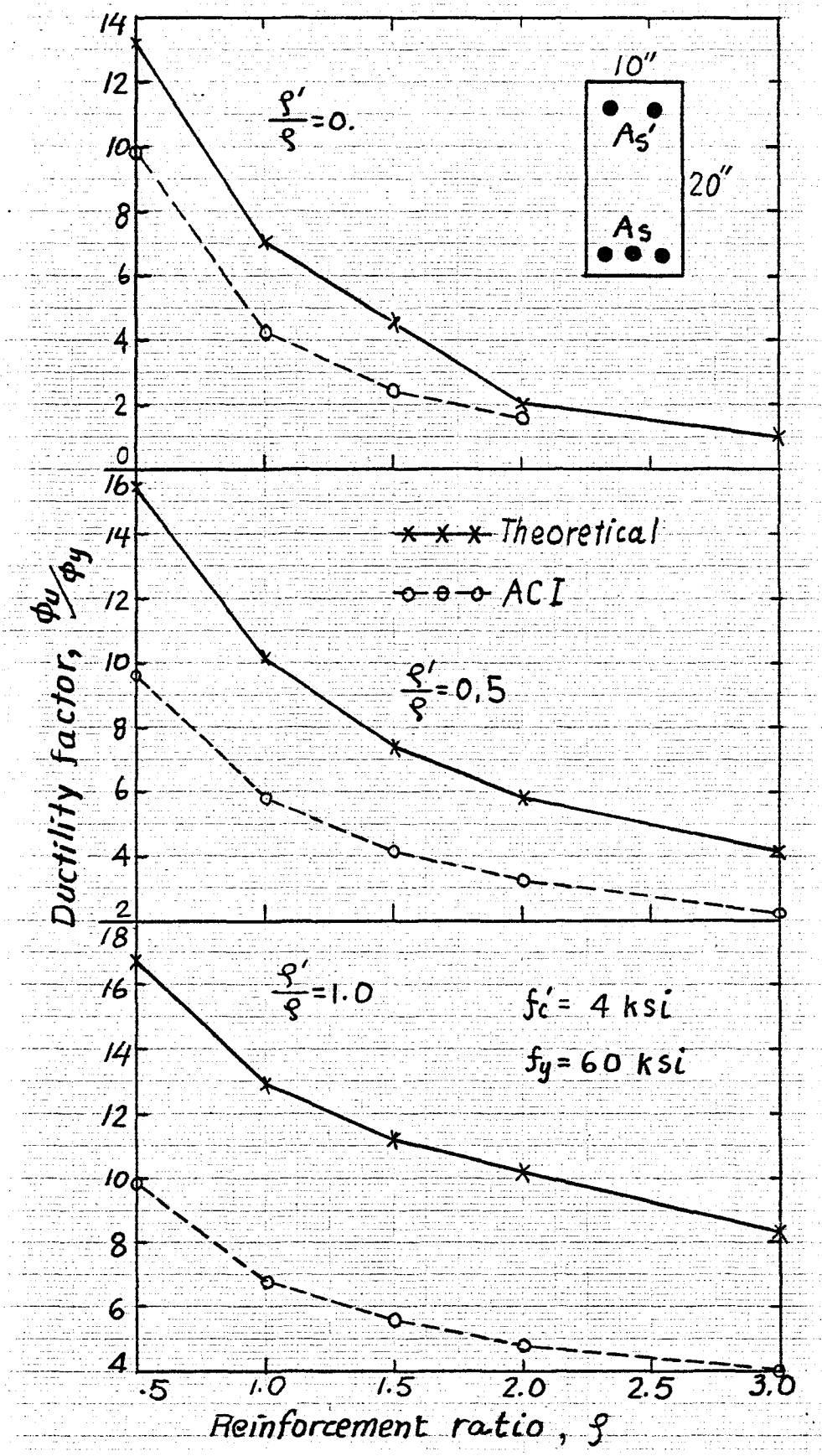

Fig. 6.6 Comparison of ductility between theoretical and ACI values for normal weight concrete.

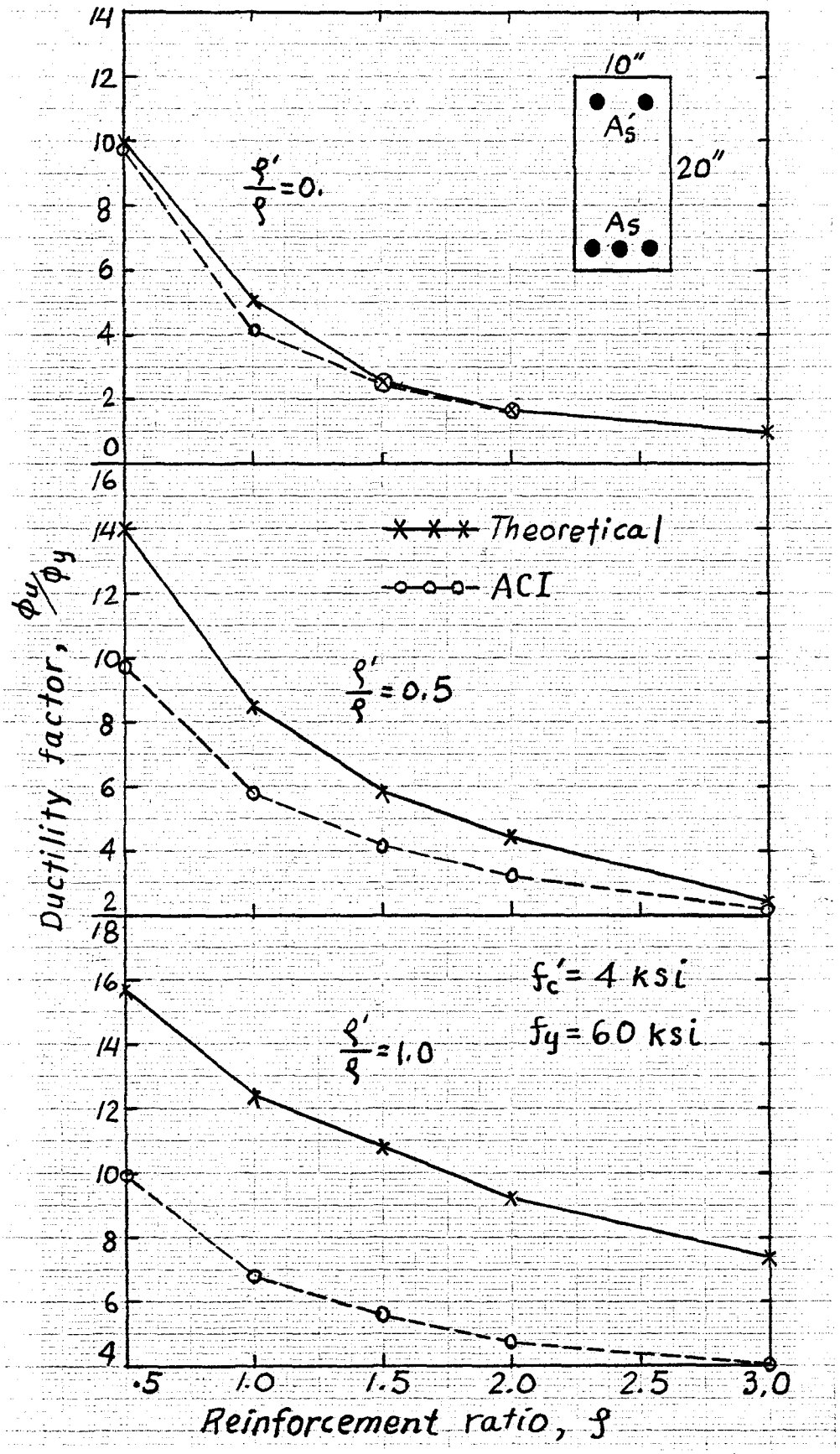

Fig. 6.7 Comparison of ductility between theoretical and ACI values for lightweight concrete.

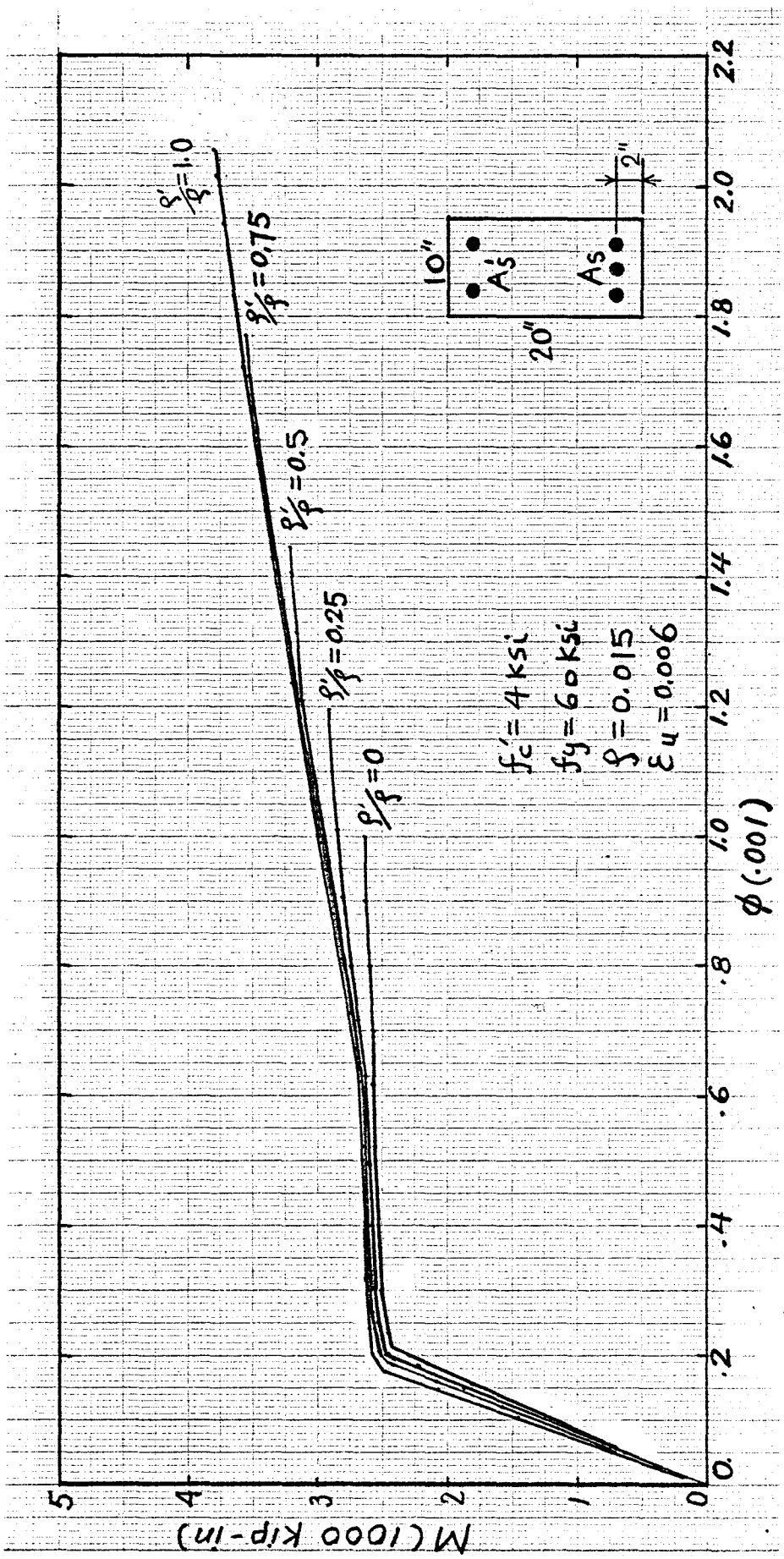

Fig. 6.8 Effect of compression reinforcement on ductility for normal weight concrete.

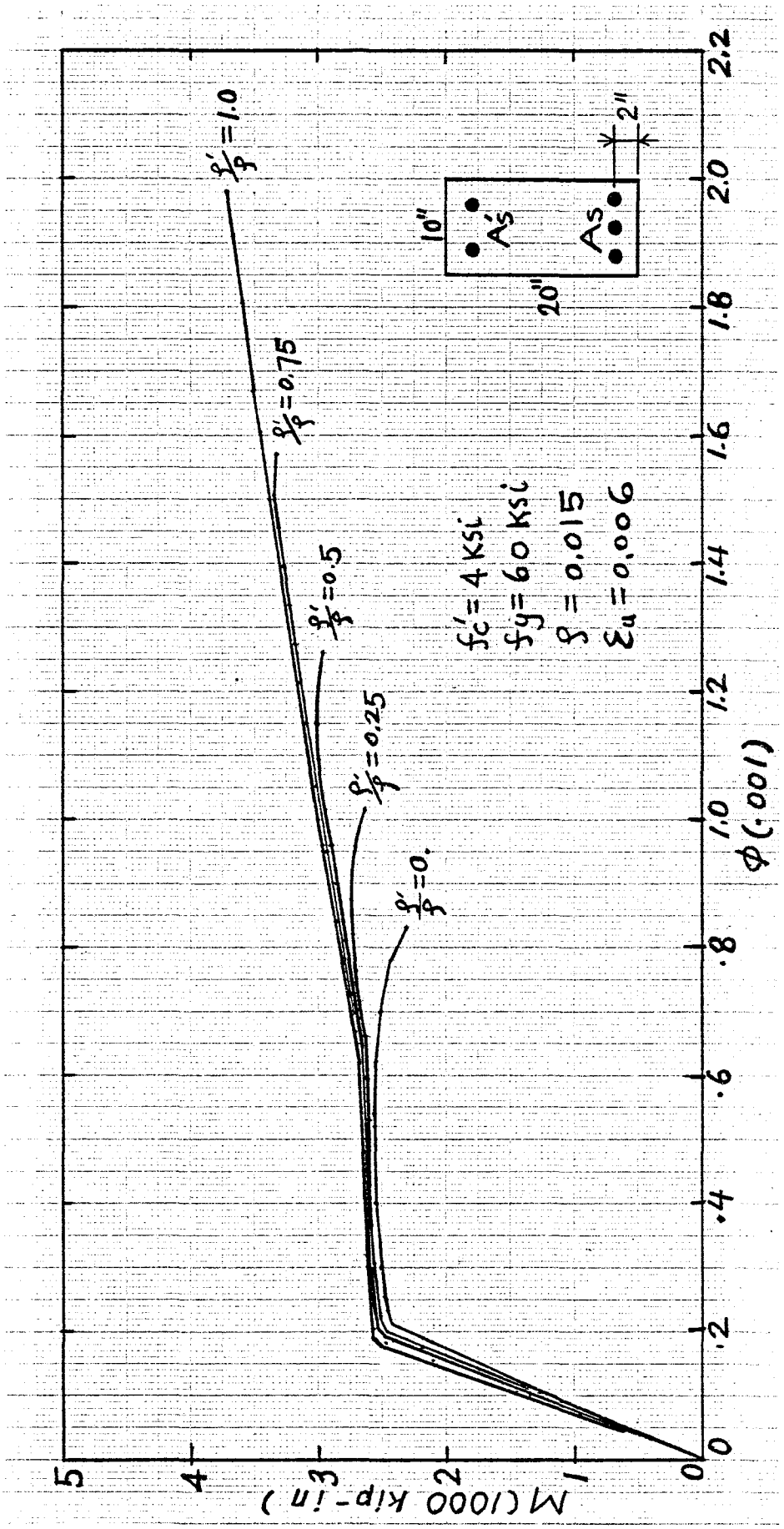

Fig. 6.9 Effect of compression reinforcement on ductility for lightweight concrete.

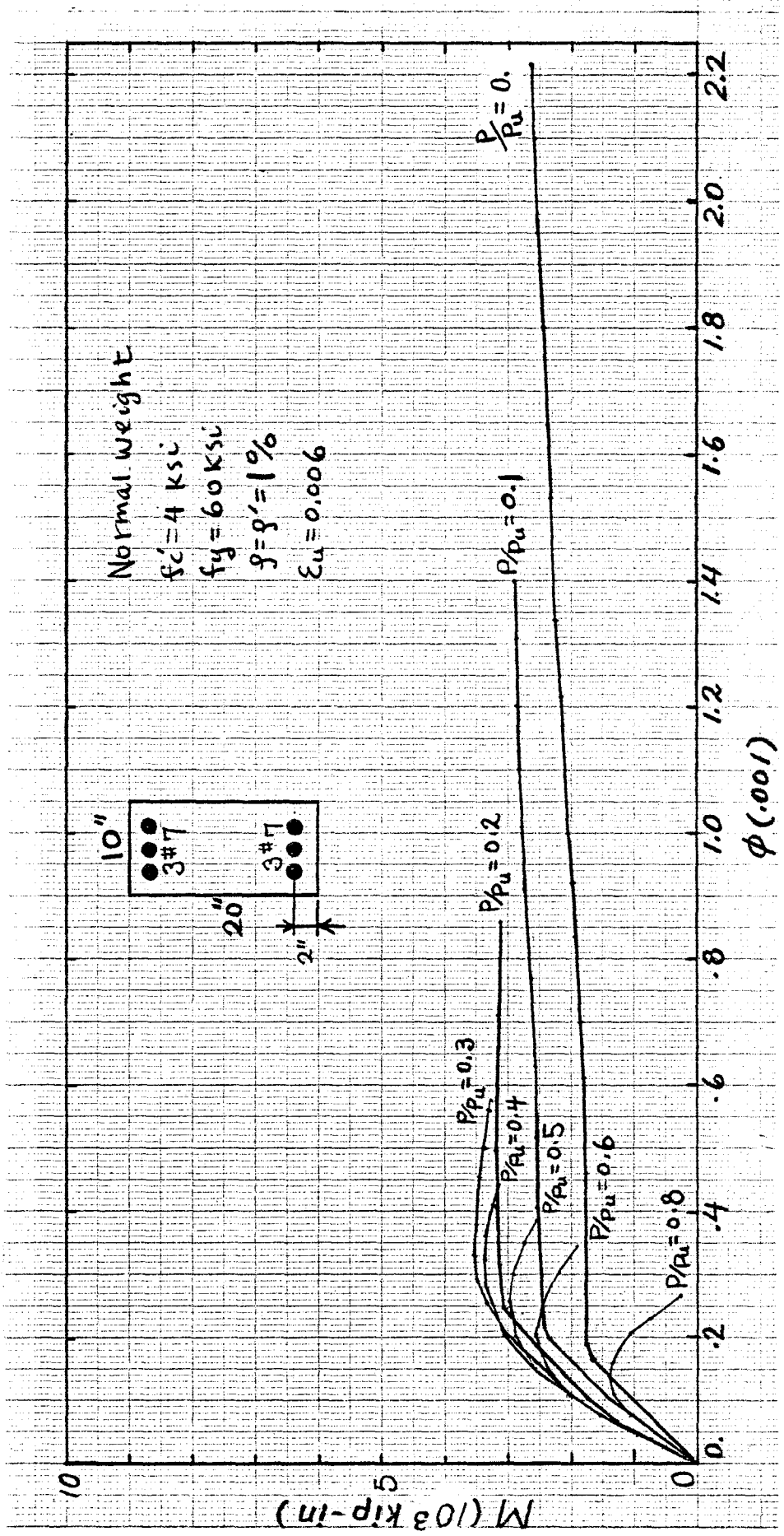

Fig. 6.10 Effect of axial loads on ductility: M-ϕ diagram for normal weight concrete.

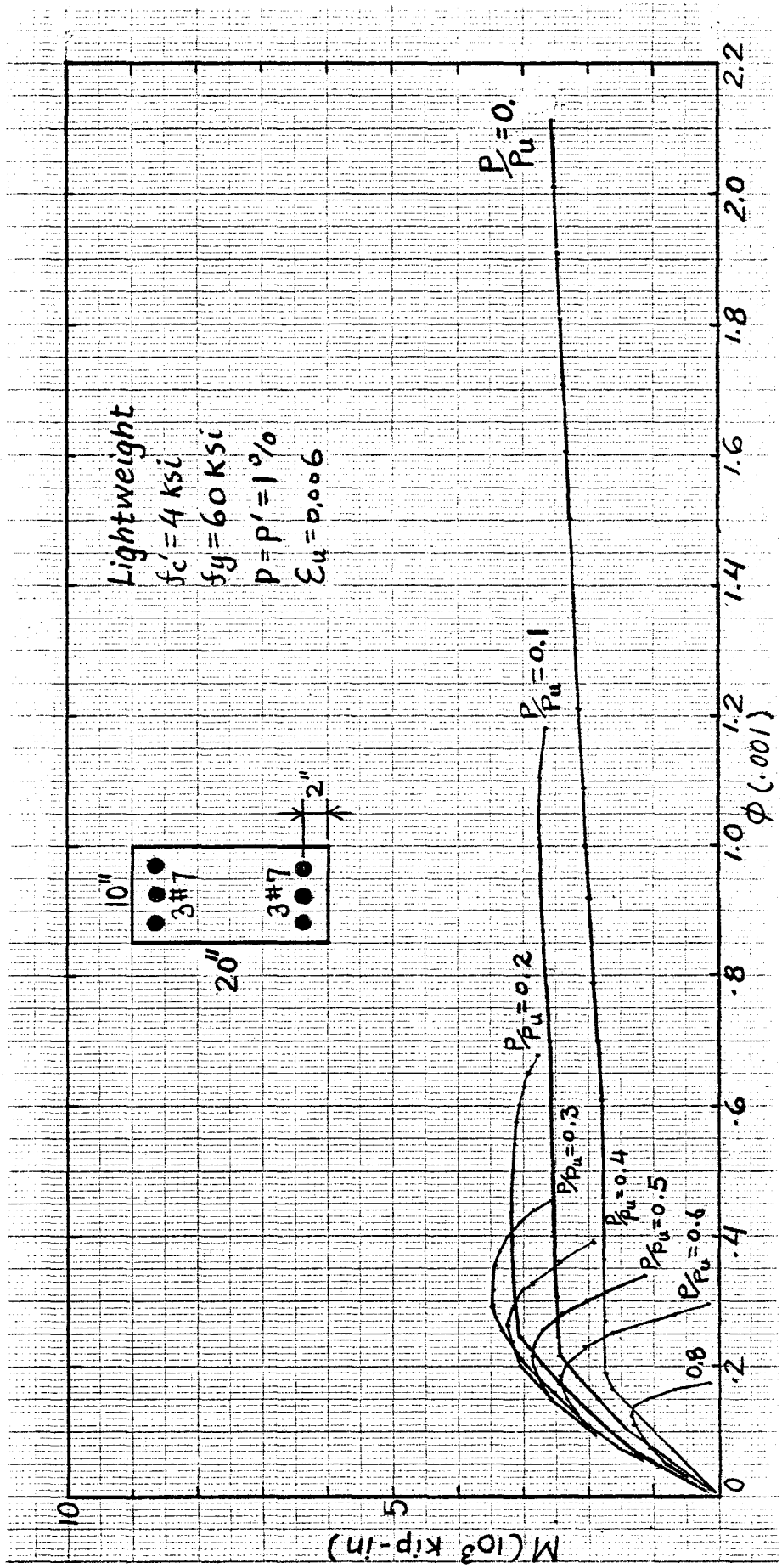

Fig. 6.11 Effect of axial loads on ductility: M-ϕ diagram for lightweight concrete.

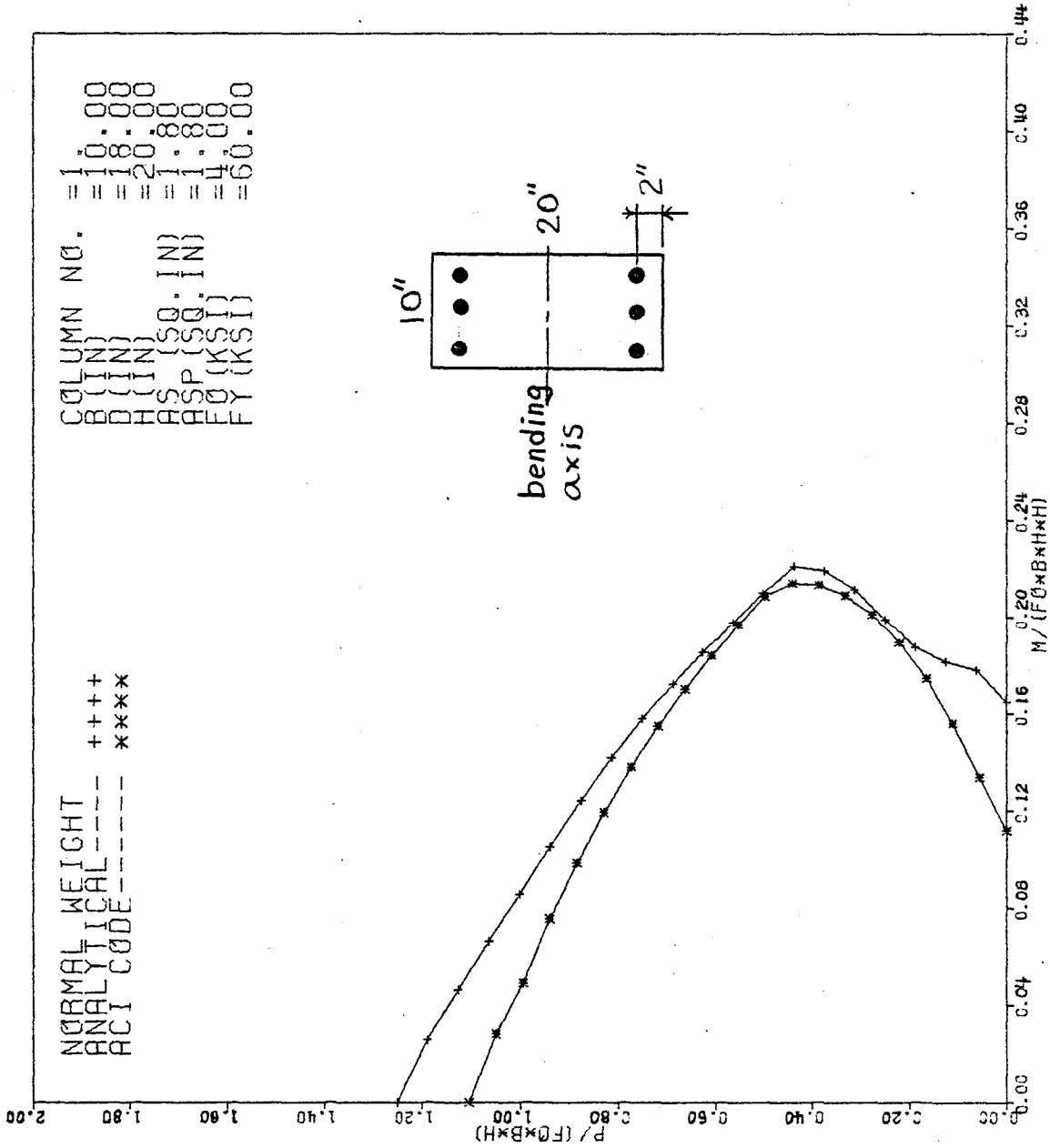

Fig. 6.12 Interaction diagram for normal weight concrete.

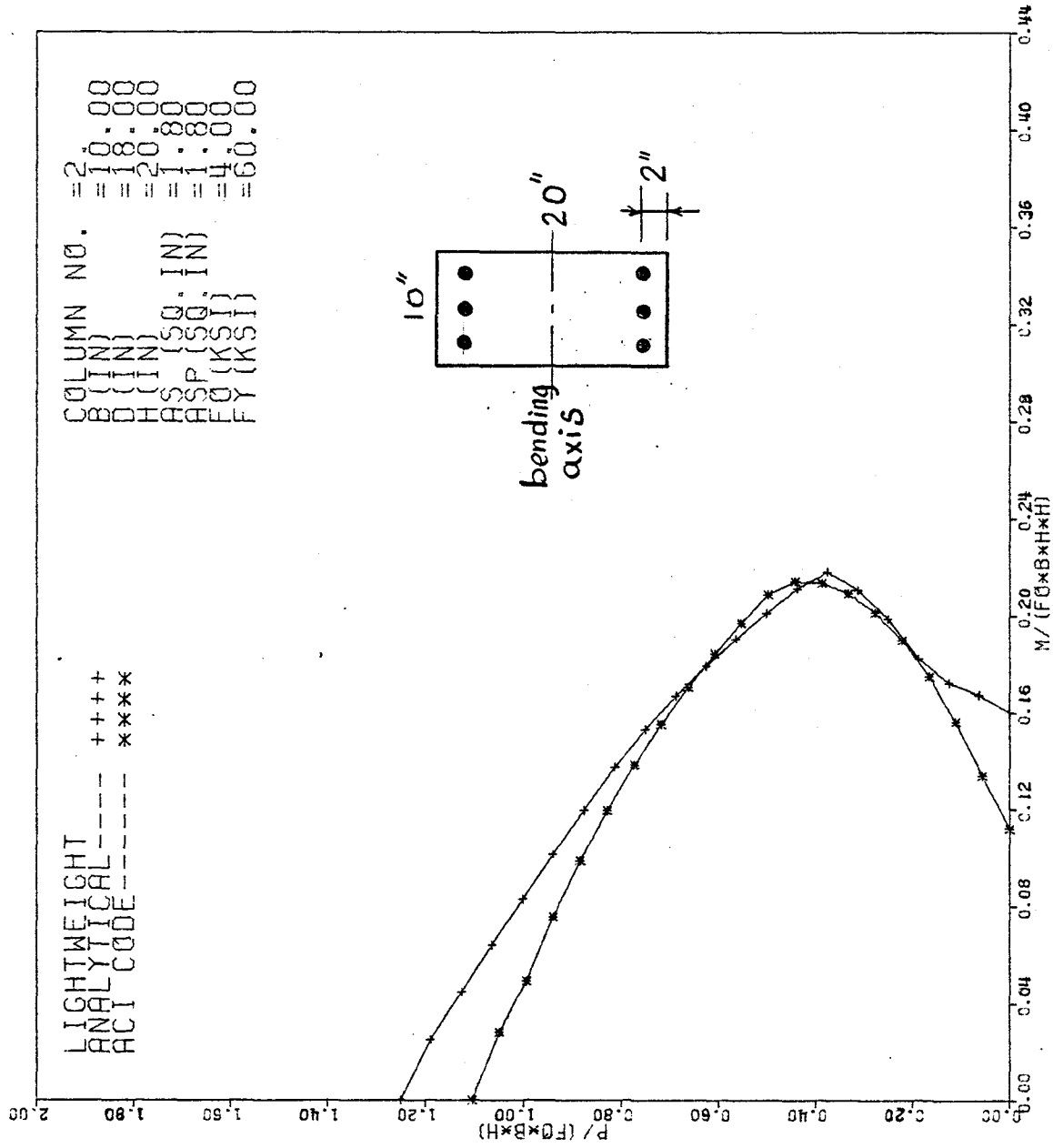

Fig. 6.13 Interaction diagram for lightweight concrete.

in Figs. 6.10 and 6.11. It can be seen that for axial loads greater than 30% of the axial load-capacity, very little ductility remains.

The effects of biaxial bending on the ductility of column sections are investigated in the following example. The materials properties are: for normal weight concrete, f'_c = 5 ksi and 9 ksi; for steel, f_y = 60 ksi. The sectional properties are shown in Fig. 6.2b for a square column having the dimensions of 10" x 10" with four #7 bars. The eccentricity angles due to biaxial bending are 0°, 22.5° and 45° measured from the centroidal axis of the cross section.

The effects of axial loads on the ductility can be observed from the moment-curvature diagrams, for $\theta = 0°$, 22.5° and 45°, respectively, plotted in Figs. 6.14, 6.15 and 6.16 for normal weight concrete with f'_c = 5 ksi. It can be seen that when the axial load approaches about 30% of the axial load-capacity, the resulting moment capacity reaches a maximum value which corresponds to the balanced moment M_b, of the column load-moment interaction surface, while the ductility factor reduces to a value of one. As the axial load continues to increase, the resulting moment decreases; the moment-curvature diagram becomes steeper on the descending portion, and the section is considered less ductile.

The effect of the eccentricity angles on the ductility can be observed from the moment-curvature diagram for f'_c = 5 ksi and 9 ksi, respectively, in Figs. 6.18 and 6.19. Therefore, everything else being equal, the higher the eccentricity angle the smaller the ductility of the section.

The effect of concrete strength on ductility can be observed by comparing Figs. 6.17 and 6.18, where the moment-curvature diagrams in biaxial bending are plotted. It can be seen that the higher strength

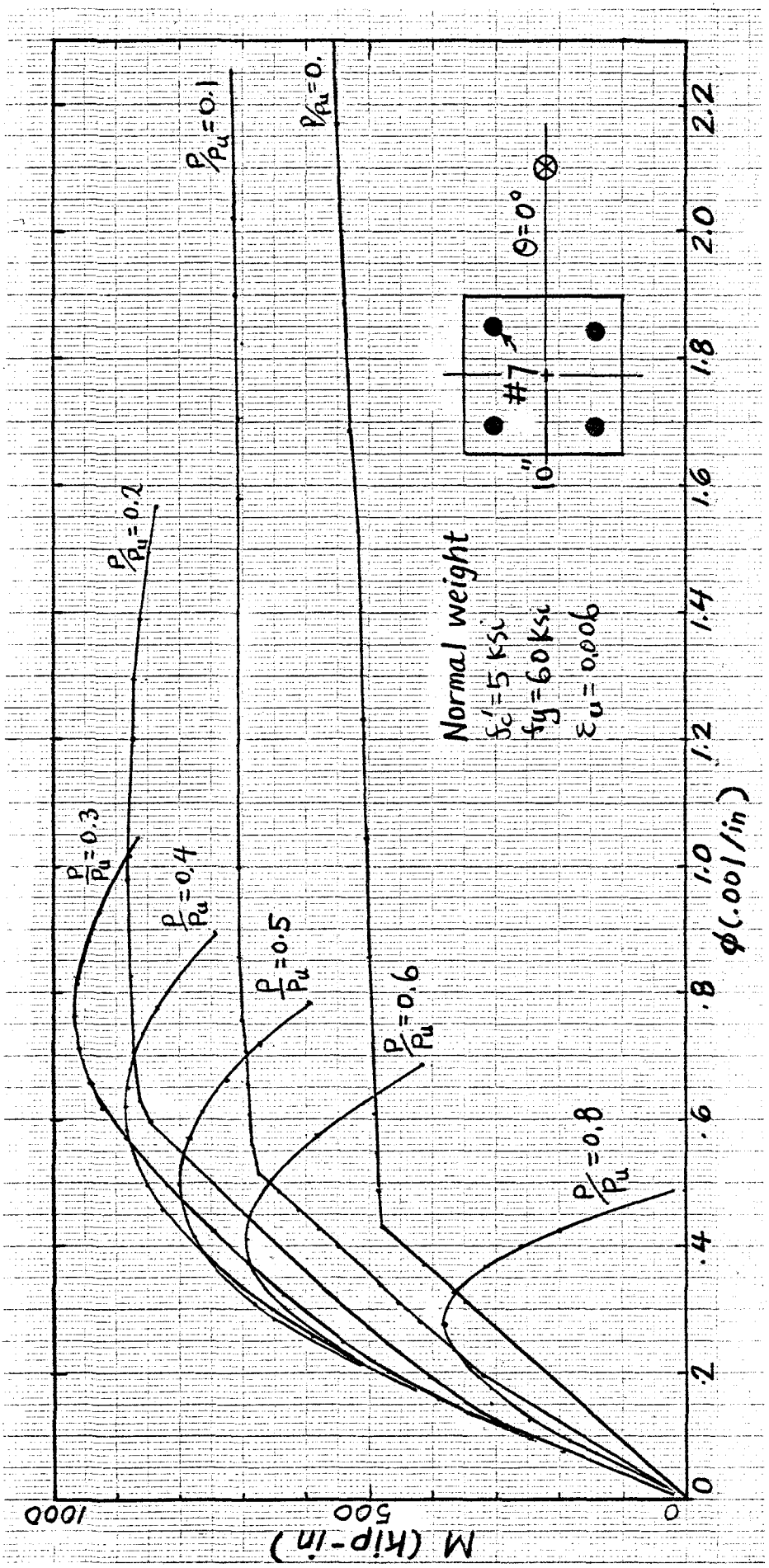

Fig. 6.14 Effect of axial loads on ductility: M-ϕ diagram for $\theta = 0^{o}$.

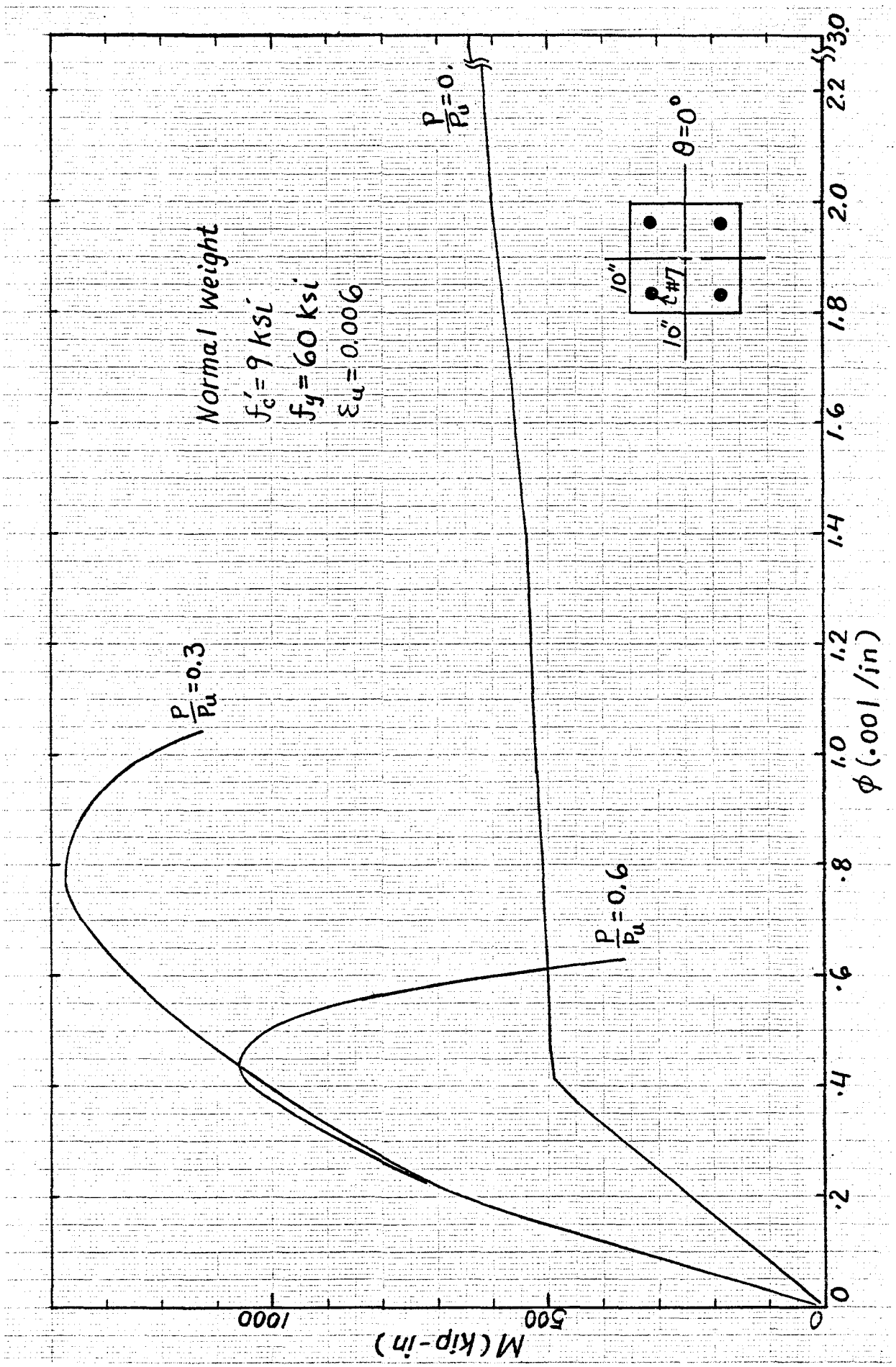

Fig. 6.14 (cont'd)

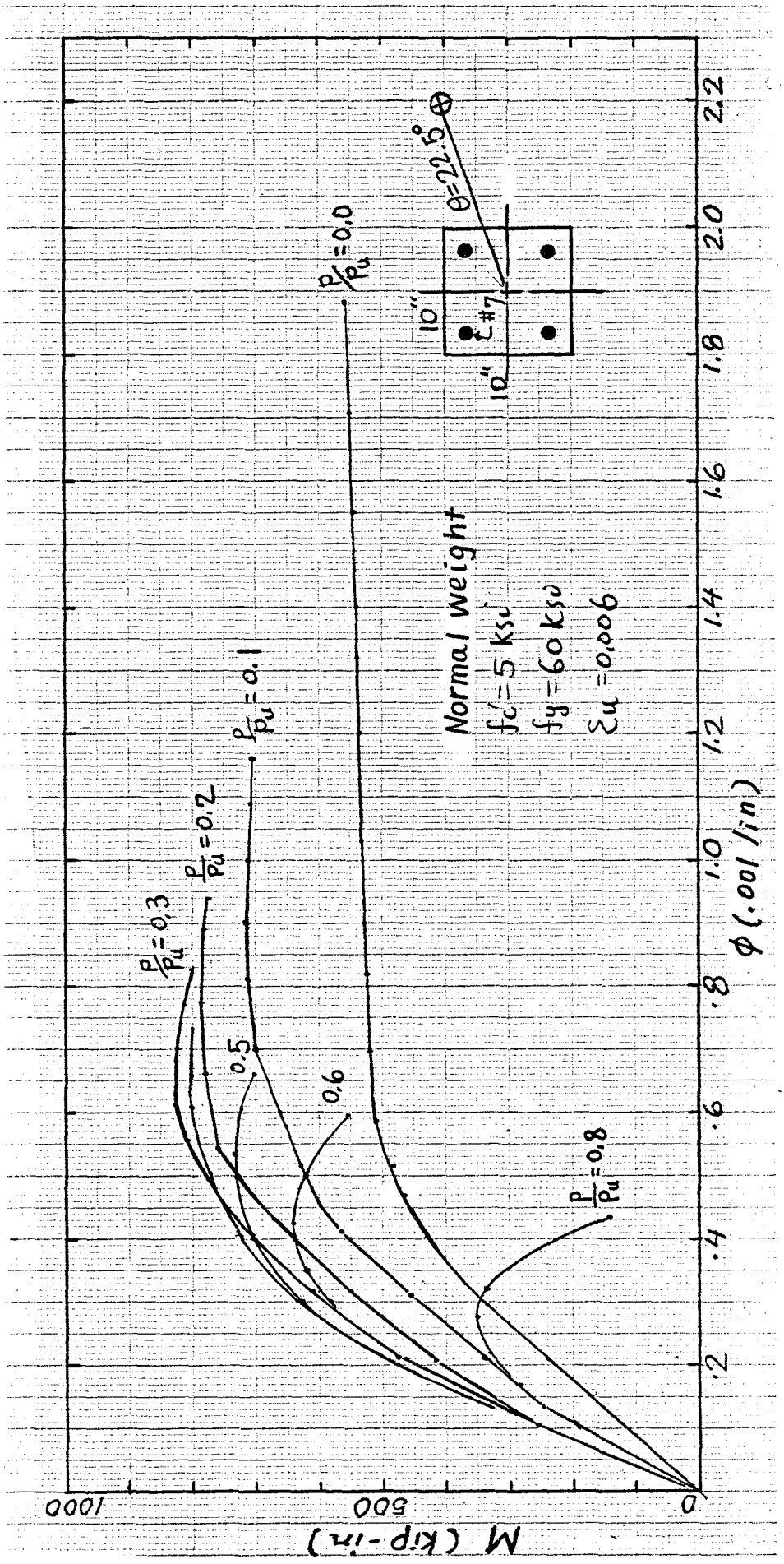

Fig. 6.15 Effect of axial load on ductility: M-φ diagram for θ = 22.5°.

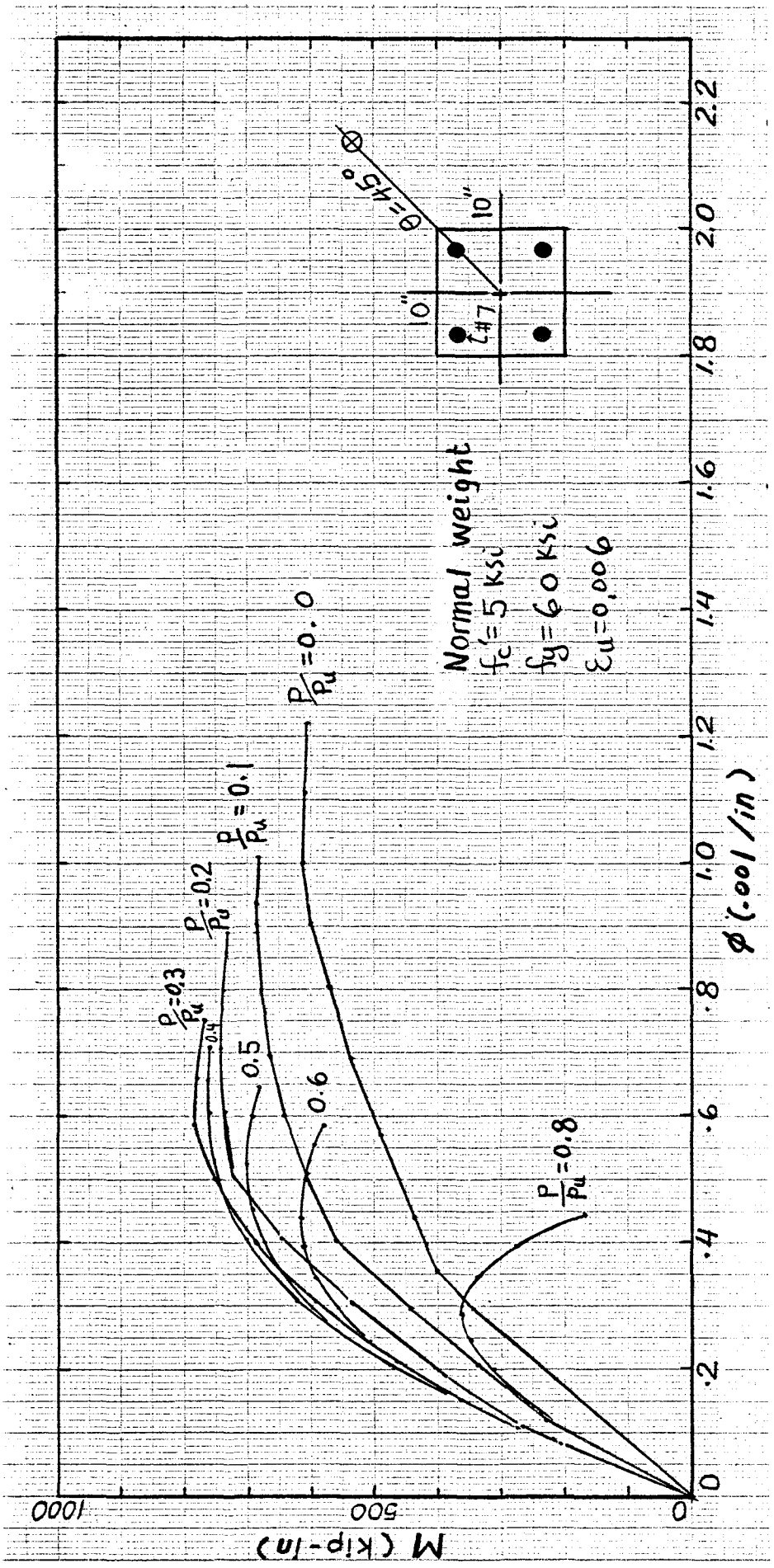

Fig. 6.16 Effect of axial load on ductility: M-φ diagram for θ = 45°.

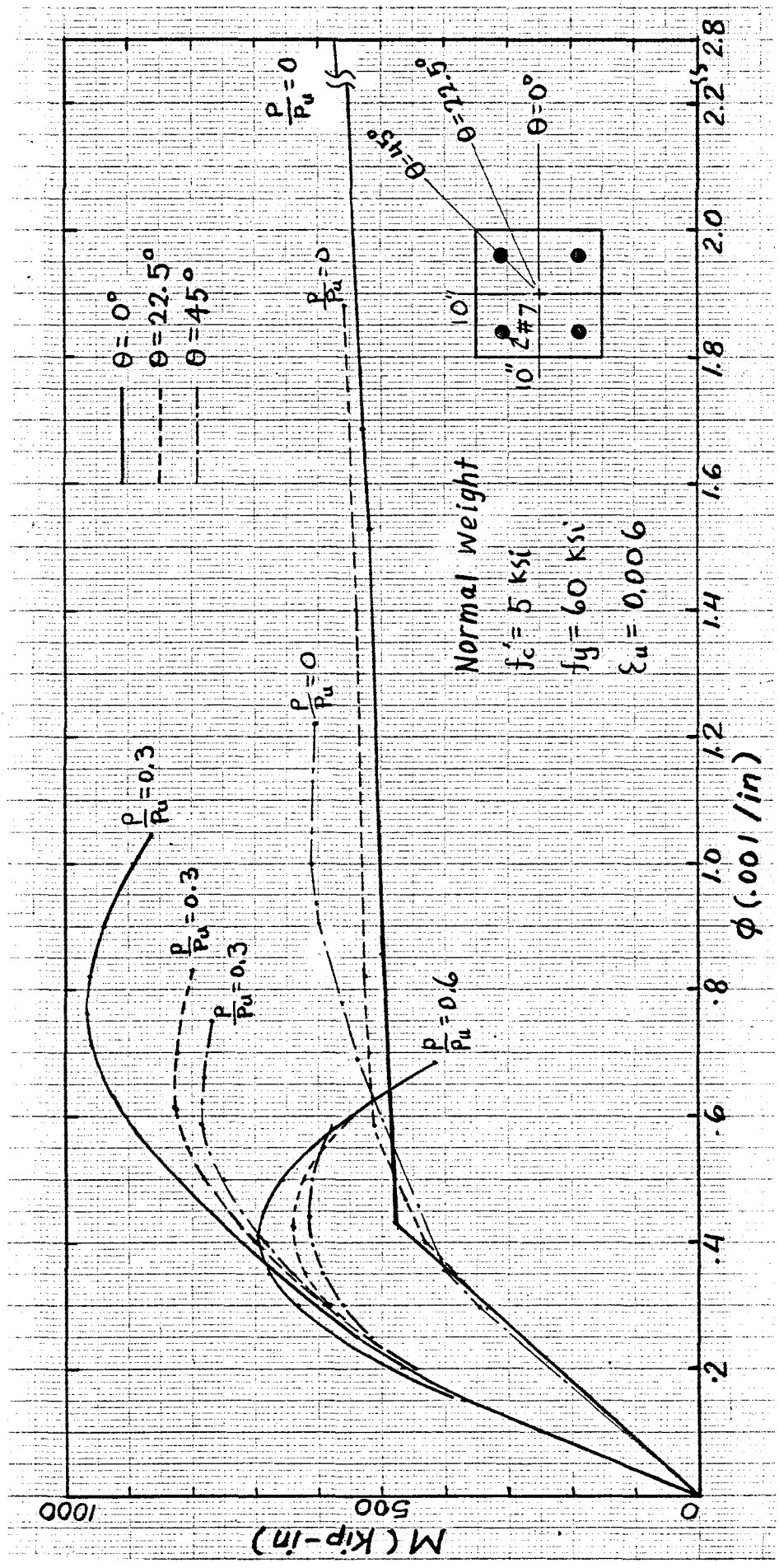

Fig. 6.17 Effect of eccentricity angles on ductility: M-φ diagram for f'_c = 5000 psi.

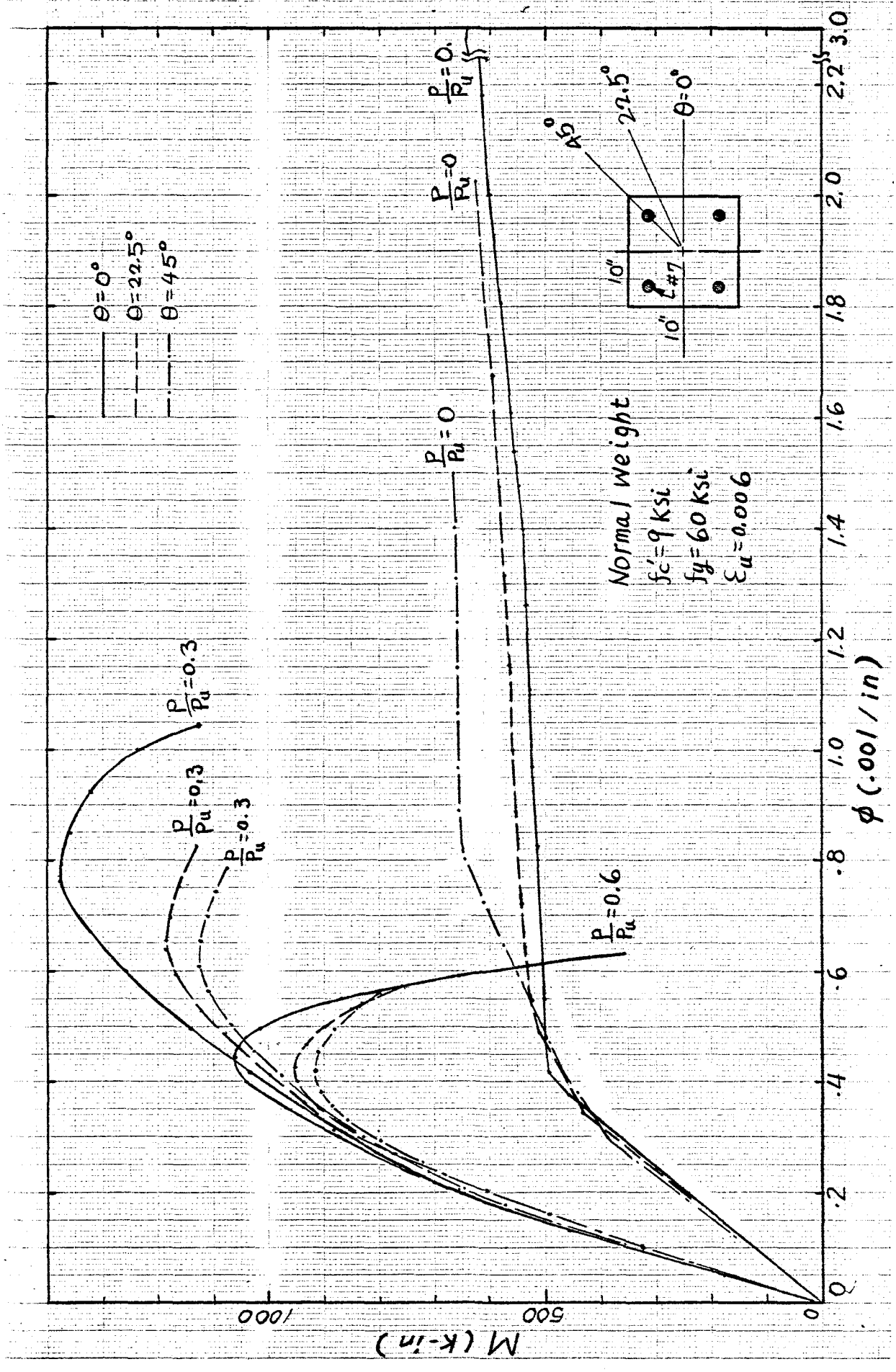

Fig. 6.18 Effect of eccentricity angles on ductility: M-φ diagram f'_c = 9000 psi.

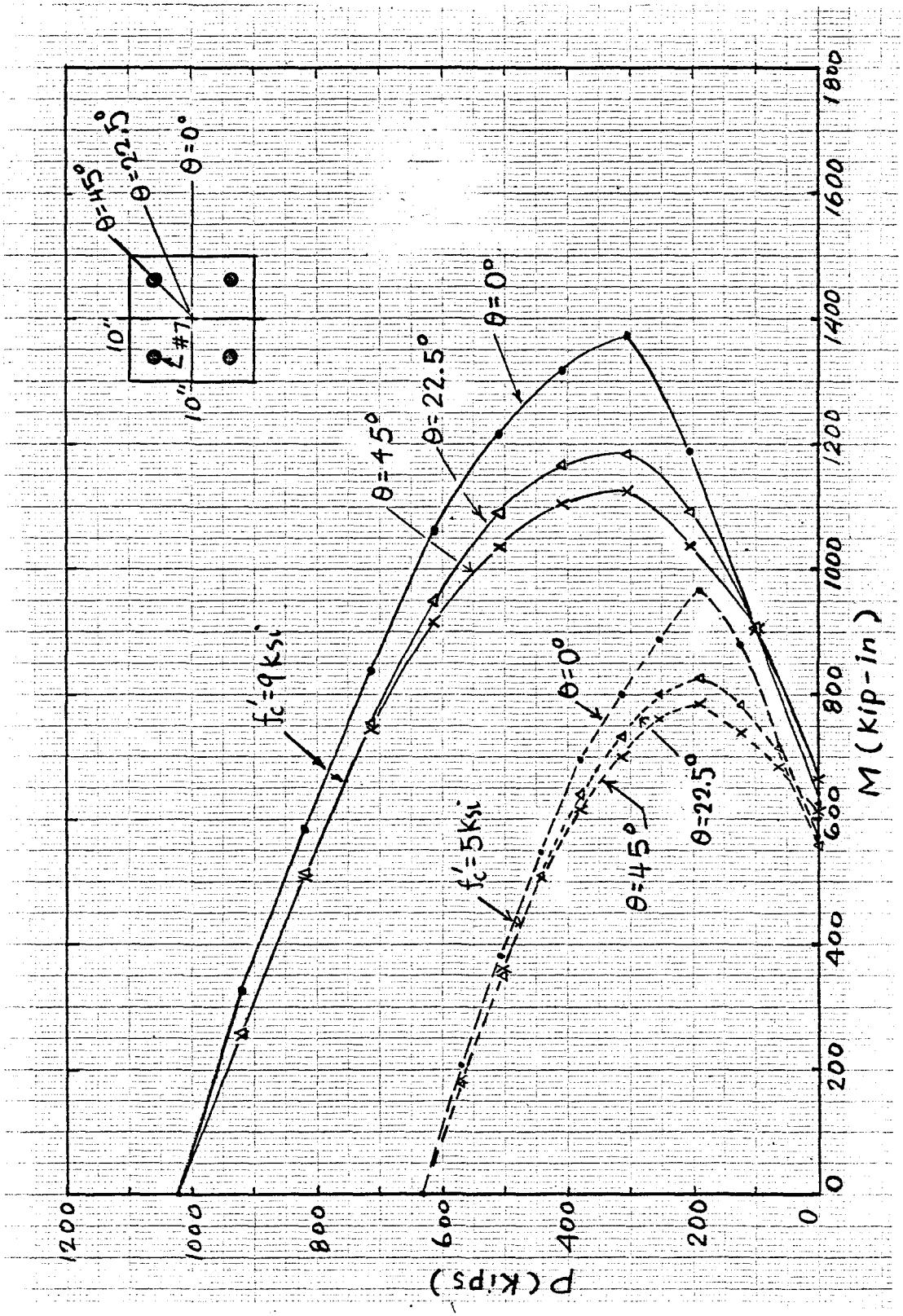

Fig. 6.19 Effect of concrete strengths on column interaction P-M diagram.

concrete section (9 ksi) shows about the same ductility as the lower strength section (5 ksi). This result is different from that observed at the material level where the higher the strength the lower the ductility.

The effects of concrete strength on the column load-moment interaction diagram are shown in Fig. 6.19. For pure bending, the higher strength concrete does not significantly improve the moment capacity of the section. However, as the axial load increases, the higher strength concrete shows a much more beneficial effect by improving the column load and moment especially at axial loads greater than about 30% of the axial load-capacity for pure compression.

The comparison of column load-moment interaction diagrams derived theoretically and according to the ACI code (where $\varepsilon_u = 0.003$) are shown in Figs. 6.20 and 6.21 for the uniaxial bending case. It can be observed that there is little difference in the diagrams especially at lower axial loads. This result strongly suggests that the ACI predictions for moment and load capacities are accurate; however, it was noted earlier for beams that although the moment capacity predicted by the code is satisfactory, there may be substantial error in estimating the curvature of the section at ultimate capacity.

6.5 ROTATIONAL CAPACITY OF HINGING REGION AND MID-SPAN DEFLECTION OF REINFORCED-CONCRETE BEAMS

6.5.1 Introduction

Both the limit design of structural concrete and the plastic design of structural steel stem from a recognition of the inelastic behavior of structures at high loads. The plastic design methods developed for steel

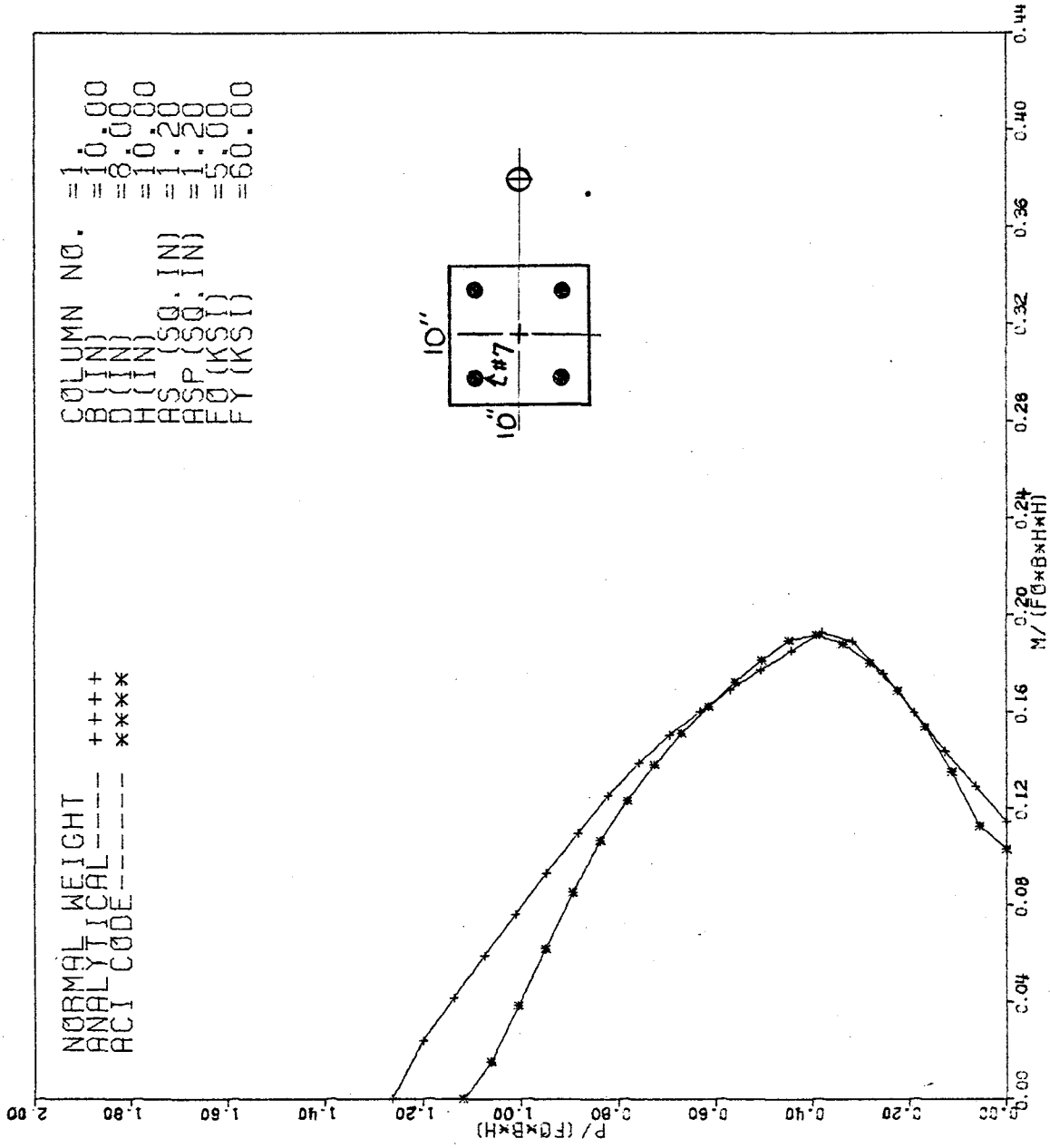

Fig. 6.20 Comparison of theoretical and the ACI column interaction P-M diagram for f'_c = 5000 psi.

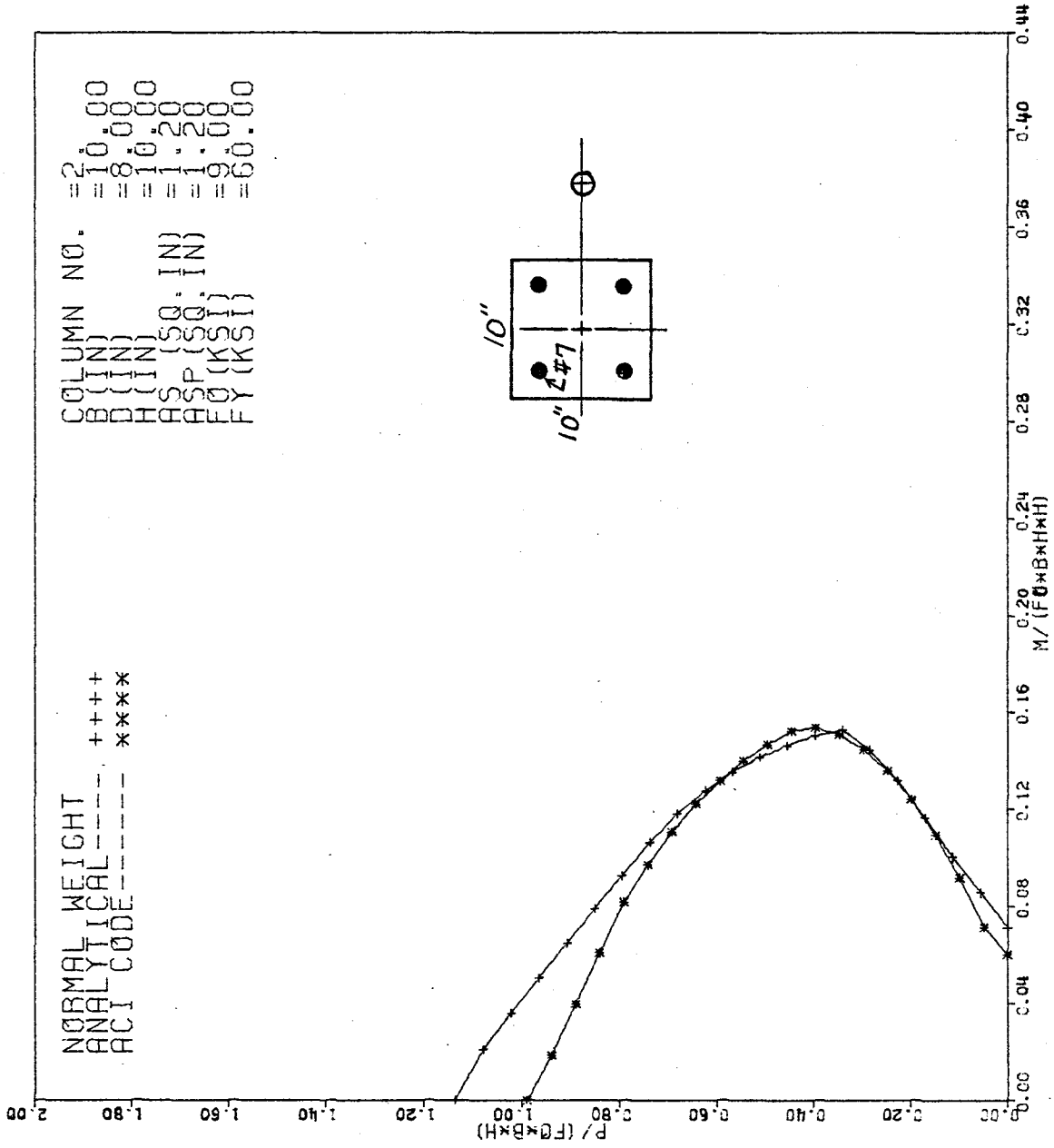

Fig. 6.21 Comparison of theoretical and the ACI column interaction P-M diagram for f'_c = 9000 psi.

concentrate on the formation of sufficient hinging mechanisms in a structure. Little attention is paid to the magnitude of the strains at the individual hinging sections as the redistribution of the moment proceeds. The strains that can be developed in the concrete and reinforcing steel in a reinforced-concrete member are considerably less than those which can be developed in a mild steel member. It is therefore necessary to consider the deformation of the hinging region in any theory of limit design for structural concrete.

6.5.2 Ultimate Strain at Extreme Fiber of Concrete and the Approximation of Moment-Curvature Diagram of a Section

The 1971 ACI code assumes that the ultimate moment capacity of a reinforced-concrete section always occurs when the compressive strain at the extreme fiber of concrete reaches a value of 0.003. This assumption is considered to be a good approximation for calculating the ultimate moment capacity, but it is quite different in calculating the ultimate curvature especially for underreinforced beams. The strain at ultimate moment may range from 0.0040 to 0.0048 as indicated, for example, in reference [39].

It is apparent that the knowledge of the moment curvature relationships for reinforced-concrete sections is necessary if calculations are to be made of the total inelastic or plastic rotations for a structural concrete member. In Fig. 6.22, two moment-curvature relationships are shown for the column case under study (pure bending) with concrete strength equal to 5 ksi and 9 ksi, respectively. A straight-line approximation for the portion between yield moment and ultimate moment is considered to be representative, and will be used in the following analysis

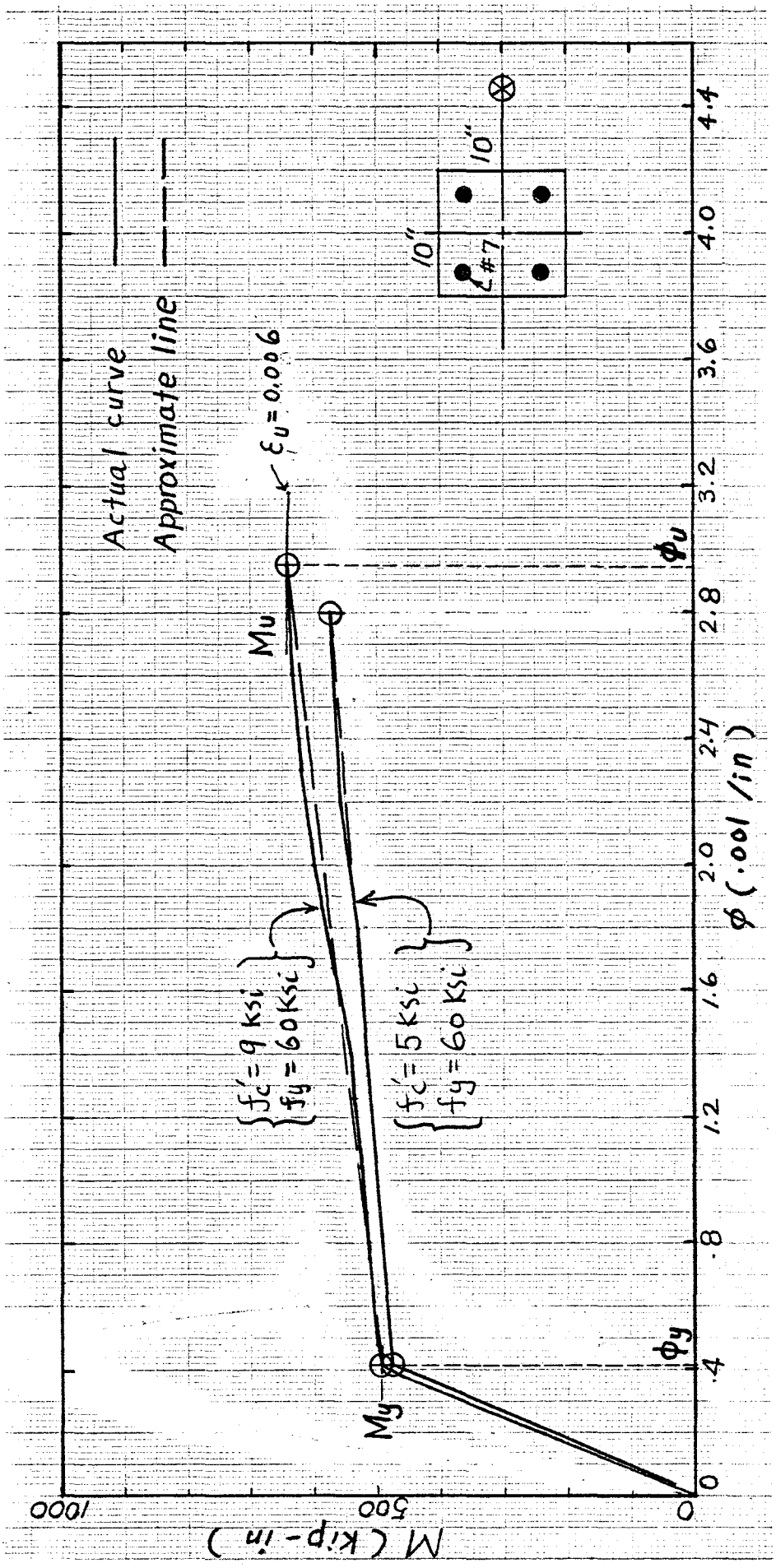

Fig. 6.22 Approximate straight lines for M-ϕ diagram.

of the rotation capacity and the mid-span deflection for reinforced-concrete beams [23].

6.5.3 Mid-Span Deflection of a Reinforced-Concrete Beam at Ultimate Capacity

A. Mid-span loading (Fig. 6.23a).

The steps suggested to calculate the mid-span deflection (see also [23]) are as follows:

1. Draw the moment diagram for the simply supported beam as shown in Fig. 6.23b.

2. Determine the shear span z, and the plastic hinge length x_p, as indicated in Fig. 6.23b where

$$z = \frac{\ell}{2} = \text{distance between maximum moment and zero moment}$$

$$x_p = \left(\frac{M_u - M_y}{M_u}\right) z \qquad (6.8)$$

M_u = ultimate moment

M_y = yield moment

3. Determine the moment-curvature relationship. The actual M-ϕ diagram for a given sectional and material property has been simplified by two straight-lines meeting at the yield point as shown in Fig. 6.22.

4. Draw the curvature distribution diagram along the beam as shown in Fig. 6.23c.

5. Calculate the elastic deflection at the mid-span (Fig. 6.23d)

$$\Delta_e = \phi_y \left(\frac{M_u}{M_y}\right) \frac{\ell}{4} \left(\frac{\ell}{2} - \frac{\ell}{6}\right) = \phi_y \left(\frac{M_u}{M_y}\right) \left(\frac{\ell^2}{12}\right) \qquad (6.9)$$

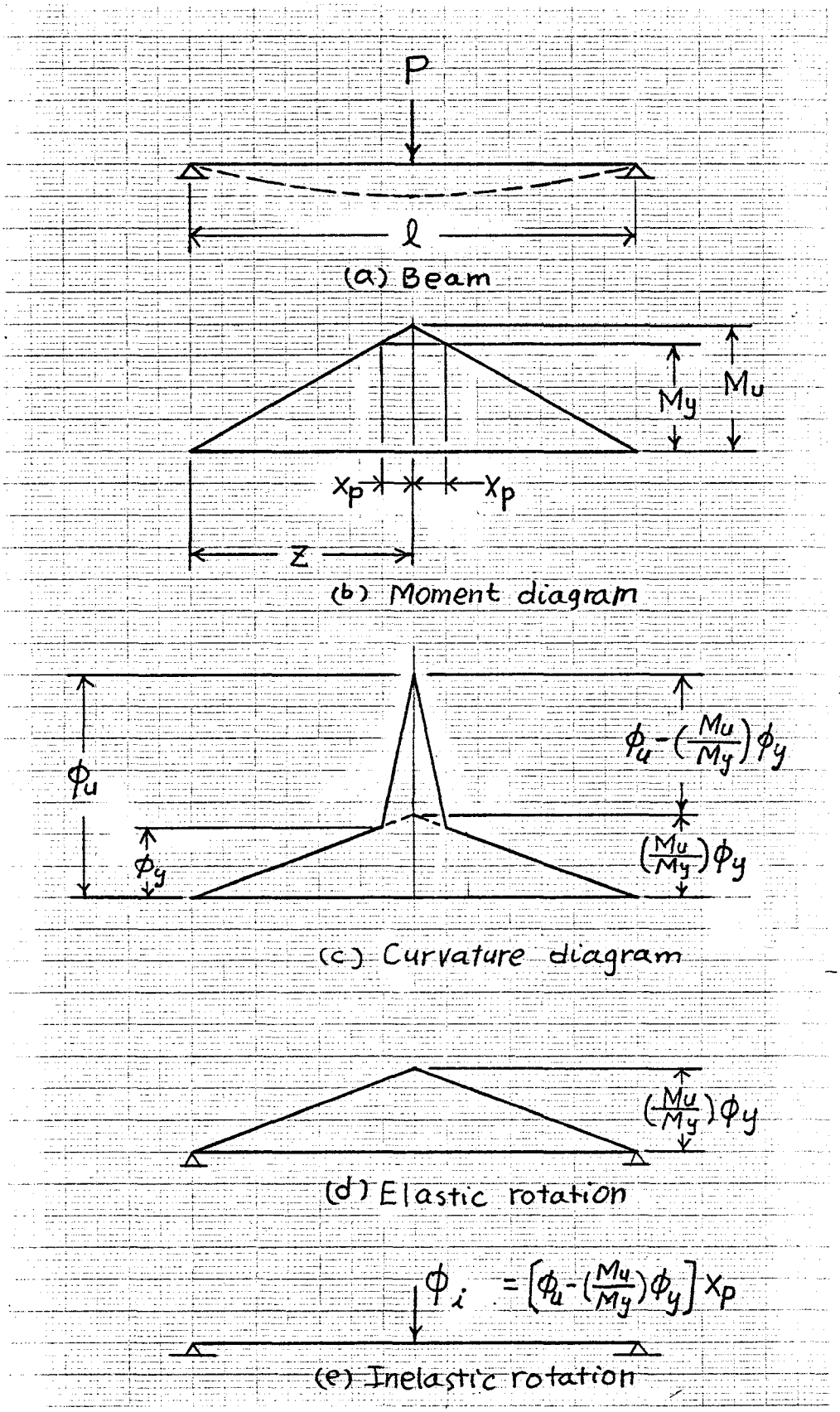

Fig. 6.23 Calculation of mid-span deflection for beam loaded at mid-span.

where

ϕ_y = yield curvature

6. Calculate the inelastic deflection at the mid-span (Fig. 6.23e)

$$\phi_i = \left[\phi_u - \left(\frac{M_u}{M_y}\right)\phi_y\right] x_p \tag{6.10}$$

$$\Delta_i = \frac{\phi i}{2}\left(\frac{\ell}{2}\right) = \left(\frac{\ell}{4}\right)\left(x_p\right)\left[\phi_u - \left(\frac{M_u}{M_y}\right)\phi_y\right] \tag{6.11}$$

where

ϕ_u = ultimate curvature

7. Calculate the total deflection at the ultimate stage

$$\Delta_u = \Delta_e + \Delta_i \tag{6.12}$$

8. Calculate the total deflection at the yield stage by substituting $M_u = M_y$ into Eq. (6.9) which leads to:

$$\Delta_y = \phi_y\left(\frac{\ell^2}{12}\right) \tag{6.13}$$

9. Calculate the ductility factor in terms of deflections where

$$\text{Ductility Factor} = \frac{\Delta_u}{\Delta_y} \tag{6.14}$$

B. Third-point loading (Fig. 6.24a)

The steps to calculate the mid-span deflection are similar to those for the beam loaded at the mid-span. The calculation steps are as follows:

1. The total mid-span deflection at the ultimate stage (Fig. 6.24b)

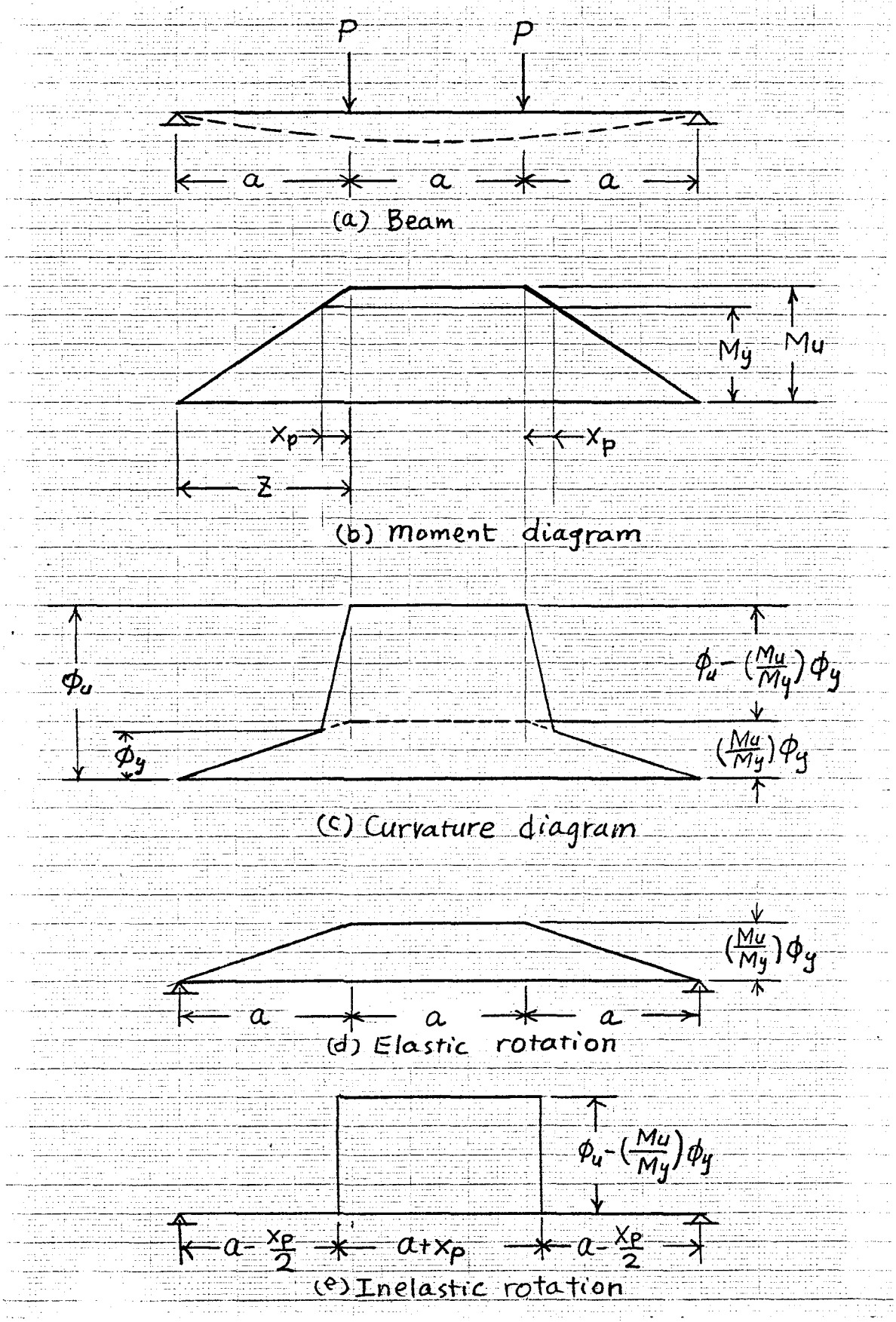

Fig. 6.24 Calculation of mid-span deflection for beam loaded at one-third span.

Deflection due to elastic rotation

$$\Delta_e = \left[\left(\frac{M_u}{M_y}\right)\phi_y\left(\frac{a}{2}\right) + \left(\frac{M_u}{M_y}\right)\phi_y\left(\frac{a}{2}\right)\right]\left(\frac{3a}{2}\right) - \left(\frac{M_u}{M_y}\right)\phi_y\left(\frac{a}{2}\right)\left[\left(\frac{a}{2} + \frac{a}{3}\right) + \left(\frac{a}{4}\right)\right]$$

or

$$\Delta_e = \left(\frac{M_u}{M_y}\right)\phi_y a^2\left(\frac{23}{24}\right) = 0.9583\left(\frac{M_u}{M_y}\right)\phi_y a^2 \qquad (6.15)$$

Deflection due to inelastic rotation

$$\Delta_i = \left[\phi_u - \left(\frac{M_u}{M_y}\right)\phi_y\right]\left(\frac{a + x_p}{2}\right)\left[\frac{\ell}{2} - \left(\frac{a + x_p}{4}\right)\right] \qquad (6.16)$$

where

$$x_p = \left(\frac{M_u - M_y}{M_u}\right) z$$

$z = a =$ shear span

Total deflection

$$\Delta_u = \Delta_e + \Delta_i \qquad (6.17)$$

2. The total mid-span deflection at the yield stage obtained by substituting $M_u = M_y$ into Eq. (6.15) which leads to:

$$\Delta_y = 0.9583\,\phi_y a^2 \qquad (6.18)$$

3. Ductility factor = Δ_u/Δ_y

CHAPTER VII

STUDY OF THE ULTIMATE STRENGTH PARAMETERS FOR THE DESIGN OF REINFORCED-CONCRETE SECTIONS

7.1 INTRODUCTION

In analyzing the flexural behavior of reinforced-concrete sections, several key parameters are considered, namely: the strain at the extreme compressive fiber of concrete, ε_{cu}; the properties of the compression zone of concrete described by α and β (see Fig. 5.5); the strain in the tensile steel, ε_s; the load-moment-curvature interaction diagram and the ductility factor. The above parameters will be investigated for normal weight concrete strength from 3 ksi to 13 ksi, and lightweight concrete strength from 3 ksi to 7 ksi. The stress-strain curves of concrete for the various strengths considered are shown in Figs. 7.1 and 7.2. The stress-strain curve for Grade 60 steel with a yield strength of 60 ksi is shown in Fig. 6.4.

7.2 PARAMETERS α AND β OF THE CONCRETE COMPRESSION ZONE

For a given concrete stress-strain curve, two important parameters α and β can describe the properties of that curve at any specified strain. These parameters are explained in Fig. 5.5. The parameter α relates to the area under the curve for a given strain, while β relates to the moment arm of that area with respect to the extreme compressive strain, ε_c. Since the compression zone of the reinforced-concrete section can be represented by these two parameters, a detailed study on their relationship with the entire range of strain is needed.

In Figs. 7.3 and 7.4, the variations of α, β (or β_1) and ε_c are plotted for various stress-strain curves of normal and lightweight concretes.

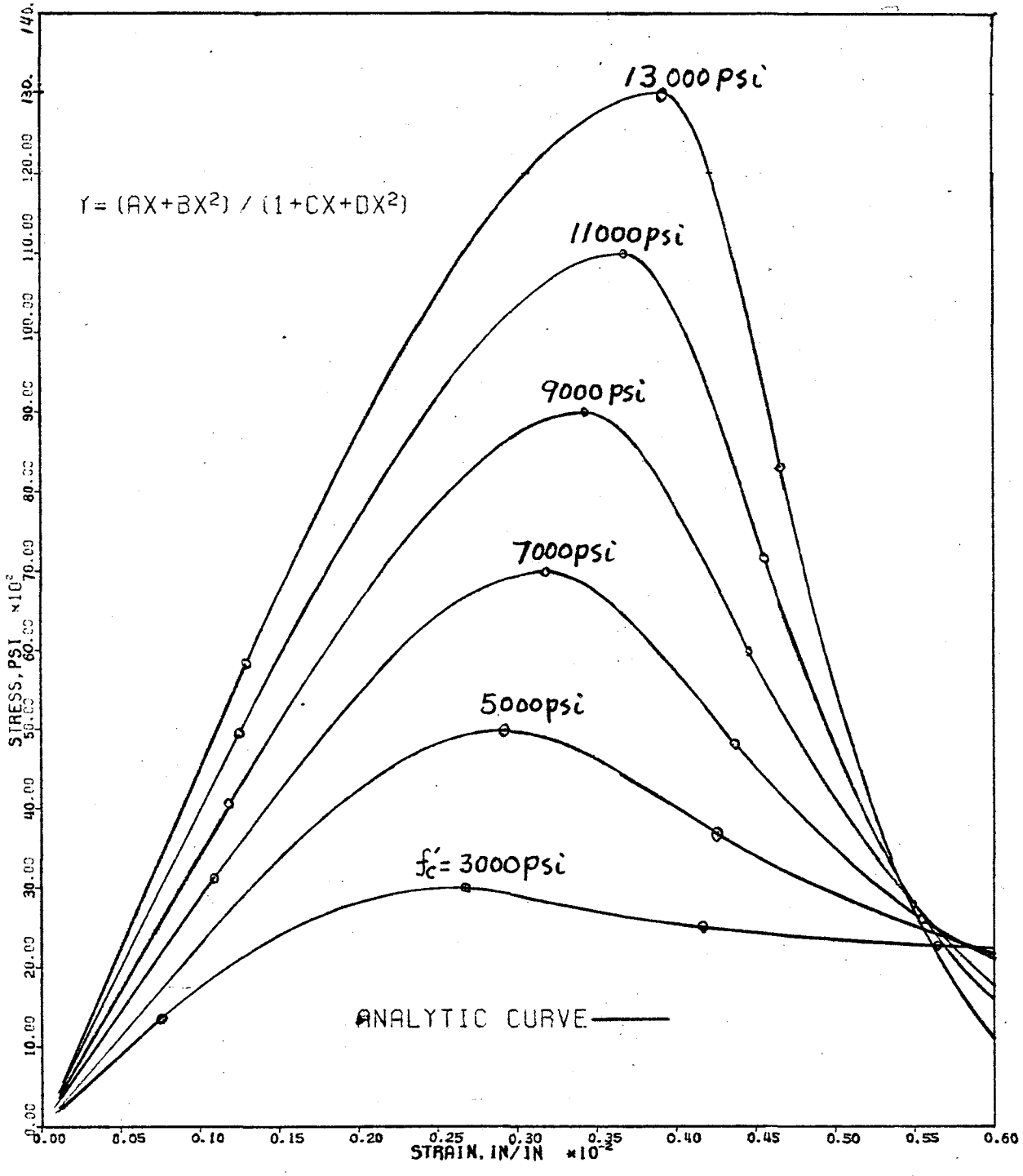

Fig. 7.1 Stress-strain curves of normal weight concrete with f'_c = 3,000 to 13,000 psi.

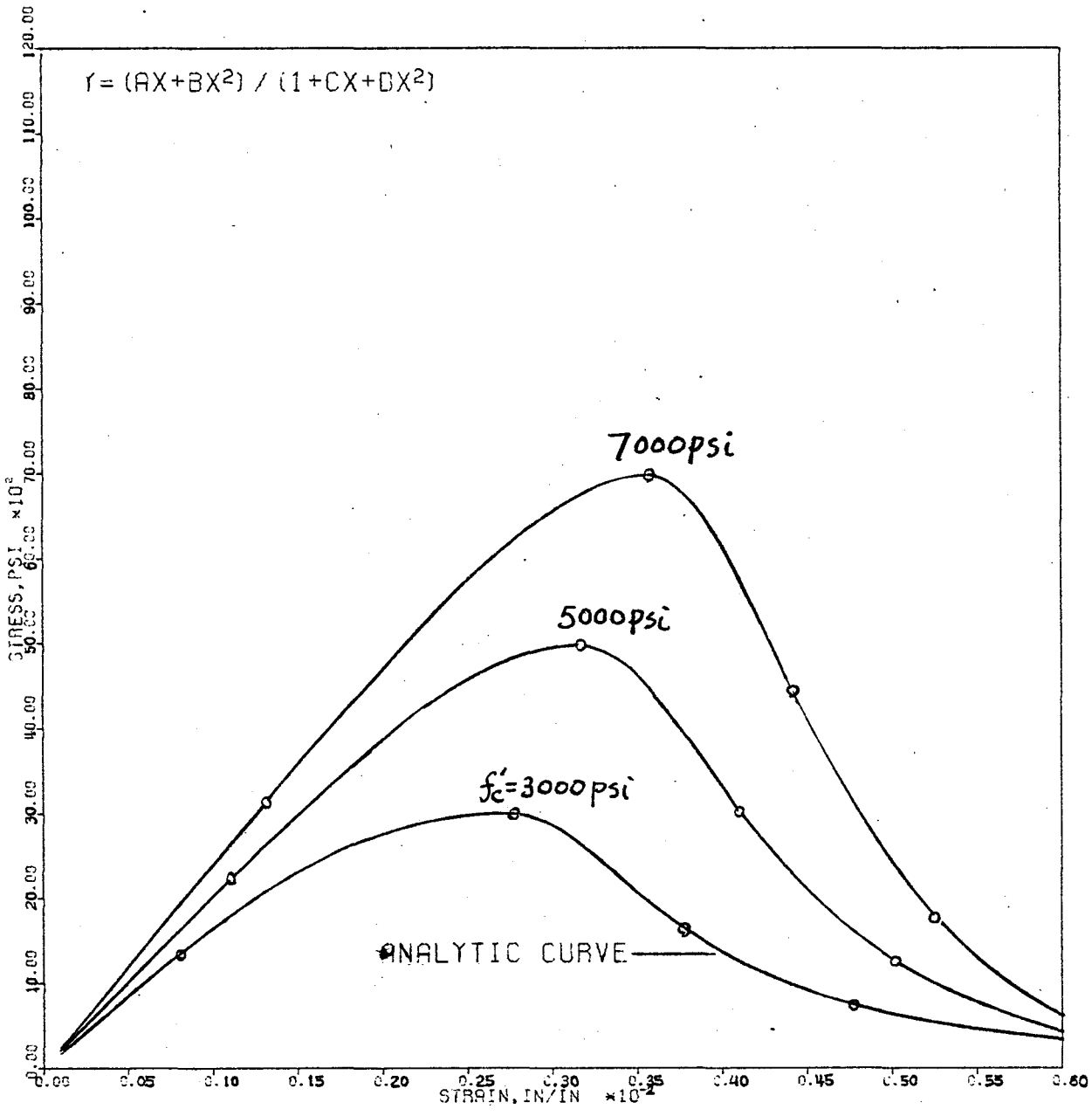

Fig. 7.2 Stress-strain curves of lightweight concrete with f'_c = 3,000 to 7,000 psi.

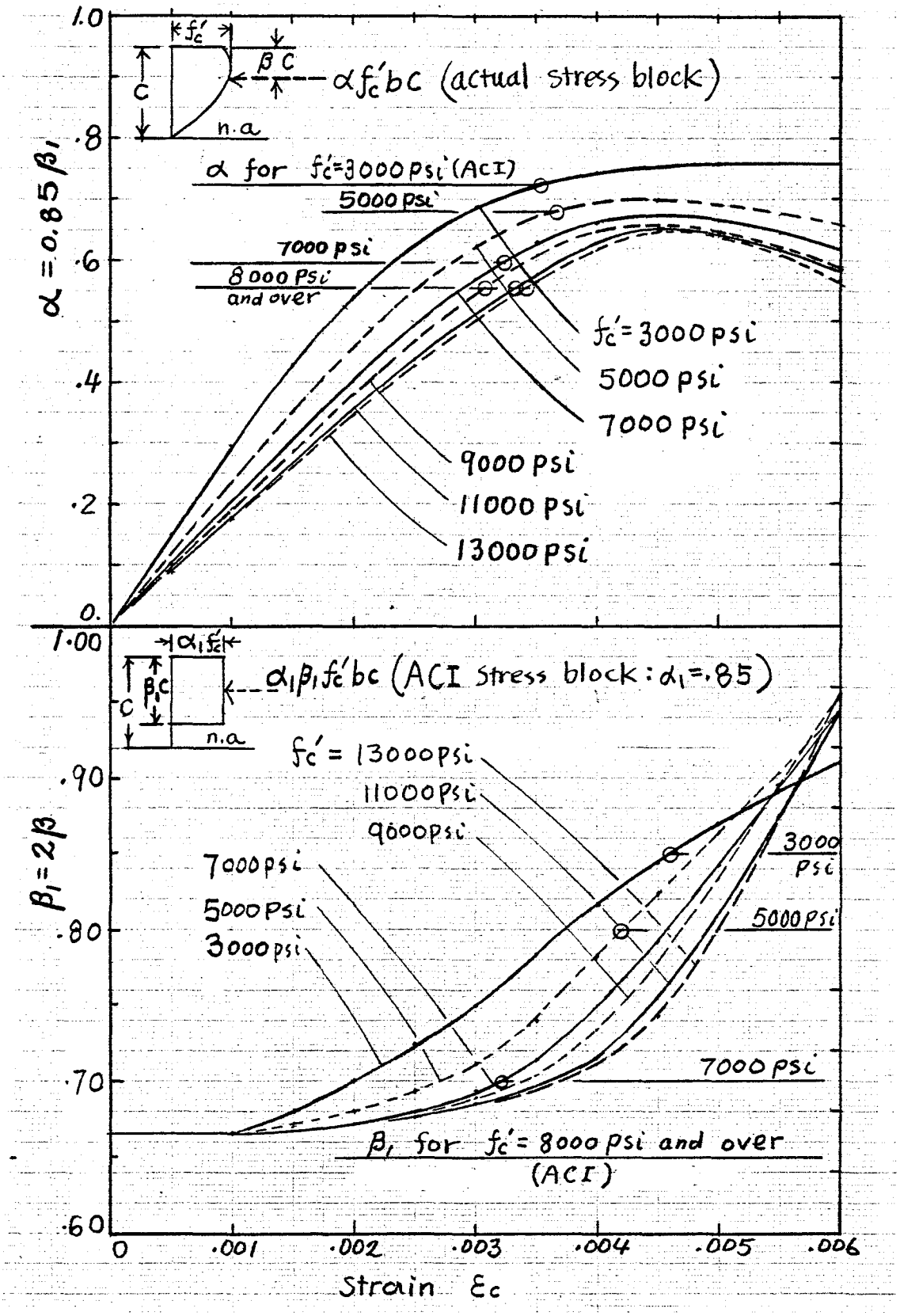

Fig. 7.3 Relationship of α, β vs. ε_c for stress-strain curves of normal weight concrete.

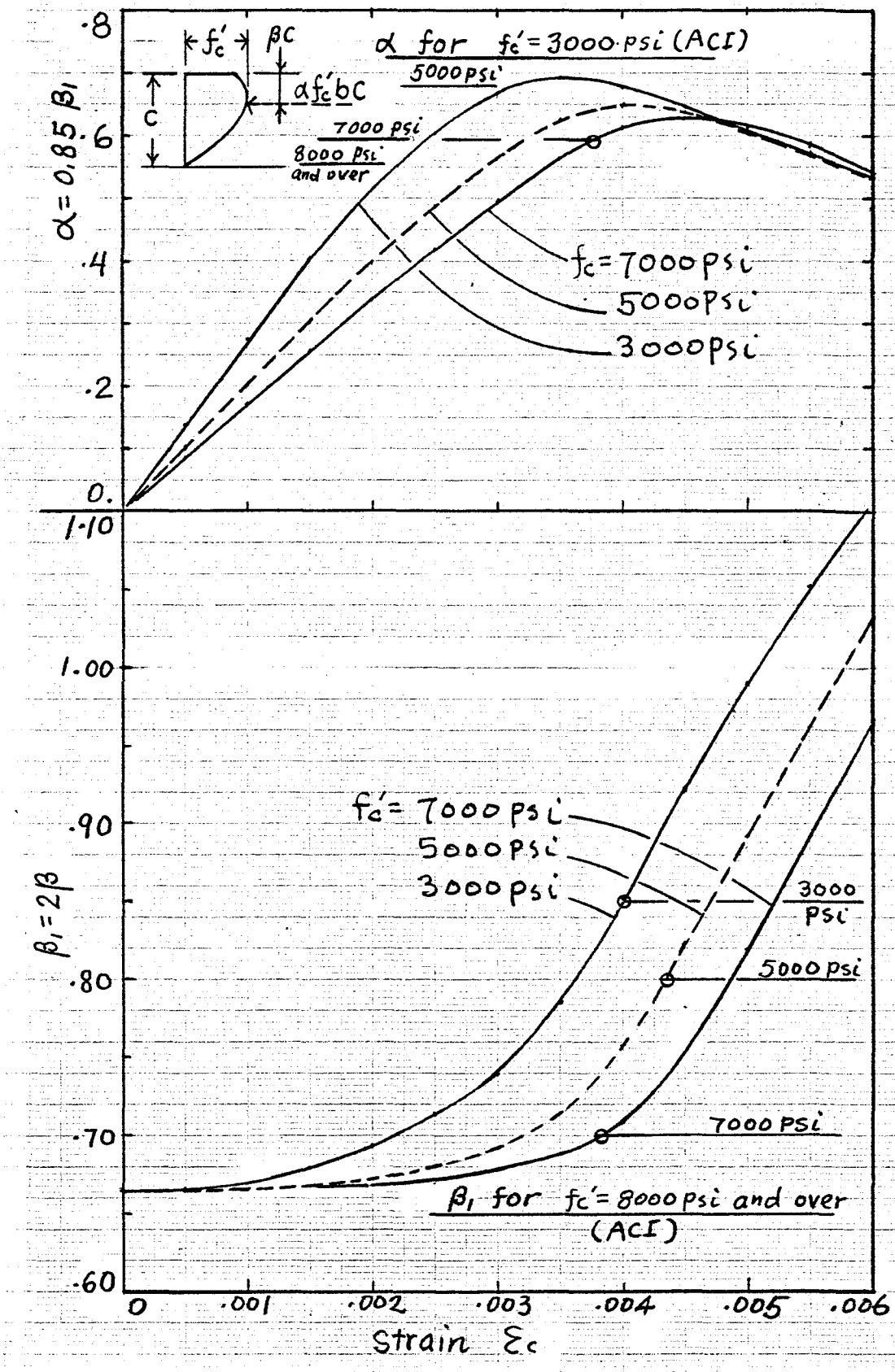

Fig. 7.4 Relationship of α, β vs. ε_c for stress-strain curves of light-weight concrete.

The corresponding values using the ACI assumptions are also plotted for comparison. In order to determine the maximum resisting moment of the compression zone with respect to the tensile steel, one attempts to maximize the value of α and minimize the value of β. From the α, ε_c relationship, the maximum α occurs at about $\varepsilon_c = 0.0045$ for most normal weight concrete strengths from 3000 psi to 13,000 psi, and at about $\varepsilon_{cu} = 0.0035$, 0.004, 0.0045, respectively, for lightweight concrete strengths of 3000, 5000 and 7000 psi. Therefore, the location of the maximum value of α can be written as follows:

$$\left\{ \begin{array}{ll} \varepsilon_{c\alpha} = 0.0045 & \text{for normal weight concrete of } f'_c = 3000 \text{ psi to } 13{,}000 \text{ psi} \\ \varepsilon_{c\alpha} = 0.0035 + 0.00025[(f'_c/1000) - 3] & \text{for lightweight concrete of } f'_c = 3000 \text{ psi to } 7000 \text{ psi} \end{array} \right\} \quad (7.1)$$

In most cases, the resisting moment of the compression zone of concrete, using $\varepsilon_{c\alpha}$ as the strain at the extreme compressive fiber, is not much different from that obtained using the value of ε_{cu}. This can be verified from the following example with $\rho = 0.015$, $\rho' = 0$ and $f'_c = 3000$ psi to 13,000 psi for normal weight concrete and $f'_c = 3000$ psi to 7000 psi for lightweight concrete. Figs. 7.5a and 7.6a compare the resisting moments obtained according to Eqs. (7.1) for the approximate value of ε_{cu} and the actual value of ε_{cu}. It can be seen that Eqs. (7.1) is a good approximation for the value of ε_{cu} as far as the ultimate moment is concerned. Figures 7.5b and 7.6b show the corresponding moment-curvature relationships. It can be seen that using $\varepsilon_{c\alpha}$ leads to a curvature closer to the exact curvature at ultimate than the ACI approximation.

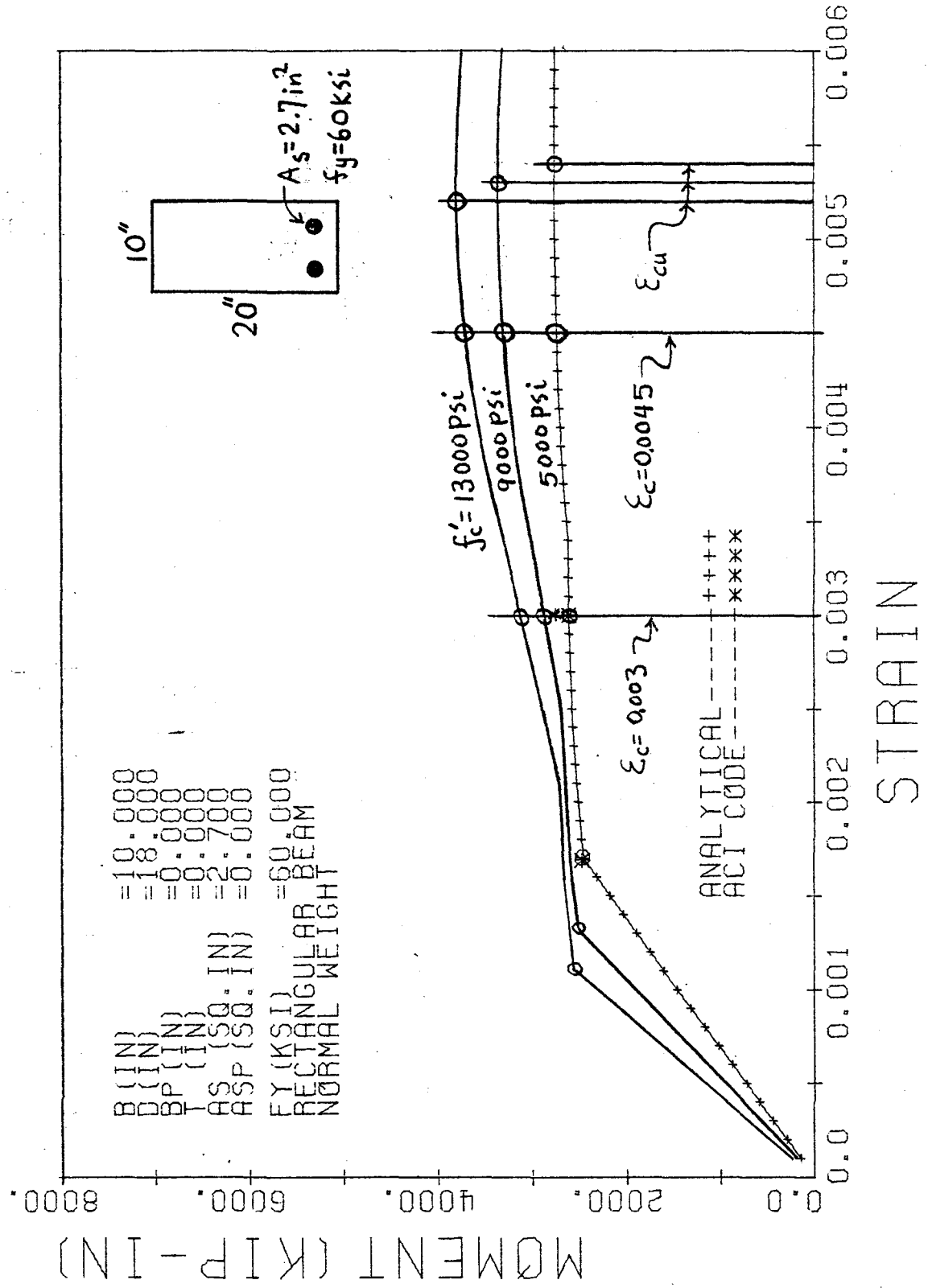

Fig. 7.5a Moment-strain relationship for normal weight concrete with f'_c = 5,000 psi to 13,000 psi.

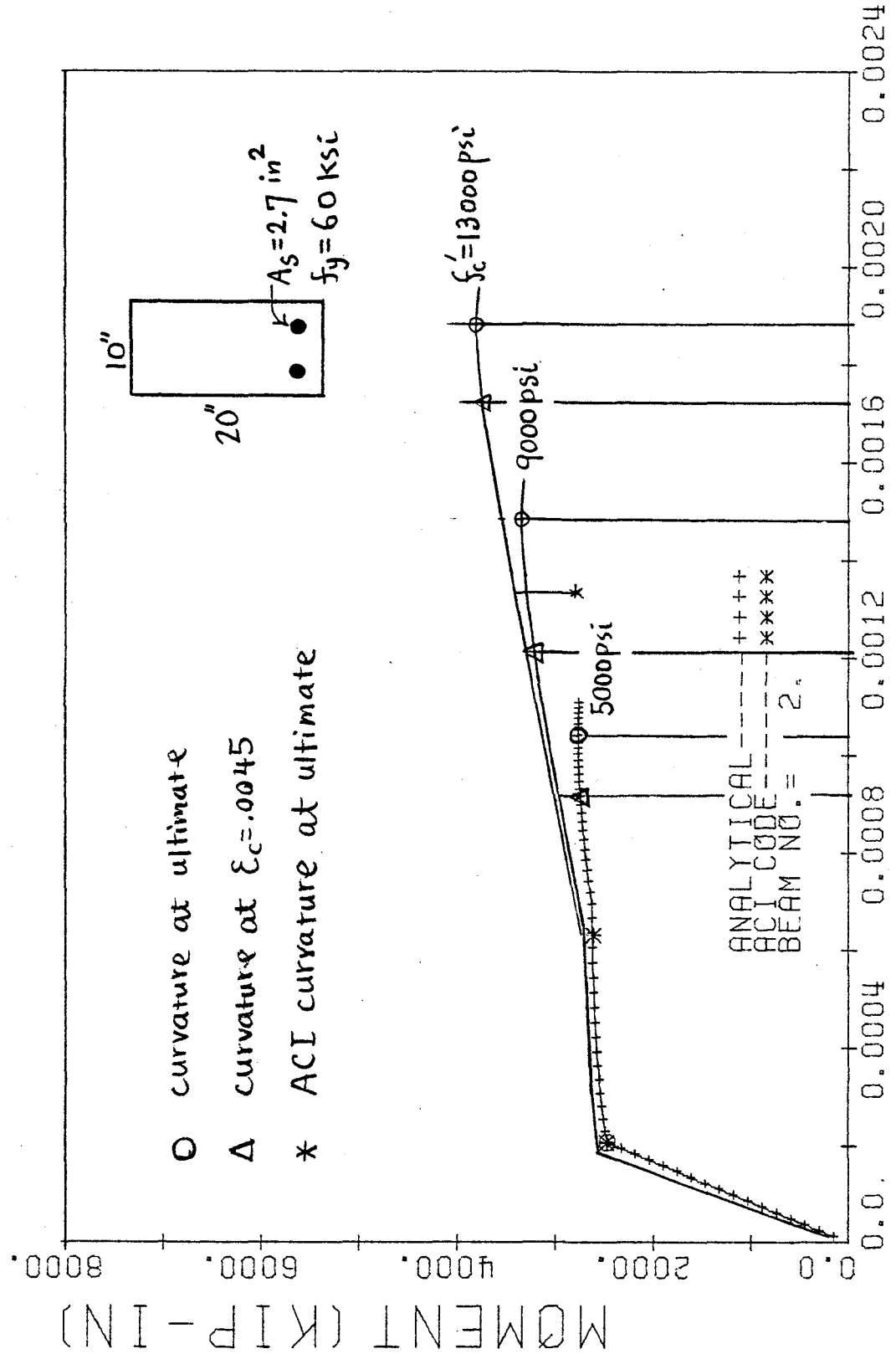

Fig. 7.5b Moment-curvature relationship for normal weight concrete with f'_c = 5,000 psi to 13,000 psi.

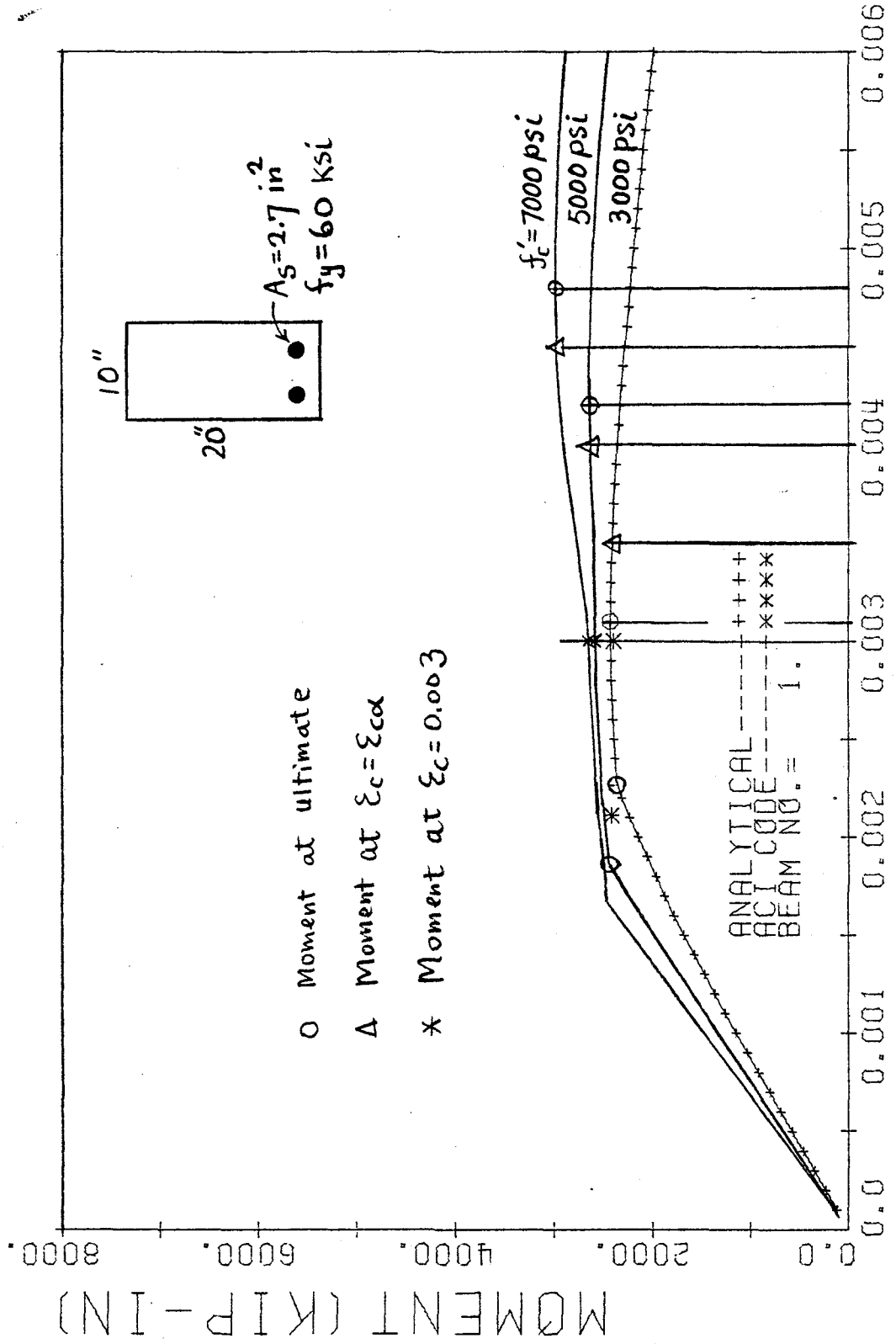

Fig. 7.6a Moment-strain relationship for lightweight concrete with f'_c = 3,000 psi to 7,000 psi.

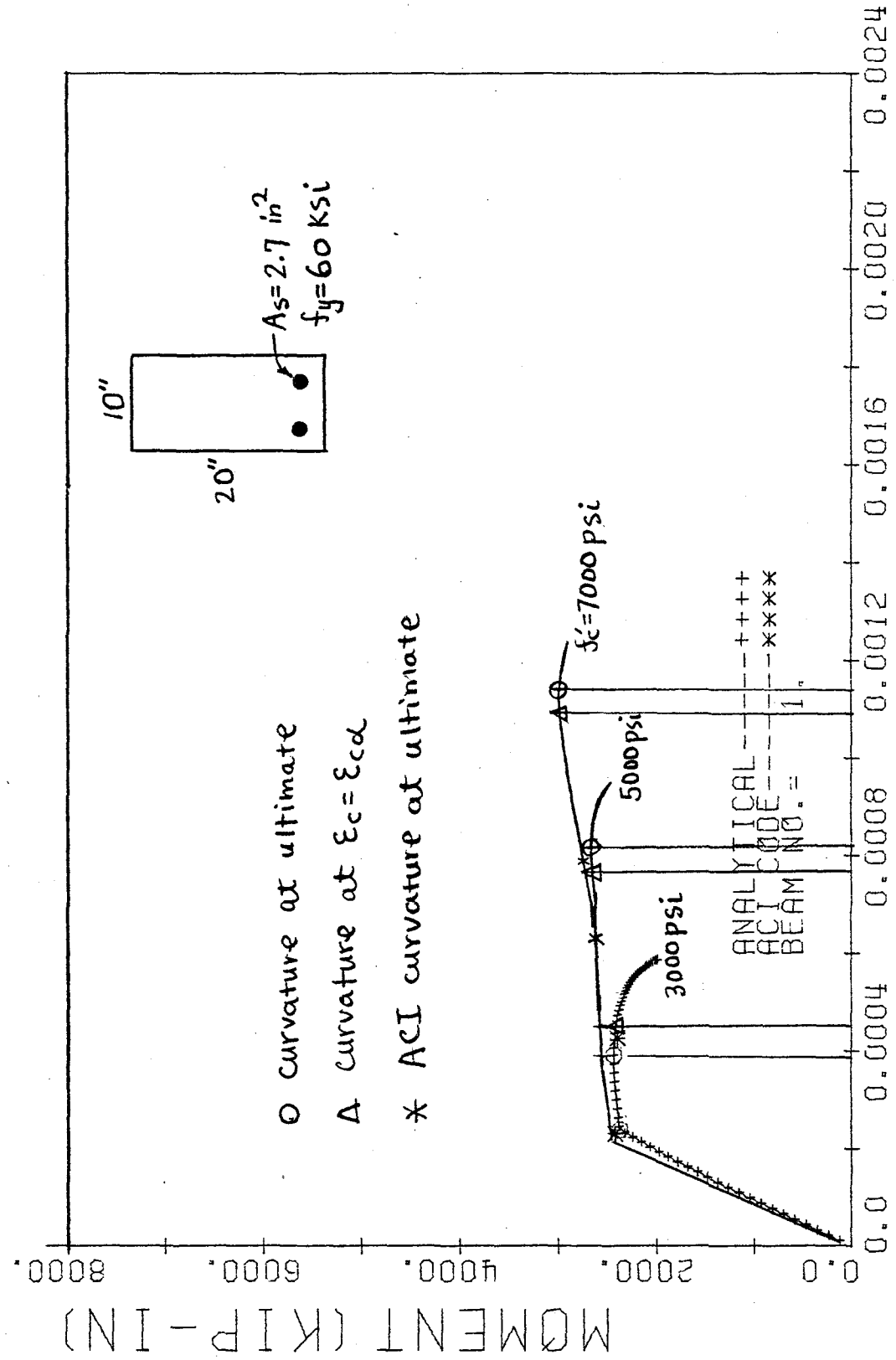

Fig. 7.6b Moment-curvature relationship for lightweight concrete with f'_c = 3,000 psi to 7,000 psi.

7.3 CONCRETE STRAIN ε_{cu} AT MAXIMUM MOMENT

The strain at the extreme compressive fiber of concrete at ultimate are plotted for various concrete strengths and reinforcement ratios in Figs. 7.7 and 7.8 for normal and lightweight concretes, respectively, assuming a rectangular section. It can be seen that except for the case of singularly reinforced sections with a high reinforcement ratio, the ACI constant value $\varepsilon_{cu} = 0.003$ is over-conservative. The use of $\varepsilon_{cu} = \varepsilon_{c\alpha} = 0.0045$ for normal weight concrete and Eqs. (7.1) for lightweight concrete seem more appropriate.

7.4 STRESS BLOCK DEPTH PARAMETER β_1 FROM THE ACI CODE

The actual compression zone of concrete at ultimate (maximum moment) is represented by an equivalent rectangular stress block by the ACI code as shown in Fig. 7.3. Two conditions should be satisfied if this transformation is equivalent in terms of the statics of the section, namely, the magnitude of the resultant force and the location of that force should remain unchanged. These conditions are expressed as follows:

For the equilibrium of forces:

$$\alpha_1 \beta_1 = \alpha$$

or

$$\beta_1 = \frac{\alpha}{\alpha_1} \tag{7.2}$$

and

For the equilibrium of moments:

$$\beta_1 = 2\beta \tag{7.3a}$$

The value of α_1 as stipulated by the ACI code can be substituted into Eq. (7.2) and leads to:

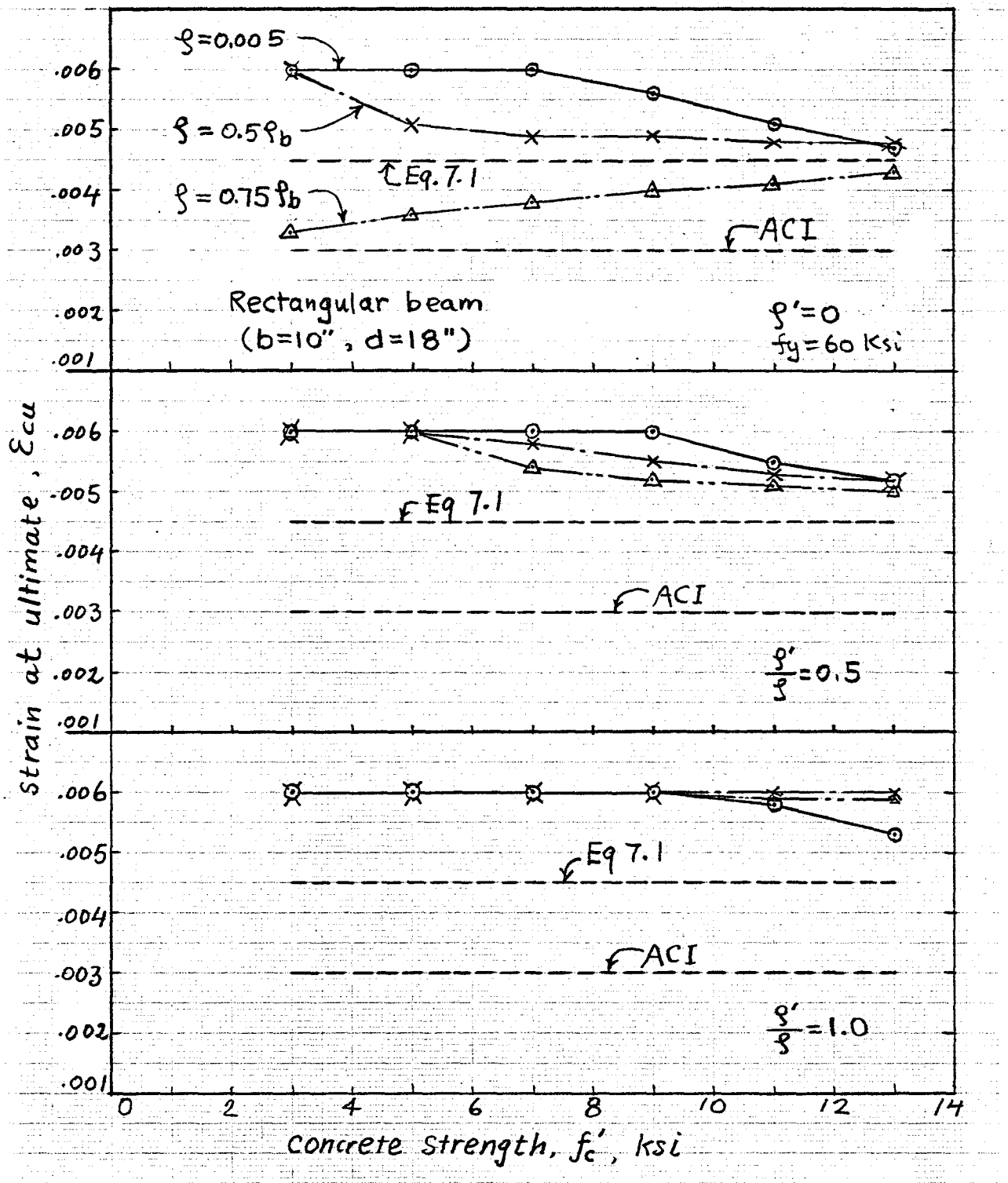

Fig. 7.7 Relationship of ε_{cu} vs. f'_c for normal weight concrete.

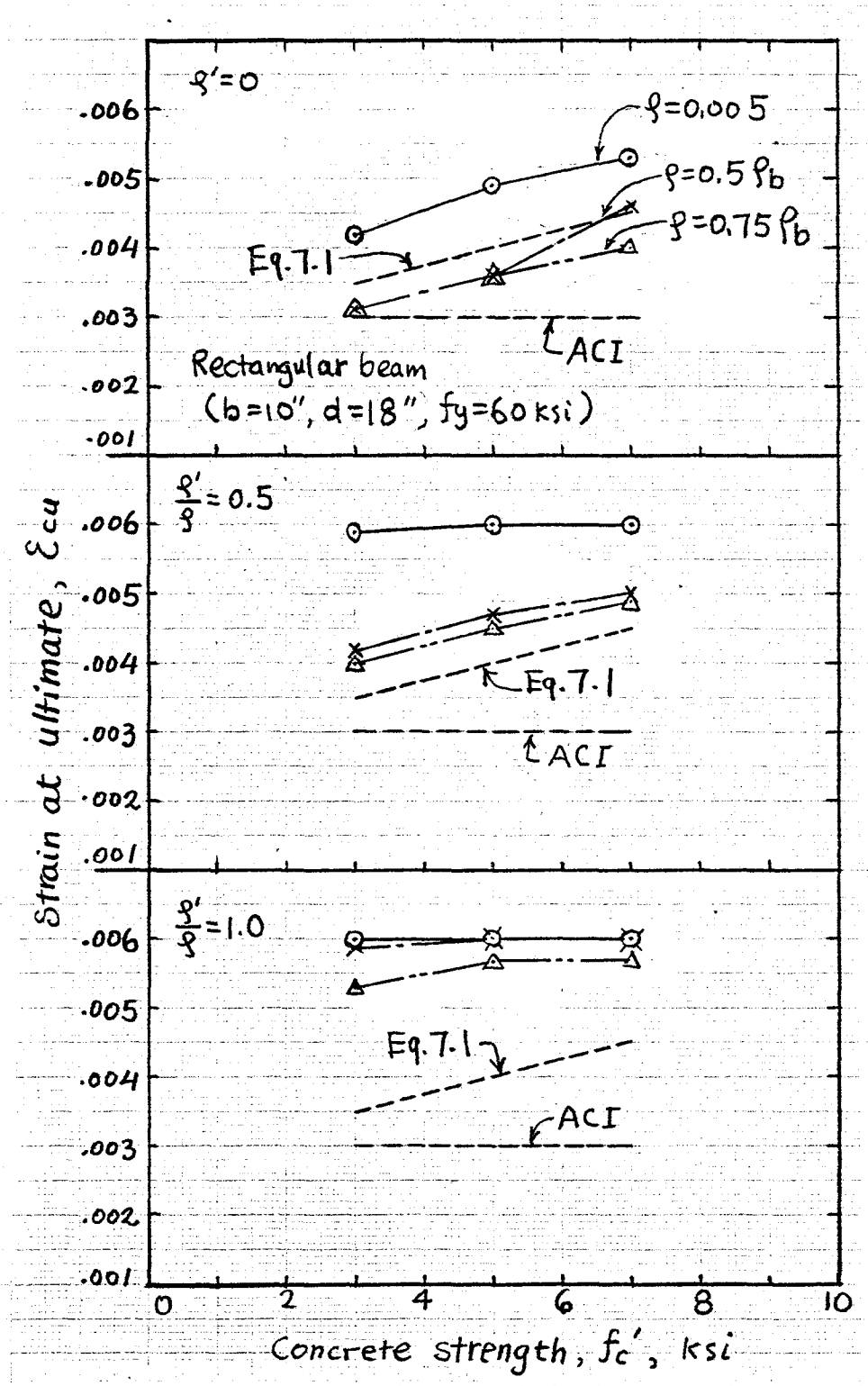

Fig. 7.8 Relationship of ε_{cu} vs. f'_c for lightweight concrete.

$$\beta_1 = \frac{\alpha}{0.85} \tag{7.3b}$$

Furthermore, the ACI code stipulates the value of β_1 as follows:

$$\left.\begin{aligned} \beta_1 &= 0.85 && \text{for } f'_c \leq 4000 \text{ psi} \\ \beta_1 &= 0.85 - 0.05\left(\frac{f'_c}{1000} - 4\right) && \text{for } 4000 \text{ psi} \leq f'_c \leq 8000 \text{ psi} \\ \beta_1 &= 0.65 && \text{for } f'_c \geq 8000 \text{ psi} \end{aligned}\right\} \tag{7.4}$$

The comparison of β_1 values as given by Eqs. (7.3a), (7.3b) and (7.4) are shown in Figs. 7.9 and 7.10 for various concrete strengths and reinforcement ratios. For normal weight concrete, it can be seen that the ACI formula (Eqs. (7.4)) gives a good prediction when the value of β_1 is derived from the force equilibrium (Eq. (7.3b)) as indicated by dashed lines, but is much less accurate when β_1 is derived from the location of the resultant force (Eq. (7.3a)) as indicated by solid lines. Since there is no way to narrow the differences of β_1 as obtained from Eqs (7.3a) and (7.3b) for a rectangular stress block representation, it may be possible to examine some average represention.

In order to explore the effect of β_1 on the ultimate moment and curvature, one should consider the equilibrium equations of forces and moments of the section. From the ACI code approach and for underreinforced beam, these equations are as follows

For force equilibrium:

$$A_s f_y = 0.85\, f'_c\, ba \tag{7.5}$$

which leads to:

$$a = \frac{A_s f_y}{0.85\, f'_c\, b} \tag{7.6}$$

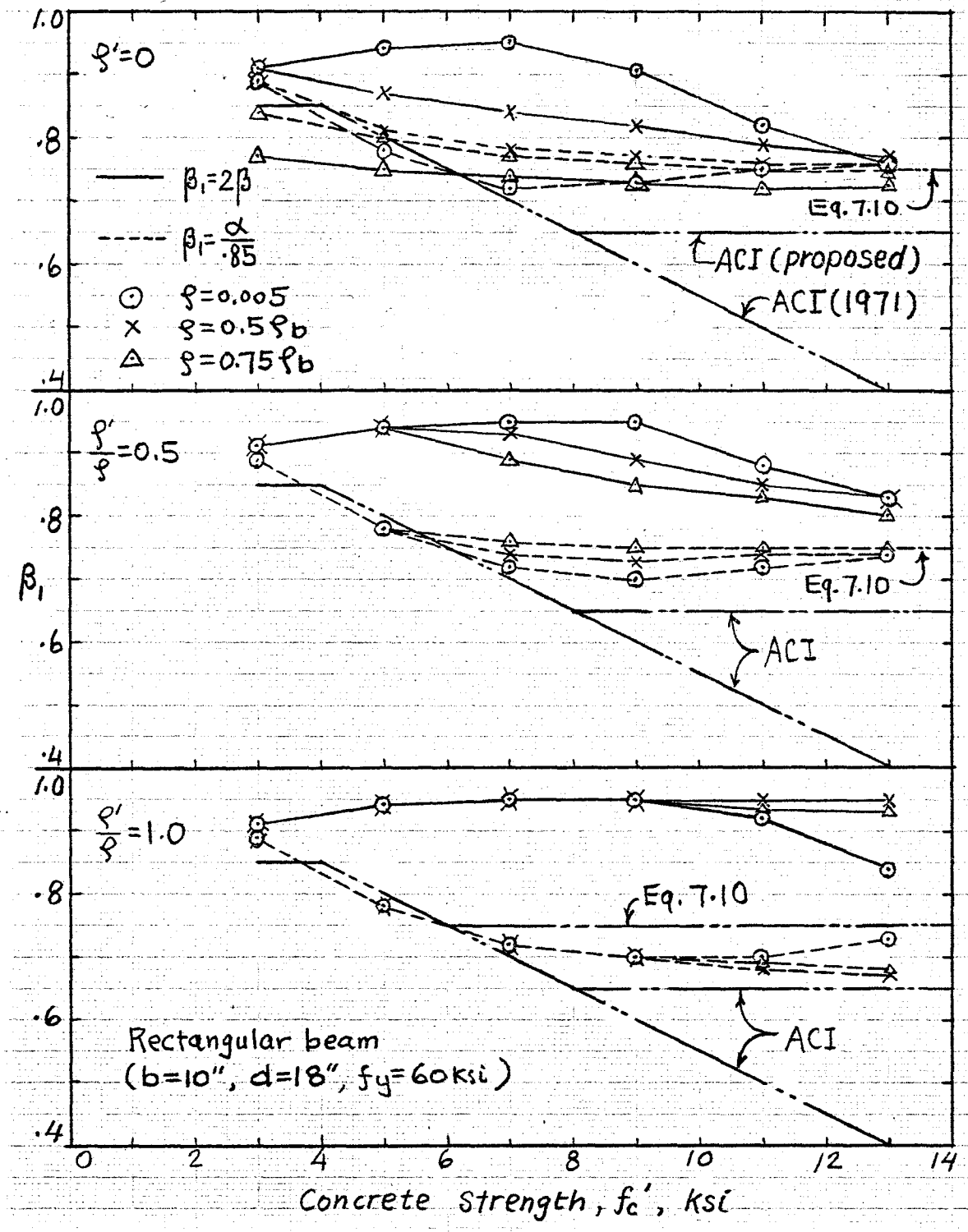

Fig. 7.9 Relationship of β_1 vs. f_c' for normal weight concrete.

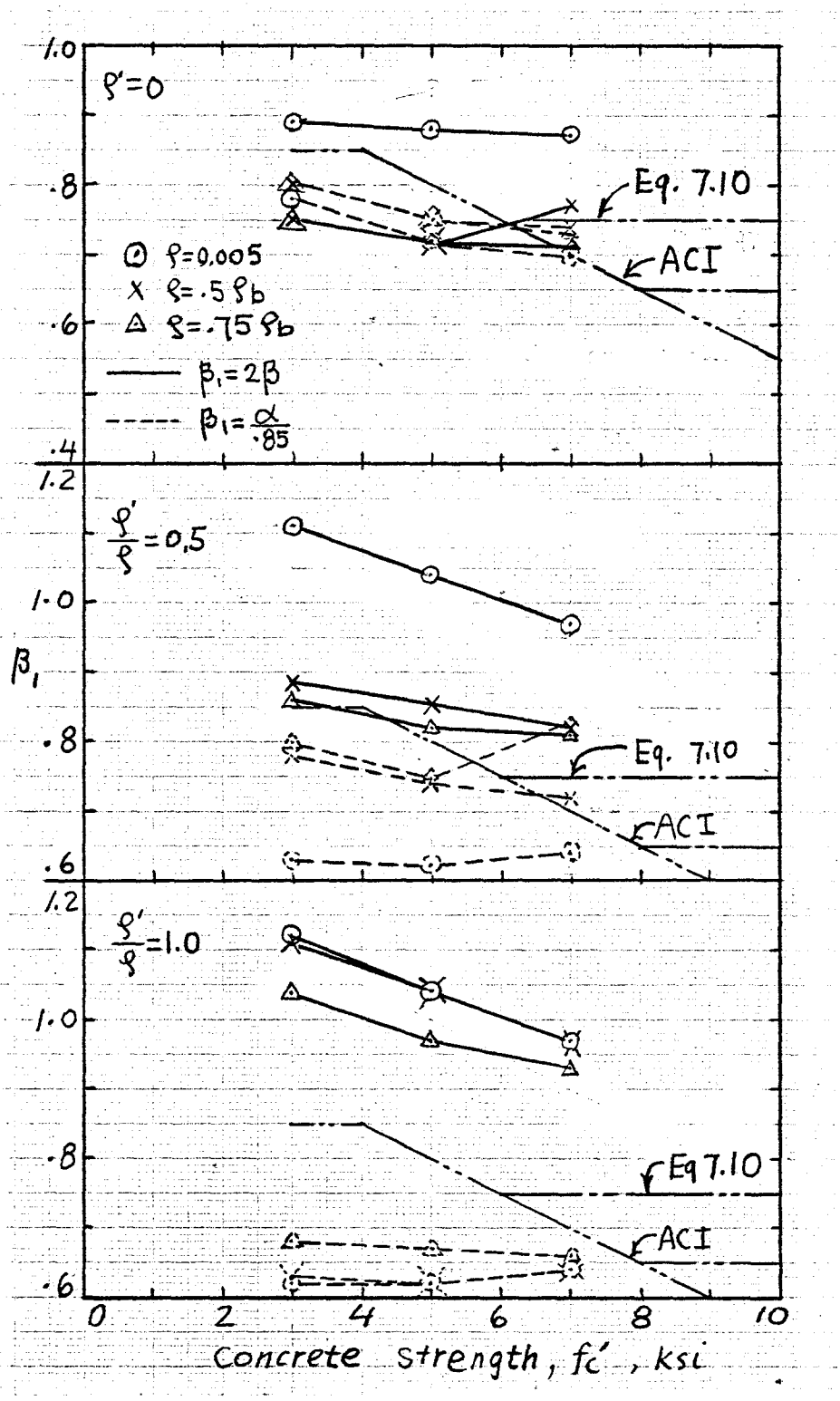

Fig. 7.10 Relationship of β_1 vs. f'_c for lightweight concrete.

where

$$\left.\begin{aligned} a &= \beta_1 c \\ \text{or} \qquad c &= \frac{a}{\beta_1} \end{aligned}\right\} \tag{7.7}$$

For moment equilibrium:

$$M_u = A_s f_y \left(d - \frac{a}{2}\right) \tag{7.8}$$

The corresponding curvature at ultimate is given by:

$$\phi_u = \frac{\varepsilon_{cu}}{c} = \frac{\beta_1 \varepsilon_{cu}}{a} \tag{7.9}$$

From the above expressions the following remarks are derived

(a) The ultimate moment M_u from Eq. (7.8) is determined by the value of a and the sectional properties, and the value of a is determined by A_s, f_y, f'_c and b only (Eq. (7.6)); therefore, changing the value of β_1 does not affect the calculation of M_u for the same properties.

(b) The ultimate curvature is determined by ε_{cu} and β_1 from Eqs. (7.9) and (7.7), so changing the value of β_1 does change the calculation of ϕ_u. A detailed study on the ultimate curvature will be discussed in the following sections.

(c) From Figs. 7.9 and 7.10, a better fitting value for β_1 representing an average can be expressed as follows:

$$\begin{aligned} \beta_1 &= 0.85 && \text{for } f'_c \le 4000 \text{ psi} \\ \beta_1 &= 0.85 - 0.05\left(\frac{f'_c}{1000} - 4\right) && \text{for } 4000 \text{ psi} \le f'_c \le 6000 \text{ psi} \\ \beta_1 &= 0.75 && \text{for } f'_c \ge 6000 \text{ psi} \end{aligned} \tag{7.10}$$

Eqs. (7.10) are also shown in Figs. 7.9 and 7.10.

7.5 THE ULTIMATE MOMENT, ULTIMATE CURVATURE AND DUCTILITY FACTOR

The effect of concrete strengths and reinforcement ratios on the ultimate moment of a given section is shown in Figs. 7.11a, 7.11b and 7.12 for normal and lightweight concrete, respectively. In the case of low tension reinforcement ratio, i.e., $\rho = 0.005$, the presence of compressive reinforcement does not significantly increase the moment capacity of the section; the reason is that the section is in tension failure. As the tension reinforcement increases (see Tables 7.1, 7.2 and 7.3), the effect of compressive reinforcement on the moment capacity becomes apparent in the theoretical analysis, but not in the ACI code approach (Fig. 7.11b). This is due to the fact that the ACI code does not take into consideration the strain-hardening portion of the stress-strain relationship of the steel. As indicated in Table 7.3, the strain in the tensile steel at ultimate for the case of $f'_c = 13{,}000$ psi, $\rho = 0.75\rho_b$ and $\rho'/\rho = 1$ reaches the value of 0.029, the corresponding stress in the steel is 84 ksi, while the ACI code still uses the yield stress $f_y = 60$ ksi in calculating the ultimate moment. Similar results are observable when lightweight concrete is used (Fig. 7.12).

The effects on the ultimate curvature are shown in Figs. 7.13 and 7.14 for normal and lightweight concrete, respectively. Note that the more the tension reinforcement, the lower the ultimate curvature. The presence of compression reinforcement increases the ultimate curvature especially for high tensile reinforcement ratios. It can also be seen in these figures that the ACI code always gives the lower bound values of ultimate curvatures. A comparison of formulas for calculating the ultimate curvature (Eq. (7.9)) according to the ACI code and to the equations proposed herein for ε_{cu} and β_1 is described next.

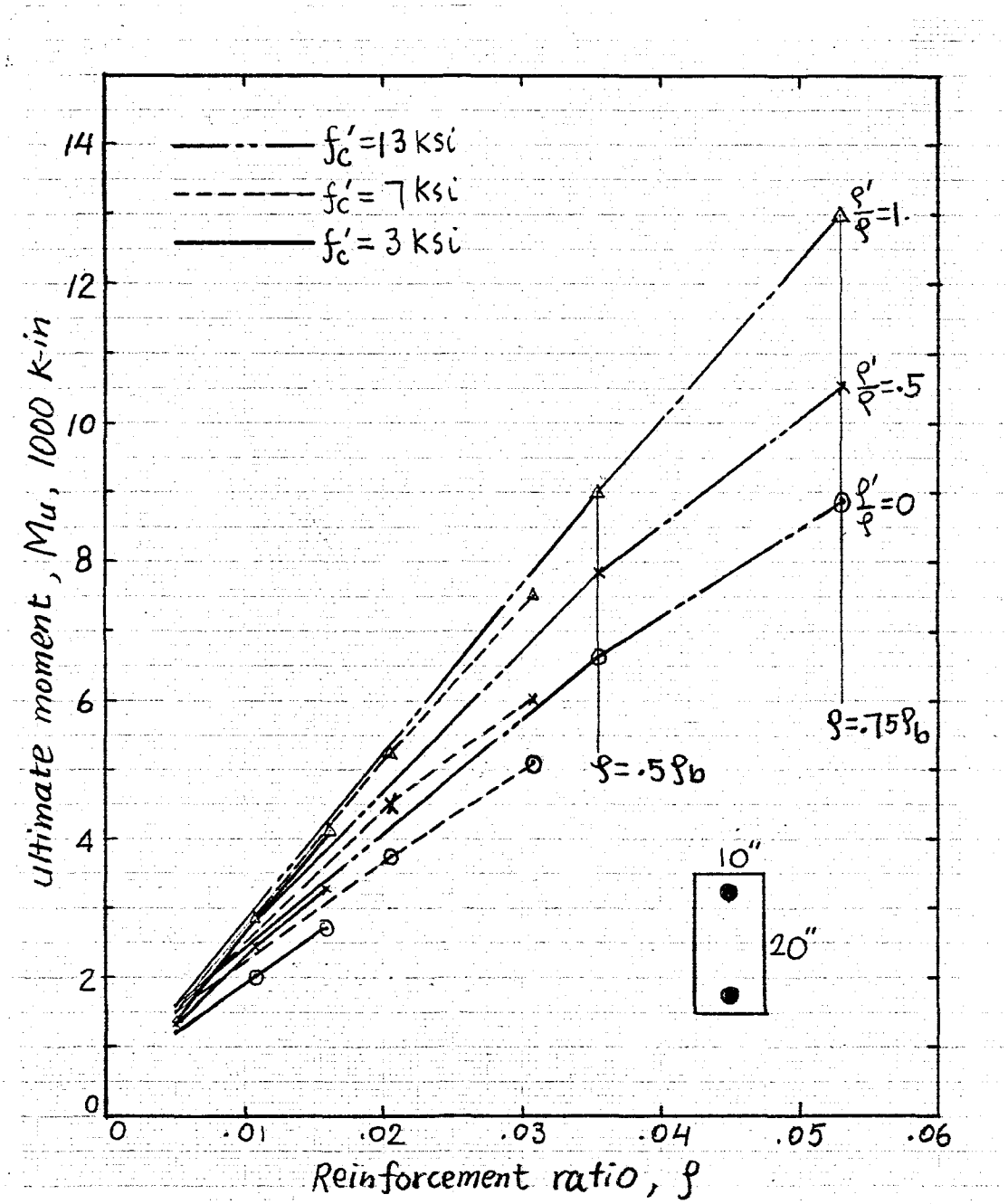

Fig. 7.11a Effect of compressive reinforcement on M_u vs. ρ relationship for normal weight concrete.

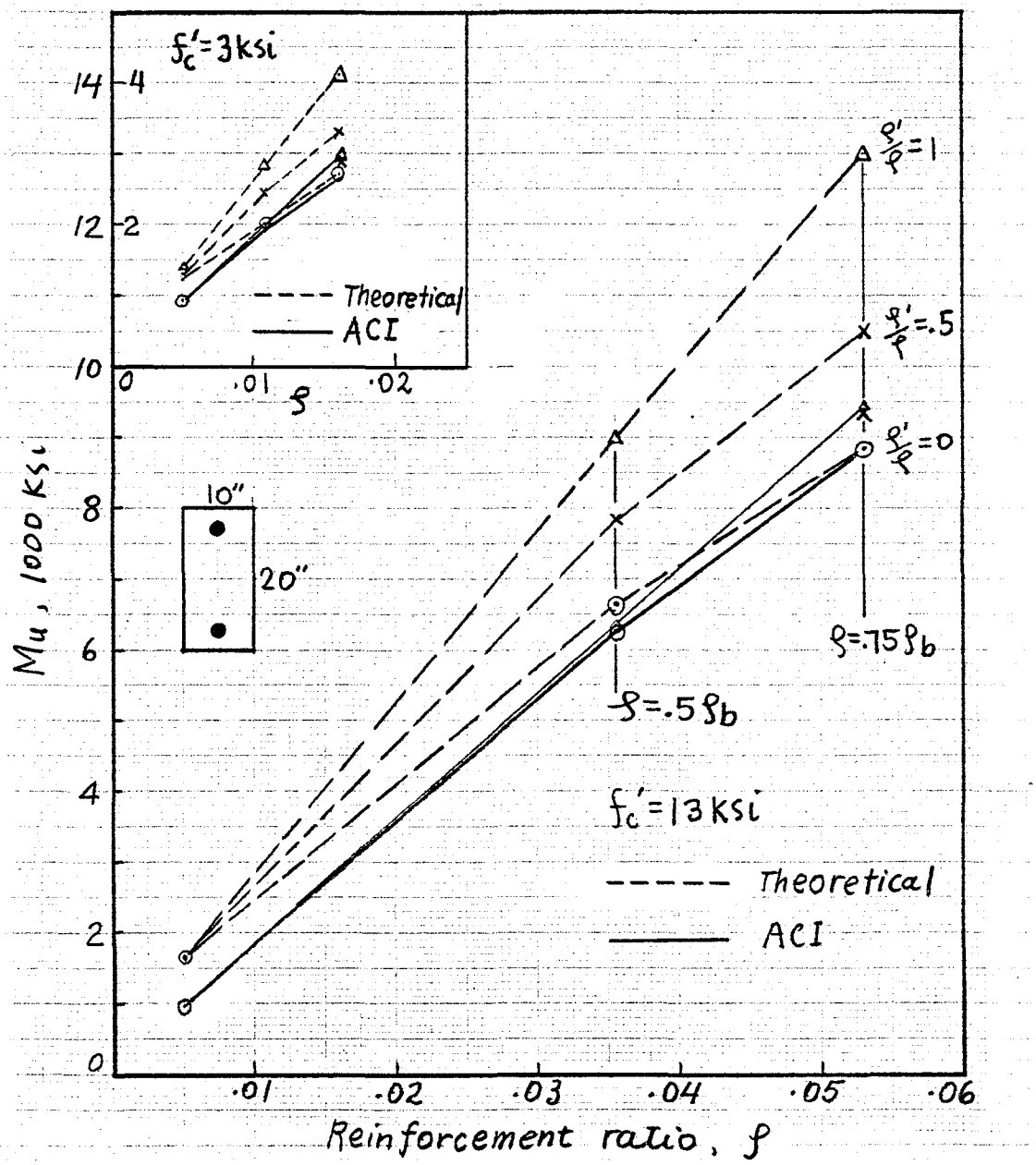

Fig. 7.11b Comparison of the theoretical and ACI values of M_u vs. ρ relationship for normal weight concrete.

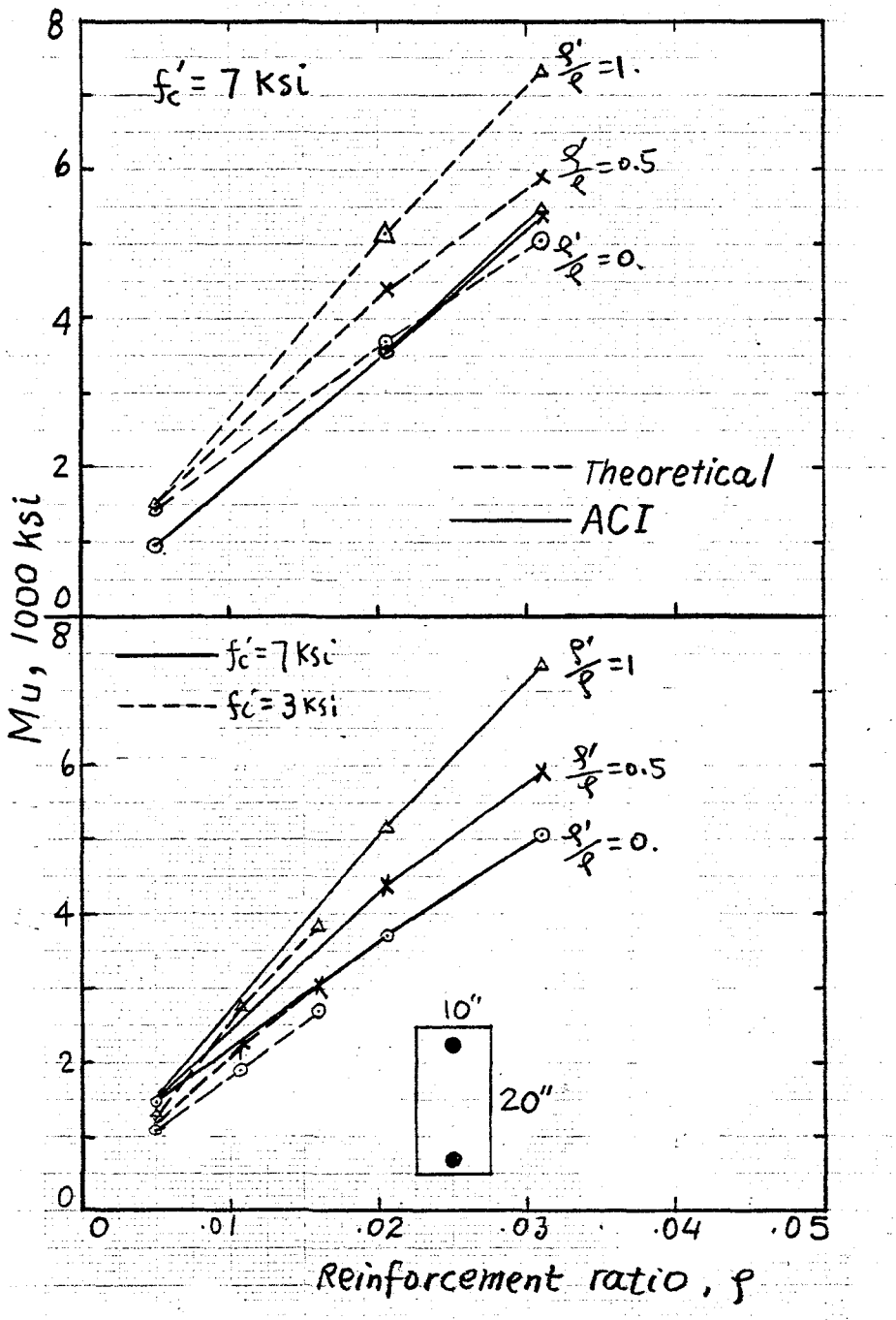

Fig. 7.12 Effect of compression reinforcement on M_u vs. ρ relationship for lightweight concrete.

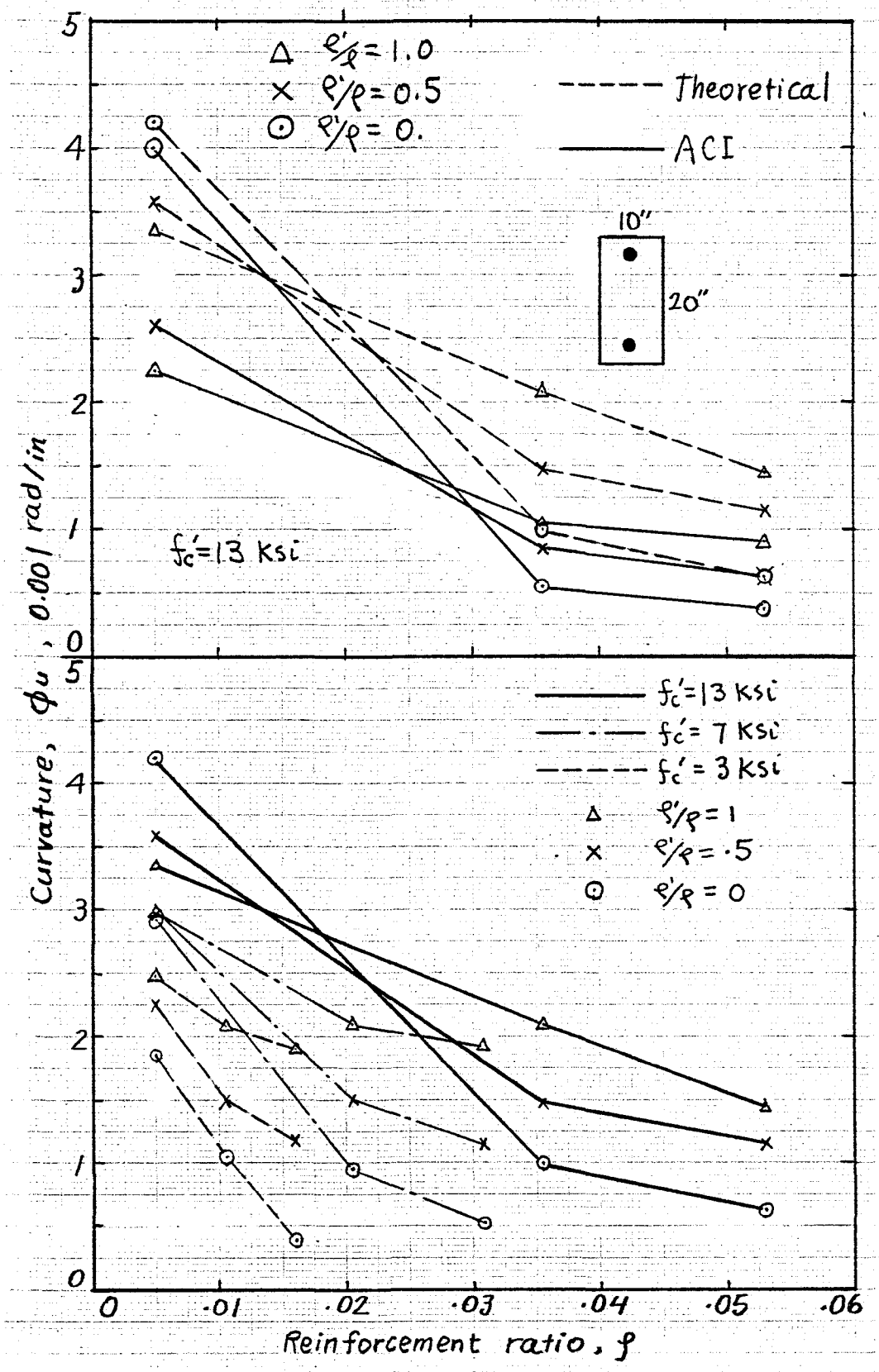

Fig. 7.13 Effect of compression reinforcement on ϕ_u vs. ρ relationship for normal weight concrete.

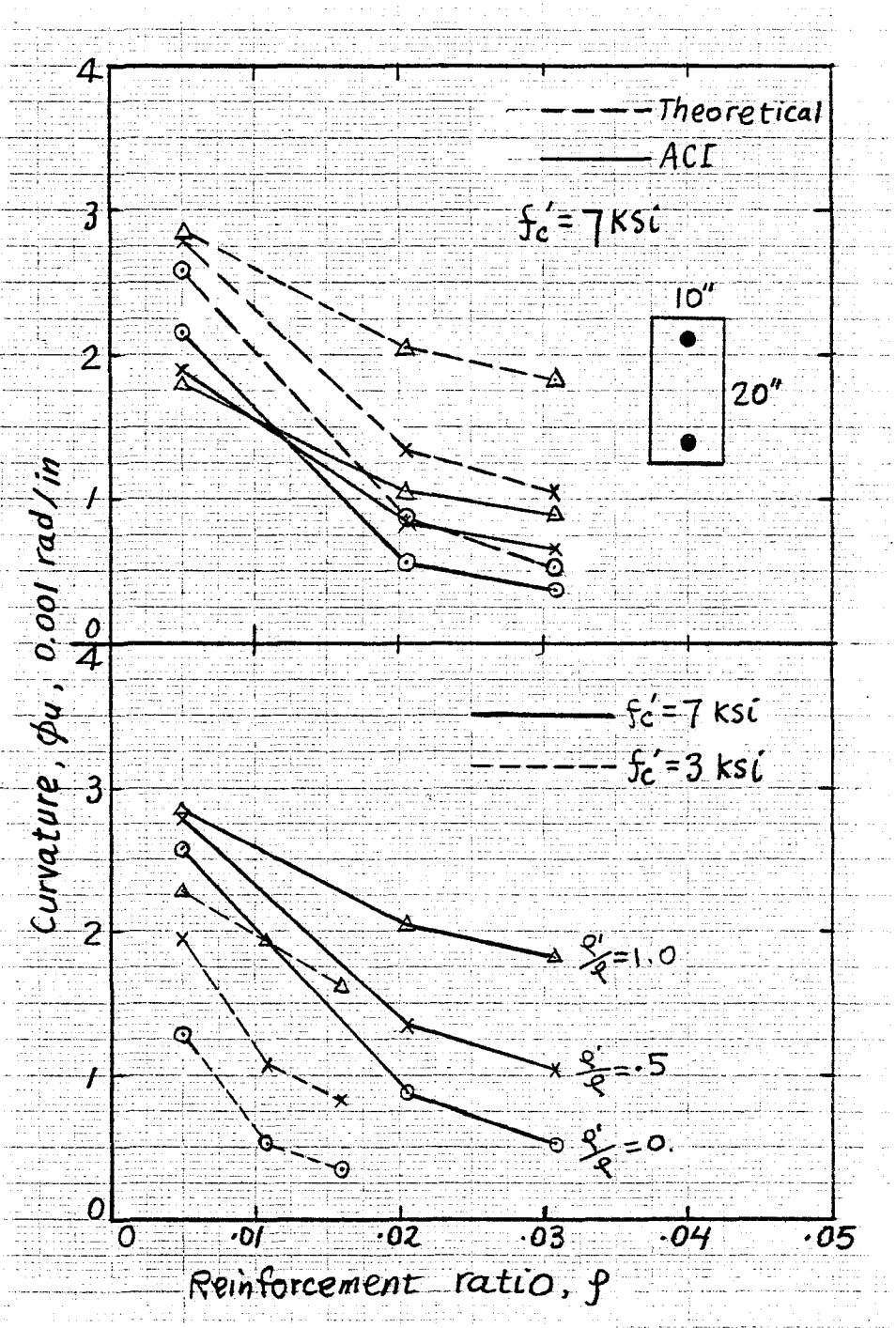

Fig. 7.14 Effect of compressive reinforcement on ϕ_u vs. ρ relationship for lightweight concrete.

For normal weight concrete of $f'_c = 7$ ksi, $\rho'/\rho = 0.5$, the analytical value of curvature at maximum moment is

$$\phi_u = 0.00151 \text{ rad/in} \quad \text{(Table 7.2)}$$

The corresponding ACI code value is

$$(\varepsilon_{cu})_{ACI} = 0.003$$

$$(\beta_1)_{ACI} = 0.7 \quad \text{(Eq. (7.4))}$$

$$(\phi_u)_{ACI} = 0.00084 \text{ rad/in} \quad \text{(Table 7.2)}$$

The proposed value is

$$(\varepsilon_{cu})_{prop.} = 0.45 \quad \text{(Eq. (7.1))}$$

$$(\beta_1)_{prop.} = 0.75 \quad \text{(Eq. (7.10))}$$

$$(\phi_u)_{prop.} = \frac{(\beta_1 \varepsilon_{cu})_{prop.}}{(\beta_1 \varepsilon_{cu})_{ACI}} (\phi_u)_{ACI} \tag{7.11}$$

or

$$(\phi_u)_{prop.} = \frac{(0.75)(0.0045)}{(0.7)(0.003)} (0.00084) = 0.00135 \text{ rad/in}$$

Figure 7.15 shows the comparison of ultimate curvatures calculated from the above two methods for normal and lightweight concretes. It can be seen that the proposed method is generally superior to the ACI code in predicting the ultimate curvature.

The effects of concrete strengths on the ductility factor are shown in Figs. 7.16 and 7.17 for normal and lightweight concretes. Note that for the case of ρ proportional to ρ_b, the ductility factors are not affected by the variation of concrete strengths if the ACI code approach is used. This seems to be also the trend in the theoretical results. The ACI code

TABLE 7.1

Moments, Curvatures and Ductility Factors at Yield and Ultimate for $\rho = 0.005$

Rectangular beam, f_y = 60 ksi (b = 10", d = 18") Note: M_y, M_u in kip-in; ϕ_y, ϕ_u in (0.001 rad/in)

	f'_c (ksi)	$\frac{\rho'}{\rho}$	Theoretical								ACI		
			At Yield			At Ultimate					At Ultimate		
			M_y	ϕ_y	ε_{cy}	M_u	ϕ_u	ε_{cu}	ε_s	ϕ_u/ϕ_y	M_u	ϕ_u	ϕ_u/ϕ_y
Normal Weight	3	0.0	863	0.168	0.0010	1223	1.846	0.0060	0.0272	11.00	915	1.275	7.60
		0.5	869	0.163	0.0009	1340	2.25	0.0060	0.0345	13.83	915	1.366	8.3
		1.0	873	0.15	0.0008	1390	2.47	0.0060	0.0384	15.5	915	1.40	8.8
	5	0.0	875	0.160	0.0009	1392	2.392	0.0060	0.0371	15.00	937	1.889	11.82
		0.5	878	0.156	0.0008	1440	2.62	0.0060	0.0412	16.8	941	1.710	10.9
		1.0	880	0.15	0.007	1460	2.73	0.0060	0.0431	17.8	942	1.65	10.7
	7	0.0	883	0.154	0.0008	1509	2.917	0.0060	0.0465	18.92	947	2.314	15.00
		0.5	885	0.152	0.0007	1514	2.95	0.0060	0.0471	19.5	959	1.197	12.6
		1.0	886	0.149	0.0007	1515	2.97	0.0060	0.0473	19.8	962	1.79	12.
	9	0.0	890	0.150	0.0007	1587	3.386	0.0056	0.0553	22.53	953	2.763	18.38
		0.5	890	0.148	0.0006	1570	3.26	0.0060	0.0527	22	972	2.116	14.2
		1.0	890	0.146	0.0006	1562	3.18	0.0060	0.0513	21.7	979	1.93	13.2
	11	0.0	895	0.147	0.0006	1633	3.822	0.0051	0.0637	25.97	956	3.376	22.93
		0.5	895	0.146	0.0006	1614	3.4	0.0055	0.0556	23.3	986	2.36	16.2
		1.0	895	0.144	0.0006	1602	3.3	0.0058	0.0540	23	997	2.10	14.6
	13	0.0	899	0.145	0.0006	1654	4.212	0.0047	0.0711	29.12	958	3.990	27.57
		0.5	899	0.143	0.0006	1653	3.57	0.0052	0.0591	24.9	999	2.59	18.06
		1.0	898	0.142	0.0005	1641	3.33	0.0053	0.0548	23.4	1013	2.26	15.9
Lightweight	3	0.0	860	0.170	0.0011	1077	1.285	0.0042	0.0189	7.55	914	1.275	7.49
		0.5	867	0.164	0.0010	1228	1.940	0.0059	0.0290	11.78	915	1.36	8.3
		1.0	871	0.160	0.0009	1318	2.27	0.0060	0.0348	14.1	915	1.41	8.8
	5	0.0	869	0.160	0.0009	1299	1.95	0.0049	0.0302	11.9	938	1.889	11.5
		0.5	874	0.16	0.0009	1371	2.39	0.0060	0.0371	15	941	1.71	10.7
		1.0	876	0.15	0.0008	1409	2.57	0.0060	0.0402	16.4	942	1.65	10.5
	7	0.0	876	0.16	0.0008	1463	2.57	0.0053	0.0410	16.1	947	2.314	14.5
		0.5	879	0.15	0.0008	1476	2.78	0.0060	0.0442	17.9	958	1.91	12.3
		1.0	880	0.15	0.0007	1486	2.85	0.0060	0.0453	18.6	962	1.79	11.7

TABLE 7.2

Moments, Curvatures and Ductility Factors at Yield and Ultimate for $\rho = 0.5\ \rho_b$

Rectangular beam, f_y = 60 ksi (b = 10", d = 18") Note: M_y, M_u in kip-in; ϕ_y, ϕ_u in (0.001 rad/in)

	f'_c (ksi)	$\frac{\rho'}{\rho}$	Theoretical								ACI		
			At Yield			At Ultimate					At Ultimate		
			M_y	ϕ_y	ε_{cy}	M_u	ϕ_u	ε_{cu}	ε_s	ϕ_u/ϕ_y	M_u	ϕ_u	ϕ_u/ϕ_y
Normal Weight	3	0.0	1848	0.208	0.0017	2020	1.04	0.0060	0.0127	5.0	1907	0.56	2.7
		0.5	1908	0.190	0.0014	2455	1.50	0.0060	0.0209	7.8	1988	0.84	4.4
		1.0	1937	0.178	0.0012	2874	2.08	0.0060	0.0315	11.6	2002	1.04	5.8
	5	0.0	2733	0.214	0.0018	2965	0.92	0.0051	0.0115	4.3	2874	0.56	2.6
		0.5	2823	0.194	0.0015	3605	1.48	0.0060	0.0206	7.6	2966	0.84	4.3
		1.0	2866	0.181	0.0012	4246	2.07	0.0060	0.0313	11.4	2980	1.04	5.7
	7	0.0	3357	0.213	0.0018	3761	0.96	0.0049	0.0124	4.5	3580	0.56	2.6
		0.5	3461	0.194	0.0015	4499	1.51	0.0058	0.0214	7.8	3661	0.84	4.3
		1.0	3512	0.181	0.0012	5230	2.09	0.0060	0.0317	11.5	3668	1.04	5.7
	9	0.0	4008	0.213	0.0018	4591	1.00	0.0049	0.0131	4.7	4308	0.56	2.6
		0.5	4132	0.194	0.0015	5445	1.52	0.0055	0.0219	7.8	4386	0.83	4.3
		1.0	4193	0.181	0.0012	6264	2.11	0.0060	0.0320	11.6	4390	1.04	5.7
	11	0.0	4882	0.217	0.0019	5609	0.98	0.0048	0.0129	4.5	5266	0.56	2.6
		0.5	5042	0.196	0.0015	6636	1.48	0.0053	0.0215	7.5	5361	0.84	4.2
		1.0	5121	0.183	0.0013	7640	2.10	0.0060	0.0318	11.5	5366	1.04	5.7
	13	0.0	5755	0.219	0.0019	6639	0.98	0.0048	0.0128	4.5	6224	0.56	2.6
		0.5	5953	0.198	0.0015	7839	1.47	0.0052	0.0213	7.4	6336	0.84	4.2
		1.0	6049	0.184	0.0013	9016	2.09	0.006	0.0317	11.4	6341	1.04	5.6
Lightweight	3	0.0	1841	0.212	0.0018	1925	0.52	0.0031	0.0062	2.4	1907	0.56	2.7
		0.5	1905	0.192	0.0015	2232	1.08	0.0042	0.0153	5.6	1988	0.84	4.3
		1.0	1935	0.180	0.0012	2755	1.93	0.0059	0.289	10.7	2002	1.04	5.7
	5	0.0	2711	0.22	0.0020	2887	0.63	0.0036	0.0078	2.8	2874	0.56	2.5
		0.5	2814	0.20	0.0016	3427	1.21	0.0047	0.0171	6.3	2966	0.84	4.2
		1.0	2861	0.18	0.0013	4160	2.00	0.0060	0.0301	10.8	2980	1.04	5.6
	7	0.0	3319	0.22	0.0020	3691	0.87	0.0046	0.0111	3.8	3580	0.56	2.5
		0.5	3445	0.20	0.0016	4383	1.35	0.0050	0.0193	6.7	3661	0.84	4.2
		1.0	3503	0.18	0.0013	5168	2.05	0.0060	0.031	11.0	3668	1.04	5.6

TABLE 7.3

Moments, Curvatures and Ductility Factors at Yield and Ultimate for $\rho = 0.75\ \rho_b$

Rectangular beam, f_y = 60 ksi (b = 10", d = 18") Note: M_y, M_u in kip-in; ϕ_y, ϕ_u in (0.001 rad/in)

	f'_c (ksi)	$\frac{\rho'}{\rho}$	Theoretical								ACI		
			At Yield			At Ultimate					At Ultimate		
			M_y	ϕ_y	ε_{cy}	M_u	ϕ_u	ε_{cu}	ε_s	ϕ_u/ϕ_y	M_u	ϕ_u	ϕ_u/ϕ_y
Normal Weight	3	0.0	2648	0.247	0.0024	2693	0.38	0.0033	0.0036	1.6	2641	0.37	1.6
		0.5	2824	0.208	0.0017	3278	1.18	0.0060	0.0153	5.6	2925	0.65	3.1
		1.0	2887	0.19	0.0014	4121	1.90	0.0060	0.0283	10	2972	0.91	4.8
	5	0.0	3953	0.250	0.0025	4073	0.45	0.0036	0.0045	1.7	4021	0.37	1.5
		0.5	4188	0.21	0.0018	4813	1.16	0.0060	0.150	5.4	4370	0.65	3.1
		1.0	4278	0.19	0.0014	6075	1.89	0.0060	0.0280	9.8	4422	0.91	4.7
	7	0.0	4876	0.247	0.0024	5102	0.52	0.0038	0.0056	2.1	5059	0.37	1.5
		0.5	5137	0.212	0.0018	6016	1.16	0.0054	0.0154	5.4	5398	0.65	3.1
		1.0	5243	0.19	0.0014	7530	1.93	0.0060	0.0289	10	5440	0.91	4.7
	9	0.0	5829	0.247	0.0024	6160	0.58	0.0040	0.0065	2.4	6120	0.37	1.5
		0.5	6134	0.212	0.0018	7288	1.17	0.0052	0.0159	5.5	6471	0.65	3.1
		1.0	6259	0.19	0.0014	9053	1.97	0.0060	0.0294	10.2	6508	0.91	4.7
	11	0.0	7097	0.251	0.0025	7525	0.59	0.0041	0.0065	2.3	7480	0.37	1.5
		0.5	7490	0.21	0.0018	8893	1.15	0.0051	0.0157	5.3	7909	0.65	3.0
		1.0	7648	0.19	0.0015	11021	1.94	0.0059	0.0290	10	7955	0.91	4.7
	13	0.0	8364	0.25	0.0026	8893	0.62	0.0043	0.0069	2.4	8839	0.37	1.5
		0.5	8846	0.21	0.0019	10511	1.14	0.0050	0.0155	5.3	9347	0.65	3.0
		1.0	9036	0.19	0.0015	12990	1.93	0.0059	0.0288	9.9	9401	0.91	4.7
Lightweight	3	0.0	2642	0.25	0.0025	2682	0.34	0.0031	0.0031	1.3	2641	0.37	1.5
		0.5	2823	0.21	0.0018	3032	0.82	0.0040	0.0023	3.9	2925	0.65	3.1
		1.0	2886	0.19	0.0014	3857	1.62	0.0053	0.0240	8.5	2972	0.91	4.7
	5	0.0	3928	0.26	0.0027	4050	0.42	0.0036	0.0040	1.6	4021	0.37	1.4
		0.5	4181	0.22	0.0019	4631	0.93	0.0045	0.0122	4.2	4370	0.65	3.0
		1.0	4275	0.19	0.0015	5846	1.71	0.0055	0.0254	8.7	4422	0.91	4.6
	7	0.0	4826	0.26	0.0027	5077	0.52	0.0040	0.0053	2.0	5059	0.37	1.4
		0.5	5123	0.22	0.0019	5897	1.05	0.0049	0.0147	4.7	5398	0.65	2.9
		1.0	5237	0.20	0.0015	7365	1.82	0.0057	0.0272	9.2	5440	0.91	4.6

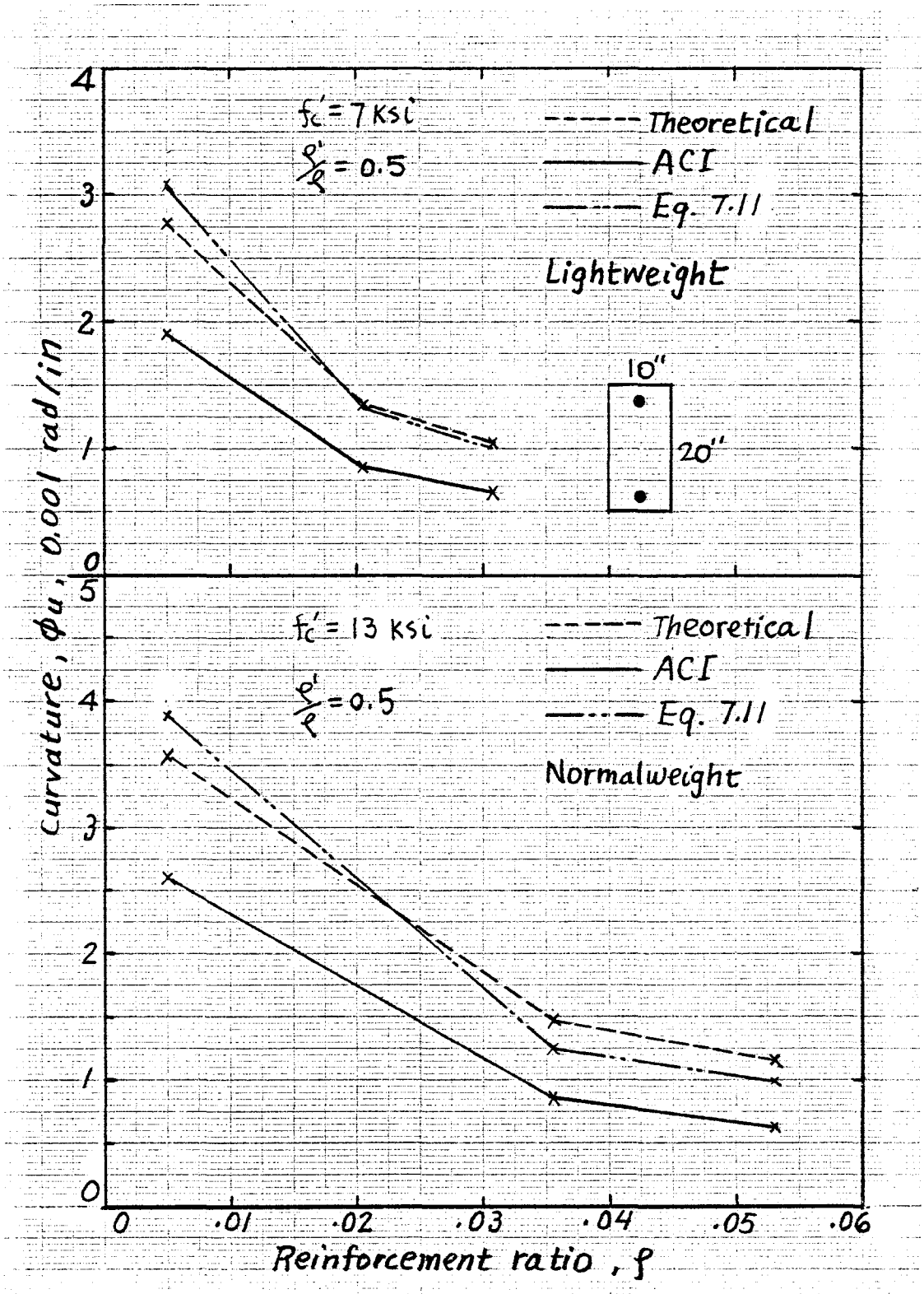

Fig. 7.15 Comparison of ultimate curvatures from the theoretical ACI and proposed values.

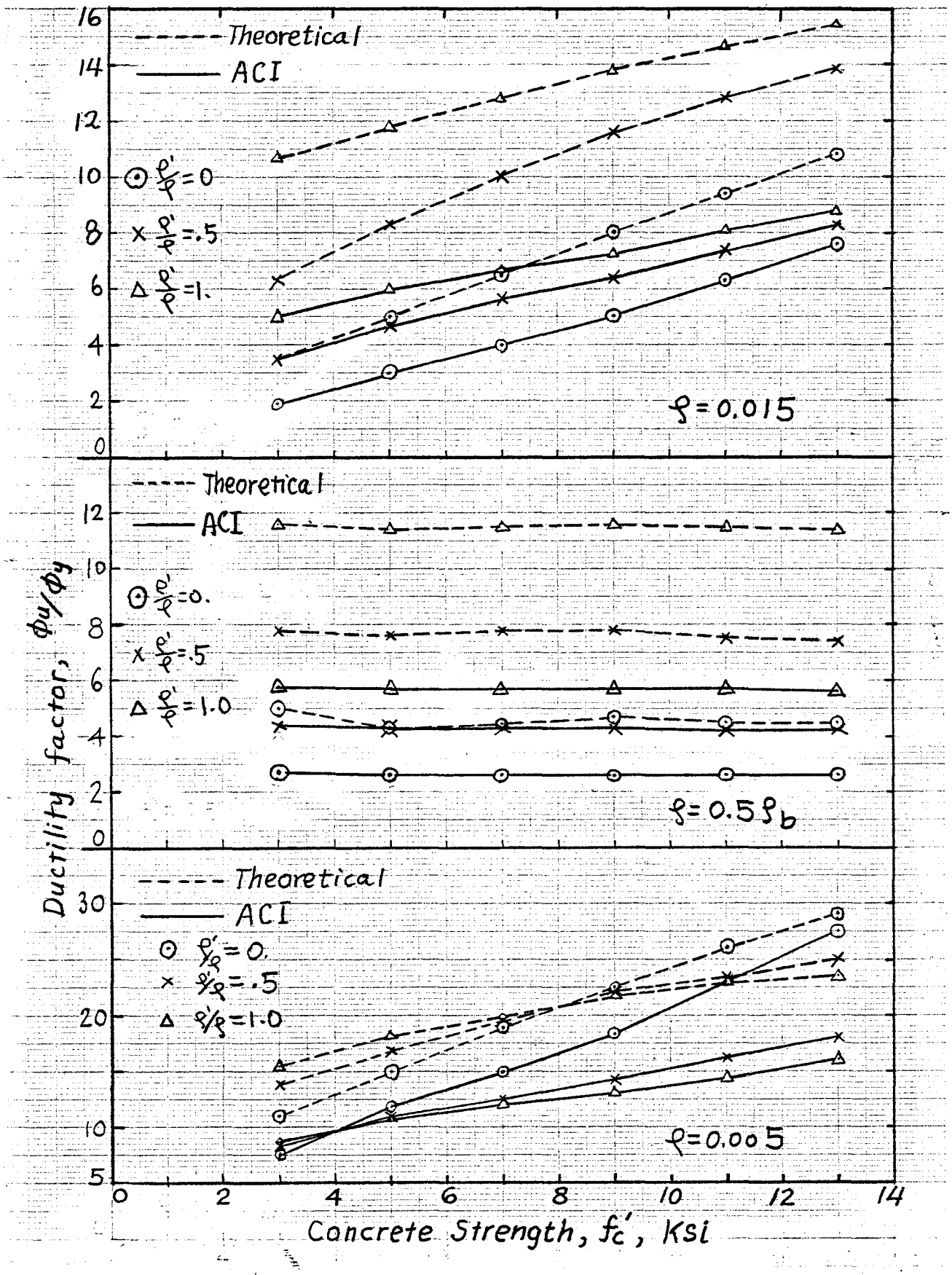

Fig. 7.16 Comparison of ductility factors between the theoretical and ACI values for normal weight concrete.

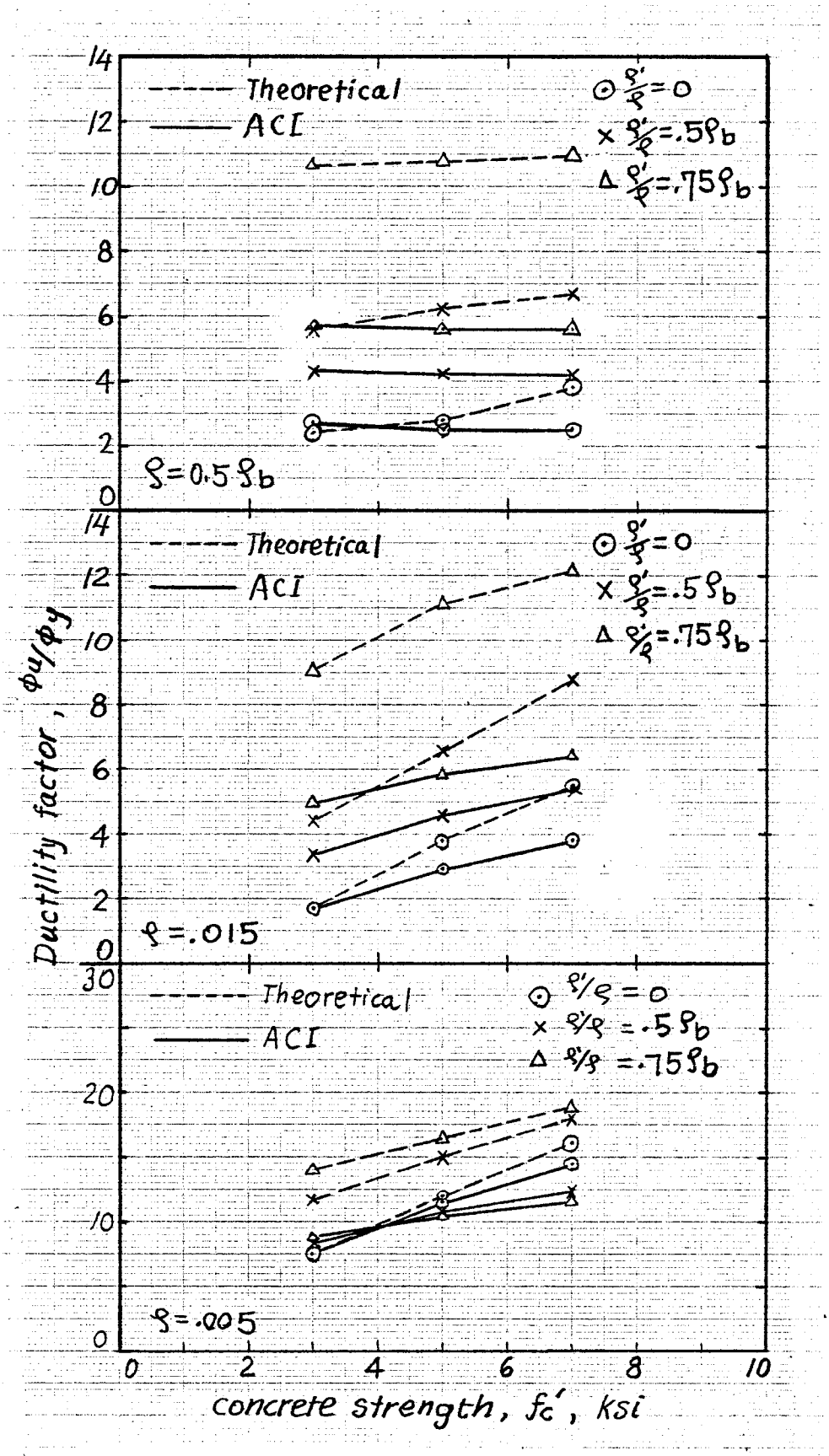

Fig. 7.17 Comparison of ductility factors between the theoretical and ACI values for lightweight concrete.

values give a lower bound of ductility factors as expected due to lower values of ultimate curvatures. The additions of compression reinforcement increases the ductility factor. For a given reinforcement ratio, the higher the concrete strength the larger the ductility factor. The lower ductility of higher strength concrete at the material level as compared to regular concrete does not imply a smaller ductility factor at the sectional level.

CHAPTER VIII

SUMMARY AND CONCLUSIONS

Based on the results of this study, the following conclusions can be drawn:

1. The complete stress-strain curve of concrete in compression including the descending portion can be obtained using the simple experimental technique developed in this investigation; this technique eliminates the effect of the testing system during unloading of the specimen and is adaptable to any testing machine.

2. High strength, normal weight and lightweight concretes do not fail in a brittle manner (provided special precautions are taken during testing) and exhibit a reproducible descending portion of the stress-strain curve.

3. Most analytical relationships representing the stress-strain curve of concrete in compression are based on the characteristics of the ascending portion only and do not consider the characteristics of the descending portion. The analytic expression for the stress-strain curve should contain constants which reflect not only the properties of the ascending portion but also those of the descending portion. The presence of lateral reinforcement can then be accounted for more rationally.

4. An inflection point was generally observed along the descending portion of the stress-strain curves. For normal weight concretes strains at the inflection point and at the peak did not change substantially with the compressive strength; whereas for lightweight concrete these strain values increased almost linearly with strength.

5. There is some indication that the coordinates of the inflection point may be a property of the material and thus are useful in the analytical characterization of the descending portion of the stress-strain curve.

6. The analytical expression developed here for the stress-strain curves of concretes in compression correlates well with experimental observations up to strains of 0.020.

7. Based on data of 50 random specimens of Grade 60 reinforcing bars tested according to ASTM standards, the observed yield strength of reinforcing bars with a specified yield strength of 60 ksi can vary from about 60 to 75 ksi.

8. The analytical expression proposed to describe the entire stress-strain curve of reinforcing bars with yield strength of 60 to 75 ksi shows close correlation with experimental observed curves.

9. The computerized nonlinear analysis model (developed in this study) which uses the actual stress-strain properties of steel and concrete with general assumptions of equilibrium and compatibility, leads to acceptable predictions of the structural behavior of reinforced concrete sections; this includes ultimate loads, moments, curvatures and ductility factors as reported in the technical literature for beams and columns.

Based on the analytical results derived from the use of the computerized model to predict the structural response of reinforced concrete section, the following conclusions are drawn:

10. Although the shape of the descending portion of the stress-strain curve of concrete has little influence on the ultimate moment of reinforced concrete sections, it does significantly affect curvatures and ductility factors for both normal weight and lightweight concretes.

11. For the same specified concrete strengths and everything else being equal, members reinforced with normal weight concrete exhibit a higher ductility factor than those with lightweight concrete. Similar ductilities can be achieved by adding compressive reinforcement.

12. The presence of compressive reinforcement in beams increases the ductility factor but has little effect on the yield moment and curvature for both normal weight and lightweight concrete sections.

13. Given a reinforcement ratio of the section, the use of high strength concrete does not significantly improve the moment capacity of flexural members. It has however a substantial influence on the load and load-moment capacity of column.

14. As the tensile reinforcement increases in reinforced concrete sections, the effect of compressive reinforcement on the moment capacity becomes apparent in the theoretical analysis, but is not reflected in the ACI code approach. This is due to the fact that the ACI code does not take into consideration the strain-hardening portion of the stress-strain relationship of the tensile steel. This strain always exceeds the onset of strain-hardening for high compressive reinforcement ratio; thus leading to a stress higher than the yield stress.

15. The increase of axial load leads to a decrease in the ductility factor for columns. When the axial load approaches about 30% of the axial load capacity of the column, the ductility factor in bending approaches one, and the resisting moment capacity reaches its maximum value which corresponds to the balanced moment, M_b, in the column load-moment interaction diagram.

16. For a symmetrically reinforced column under biaxially eccentric loading, the effect of the eccentricity angle becomes significant only around the balanced conditions as shown in the load-moment interaction diagram; the eccentricity angle tends to decrease the load capacity and the ductility of the column section.

17. Although high strength concrete as a material shows lesser ductility than low strength concrete, the ductility at ultimate of reinforced concrete sections made with both materials are not significantly different.

18. There is evidence that the strain on the extreme compressive fiber of concrete at ultimate behavior of flexural members can be approximated by the value of 0.0045 for normal weight concrete with strength from 3 to 13 ksi and by the values of 0.0035, 0.0040 and 0.0045, respectively, for lightweight concrete of 3, 5 and 7 ksi strengths. This conclusion is substantially different from the ACI recommended value of 0.0030 for all concretes.

19. The parameter β_1 for the depth of the rectangular stress block defined in the ACI code, does not affect the calculation of the ultimate moment of under-reinforced beams, but affects the calculation of the ultimate curvature. Since two values of β_1 can be derived from the

actual stress block by satisfying two static conditions, an average value of $\beta_1 = 0.75$ for both normal and lightweight concretes with strengths greater than 6 ksi, was found adequate in predicting ultimate curvature more accurately than the ACI recommended value.

REFERENCES

[1] ACI Committee 318, Building Code Requirements for Reinforced Concrete (ACI 318-71), American Concrete Institute, Detroit, 1971.

[2] Barnard, P. R., "Researches into the Complete Stress-Strain Curve for Concrete," Magazine of Concrete Research, Vol. 16, No. 49, Dec. 1964, pp. 203-210.

[3] Behr, R., Goodspeed, C., and Romualdi, J., "Analytical and Experimental Investigation of Ferrocement Sandwich Panel,"

[4] Bresler, B., "Reinforced Concrete Engineering," Vol. 1, John Wiley & Sons, Inc., New York, 1974.

[5] Bresler, B., "Lightweight Aggregate Reinforced Concrete Columns," ACI Symposium on Lightweight Aggregate Concrete, New York ACI SP 2 9-7, pp. 81-130, April 1971.

[6] Brock, G., "Concrete: Complete Stress-Strain Curves," Engineering, London, Vol. 193, No. 5011, 1962, p. 606.

[7] Burns, N. H. and Siess, C. P., "Plastic Hinge in Reinforced Concrete," Proceeding of ASCE, J. STD., Oct. 1966, pp. 45-64.

[8] "High Strength Concrete in Chicago High-Rise Buildings," Preliminary report published by Chicago Committee on High-Rise Buildings, 10 South Wabash Avenue, Chicago, 1976, 63 pp.

[9] Cismigiu, A. and Dougariu, L., "Automatic Design of Strength and Ductility of Reinforced Concrete Members," Rev. Roum. Sci. Tech.-Mech. Appl., Tome 21, No. 2, Bucarest, 1976, pp. 165-181.

[10] Cohn, M. Z. and Ghosh, S. K., "The Flexural Ductility of Reinforced Concrete Sections," S. M. Report No. 100, Solid Mech. Div., University of Waterloo and Publications International Association of Bridge and Structural Engineers, Vol. 32-2, 1972.

[11] Corley, W. G., "Rotation Capacity of Reinforced Concrete Beam," Proceeding of ASCE, J. STD., Oct. 1966, pp. 121-146.

[12] Desayi, P. and Krishnan, S., "Equation for Stress-Strain Curve of Concrete," Journal of the American Concrete Institute, Proc. V. 61, March 1964, pp. 345-350.

[13] Ferguson, P. M., "Reinforced Concrete Fundamentals," John Wiley & Sons, Inc., New York, 1973.

[14] Fintel, M., "Handbook of Concrete Engineering," Van Nostrand Reinhold Company, 1974, p. 229 - p. 245.

[15] Ghosh, S. K. and Cohn, M. Z., "Computer Analysis of Reinforced Concrete Sections under Combined Bending and Compression," International Association of Bridge and Structural Engineering, Proceedings, Vol. 34-I, Zurich, 1974.

[16] Goldberg, J. E. and Richard R. M., "Analysis of Nonlinear Structures," ASCE, SDJ, Vol. 89, No. ST4, Aug. 1963.

[17] Heimdahl, P. D. and Bianchini, A. C., "Ultimate Strength of Beams Reinforced with Steel Having No Definite Yield Point," ACI, J. Dec. 1974.

[18] Heimdahl, P. D. and Bianchini, A. C., "Ultimate Strength of Biaxially Eccentrically Loaded Concrete Columns Reinforced with High Strength Steel," ACI SP50-4, pp. 93-117.

[19] Hognestad, E., "A Study of Combined Bending and Axial Load in Reinforced Concrete Members," University of Illinois Engineering Experiment Station Bulletin No. 399, 1951.

[20] Hognestad, E., Hanson, N. W., and McHenry, D., "Concrete Stress Distribution in Ultimate Strength Design," ACI Journal, Proceeding Vol. 52, No. 4, Dec. 1955, pp. 455-480.

[21] Kulicki, J. M. and Kostem, C. N., "Inelastic Response of Prestressed Concrete Beams," International Association of Bridge and Structural Engineering, Vol. 35-II, Zurich, 1975.

[22] Mattock, A. H., Kriz, L. B., and Hognestad, E., "Rectangular Concrete Stress Distribution in Ultimate Strength Design," ACI Journal Proceedings, Vol. 32, No. 8, Feb. 1961, pp. 875-920.

[23] Mattock, A. H., "Rotational Capacity of Hinging Regions in Reinforced Concrete Beams," Proceedings of the International Symposium, Flexural Mechanics of Reinforced Concrete, Miami, Fla., Nov. 1964, pp. 143-181.

[24] Naaman, A. E., "Ultimate Analysis of Prestressed and Partially Prestressed Sections by Strain Compatibility," to be published in the Journal of the Prestressed Concrete Institute.

[25] Popovics, S., "A Review of Stress-Strain Relationships for Concrete," Journal of the American Concrete Institute, Proc. 67, March 1970, pp. 243-248.

[26] Popovics, S., "A Numerical Approach to the Complete Stress-Strain Curve of Concrete," Cement and Concrete Research, Vol. 3, 1973, pp. 583-599.

[27] Ramberg, W. and Osgood, W. R., "Description of Stress-Strain Curves by Three Parameters, NACA TN 902, July 1943.

[28] Roy, H.E.H. and Sozen, Mete A., "Ductility of Concrete," Flexural Mechanics of Reinforced Concrete, Proceedings of the International Symposium, Miami, Fla, Nov. 1964.

[29] Saenz, L. P., Discussion of Reference [38], Journal of the American Concrete Institute, Proc. Vol. 61, No. 9, Sept. 1964, pp. 1229, 1236.

[30] Salse, E.A.B. and Fintel, M., "Strength, Stiffness and Ductility of Slender Shear Walls,"Fifth World Conference on Earthquake Engineering, Rome 1973, Session 3A.

[31] Sangha, C. M. and Dhir, R. K., "Strength and Complete Stress-Strain Relationships for Concrete Tested in Uniaxial Compression under Different Test Conditions," Materiaux et Construction, RILEM, Vol. 5, No. 30, 1972.

[32] Sargin, M., "Stress-Strain Relationship for Concrete and the Analysis of Structural Concrete Sections," Study No. 4, Solid Mechanics Division, University of Waterloo, Waterloo, Ontario, Canada, 1971, 167 pp.

[33] Shah, S. P. and Rangan, B. V., "Effects of Reinforcements on Ductility of Concrete," ACI Journal, June 1970.

[34] Smith, G. M. and Young, L. E., "Ultimate Flexural Analysis Based on Stress-Strain Curve of Cylinders," Journal of the American Concrete Institute, Proc. Vol. 63, Dec. 1956, pp. 597-609.

[35] Smith, G. M. and Young, L. E., "Ultimate Theory in Flexure by Exponential Function," ACI Journal, Proc. Vol. 52, No. 3, Nov. 1955, pp. 349-360.

[36] Spooner, D. C., "Progressive Damage and Energy Dissipation in Concrete in Uniaxial Compression," Ph.D. Thesis, University of London, Kings College, 1974, 262 pp.

[37] Sturman, G. M., Shah, S. P. and Winter, G., "Effect of Flexural Strain Gradients on Microcracking and Stress-Strain Behavior of Concrete," ACI Journal, Proc. Vol. 62, No. 7, July 1965, pp. 805-822.

[38] Turner, P. W. and Barnard, P. R., "Stiff Constant Strain Rate Testing Machine," The Engineer (London), Vol. 214, No. 5557, July 1962, pp. 146-148.

[39] Wang, P., Shah, S. P. and Naaman, A. E., Dicussion of "Flexural Behavior of High Strength Concrete Beam," by Leslie, K. E., Rajgopalan, K. S. and Everard, N. J., ACI Journal, Proc. Vol. 74, No. 9, March 1977, pp. 143-145.

[40] Winter, G. and Nilson, A. H., "Design of Concrete Structures," McGraw-Hill Book Company, New York, 1972.

[41] Wiss, Janney, Elstner & Associates, Inc., "Tensile Test Load-Elongation Autographic Plots for Associated Reinforcing Bar Producers Technical Committee," WJE No. 74458, Oct. 31, 1975.

[42] Berwanger, C., "Effect of Axial Load on the Moment-Curvature Relationship of Reinforced Concrete Members," ACI SP-50, pp. 263-288.

[43] Leslie, K. E., Rajagopalan, K. S. and Everard, N. J., "Flexural Behavior of High-Strength Concrete Beams," ACI Journal, Sept. 1976, pp. 517-521.

APPENDIX I

COMPUTER PROGRAM FOR THE NONLINEAR ANALYSIS OF RECTANGULAR AND T-SECTIONS

```
RELEASE 2.0              MAIN              DATE = 77161          20/37/15

      CCC
      CCC   PURE BENDING OF RECTANGULAR AND T-BEAM (Appendix 1)
      CCC
            DIMENSION FF(900),EE(900),XALPHA(900),XBETA(900)
            DIMENSION BXM(100),BCURV(100),BEU(100),BFS(100)
        105 READ(5,240) JOB
        240 FORMAT(I5)
            IF(JOB.EQ.0) STOP
            WRITE(6,250)  JOB
        250 FORMAT(////' BEAM   NO.',I5//)
      CCC   FO=CONCRETE PEAK STRESS(KSI), FY=STEEL YIELD STRE(KSI)
      CCC   ICONC=2....NORMAL WEIGHT
      CCC   ICONC=1....LIGHTWEIGHT
            READ(5,111) FO,FY,ICONC
        111 FORMAT(2F10.4,I5)
            READ(5,222) B,D,H, AS, ASP,DPP,BP,T
        222 FORMAT(8F10.4)
      CCC   END OF DATA
      CCC
            IF(ICONC.EQ. 1) GO TO 11
            IF(ICONC.EQ. 2) GO TO 22
         11 WRITE(6,15)
            GO TO 50
         22 WRITE(6,25)
         50 CONTINUE
         15 FORMAT(/' LIGHTWEIGHT'/)
         25 FORMAT(/' NORMAL WEIGHT'/)
      CCC
            PFIX=0.
      CCC
            BT1=0.85-0.05*(FO-4.)
            IF(FO.GT. 8.) BT1=0.65
      CCC   PBAL= BALANCED REINFORCEMENT RATIO FROM ACI CODE
            PBAL=(0.85*BT1*FO/FY)*(87./(87.+FY))
      CCC
            IF(AS.NE. 0.) GO TO 10
            AS=0.50*PBAL*B*D
            AS=0.75*PBAL*B*D
            AS=0.005*B*D
            AS=0.015*B*D
      CCC
            ASP=0.5*AS
            ASP=0.
            ASP=AS
        10 CONTINUE
      CCC
            PAS=AS/(B*D)
            PASP=ASP/(B*D)
      CCC   BP=T=0.0  FOR RECTANGULAR BEAM
            ETS=0.001
      CCC   COMPUTE CONCRETE PROPERTIES
      CCC
            CALL ALPBET(FO,EO,FF,EE,XALPHA,XBETA,DE,ICONC,EMC)
      CCC
            IF(BP.NE.0.) GO TO 1000
      CCC
      CCC   RECTANGULAR BEAM
      CCC
            WRITE(6,888)
```

```
  888 FORMAT(/' RECTANGULAR BEAM'//)
      WRITE(6,666)
  666 FORMAT(/' SECTION PROPERTIES'//
     1  4X,1HB,10X,1HD,10X,1HH,10X,3HDPP, 9X,2HBP,9X,1HT,9X
     1    3HPAS, 8X,4HPASP,7X,2HAS, 9X,3HASP, 8X,2HFO, 9X,2HFY/)
      WRITE(6,777) B,D,H,DPP,BP,T,PAS,PASP,AS,ASP,FO,FY
  777 FORMAT(12(F10.4,1X))
      WRITE(6,444)
  333 FORMAT(4(F10.4,1X),2(F10.5,1X),2(F10.3,1X),F10.4,1X,2(F10.3,1X),
     1  5X,F6.5/)
  444 FORMAT(//' ANALYSIS RESULTS'//
     1           4X,' EU',7X,' ALPHA',5X,' BETA', 6X,' C(INS)',4X,
     2  ' ES',8X,' ESP',6X, ' FS(KSI)',3X,' FSP(KSI)',1X,' XP(KIP) ',
     3  2X,' XM(K-IN)',1X,' CURV(.001/IN)',' XM/FOBDD'//)
      TXM=0.
      CPREV=0.4*D
      NPTS=60
      DO 300 I= 1,NPTS
      EU=0.0001*I
      AN=EU/DE
      AAN=AN+0.5
      N=AAN
      N1=N+1
      ALPHA=XALPHA(N)
      BETA=XBETA(N)
      FU=FF(N1)
CCC
CCC   TRY NEUTUAL AXIS, C
CCC
      C=CPREV
      DELTA=0.1
      YKK=1000.
      GO TO 370
  310 C=C+DELTA
      GO TO 370
  320 C=C-DELTA
  370 CONTINUE
      IF(T.EQ. 0.) GO TO 200
      IF(C.GT. T) GO TO 1340
  200 CONTINUE
      ES=EU*((D-C)/C)
      CALL STEELA(FS,ES,FY,EMS)
      IF(ASP.EQ. 0.) GO TO 325
      ESP=EU*((C-DPP)/C)
      CALL STEELA(FSP,ESP,FY,EMS)
      GO TO 335
  325 ESP=0.
      FSP=0.
  335 CONTINUE
      XP=ALPHA*FO*B*C+ASP*FSP-AS*FS
      IF(YKK.EQ. 1000.) GO TO 380
      IF((ABS(XP-PFIX)+ABS(XPP-PFIX)).NE.ABS(XP+XPP-2.*PFIX)) GO TO 270
  380 XPP=XP
      XCC=C
      YKK=2000.
      IF(ABS(XP-PFIX).LT. ETS ) GO TO 330
      IF(XP-PFIX) 310,330,320
  270 DELTA=ABS(0.1*(C-XCC))
      C=(C+XCC)/2.
      GO TO 370
  330 CONTINUE
```

```
  400 XM=ALPHA*FO*B*C*(D-BETA*C)+ASP*FSP*(D-DPP)
  390 CONTINUE
      IF(T.EQ. 0.) GO TO 392
      WRITE(6,990)
  990 FORMAT( '     DESIGNED AS RECT.-SECTION')
  392 CONTINUE
      RATIO=XM/(FO*B*D*D)
      CURV=EU/C
      CURV=CURV*1000.
      WRITE(6,333) EU,ALPHA,BETA,C,ES,ESP,FS,FSP,XP,XM,CURV,RATIO
      IF(T.NE. 0.) GO TO 1200
      IF(ICODE.EQ.2) GO TO 205
      BXM(I)=XM
      BCURV(I)=CURV
      BEU(I)=EU
      BFS(I)=FS
      IF(XM-TXM) 410,410,420
  420 TXM=XM
      TCURV=CURV
      TEU=EU
  410 CONTINUE
      CPREV=C
  290 CONTINUE
  300 CONTINUE
CCC
CCC   COMPUTE YIELDING MOMENT BY INTERPOLATING ANALYTICAL RESULTS
CCC
      I=1
  470 CONTINUE
      IF(BFS(I)- FY) 450,460,460
  450 I=I+1
      GO TO 470
  460 KK=I-1
      KA=KK-1
      RR=( FY-BFS(KK))/(BFS(KK)-BFS(KA))
      REU=BEU(KK)+0.0001*RR
      RXM=BXM(KK)+RR*(BXM(KK)-BXM(KA))
      RCURV=BCURV(KK)+RR*(ECURV(KK)-BCURV(KA))
      WRITE(6,515)
  515 FORMAT(//' AT YIELDING OF REINFORCEMENT'//)
      WRITE(6,535) REU,RXM,RCURV
      WRITE(6,525)
  525 FORMAT(//' AT ULTIMATE'//)
      WRITE(6,535) TEU,TXM,TCURV
  535 FORMAT(' EU              =',F10.5//' XM(K-IN)      =',F10.3//
     1   ' CURV(.001/IN)=',F10.6)
CCC
CCC   DUCTILITY FACTOR
CCC
      DUCT=TCURV/RCURV
      WRITE(6,545) DUCT
  545 FORMAT(/' DUCTILITY FACTOR=',F10.4/)
CCC
CCC   ACI MOMENT FOR UNDERREINFOTCED BEAM(FOR THE CASE OF NO AXIAL LOAD)
CCC
      WRITE(6,2222)
 2222 FORMAT(///' ACI CODE MOMENT FOR UNDERREINFORCED BEAM'/)
      WRITE(6,444)
      EU=0.003
      ALPHA=0.85*BT1
      BETA=BT1/2.
```

```
      EY=FY/EMS
      XN=EMS/EMC
      XNP=XN*PAS
      XNPP=XN*PASP
 2000 CONTINUE
CCC
CCC   SECTION WITHOUT COMPRESSION STEEL
CCC
      IF(ASP.NE. 0.) GO TO 2200
      PMAX=0.75*PBAL
      IF(PAS-PMAX) 2260,2260,2270
 2270 WRITE(6,2250)
 2250 FORMAT(//' OVERREINFORCED BEAM----NO SOLUTION'//)
      GO TO 205
 2260 CONTINUE
CCC
CCC   AT YIELD OF REINFORCEMENT
CCC
      WRITE(6,515)
      XK=-XNP+SQRT(XNP*XNP+2.*XNP)
      C=XK*D
      ES=EY
      FS=FY
      ESP=0.
      FSP=0.
      XP=0.
      XM=AS*FY*(D-C/3.)
      CURV=EY/(D-C)
      CURV=CURV*1000.
      EC=EY*(C/(D-C))
      RATIO=XM/(FO*B*D*D)
      ALPHY=0.5
      BETY=0.33333
      WRITE(6,333) EC,ALPHY,BETY,C,ES,ESP,FS,FSP,XP,XM,CURV,RATIO
      XMYYY=XM
      CURYYY=CURV
      ECYYY=EC
CCC
CCC   AT ULTIMATE
CCC
      WRITE(6,525)
      A=(AS*FY)/(0.85*FO*B)
      C=A/BT1
      XM=AS*FY*(D-A/2.)
      XP=0.
      ESP=0.
      FSP=0.
      ES=EU*((D-C)/C)
      CALL STEELA(FS ,ES ,FY,EMS)
      CURV=EU/C
      CURV=CURV*1000.
      RATIO=XM/(FO*B*D*D)
      WRITE(6,333) EU,ALPHA,BETA,C,ES,ESP,FS,FSP,XP,XM,CURV,RATIO
      XMCCD=XM
      EUCCD=EU
      CURCOD=CURV
      DUCTCD= CURCOD/CURYYY
      WRITE(6,545) DUCTCD
      GO TO 205
 2200 CONTINUE
CCC
```

```
CCC    SECTION WITH COMPRESSION STEEL
CCC
       PMAX=0.75*(PBAL+PASP)
       PMIN=PASP+0.85*BT1*(FO/FY)*(DPP/D)*(87./(87.-FY))
       IF(PAS-PMAX) 2230,2230,2240
 2240  WRITE(6,2250)
       GO TO 205
 2230  CONTINUE
CCC
CCC    AT YIELD OF REINFORCEMENT
CCC
       WRITE(6,515)
       AA=XNP+XNPP
       XK=-AA+SQRT(AA*AA+2.*XNP+2.*XNPP*(DPP/D))
       C=XK*D
       ES=EY
       FS=FY
       EC=EY*(C/(D-C))
       ESP=EC*(C-DPP)/C
       FSP=EMS*ESP
       XMS=ASP*FSP*(D-DPP)
       XMC=0.5*B*C*FY/XN*(C/(D-C))*(D-C/3.)
       XM=XMS+XMC
       XP=0.
       CURV=EY/(D-C)
       CURV=CURV*1000.
       RATIO=XM/(FO*B*D*D)
       ALPHY=0.5
       BETY=0.33333
       WRITE(6,333) EC,ALPHY,BETY,C,ES,ESP,FS,FSP,XP,XM,CURV,RATIO
       XMYYY=XM
       CURYYY=CURV
       ECYYY=EC
CCC
CCC    AT ULTIMATE
CCC
       WRITE(6,525)
       IF(PAS-PMIN) 2210,2220,2220
 2220  CONTINUE
CCC
CCC    COMPRESSION STEEL YIELD
CCC
       A=(AS-ASP)*FY/(0.85*FO*B)
       C=A/BT1
       XM=ASP*FY*(D-DPP)+(AS-ASP)*FY*(D-A/2.)
       XP=0.
       GO TO 2300
 2210  CONTINUE
CCC
CCC    COMPRESSION STEEL NOT YIELD
CCC
CCC    DETERMINE N.A. BY QUADRATIC EQUATION
       AA=0.85*BT1*FO*B
       BB=ASP*EU*EMS-AS*FY
       CC=ASP*EU*EMS*DPP
       ROOT2=BB*BB+4.*AA*CC
       ROOT=ROOT2**0.5
       C=(-BB+ROOT)/(2.*AA)
       A=C*BT1
       FSP=EMS*EU*(C-DPP)/C
       XM=0.85*FO*A*B*(D-A/2.)+ASP*FSP*(D-DPP)
```

```
      XP=0.
 2300 CONTINUE
      ES=EU*((D-C)/C)
      ESP=EU*((C-DPP)/C)
      CALL STEELA(FS ,ES ,FY,EMS)
      CALL STEELA(FSP,ESP,FY,EMS)
      CURV=EU/C
      CURV=CURV*1000.
      RATIO=XM/(FO*B*D*D)
      WRITE(6,333) EU,ALPHA,BETA,C,ES,ESP,FS,FSP,XP,XM,CURV,RATIO
      CURCOD=CURV
      XMCOD=XM
      EUCOD=EU
      DUCTCD= CURCOD/CURYYY
      WRITE(6,545) DUCTCD
      GO TO 205
CCC
CCC   T-BEAM
CCC
 1000 CONTINUE
      WRITE(6,555)
  555 FORMAT(/' T-BEAM'//)
      WRITE(6,666)
      WRITE(6,777) B,D,H,DPP,BP,T,PAS,PASP,AS,ASP,FO,FY
      WRITE(6,444)
      TXM=0.
      CPREV=0.4*D
      NPTS=60
      DO 1300 I= 1,NPTS
      EU=0.0001*I
      AN=EU/DE
      AAN=AN+0.5
      N=AAN
      N1=N+1
      ALPHA=XALPHA(N)
      BETA=XBETA(N)
      FU=FF(N1)
CCC
CCC   TRY NEUTUAL AXIS, C
CCC
 3100 CONTINUE
      ITEST=1
      C=CPREV
      DELTA=0.1
      YKK=1000.
      GO TO 1370
 1310 C=C+DELTA
      GO TO 1370
 1320 C=C-DELTA
 1370 CONTINUE
      ITEST=ITEST+1
      IF(ITEST.GT.30) GO TO 1375
      IF(C.LT. T) GO TO 370
 1340 CONTINUE
      ES=EU*((D-C)/C)
      EFB=EU*((C-T)/C)
CCC   EFB= STRAIN AT BOTTOM OF FLANGE
      IF(ICODE.EQ.2) GO TO 3200
      AN=EFB/DE
      AAN=AN+0.5
      N=AAN
```

```
      N1=N+1
      ALPHAT=XALPHA(N)
      BETAT=XBETA(N)
      FFB=FF(N1)
 3200 CONTINUE
      CALL STEELA(FS,ES,FY,EMS)
      IF(ASP.EQ. 0.) GO TO 1325
      ESP=EU*((C-DPP)/C)
      CALL STEELA(FSP,ESP,FY,EMS)
      GO TO 1335
 1325 ESP=0.
      FSP=0.
 1335 CONTINUE
      XP=ALPHA*FO*B*C+ASP*FSP-AS*FS-ALPHAT*FO*(B-BP)*(C-T)
      IF(ABS(XP-PFIX).LT. ETS ) GO TO 1330
      IF(YKK.EQ. 1000.) GO TO 1380
      IF((ABS(XP-PFIX)+ABS(XPP-PFIX)).NE.ABS(XP+XPP-2.*PFIX)) GO TO 1270
      IF(XP.GT. 0.) GO TO 1380
 1380 XPP=XP
      XCC=C
      YKK=2000.
      IF(XP-PFIX) 1310,1310,1320
 1270 DELTA=ABS(0.1*(C-XCC))
      C=(C+XCC)/2.
      GO TO 1370
 1330 CONTINUE
 1400 XM=ALPHA*FO*B*C*(D-BETA*C)+ASP*FSP*(D-DPP)
     1  -ALPHAT*FO*(B-BP)*(C-T)*(D-T-BETAT*(C-T))
 1390 CONTINUE
      WRITE(6,880)
  880 FORMAT( '     DESIGNED AS T-SECTION')
      RATIO=XM/(FO*BP*D*D)
      CURV=EU/C
      CURV=CURV*1000.
      WRITE(6,333) EU,ALPHA,BETA,C,ES,ESP,FS,FSP,XP,XM,CURV,RATIO
 1200 CONTINUE
      CPREV=C
      BXM(I)=XM
      BCURV(I)=CURV
      BEU(I)=EU
      BFS(I)=FS
      IF(XM-TXM) 430,430,440
  440 TXM=XM
      TCURV=CURV
      TEU=EU
  430 CONTINUE
 1300 CONTINUE
      GO TO 600
 1375 CONTINUE
CCC
CCC   NO SOLUTION AT THAT PARTICULAR STRAIN
CCC
      NPTS=I-1
  600 CONTINUE
CCC
CCC   COMPUTE YIELDING MOMENT BY INTERPOLATING ANALYTICAL RESULTS
CCC
      I=1
  480 CONTINUE
      IF(BFS(I)- FY) 485,495,495
  485 I=I+1
```

```
      GO TO 480
  495 KK=I-1
      KA=KK-1
      RR=( FY-BFS(KK))/(BFS(KK)-BFS(KA))
      REU=BEU(KK)+0.0001*RR
      RXM=BXM(KK)+RR*(BXM(KK)-BXM(KA))
      RCURV=BCURV(KK)+RR*(BCURV(KK)-BCURV(KA))
      WRITE(6,515)
      WRITE(6,535) REU,RXM,RCURV
      WRITE(6,525)
      WRITE(6,535) TEU,TXM,TCURV
CCC
CCC   DUCTILITY FACTOR
CCC
      DUCT=(TCURV-RCURV)/RCURV
      WRITE(6,545) DUCT
CCC
CCC   ACI MOMENT FOR UNDERREINFOTCED BEAM(FOR THE CASE OF NO AXIAL LOAD)
CCC
      WRITE(6,2222)
      WRITE(6,444)
      EU=0.003
      ALPHA=0.85*BT1
      BETA=BT1/2.
      EY=FY/EMS
      XN=EMS/EMC
      XNP=XN*PAS
      XNPP=XN*PASP
 4000 CONTINUE
      PASW=AS/(BP*D)
      PASPW=ASP/(BP*D)
      ASF=0.85*FO*(B-BP)*T/FY
      PASF=ASF/(BP*D)
      PBALW=PBAL+PASF+PASPW
      PMAXW=0.75*PBALW
      IF(PASW-PMAXW) 4230,4230,4240
 4240 WRITE(6,2250)
      GO TO 205
 4230 CONTINUE
CCC
CCC   TESTING BEAM DESIGNED AS RECTANGULAR OR T-SECTION
CCC   ASSUME COMPRESSION STEEL YIELD
CCC
      A=(AS-ASP)*FY/(0.85*FO*B)
      IF(A-T) 4100,4200,4200
 4100 CONTINUE
CCC
CCC   BEAM DESIGNED AS RECT.-SECTION
CCC
      GO TO 2000
CCC
CCC   BEAM DESIGNED AS T-SECTION
CCC
 4200 CONTINUE
CCC
CCC   AT YIELD OF REINFORCEMENT
CCC
      WRITE(6,515)
      BB=(XNP+XNPP)*(B/BP)-(T/D)
      CC=2.*XNP+2.*XNPP*(DPP/D)*(B/BP)-(T/D)**2
      XK=-BB+SQRT(BB*BB+CC)
```

```
      C=XK*D
      ES=EY
      FS=FY
      EC=EY*(C/(D-C))
      ESP=EC*(C-DPP)/C
      FSP=EMS*ESP
      EFB=EC*(C-T)/C
      FFB=EMC*EFB
      CA=0.5*B*C*FY/XN*C/(D-C)
      CB=0.5*(B-BP)*(C-T)*FFB
       XM=CA*(D-C/3.)+ASP*FSP*(D-DPP)-CB*(D-T-(C-T)/3.)
      XP=0.
      CURV=EY/(D-C)
      CURV=CURV*1000.
      RATIO=XM/(FO*BP*D*D)
      ALPHY=0.5
      BETY=0.33333
      WRITE(6,333) EC,ALPHY,BETY,C,ES,ESP,FS,FSP,XP,XM,CURV,RATIO
      XMYYY=XM
      CURYYY=CURV
      ECYYY=EC
CCC
CCC   AT ULTIMATE
CCC
      WRITE(6,525)
      ASF=0.85*FO*(B-BP)*T/FY
      CCF=(AS-ASF-ASP)*FY
      A=CCF/(0.85*FO*BP)
      C=A/BT1
      XM=CCF*(D-A/2.)+ASF*FY*(D-T/2.)+ASP*FY*(D-DPP)
      XP=0.
      ES=EU*((D-C)/C)
      ESP=EU*((C-DPP)/C)
      CURV=EU/C
      CURV=CURV*1000.
      RATIO=XM/(FO*BP*D*D)
      WRITE(6,333) EU,ALPHA,BETA,C,ES,ESP,FS,FSP,XP,XM,CURV,RATIO
      XMCOD=XM
      EUCOD=EU
      CURCOD=CURV
      DUCTCD= CURCOD/CURYYY
      WRITE(6,545) DUCTCD
CCC
  205 CONTINUE
CCC
CCC
      GO TO 105
      END
```

```
RELEASE 2.0                ALPBET              DATE = 77161          20/37/15

      SUBROUTINE ALPBET(FO,EO,FF,EE,XALPHA,XBETA,DE,ICONC,EMC)
      DIMENSION FF(900),EE(900),A(900),DX(900),ATOT(900),AMTOT(900)
      DIMENSION XALPHA(900),XBETA(900)
      Y1(X)=(A1*X+B1*X*X)/(1.+C1*X+D1*X*X)
      Y2(X)=(A2*X+B2*X*X)/(1.+C2*X+D2*X*X)
CCC   ICONC=2....NORMAL WEIGHT
CCC   ICONC=1....LIGHTWEIGHT
      IF(ICONC.EQ.2) GO TO 205
      IF(ICONC.EQ.1) GO TO 105
  205 CONTINUE
CCC
CCC   NORMAL WEIGHT
      IF(FO.EQ. 3.    ) GO TO 3000
      IF(FO.EQ. 5.    ) GO TO 5000
      IF(FO.EQ. 7.    ) GO TO 7000
      IF(FO.EQ. 9.    ) GO TO 9000
      IF(FO.EQ. 11.   ) GO TO 11000
      IF(FO.EQ. 13.   ) GO TO 13000
 3000 CONTINUE
CCC   FO=3.     KSI....NORMAL WEIGHT
      EO=0.00267
      A1=1.596974
      B1=-0.352041
      C1=-0.403026
      D1=0.647959
      A2=-1.275770
      B2=1.479521
      C2=-3.275770
      D2=2.479521
      GO TO 9999
 5000 CONTINUE
CCC   FO=5.     KSI....NORMAL WEIGHT
      EO=0.00292
      A1=1.364804
      B1=-0.758034
      C1=-0.635196
      D1=0.241966
      A2=0.326434
      B2=0.047969
      C2=-1.673566
      D2=1.047969
      GO TO 9999
 7000 CONTINUE
CCC   FO=7.     KSI....NORMAL WEIGHT
      EO=0.00317
      A1=1.304017
      B1=-0.831953
      C1=-0.695983
      D1=0.168047
      A2=0.357600
      B2=-0.095550
      C2=-1.642400
      D2=0.904450
      GO TO 9999
 9000 CONTINUE
CCC   FO=9.     KSI....NORMAL WEIGHT
      EO=0.00343
      A1=1.300358
      B1=-0.835974
```

```
      C1=-0.699642
      D1=0.164026
      A2=0.301863
      B2=-0.124428
      C2=-1.698137
      D2=0.875572
      GO TO 9999
11000 CONTINUE
CCC   FO=11.   KSI....NORMAL WEIGHT
      EO=0.00368
      A1=1.322665
      B1=-0.810704
      C1=-0.677335
      D1=0.189296
      A2=0.238022
      B2=-0.121764
      C2=-1.761978
      D2=0.878236
      GO TO 9999
13000 CONTINUE
CCC   FO=13.   KSI....NORMAL WEIGHT
      EO=0.00392
      A1=1.358955
      B1=-0.765732
      C1=-0.641045
      D1=0.234268
      A2=0.179553
      B2=-0.107095
      C2=-1.820447
      D2=0.892905
      GO TO 9999
CCC
  105 CONTINUE
CCC
CCC   LIGHTWEIGHT
CCC
      IF(FO.EQ. 3.    ) GO TO 30
      IF(FO.EQ. 5.    ) GO TO 50
      IF(FO.EQ. 7.    ) GO TO 70
   30 CONTINUE
CCC   FO=3000. PSI....LIGHTWEIGHT CONCRETE
      EO=0.00277
      A1=1.541689
      B1=-0.466498
      C1=-0.458311
      D1=0.533502
      A2=0.178520
      B2=-0.046208
      C2=-1.821480
      D2=0.953792
      GO TO 9999
   50 CONTINUE
CCC   FO=5000. PSI....LIGHTWEIGHT CONCRETE
      EO=0.00317
      A1=1.287970
      B1=-0.849227
      C1=-0.712030
      D1=0.150773
      A2=0.235274
      B2=-0.103281
      C2=-1.764726
```

```
      D2=0.896719
      GO TO 9999
   70 CONTINUE
CCC   FO=7000. PSI....LIGHTWEIGHT CONCRETE
      EO=0.00357
      A1=1.220582
      B1=-0.911536
      C1=-0.779418
      D1=0.088464
      A2=0.219928
      B2=-0.114448
      C2=-1.780072
      D2=0.885552
      GO TO 9999
 9999 CONTINUE
      EMC=A1*FO/EO
CCC   DE=INTERVAL IN STRAIN-AXIS
      EU=0.006
      DE=0.00001
      AN=EU/DE
      AAN=AN+0.5
      N=AAN
      N1=N+1
CCC   N=NOS. OF INTERVAL
      DO 500 I=1,N1
  500 FF(I)=0.
      DO 100 I=1,N1
      EE(I)=DE*FLOAT(I-1)
      X=EE(I)/EO
      IF(X.LT. 1.) GO TO 200
      FF(I)=FO*Y2(X)
      GO TO 300
  200 FF(I)=FO*Y1(X)
  300 CONTINUE
  100 CONTINUE
      FU=FF(N1)
CCC   AREA AND MOMENT UNDER CURVE
      DO 400 I=1,N
      A(I)=0.5*DE*(FF(I)+FF(I+1))
      DDX=(DE/3.)*((FF(I)+2.*FF(I+1))/(FF(I)+FF(I+1)))
      DX(I)=DDX+DE*FLOAT(I-1)
  400 CONTINUE
      DO 800 K=1,N
      EU=DE*K
      AMON=0.
      AREA=0.
      DO 700 I=1,K
      AREA=AREA+A(I)
      AMON=AMON+A(I)*DX(I)
  700 CONTINUE
      ATOT(K)=AREA
      AMTOT(K)=AMON
      XALPHA(K)=ATOT(K)/(FC*EU)
      BETA=AMTOT(K)/ATOT(K)
      BETA=BETA/EU
      BETA=1.-BETA
      XBETA(K)=BETA
  800 CONTINUE
      RETURN
      END
```

```
RELEASE 2.0                STEELA              DATE = 77161          20/37/15

      SUBROUTINE STEELA(FS,ES,FY,EMI)
      IF(FY.EQ. 60.    ) GO TO 60000
60000 CONTINUE
      FSU=104.58
      FSF=93.44
      EMI=29760.
      EMSH=1222.
      ESH=0.0091
      ESU=0.0729
      ESF=0.1542
      A=1.748272
      B=0.173674
      C=-0.251726
      D=1.173672
      GO TO 9999
 9999 CONTINUE
      EY=FY/EMI
      XO=ESU-ESH
      YO=FSU-FY
      IF(ES.LT.EY ) GO TO 1300
      IF(ES.GT.EY.AND.ES.LT.ESH) GO TO 1200
      IF(ES.GT.ESH.AND.ES.LT.ESF) GO TO 1100
      IF(ES.GT.ESF) GO TO 1400
 1300 FS=EMI*ES
      GO TO 500
 1200 FS=FY
      GO TO 500
 1100 CONTINUE
      XX=(ES-ESH)/XO
      YY=(A*XX+B*XX*XX)/(1.+C*XX+D*XX*XX)
      FS=YY*YO+FY
      GO TO 500
 1400 FS=0.
      GO TO 500
  500 CONTINUE
      RETURN
      END
```

BEAM NO. 1

NORMAL WEIGHT

RECTANGULAR BEAM

SECTION PROPERTIES

B	D	H	DPP	BP	T	PAS	PASP	AS	ASP	FO	FY
10.0000	18.0000	20.0000	2.0000	0.0	0.0	0.0150	0.0150	2.7000	2.7000	3.0000	60.0000

ANALYSIS RESULTS

EU	ALPHA	BETA	C(INS)	ES	ESP	FS(KSI)	FSP(KSI)	XP(KIP)	XM(K-IN)	CURV(.001/IN)	XM/FOBOD
0.0001	0.0300	0.3330	7.1413	0.00015	0.00007	4.525	2.143	0.0006	193.064	0.014	.01986
0.0002	0.0603	0.3328	7.1360	0.00030	0.00014	9.061	4.284	0.0003	386.624	0.028	.03978
0.0003	0.0906	0.3327	7.1322	0.00046	0.00022	13.604	6.424	0.0001	580.477	0.042	.05972
0.0004	0.1210	0.3328	7.1298	0.00061	0.00029	18.149	8.565	0.0003	774.401	0.056	.07967
0.0005	0.1513	0.3329	7.1289	0.00076	0.00036	22.691	10.705	0.0005	968.166	0.070	.09961
0.0006	0.1815	0.3332	7.1296	0.00091	0.00043	27.225	12.847	-0.0001	1161.534	0.084	.11950
0.0007	0.2115	0.3336	7.1318	0.00107	0.00050	31.746	14.990	-0.0002	1354.275	0.098	.13933
0.0008	0.2411	0.3342	7.1355	0.00122	0.00058	36.250	17.135	-0.0008	1546.147	0.112	.15907
0.0009	0.2703	0.3349	7.1408	0.00137	0.00065	40.731	19.282	-0.0003	1736.923	0.126	.17870
0.0010	0.2991	0.3357	7.1476	0.00152	0.00072	45.185	21.433	-0.0007	1926.366	0.140	.19819
0.0011	0.3273	0.3367	7.1560	0.00167	0.00079	49.607	23.587	-0.0000	2114.262	0.154	.21752
0.0012	0.3548	0.3378	7.1659	0.00181	0.00087	53.992	25.745	-0.0008	2300.391	0.167	.23667
0.0013	0.3816	0.3390	7.1773	0.00196	0.00094	58.337	27.907	-0.0007	2484.566	0.181	.25561
0.0014	0.4076	0.3404	6.7677	0.00232	0.00099	60.000	29.351	0.0002	2566.884	0.207	.26408
0.0015	0.4328	0.3419	6.1927	0.00286	0.00102	60.000	30.223	0.0002	2582.589	0.242	.26570
0.0016	0.4570	0.3435	5.7183	0.00344	0.00104	60.000	30.962	0.0005	2594.820	0.280	.26696
0.0017	0.4804	0.3452	5.3238	0.00405	0.00106	60.000	31.586	0.0009	2604.455	0.319	.26795

0.0018	0.5027	0.3471	4.9930	0.00469	0.00108	60.000	32.111	0.0005	2612.123	0.361	.26874
0.0019	0.5241	0.3490	4.7137	0.00536	0.00109	60.000	32.552	0.0002	2618.300	0.403	.26937
0.0020	0.5444	0.3511	4.4760	0.00604	0.00111	60.000	32.925	0.0002	2623.331	0.447	.26989
0.0021	0.5637	0.3532	4.2724	0.00675	0.00112	60.000	33.241	0.0001	2627.459	0.492	.27031
0.0022	0.5819	0.3555	4.0968	0.00747	0.00113	60.000	33.510	0.0007	2630.888	0.537	.27067
0.0023	0.5992	0.3578	3.9444	0.00820	0.00113	60.000	33.741	0.0007	2633.734	0.583	.27096
0.0024	0.6153	0.3603	3.8112	0.00893	0.00114	60.000	33.943	0.0	2636.103	0.630	.27120
0.0025	0.6305	0.3628	3.7269	0.00957	0.00116	60.581	34.474	0.0007	2662.787	0.671	.27395
0.0026	0.6446	0.3654	3.6612	0.01018	0.00118	61.330	35.108	0.0009	2696.368	0.710	.27740
0.0027	0.6578	0.3680	3.6030	0.01079	0.00120	62.081	35.749	0.0003	2729.813	0.749	.28084
0.0028	0.6699	0.3708	3.5513	0.01139	0.00122	62.831	36.400	0.0007	2763.073	0.788	.28427
0.0029	0.6808	0.3738	3.5055	0.01199	0.00125	63.580	37.065	0.0004	2796.031	0.827	.28766
0.0030	0.6905	0.3769	3.4647	0.01259	0.00127	64.325	37.744	0.0007	2828.693	0.866	.29102
0.0031	0.6992	0.3801	3.4283	0.01318	0.00129	65.068	38.436	0.0007	2861.065	0.904	.29435
0.0032	0.7068	0.3835	3.3956	0.01376	0.00132	65.808	39.140	0.0001	2893.171	0.942	.29765
0.0033	0.7136	0.3668	3.3660	0.01435	0.00134	66.545	39.856	0.0009	2925.067	0.980	.30093
0.0034	0.7196	0.3902	3.3392	0.01493	0.00136	67.280	40.580	0.0009	2956.751	1.018	.30419
0.0035	0.7250	0.3936	3.3147	0.01551	0.00139	68.012	41.312	0.0009	2988.251	1.056	.30743
0.0036	0.7297	0.3970	3.2922	0.01608	0.00141	68.741	42.050	0.0005	3019.582	1.094	.31066
0.0037	0.7338	0.4002	3.2714	0.01666	0.00144	69.468	42.794	0.0003	3050.761	1.131	.31386
0.0038	0.7375	0.4035	3.2522	0.01723	0.00146	70.192	43.543	0.0002	3081.800	1.168	.31706
0.0039	0.7407	0.4066	3.2344	0.01780	0.00149	70.914	44.294	0.0007	3112.706	1.206	.32024
0.0040	0.7436	0.4097	3.2177	0.01838	0.00151	71.633	45.049	0.0009	3143.472	1.243	.32340
0.0041	0.7461	0.4127	3.2021	0.01895	0.00154	72.349	45.805	0.0005	3174.097	1.280	.32655
0.0042	0.7483	0.4156	3.1874	0.01952	0.00156	73.062	46.562	0.0004	3204.590	1.318	.32969
0.0043	0.7502	0.4185	3.1735	0.02009	0.00159	73.772	47.320	0.0003	3234.945	1.355	.33281
0.0044	0.7518	0.4212	3.1604	0.02066	0.00162	74.479	48.078	0.0006	3265.161	1.392	.33592
0.0045	0.7533	0.4239	3.1479	0.02123	0.00164	75.182	48.835	0.0006	3295.223	1.430	.33901
0.0046	0.7545	0.4265	3.1360	0.02180	0.00167	75.882	49.590	0.0009	3325.135	1.467	.34209
0.0047	0.7556	0.4290	3.1247	0.02237	0.00169	76.578	50.344	0.0004	3354.875	1.504	.34515

0.0048	0.7565	0.4314	3.1138	0.02295	0.00172	77.270	51.096	0.0002	3384.449	1.542	.34819
0.0049	0.7573	0.4338	3.1034	0.02352	0.00174	77.957	51.846	0.0009	3413.855	1.579	.35122
0.0050	0.7579	0.4360	3.0933	0.02410	0.00177	78.640	52.592	0.0005	3443.061	1.616	.35422
0.0051	0.7584	0.4382	3.0836	0.02467	0.00179	79.318	53.335	0.0005	3472.073	1.654	.35721
0.0052	0.7588	0.4404	3.0742	0.02525	0.00182	79.992	54.074	0.0010	3500.887	1.692	.36017
0.0053	0.7591	0.4424	3.0651	0.02582	0.00184	80.660	54.808	0.0004	3529.470	1.729	.36311
0.0054	0.7593	0.4444	3.0562	0.02640	0.00187	81.323	55.539	0.0006	3557.838	1.767	.36603
0.0055	0.7594	0.4463	3.0476	0.02698	0.00189	81.980	56.264	0.0004	3585.964	1.805	.36893
0.0056	0.7595	0.4482	3.0392	0.02757	0.00191	82.631	56.984	0.0010	3613.852	1.843	.37180
0.0057	0.7595	0.4500	3.0310	0.02815	0.00194	83.276	57.699	0.0007	3641.472	1.881	.37464
0.0058	0.7594	0.4518	3.0229	0.02874	0.00196	83.915	58.408	0.0003	3668.824	1.919	.37745
0.0059	0.7593	0.4534	3.0150	0.02932	0.00199	84.547	59.111	0.0010	3695.910	1.957	.38024
0.0060	0.7591	0.4551	3.0073	0.02991	0.00201	85.172	59.807	0.0005	3722.691	1.995	.38299

AT YIELDING OF REINFORCEMENT

EU = 0.00134
XM(K-IN) = 2555.048
CURV(.001/IN)= 0.186355

AT ULTIMATE

EU = 0.00600
XM(K-IN) = 3722.691
CURV(.001/IN)= 1.995175
DUCTILITY FACTOR= 10.7063

ACI CODE MOMENT FOR UNDERREINFORCED BEAM

ANALYSIS RESULTS

EU	ALPHA	BETA	C(INS)	ES	ESP	FS(KSI)	FSP(KSI)	XP(KIP)	XM(K-IN)	CURV(.001/IN)	XM/FOBDD
AT YIELDING OF REINFORCEMENT											
0.0013	0.5000	0.3333	7.1477	0.00202	0.00096	60.000	28.461	0.0	2559.418	0.186	.26331
AT ULTIMATE											
0.0030	0.7650	0.4500	3.1739	0.01401	0.00111	66.124	33.022	0.0	2633.642	0.945	.27095

DUCTILITY FACTOR= 5.0878

APPENDIX II

COMPUTER PROGRAM FOR NONLINEAR ANALYSIS OF UNIAXIALLY LOADED COLUMNS

```
RELEASE 2.0              MAIN                DATE = 77111          16/24/23

  CCC
  CCC    COLUMN....AXIAL LOAD PLUS UNIAXIAL BENDING (Appendix 2)
  CCC    REINFORCEMENT ALONG TWO FACES ONLY
  CCC
        DIMENSION FF(900),EE(900),XALPHA(900),XBETA(900),BXP(100),BXM(100)
       1  ,BCURV(100),BC(100),HXP(100),HXM(100),HCURV(100),HC(100),
       2  BEU(100)
        XPA(A)=0.85*FO*B*A+ASP*FSP-AS*FS
        XMA(A )=0.85*FO*B*A*(H/2.-A/2.)+ASP*FSP*(H/2.-DPP)+
       1  AS*FS*(D-H/2.)
        XPB(FS)=0.85*FO*B*A+ASP*FY +AS*FS
        XMB(FS)=(ASP*FY-AS*FS)*(H/2.-DPP)
    105 READ(5,240) JOB
    240 FORMAT(I5)
        IF(JOB.EQ.0) STOP
        WRITE(6,250)  JOB
    250 FORMAT(////' COLUMN NO.',I5//' UNIAXIAL BENDING'//)
  CCC   READ PARAMETERS OF CONCRETE STRESS-STRAIN CURVE
  CCC   FO=PEAK STRESS IN CONCRETE, KSI
  CCC   FY=YIELD STRESS IN STEEL, KSI
  CCC   ICONC=2....NORMAL WEIGHT
  CCC   ICONC=1....LIGHTWEIGHT
        READ(5,111) FO,FY,ICONC
    111 FORMAT(2F10.4,I5)
        READ(5,222) B,D,H, AS, ASP,DPP
    222 FORMAT(6F10.4)
        DP=H-D
        PAS=AS/(B*D)
        PASP=ASP/(B*D)
        WRITE(6,666)
    666 FORMAT(/4X,1HB,12X,1HD,12X,1HH,12X,3HDPP,10X,
       1    3HPAS,10X,4HPASP,9X,2HAS,11X,3HASP,10X,2HFO,11X,2HFY/)
        WRITE(6,777) B,D,H,DPP,PAS,PASP,AS,ASP,FO,FY
    777 FORMAT(10(F10.4,3X))
  CCC
  CCC   COMPUTE CONCRETE PROPERTIES
  CCC
        CALL ALPBET(FO,EO,FF,EE,XALPHA,XBETA,DE,ICONC,EMC)
  CCC
        ES=EO
        CALL STEELA(FS,ES,FY,EMI)
  CCC
        PMAX=FO*(B*H-AS-ASP)+FS*(AS+ASP)
        WRITE(6,999)  PMAX
    999 FORMAT(///' MAX. AXIAL LOAD(KIPS)=',F12.3/)
        ETS=0.001
        ETS=0.01
  CCC
        DO 600 II=1,20
  CCC
        FACTOR=0.05*(II-1)
        PFIX=PMAX*FACTOR
        WRITE(6,888)  PFIX
    888 FORMAT(//' AXIAL LOAD(KIPS)      =',F12.3//)
        WRITE(6,551) FACTOR
    551 FORMAT(/' FACTOR OF LOAD        =',F5.2//)
        WRITE(6,444)
    444 FORMAT(///4X,' EU',7X,' ALPHA',5X,' BETA', 6X,' C(INS)',4X,
       1   ' ES',8X,' ESP',6X, ' FS(KSI)',3X,' FSP(KSI)',1X,' XP(KIPS)',
```

```
     2  2X,' XM(K-IN)',1X,' CURV(.001/IN)',//)
  333 FORMAT(4(F10.4,1X),2(F10.5,1X),5(F10.3,1X)/)
      TXM=0.
      CPREV=0.4*D
CCC
      DO 300 I=10,60
CCC
      EU=0.0001*I
      AN=EU/DE
      AAN=AN+0.5
      N=AAN
      N1=N+1
      ALPHA=XALPHA(N)
      BETA=XBETA(N)
      FU=FF(N1)
     .ES=EU
      CALL STEELA(FS,ES,FY,EMI)
      PMAX1=FU*(B*H-AS-ASP)+FS*(AS+ASP)
      IF(EU-E0) 410,410,420
  410 IF(PMAX1.LT. PFIX) GO TO 290
  420 CONTINUE
CCC
CCC   TRY NEUTUAL AXIS, C
CCC
      C=CPREV
      DELTA=0.1
      YKK=1000.
  310 C=C+DELTA
      GO TO 370
  320 C=C-DELTA
  370 CONTINUE
      IF(C.GT. D) GO TO 1000
      ES=EU*((D-C)/C)
      ESP=EU*((C-DPP)/C)
      CALL STEELA(FS,ES,FY,EMI)
      CALL STEELA(FSP,ESP,FY,EMI)
      XP=ALPHA*F0*B*C+ASP*FSP-AS*FS
      IF(YKK.EQ. 1000.) GO TO 380
      AXP=XP-PFIX
      AXPP=XPP-PFIX
      IF((ABS(AXP)+ABS(AXPP)).NE. ABS(AXP+AXPP)) GO TO 270
  380 XPP=XP
      XCC=C
      YKK=2000.
      IF(ABS(XP-PFIX).LT. ETS ) GO TO 330
      IF(XP-PFIX) 310,330,320
  270 DELTA=ABS(0.1*(C-XCC))
      C=(C+XCC)/2.
      GO TO 310
  330 CONTINUE
CCC   XM= MOMENT ABOUT CENTER OF SECTION
  400 XM=ALPHA*F0*B*C*(H/2.-BETA*C)+ASP*FSP*(H/2.-DPP)+AS*FS*(D-H/2.)
      CURV=EU/C
      CURV=CURV*1000.
      WRITE(6,333) EU,ALPHA,BETA,C,ES,ESP,FS,FSP,XP,XM,CURV
      GO TO 290
CCC
CCC   C GREATER THAN D
CCC
 1000 CONTINUE
      ES=0.
```

```
      DELTA=0.05*EU
      YKK=1000.
      GO TO 1340
 1310 ES=ES+DELTA
      GO TO 1340
 1320 ES=ES-DELTA
 1340 CONTINUE
      IF(ES-EU) 1440,1450,290
 1440 CONTINUE
      IF(ES.LT. 0.) GO TO 290
      C=D*(EU/(EU-ES))
      ESP=EU*((C-DPP)/C)
      EFB=EU*((C-H)/C)
CCC   EFB= STRAIN AT FACE OF LESS COMPRESSION
      GO TO 1490
 1450 ESP=EU
      EFB=EU
 1490 CONTINUE
      CALL STEELA(FS,ES,FY,EMI)
      CALL STEELA(FSP,ESP,FY,EMI)
      IF(C.GT. H) GO TO 1350
      ALPHAT=0.
      BETAT=0.
      GO TO 1360
 1350 CONTINUE
      AN=EFB/DE
      AAN=AN+0.5
      N=AAN
      N1=N+1
      FFB=FF(N1)
      ALPHAT=XALPHA(N)
      BETAT=XBETA(N)
 1360 CONTINUE
      XP=ALPHA*FO*B*C+ASP*FSP+AS*FS-ALPHAT*FO*B*(C-H)
      AXP=XP-PFIX
      AXPP=XPP-PFIX
      IF(YKK.EQ. 1000.) GO TO 1380
      IF((ABS(AXP)+ABS(AXPP)).NE. ABS(AXP+AXPP)) GO TO 1270
 1380 XPP=XP
      YKK=2000.
      IF(ABS(XP-PFIX).LT. ETS ) GO TO 1330
      IF(XP-PFIX) 1310,1330,1320
 1270 ES=ES-DELTA
      DELTA=DELTA/10.
      IF(DELTA.LT.0.00000001) GO TO 1400
      GO TO 1310
 1330 CONTINUE
CCC   XM= MOMENT ABOUT CENTER OF SECTION
 1400 XM=ALPHA*FO*B*C*(H/2.-BETA*C)+ASP*FSP*(H/2.-DPP)-AS*FS*(H/2.-DP)
     1   +ALPHAT*FO*B*(C-H)*(BETAT*(C-H)+H/2.)
      CURV=EU/C
      CURV=CURV*1000.
      WRITE(6,333) EU,ALPHA,BETA,C,ES,ESP,FS,FSP,XP,XM,CURV
  290 CONTINUE
      IF(XM-TXM) 2100,2100,2200
 2200 TXM=XM
      TCURV=CURV
      TC=C
      TEU=EU
 2100 CONTINUE
  300 CONTINUE
```

```
      BXM(II)=TXM
      BXP(II)= PFIX
      BCURV(II)=TCURV
      BEU(II)=TEU
      BC(II)=TC
  600 CONTINUE
      NPTS=II+1
      N1=NPTS
      BXM(N1)=0.
      BXP(N1)= PMAX
      WRITE(6,2222)
      DO 2300 II=1,N1
      WRITE(6,2111) BXP(II),BXM(II),BCURV(II),BEU(II),BC(II)
 2300 CONTINUE
 2222 FORMAT(//' INTERACTION CURVE'//' AXIAL LOAD(KIPS)',2X,
     1   ' MOMENT(KIP-INS)',2X,' CURV(.001/IN)',5X,' EU',6X,' C(IN)'/)
 2111 FORMAT(2(5X,F10.3),6X,F10.4,4X,F10.4,2X,F10.4/)
CCC
CCC   ACI INTERACTION DIAGRAM
CCC
CCC   MAXIMUM CONCENTRIC LOAD
CCC
      POP=0.85*FO*(B*H-AS-ASP)+FY*(AS+ASP)
      DP=H-D
      EU=0.003
      BT1=0.85-0.05*(FO/1000.-4.)
      EMIEU=EMI*EU
      PBAL=(0.85*BT1*FO/FY)*(EMIEU /(EMIEU +FY))
      EY=FY/EMI
CCC
CCC   BALANCED CONTION
CCC
      C=D*(EU/(EU+EY))
      A=C*BT1
      FS=FY
      ESP=EU*((C-DPP)/C)
      IF(ESP.LT.EY) GO TO 3100
      FSP=FY
      GO TO 3200
 3100 FSP=ESP*EMI
 3200 CONTINUE
      XPBAL=XPA(A)
      XMBAL=XMA(A)
      ECCBAL=XMBAL/XPBAL
      CURBAL=(EU/C)*1000.
      CBAL=C
CCC
CCC   N.A. LOCATED AT TENSSION STEEL
CCC
      C=D
      A=C*BT1
      FSP=FY
      H2=H/2.
      C1=0.85*FO*B*A
      C2=ASP*FY
      XP1=C1+C2
      XM1=C1*(H2-A/2.)+C2*(H2-DPP)
      CNA1=C
      CURV1=(EU/C)*1000.
CCC
CCC   N.A. LOCATED AT FACE OF CONCRETE
```

```
CCC
      C=H
      A=C*BT1
      FSP=FY
      ES=EU*(DP/H)
      FS=ES*EMI
      C1=0.85*F0*B*A
      C2=ASP*FY
      C3=AS*FS
      XP2=C1+C2+C3
      XM2=C1*(H2-A/2.)+C2*(H2-DPP)-C3*(H2-DP)
      CNA2=C
      CURV2=(EU/C)*1000.
CCC
CCC   N.A. LOCATED OUTSIDE OF SECTION, DEPTH OF STRESS BLOCK EQUAL TO H
CCC
      A=H
      C=H/BT1
      ES=EU*((C-D)/C)
      IF(ES-EY) 5110,5110,5120
 5110 FS=ES*EMI
      GO TO 5130
 5120 FS=FY
 5130 CONTINUE
      C1=0.85*F0*B*A
      C2=ASP*FY
      C3=AS*FS
      XP3=C1+C2+C3
      XM3=C1*(H2-A/2.)+C2*(H2-DPP)-C3*(H2-DP)
      CNA3=C
      CURV3=(EU/C)*1000.
CCC
CCC   PURE BENDING FOR DOUBLE REINFORCED SECTION
CCC
      PMAX=0.75*(PBAL+PASP)
      PMIN=PASP+0.85*BT1*(F0/FY)*(DPP/D)*(EMIEU /(EMIEU -FY))
      IF(PAS-PMAX) 2230,2230,2240
 2240 WRITE(6,2250)
      GO TO 5900
 2230 CONTINUE
      IF(PAS-PMIN) 2210,2220,2220
 2220 CONTINUE
CCC
CCC   COMPRESSION STEEL YIELD
CCC
      A=(AS-ASP)*FY/(0.85*F0*B)
      C=A/BT1
      XM=ASP*FY*(D-DPP)+(AS-ASP)*FY*(D-A/2.)
      XP=0.
      GO TO 2270
 2210 CONTINUE
CCC
CCC   COMPRESSION STEEL NOT YIELD
CCC   DETERMINE N.A. BY QUADRATIC EQUATION
CCC
      AA=0.85*BT1*F0*B
      BB=ASP*EU*EMI-AS*FY
      CC=ASP*EU*EMI*DPP
      ROOT2=BB*BB+4.*AA*CC
      ROOT=ROOT2**0.5
      C=(-BB+ROOT)/(2.*AA)
```

```
      A=C*BT1
      IF(C.LT. DPP) GO TO 2260
      FSP=EMI*EU*(C-DPP)/C
      FS=FY
      XM=XMA(A)
      XP=0.
      GO TO 2270
 2260 CONTINUE
CCC
CCC   ASSUME COMPRESSION STEEL NOT EXIST
CCC
      A=(AS*FY)/(0.85*FO*B)
      C=A/BT1
      XM=AS*FY*(D-A/2.)
      XP=0.
 2270 CONTINUE
      XMBD=XM
      XPBD=XP
      CNABD=C
      CURVBD=(EU/C)*1000.
 2250 FORMAT(//' OVERREINFORCED BEAM----NO SOLUTION'//)
      HXP( 1)=0.
      HXM( 1)= XMBD
      HCURV( 1)=CURVBD
      HC(1)=CNABD
      HXP(21)=POP
      HXM(21)=0.
      HCURV(21)=0.
      HC(21)=99999.
CCC
      DO 6000 II=2,20
CCC
      FACTOR=0.05*(II-1)
      PFIX=POP*FACTOR
      HXP(II)=PFIX
      IF(PFIX.LT. XPBAL) GO TO 5000
      IF(PFIX.GT. XPBAL) GO TO 5100
 5000 CONTINUE
      FS=FY
      FSP=FY
      A=(PFIX-ASP*FSP+AS*FS)/(0.85*FO*B)
      C=A/BT1
      HXM(II)=XMA(A)
      HCURV(II)=(EU/C)*1000.
      HC(II)=C
      GO TO 5900
 5100 CONTINUE
CCC
CCC   FAILURE BY COMPRESSION OF CONCRETE
CCC
      IF(PFIX.LT. XP1) GO TO 5200
      IF(PFIX.LT. XP2) GO TO 5300
      IF(PFIX.LT. XP3) GO TO 5400
      IF(PFIX.GT. XP3) GO TO 5500
 5200 CONTINUE
CCC
CCC   LOCATE N.A.
CCC
      AA=0.85*BT1*FO*B
      BB=ASP*FY+AS*EU*EMI-PFIX
      CC=AS*EU*EMI*D
```

```
      ROOT2=BB*BB+4.*AA*CC
      ROOT=ROOT2**0.5
      C=(-BB+ROOT)/(2.*AA)
      A=C*BT1
      FSP=FY
      ES=EU*((D-C)/C)
      FS=ES*EMI
      HXM(II)=XMA(A)
      HCURV(II)=(EU/C)*1000.
      HC(II)=C
      GO TO 5900
 5300 CONTINUE
      RR=(PFIX-XP1)/(XP2-XP1)
      HXM(II)=XM1+(XM2-XM1)*RR
      C=CNA1+(CNA2-CNA1)*RR
      HCURV(II)=(EU/C)*1000.
      HC(II)=C
      GO TO 5900
 5400 CONTINUE
      RR=(PFIX-XP2)/(XP3-XP2)
      HXM(II)=XM2+(XM3-XM2)*RR
      C=H+(CNA3-CNA2)*RR
      HCURV(II)=(EU/C)*1000.
      HC(II)=C
      GO TO 5900
 5500 CONTINUE
      ASFS=PFIX-0.85*FO*B*H-ASP*FY
      HXM(II)=ASP*FY*(H2-DPP)-ASFS*(H2-DP)
      FS=ASFS/AS
      ES=FS/EMI
      C=D*(EU/(EU-ES))
      HCURV(II)=(EU/C)*1000.
      HC(II)=C
      GO TO 5900
 5900 CONTINUE
 6000 CONTINUE
      WRITE(6,6200)
 6200 FORMAT(//' ACI CODE'//)
      WRITE(6,2222)
      DO 6300 II=1,21
      WRITE(6,2111) HXP(II),HXM(II),HCURV(II), EU     ,HC(II)
 6300 CONTINUE
      WRITE(6,6400)
 6400 FORMAT(//' BALANCED CONDITION'/)
      WRITE(6,2111) XPBAL,XMBAL,CURBAL,EU,CBAL
      WRITE(6,6500)
 6500 FORMAT(/' N.A. LOCATED AT TENSION STEEL'/)
      WRITE(6,2111) XP1,XM1,CURV1,EU,CNA1
      WRITE(6,6600)
 6600 FORMAT(/' N.A. LOCATED AT FACE OF CONCRETE'/)
      WRITE(6,2111) XP2,XM2,CURV2,EU,CNA2
      WRITE(6,6700)
 6700 FORMAT(/' DEPTH OF STRESS BLOCK EQUAL TO H'/)
      WRITE(6,2111) XP3,XM3,CURV3,EU,CNA3
CCC
      CALL PLOTER(BXP,BXM,NPTS,B,D,H,AS,ASP,FO,FY,JOB,ICONC,HXP,HXM)
CCC
      GO TO 105
      END
```

COLUMN NO.

UNIAXIAL BENDING

B	D	H	DPP	PAS	PASP
10.0000	8.0000	10.0000	2.0000	0.0150	0.0150

AS	ASP	FO	FY
1.2000	1.2000	9.0000	60.0000

INTERACTION CURVE

AXIAL LOAD(KIPS)	MOMENT(KIP-INS)	CURV(.001/IN)	EU	C(IN)
0.0	642.095	2.9475	0.0054	1.8320
51.120	772.150	2.3380	0.0049	2.0958
102.240	904.693	1.8655	0.0046	2.4658
153.360	1049.393	1.3143	0.0040	3.0434
204.480	1186.809	1.0943	0.0040	3.6554
255.600	1299.827	0.9105	0.0040	4.3932
306.720	1374.959	0.7587	0.0040	5.2719
357.840	1353.922	0.7241	0.0042	5.8002
408.960	1315.765	0.6431	0.0041	6.3755
460.080	1271.219	0.5874	0.0041	6.9799
511.200	1216.367	0.5224	0.0040	7.6573
562.320	1147.709	0.4801	0.0040	8.3312
613.439	1061.768	0.4430	0.0040	9.0300
664.560	956.182	0.4102	0.0040	9.7502
715.679	834.406	0.3671	0.0039	10.6243
766.800	709.886	0.3371	0.0039	11.5695
817.919	582.224	0.2929	0.0038	12.9755
869.039	453.228	0.2608	0.0038	14.5707
920.159	322.995	0.2132	0.0037	17.3561
971.279	188.496	0.1678	0.0037	22.0533
1022.399	0.0	0.0	0.0	0.0

ACI CODE

INTERACTION CURVE

AXIAL LOAD(KIPS)	MOMENT(KIP-INS)	CURV(.001/IN)	EU	C(IN)
0.0	542.117	3.3454	0.0030	0.8967
44.532	641.698	5.4090	0.0030	0.5546
89.064	825.473	2.7045	0.0030	1.1093
133.596	983.326	1.8030	0.0030	1.6639
178.128	1115.256	1.3522	0.0030	2.2185
222.660	1221.263	1.0818	0.0030	2.7732
267.192	1301.347	0.9015	0.0030	3.3278
311.724	1355.508	0.7727	0.0030	3.8824
356.256	1383.747	0.6761	0.0030	4.4371
400.788	1369.766	0.6099	0.0030	4.9192
445.320	1319.650	0.5645	0.0030	5.3146
489.852	1259.037	0.5239	0.0030	5.7267
534.384	1185.975	0.4875	0.0030	6.1537
578.916	1098.707	0.4550	0.0030	6.5941
623.448	995.676	0.4258	0.0030	7.0463
667.979	875.518	0.3995	0.0030	7.5089
712.511	737.057	0.3759	0.0030	7.9806
757.043	548.271	0.3542	0.0030	8.4702
801.575	357.773	0.3348	0.0030	8.9603
846.107	167.275	0.3174	0.0030	9.4505
890.639	0.0	0.0	0.0030	99999.0000

BALANCED CONDITION

371.271	1355.999	0.6305	0.0030	4.7580

N.A. LOCATED AT TENSION STEEL

714.323	731.017	0.3750	0.0030	8.0000

N.A. LOCATED AT FACE OF CONCRETE

896.038	-46.316	0.3000	0.0030	10.0000

DEPTH OF STRESS BLOCK EQUAL TO H

853.944	165.165	0.3149	0.0030	9.5279

APPENDIX III

COMPUTER PROGRAM FOR NONLINEAR ANALYSIS OF BIAXIALLY LOADED COLUMNS

```
RELEASE 2.0                MAIN                DATE = 77113          15/02/53

  CCC
  CCC    COLUMN--BIAXIAL BENDING (Appendix 3)
  CCC
        DIMENSION BXP(100),BXM(100),BCURV(100),BEU(100),BC(100)
        DIMENSION AS(50),XS(50),YS(50),DISTS(50),CS(50),XMS(50),YMS(50),
       1  FS(50),ES(50),SIGN(50),
       2  XELE(1000),YELE(1000),DISTE(1000),NENA(1000),EC(1000),EC(1000),
       3  CC(1000),XMC(1000),YMC(1000),XELA(1000),YELA(1000),DISTA(1000)
  CCC
        DISTAN(X,Y)=(Y-SLP*X-YB )/((1.+SLP*SLP)**0.5)
  CCC
    105 READ(5,112) JOB
        IF(JOB.EQ.0) STOP
        WRITE(6,221)  JOB
    221 FORMAT(///' COLUMN NO.=',I5//' BIAXIAL BENDING'//)
  CCC
  CCC    FC=CONCRETE PEAK STRESS(KSI), FY=STEEL YIELD STRE(KSI)
  CCC    H=LENGTH IN X-DIRECTION, B=WIDTH IN Y-DIRECTION
  CCC
        RAD=0.01745329
        DEG=57.29577951
        READ(5,111) FC,FY
    111 FORMAT(8F10.4)
        READ(5,111) H,B
        READ(5,112) NBAR
    112 FORMAT(I5)
        ASTOL=0.
  CCC    ASTOL=TOTAL AREA OF REINFORCEMENT, PAS=RATIO OF REINFORCEMENT
        DO 100 I=1,NBAR
        READ(5,111) AS(I),XS(I),YS(I)
        ASTOL=ASTOL+AS(I)
    100 CONTINUE
        PAS=ASTOL/(B*H)
        READ(5,111) THETA
  CCC
  CCC    END OF INPUT DATA
  CCC    ECC=ECCENTRICITY(INCH), THETA=ANGLE FROM X-AXIS(DEGREE)
  CCC    THETAR=THETA IN RADIAN
  CCC    RMXY=RATIO OF ECCENTRICITY=ECCY/ECCX
  CCC
        THETAR=THETA*0.01745329
        IF(THETA.EQ. 0.) GO TO 102
        IF(THETA.EQ.90.) GO TO 102
        RMXY=TAN(THETAR)
        SLPRA=-1./RMXY
    102 CONTINUE
  CCC
  CCC    CONCRETE PROPERTIES
  CCC
        ECA=0.001
        CALL CONCRE(ECA,ECA,FC,EC)
  CCC
  CCC    STEEL PROPERTIES
  CCC
        ESA=0.001
        CALL STEELA(FSA,FSA,FY,EY)
        WRITE(6,222) B,H,ASTOL,PAS,FC,EC,FY,EY
    222 FORMAT(/' SECTION PROPERTIES'//
       1  5X,5HB(IN),6X,5HH(IN),4X,9HAS(SQ.IN),5X,3HPAS,4X,7HFC(KSI),
```

```
     2 7X,2HFO,6X,7HFY(KSI),7X,2HFY//
     3 5(F10.3,1X),F10.5,1X,F10.3,1X,F10.5/)
       WRITE(6,223)
  223 FORMAT(/' ARRANGEMENT OF REINFORCING BARS( ORIGIN AT CENTER OF SE
     1CTION)'//1X,7HBAR NO.,3X,9HAS(SQ.IN),3X,5HX(IN),6X,5HY(IN)//)
       DO 101 I=1,NBAR
       WRITE(6,224) I,AS(I),XS(I),YS(I)
  101 CONTINUE
  224 FORMAT(I5,3X,3(F10.3,1X)/)
       WRITE(6,225) THETA,THETAR
  225 FORMAT(/' LOCATION OF APPLIED LOADING'//
     1       ' THETA                (DEGREE)=',F10.5//
     2  ' THETAR              (RADIAN)=',F10.5/)
CCC
CCC    ELEMENT PROPERTIES
CCC    DES=DIMENSION OF ELEMENT SQUARE(INCH)
CCC    NEX=NOS. OF ELEMENT IN X-DIRECTION
CCC    NEY=NOS. OF ELEMENT IN Y-DIRECTION
CCC    AELE=AREA OF EACH ELEMENT
CCC    NTELE=NOS. OF TOTAL ELEMENTS
CCC    XELE=X-COORDINATE OF ELEMENT
CCC    YELE=Y-COORDINATE OF ELEMENT
CCC
       DES=0.5
       NEX=H/DES
       NEY=B/DES
       AELE=DES*DES
       NTELE=NEX*NEY
       WRITE(6,228) NTELE,NEX,NEY,AELE,DES
  228 FORMAT(/' ELEMENTS PROPERTIES' //' TOTAL NOS. OF ELEMENTS=',I5//
     1  ' NOS. OF ELEMENTS IN X-DIRECTION=',I5//
     2  ' NOS. OF ELEMENTS IN Y-DIRECTION=',I5//
     3  ' AREA OF SQUARE ELEMENT(SQ.IN)=',F10.4//
     4  ' WIDTH OF SQUARE ELEMENT(IN)  =',F10.4//)
CCC
CCC    X-Y COORDINATES OF EACH ELEMENT
CCC    XELA(I),YELA(I),DISTA(I)....NUMBERING IN ORIGINAL SYSTEM
CCC    XELE(I),YELE(I),DISTE(I)....NUMBERING IN NEW      SYSTEM
CCC
       DO 110 J=1,NEY
       NEXJ1=NEX*(J-1)
       DO 118 I=1,NEX
       K=NEXJ1+I
       YELA(K)=B/2.+DES/2.-DES*J
       XELA(K)=H/2.+DES/2.-DES*I
  118 CONTINUE
  110 CONTINUE
CCC
       PMAX=FO*(B*H-ASTOL)+FY*ASTOL
       WRITE(6,999)  PMAX
  999 FORMAT(///' MAX. AXIAL LOAD(KIPS)=',F12.3/)
       DDT=0.1
       IST=3
       LST=4
CCC
       DO 600 II=IST,LST
CCC
       FACTOR=DDT*(II-1)
       PFIX=PMAX*FACTOR
       IF(PFIX.EQ.PMAX) GO TO 700
       IF(PFIX.GT.PMAX) GO TO 700
```

```
      WRITE(6,888)  PFIX
  888 FORMAT(//' AXIAL LOAD(KIPS)      =',F12.3//)
      WRITE(6,551) FACTOR
  551 FORMAT(/' FACTOR OF LOAD         =',F5.2//)
      WRITE(6,226)
  226 FORMAT(/' ANALYSIS RESULT'//5X,2HEU,8X,6HP(KIP),3X,10HTMOM(K-IN),
     1   3X,     7HYB (IN),4X,8H XB (IN)   , 4X,3HSLP   ,4X,11HANGNA (DEG),
     2   3X,8H C   (IN),3X,6HTHETAT,5X,13HCURV(.001/IN)//)
CCC
      SLPP=SLPRA
      XBP=0.
      YBP=0.
      DELTAP=0.5+(FACTOR*6.)**2
CCC
      DO 5000 IJK=15,60
CCC
      EU=0.0001*IJK
      IF(FACTOR.GT.0.70 .AND. EU.LT.0.0025) GO TO 4900
      IF(FACTOR.GT.0.50 .AND. EU.LT.0.0020) GO TO 4900
      YKK=1000.
      CALL CONCRE(FU,EU,FO,EO)
      ESA=EU
      CALL STEELA(FSA,ESA,FY,EMI)
      PMAX1=FU*(B*H-ASTOL )+FSA*(ASTOL )
      IF(EU-EO) 611,611,622
  611 IF(PMAX1.LT. PFIX) GO TO 4900
  622 CONTINUE
CCC
CCC   TRY A NEUTRAL AXIS
CCC   N.A.......Y=SLP*X-YB=0
CCC   SLP=SLOPE OF NEUTRAL AXIS
CCC   YB=INTERSECTION ON Y-AXIS WITH N.A.
CCC   RNA=PERPENDICULAR DISTANCE FROM LOADING POSITION TO N.A.
CCC   STARTING VALUE FOR TRIAL OF NEUTRAL AXIS
CCC
      SLP=SLPP
      XB=XBP
      YB=YBP
      DELTA =DELTAP
CCC
CCC
 1000 CONTINUE
CCC
CCC
CCC   COUNTER THE ELEMENTS ABOUT NEUTRAL AXIS
CCC   DISTANCE FROM EACH ELEMENT TO NEUTRAL AXIS
CCC
      IF(THETA.EQ. 0.) GO TO 131
      IF(THETA.EQ.90.) GO TO 132
      DO 120 I=1,NTELE
      X=XELA(I)
      Y=YELA(I)
      DISTA(I)=DISTAN(X,Y)
  120 CONTINUE
      GO TO 135
  131 DO 121 I=1,NTELE
      X=XELA(I)
      DISTA(I)=X-XB
  121 CONTINUE
      GO TO 135
  132 DO 122 I=1,NTELE
```

```
      Y=YELA(I)
      DISTA(I)=Y-YB
  122 CONTINUE
  135 CONTINUE
CCC
CCC   NENA(I)=NOS. OF ELEMENTS ABOVE N.A. IN EACH ROW,(I=1,NEY)
CCC   DISTA(I)=+ ....ABOVE N.A.
CCC   DISTA(I)=- ....BELOW N.A.
CCC   NENAT=TOTAL NUMBER OF ELEMENTS ABOVE N.A.
CCC
      NENAT=0
      DO 170 J=1,NEY
      NENA(J)=0
      DO 140 I=1,NEX
      NEXJ1=NEX*(J-1)
      K=NEXJ1+I
      IF(DISTA(K)) 150,150,160
  150 INDEX=0
      GO TO 170
  160 INDEX=1
  170 NENA(J)=NENA(J)+INDEX
  140 CONTINUE
      NENAT=NENAT+NENA(J)
      IF(NENA(J).EQ. 0) GO TO 180
  130 CONTINUE
      GO TO 190
  180 IROW=J-1
      GO TO 191
  190 IROW=NEY
  191 CONTINUE
CCC
CCC   NUMBERING THE ELEMENTS ABOVE N.A. IN SEQUENCE
CCC   KAA=NUMBERING IN ORIGINAL, KBB=NUMBERING IN NEW SEQUENCE
CCC
      ICOL=NENA(1)
      DO 230 I=1,ICOL
      XELE(I)=XELA(I)
      YELE(I)=YELA(I)
      DISTE(I)=DISTA(I)
  230 CONTINUE
      KKK=0
      DO 210 J=2,IROW
      ICOL=NENA(J)
      KKK=KKK+NENA(J-1)
      NEXJ1=NEX*(J-1)
      DO 220 I=1,ICOL
      KAA=KKK+I
      KBB=NEXJ1+I
      XELE(KAA)=XELA(KBB)
      YELE(KAA)=YELA(KBB)
      DISTE(KAA)=DISTA(KBB)
  220 CONTINUE
  210 CONTINUE
CCC
CCC   DISTCN=DISTANCE FROM FARTHEST CORNER TO N.A.
CCC
      X=H/2.
      Y=B/2.
      IF(THETA.EQ. 0.) GO TO 212
      IF(THETA.EQ.90.) GO TO 213
      DISTCN=DISTAN(X,Y)
```

```
      GO TO 214
  212 DISTCN =X-XB
      GO TO 214
  213 DISTCN =Y-YB
  214 CONTINUE
CCC
CCC   STRESS AND STRAIN ON EACH CONCRETE ELEMENT
CCC
      DO 310 I=1,NENAT
      EC(I)=EU*(DISTE(I)/DISTCN)
      CALL CONCRE(FC(I),EC(I),FO,EO)
  310 CONTINUE
CCC
CCC   FORCE AND MOMENT ON EACH ELEMENT
CCC
      CCTOL=0.
      XMCT=0.
      YMCT=0.
      DO 320 I=1,NENAT
      CC(I)=AELE*FC(I)
      XMC(I)=CC(I)*YELE(I)
      YMC(I)=CC(I)*XELE(I)
      CCTOL=CCTOL+CC(I)
      XMCT=XMCT+XMC(I)
      YMCT=YMCT+YMC(I)
  320 CONTINUE
CCC
CCC   STRESS AND STRAIN ON REINFORCING BAR
CCC   REPLACEMENT OF CONCRETE AREA ON COMPRESSION ZONE BY REINFORCED BAR
CCC   BEING CONSIDERED
      IF(THETA.EQ. 0.) GO TO 412
      IF(THETA.EQ.90.) GO TO 413
CCC
      DO 401 I=1,NBAR
      X=XS(I)
      Y=YS(I)
      DISTS(I)=DISTAN(X,Y)
  401 CONTINUE
      GO TO 404
  412 DO 402 I=1,NBAR
      X=XS(I)
      DISTS(I)=X-XB
  402 CONTINUE
      GO TO 404
  413 DO 403 I=1,NBAR
      Y=YS(I)
      DISTS(I)=Y-YB
  403 CONTINUE
  404 CONTINUE
      DO 410 I=1,NBAR
      ESS=EU*(DISTS(I)/DISTCN)
      IF(ESS) 420,430,440
  420 SIGN(I)=-1.
      FCA=0.
      GO TO 450
  430 SIGN(I)=0.
      FCA=0.
      GO TO 450
  440 SIGN(I)=1.
      CALL CONCRE(FCA,ESS,FO,EO)
  450 CONTINUE
```

```
      ES(I)=ABS(ESS)
      CALL STEELA(FS(I),ES(I),FY)
      FS(I)=FS(I)*SIGN(I)-FCA
  410 CONTINUE
CCC
CCC   FORCE AND MOMENT ON REINFORCING BAR
CCC
      CSTOL=0.
      XMST=0.
      YMST=0.
      DO 460 I=1,NBAR
      CS(I)=AS(I)*FS(I)
      XMS(I)=CS(I)*YS(I)
      YMS(I)=CS(I)*XS(I)
      CSTOL=CSTOL+CS(I)
      XMST=XMST+XMS(I)
      YMST=YMST+YMS(I)
  460 CONTINUE
CCC
CCC   SUM OF FORCE AND MOMENT ON CONCRETE AND REINFORCEMENT
CCC
      P=CCTOL+CSTOL
      XM=XMCT+XMST
      YM=YMCT+YMST
      TMOM=(XM*XM+YM*YM)**0.5
CCC
      IF(THETA.EQ. 0.) GO TO 462
      IF(THETA.EQ.90.) GO TO 462
      RMXYT=XM/YM
      THETAT=ATAN(RMXYT)
      ANGNAR=ATAN(SLP)
      ANGNA =ANGNAR*DEG
      XB=-YB/SLP
      GO TO 463
  462 CONTINUE
      ANGNA=THETA
      ANGNAR=ANGNA*RAD
  463 CONTINUE
CCC
CCC
CCC
CCC   ITERATION ON POSITION OF N.A.
CCC   ETA=ALLOWABLE TOLERANCE ON AXIAL LOAD(KIP)
CCC
      ETA=0.01
      ETA=0.1
CCC
      IF(THETA.EQ. 0.) GO TO 605
CCC
      IF(YKK.EQ. 1000.) GO TO 580
      AXP= P-PFIX
      AXPP=XPP-PFIX
      IF((ABS(AXP)+ABS(AXPP)).NE. ABS(AXP+AXPP)) GO TO 540
  580 XPP=P
      YA=YB
      YKK=2000.
      IF(ABS( P-PFIX).LT. ETA ) YKK=1000.
      IF(ABS( P-PFIX).LT. ETA ) GO TO 2000
      IF( P-PFIX) 510,2000,520
  540 DELTA=ABS(0.1*(YB -YA ))
      YC=YB
```

```
      YB=(YB+YA)/2.
      YA=YC
      XPP=P
      GO TO 570
  510 YB=YB-DELTA
      GO TO 570
  520 YB=YB+DELTA
  570 CONTINUE
      GO TO 7000
  605 CONTINUE
      IF(YKK.EQ. 1000.) GO TO 680
      AXP= P-PFIX
      AXPP=XPP-PFIX
      IF((ABS(AXP)+ABS(AXPP)).NE. ABS(AXP+AXPP)) GO TO 640
  680 XPP=P
      YA=XB
      YKK=2000.
      IF(ABS( P-PFIX).LT. ETA ) GO TO 2000
      IF( P-PFIX) 610,2000,620
  640 DELTA=ABS(0.1*(XB -XA ))
      XC=XB
      XB=(XB+XA)/2.
      XA=XC
      XPP=P
      GO TO 670
  610 XB=XB-DELTA
      GO TO 670
  620 XB=XB+DELTA
  670 CONTINUE
 7000 CONTINUE
      INA=1
      GO TO 6000
 2000 CONTINUE
      INA=2
 6000 CONTINUE
CCC
CCC   ITERATION ON SLOPE OF N.A.
CCC   ETR=ALLOWABLE TOLERANCE ON SLOPE OF N.A.
CCC
      IF(THETA.EQ. 0.) GO TO 4000
      IF(THETA.EQ.90.) GO TO 4000
CCC
      ETR=0.5*RAD
      ETR=0.2*RAD
      ETR=0.1*RAD
      DANG=THETAT-THETAP
      IF(ABS(DANG).LT.ETR) GO TO 4000
      ANGNAR=ANGNAR-0.2*DANG
      SLP=TAN(ANGNAR)
      GO TO 1000
 4000 CONTINUE
      IF(INA.EQ.2) GO TO 3000
      GO TO 1000
 3000 CONTINUE
      CURV=EU/DISTCN
      CURV=CURV*1000.
      C=DISTCN
      WRITE(6,227) EU,P,TMOM,YB ,XB  ,SLP,ANGNA , C  ,THETAT,CURV
  227 FORMAT(F10.5,1X, 9(F10.4,1X)/)
      SLPP=SLP
      YBP=YB
```

```
      XBP=XB
      DELTAP=0.5+0.10*C
      IF(EU.GT.0.0030) DELTAP=0.5
CCC
      IF(XM-TXM) 2100,2100,2200
 2200 TXM=XM
      TCURV=CURV
      TC=C
      TEU=EU
 2100 CONTINUE
 4900 CONTINUE
 5000 CONTINUE
CCC
      BXM(II)=TXM
      BXP(II)= PFIX
      BCURV(II)=TCURV
      BEU(II)=TEU
      BC(II)=TC
  600 CONTINUE
      GO TO 710
  700 CONTINUE
      II=II-1
  710 CONTINUE
      NPTS=II+1
      N1=NPTS
      BXM(N1)=0.
      BXP(N1)= PMAX
      WRITE(6,2222)
      DO 2300 II=1,N1
      WRITE(6,2111) BXP(II),BXM(II),BCURV(II),BEU(II),BC(II)
 2300 CONTINUE
 2222 FORMAT(//' INTERACTION CURVE'//' AXIAL LOAD(KIPS)',2X,
     1   ' MOMENT(KIP-INS)',2X,' CURV(.001/IN)',5X,' EU',5X,' C(IN)'/)
 2111 FORMAT(2(5X,F10.3),6X,F10.4,4X,F10.4,2X,F10.4/)
      END
```

COLUMN NO.= 1

BIAXIAL BENDING

SECTION PROPERTIES

B(IN)	H(IN)	AS(SQ.IN)	PAS	FO(KSI)	EO	FY(KSI)	EY
10.000	10.000	2.400	0.024	9.000	0.00343	60.000	0.00202

ARRANGEMENT OF REINFORCING BARS(ORIGIN AT CENTER OF SECTION)

BAR NO.	AS(SQ.IN)	X(IN)	Y(IN)
1	0.600	3.000	3.000
2	0.600	-3.000	3.000
3	0.600	3.000	-3.000
4	0.600	-3.000	-3.000

LOCATION OF APPLIED LOADING

THETA (DEGREE)= 22.50000

THETAR (RADIAN)= 0.39270

ELEMENTS PROPERTIES

TOTAL NOS. OF ELEMENTS= 400

NOS. OF ELEMENTS IN X-DIRECTION= 20

NOS. OF ELEMENTS IN Y-DIRECTION= 20

AREA OF SQUARE ELEMENT(SQ.IN)= 0.2500

WIDTH OF SQUARE ELEMENT(IN) = 0.5000

MAX. AXIAL LOAD(KIPS)= 1022.400

AXIAL LOAD(KIPS) = 204.480

FACTOR OF LOAD = 0.20

ANALYSIS RESULT

EU	P(KIP)	TMOM(K-IN)	YB (IN)	XB (IN)	SLP	ANGNA (DEG)	C (IN)	THETAT	CURV(.001/IN)
0.00150	204.4973	480.4287	-7.7430	-3.3797	-2.2911	-66.4197	9.6801	0.3912	0.1550
0.00160	204.4900	515.9329	-6.7639	-2.9764	-2.2725	-66.2480	9.3147	0.3914	0.1718
0.00170	204.3873	549.7317	-5.9318	-2.6199	-2.2641	-66.1704	8.9904	0.3913	0.1891
0.00180	204.4037	582.0754	-5.2235	-2.3071	-2.2641	-66.1704	8.7042	0.3911	0.2068
0.00190	204.4583	613.0220	-4.5983	-2.0329	-2.2619	-66.1497	8.4541	0.3921	0.2247
0.00200	204.4566	643.0803	-4.0467	-1.7862	-2.2455	-66.1830	8.2274	0.3927	0.2431
0.00210	204.5266	672.4016	-3.5606	-1.5683	-2.2704	-66.2283	8.0265	0.3930	0.2616
0.00220	204.5467	701.1348	-3.1250	-1.3727	-2.2765	-66.2857	7.8455	0.3931	0.2804
0.00230	204.4541	729.2532	-2.7268	-1.1939	-2.2838	-66.3534	7.6793	0.3931	0.2995
0.00240	204.5132	756.9038	-2.3717	-1.0348	-2.2920	-66.4287	7.5307	0.3930	0.3187
0.00250	204.5564	784.2227	-2.0491	-0.8896	-2.3033	-66.5310	7.3937	0.3925	0.3381
0.00260	204.5665	811.0093	-1.7516	-0.7576	-2.3122	-66.6122	7.2693	0.3923	0.3577
0.00270	204.4014	837.3464	-1.4725	-0.6343	-2.3214	-66.6952	7.1527	0.3920	0.3775
0.00280	204.4715	863.3931	-1.2234	-0.5249	-2.3309	-66.7795	7.0487	0.3916	0.3972
0.00290	204.5246	888.9644	-0.9944	-0.4255	-2.3373	-66.8363	6.9549	0.3916	0.4170
0.00300	204.5464	914.0937	-0.7822	-0.3339	-2.3424	-66.8819	6.8688	0.3917	0.4368
0.00310	204.4857	938.9272	-0.5834	-0.2483	-2.3496	-66.9443	6.7872	0.3914	0.4567
0.00320	204.4977	963.0762	-0.4034	-0.1717	-2.3498	-66.9468	6.7166	0.3919	0.4764
0.00330	204.5032	986.9834	-0.2363	-0.1004	-2.3531	-66.9755	6.6497	0.3920	0.4963
0.00340	204.5185	1008.1426	-0.1013	-0.0431	-2.3494	-66.9438	6.5984	0.3919	0.5153
0.00350	204.4125	1018.8188	0.0644	0.0276	-2.3298	-66.7699	6.5414	0.3912	0.5351
0.00360	204.5099	1028.1941	0.2094	0.0909	-2.3045	-66.5423	6.4938	0.3913	0.5544
0.00370	204.5073	1036.9583	0.3444	0.1510	-2.2803	-66.3205	6.4488	0.3914	0.5737
0.00380	204.5766	1045.2417	0.4644	0.2058	-2.2566	-66.0999	6.4088	0.3913	0.5929
0.00390	204.4330	1052.7969	0.5800	0.2594	-2.2355	-65.9001	6.3690	0.3910	0.6123
0.00400	204.4937	1059.7656	0.6750	0.3053	-2.2111	-65.6644	6.3380	0.3913	0.6311

0.00410	204.5577	1066.1125	0.7600	0.3474	-2.1880	-65.4372	6.3101	0.3913	0.6498
0.00420	204.4879	1071.6240	0.8384	0.3972	-2.1653	-65.2114	6.2841	0.3913	0.6683
0.00430	204.4826	1076.5254	0.9051	0.4224	-2.1429	-64.9840	6.2626	0.3913	0.6866
0.00440	204.3867	1080.5925	0.9651	0.4551	-2.1207	-64.7543	6.2433	0.3913	0.7048
0.00450	204.5513	1084.2344	1.0101	0.4814	-2.0994	-64.5192	6.2301	0.3913	0.7223
0.00460	204.4826	1086.8691	1.0539	0.5076	-2.0760	-64.2798	6.2171	0.3913	0.7399
0.00470	204.5221	1088.9741	1.0876	0.5295	-2.0539	-64.0396	6.2081	0.3912	0.7571
0.00480	204.4953	1090.3574	1.1164	0.5493	-2.0323	-63.7999	6.2009	0.3911	0.7741
0.00490	204.5268	1091.1770	1.1376	0.5657	-2.0109	-63.5594	6.1968	0.3911	0.7907
0.00500	204.4960	1091.3279	1.1548	0.5804	-1.9897	-63.3162	6.1942	0.3911	0.8072
0.00510	204.4452	1090.8577	1.1673	0.5929	-1.9686	-63.0708	6.1936	0.3913	0.8234
0.00520	204.4652	1089.9343	1.1748	0.6031	-1.9480	-62.8265	6.1951	0.3912	0.8394
0.00530	204.4442	1088.4739	1.1798	0.6120	-1.9278	-62.5833	6.1975	0.3912	0.8552
0.00540	204.4613	1086.5737	1.1804	0.6186	-1.9081	-62.3422	6.2017	0.3911	0.8707
0.00550	204.5351	1084.1506	1.1754	0.6228	-1.8873	-62.0832	6.2088	0.3915	0.8858
0.00560	204.4769	1081.4524	1.1729	0.6273	-1.8668	-61.8615	6.2139	0.3912	0.9012
0.00570	204.5442	1078.2505	1.1629	0.6286	-1.8500	-61.6072	6.2231	0.3916	0.9159
0.00580	204.4599	1074.7991	1.1560	0.6306	-1.8332	-61.3884	6.2302	0.3912	0.9309
0.00590	204.5756	1070.9824	1.1410	0.6288	-1.8145	-61.1405	6.2416	0.3916	0.9453
0.00600	204.4925	1066.7939	1.1294	0.6284	-1.7973	-60.9088	6.2511	0.3916	0.9598